Optimization of chemogenetic modulation of the Locus Coeruleus in rat to study its relation to hippocampal excitability

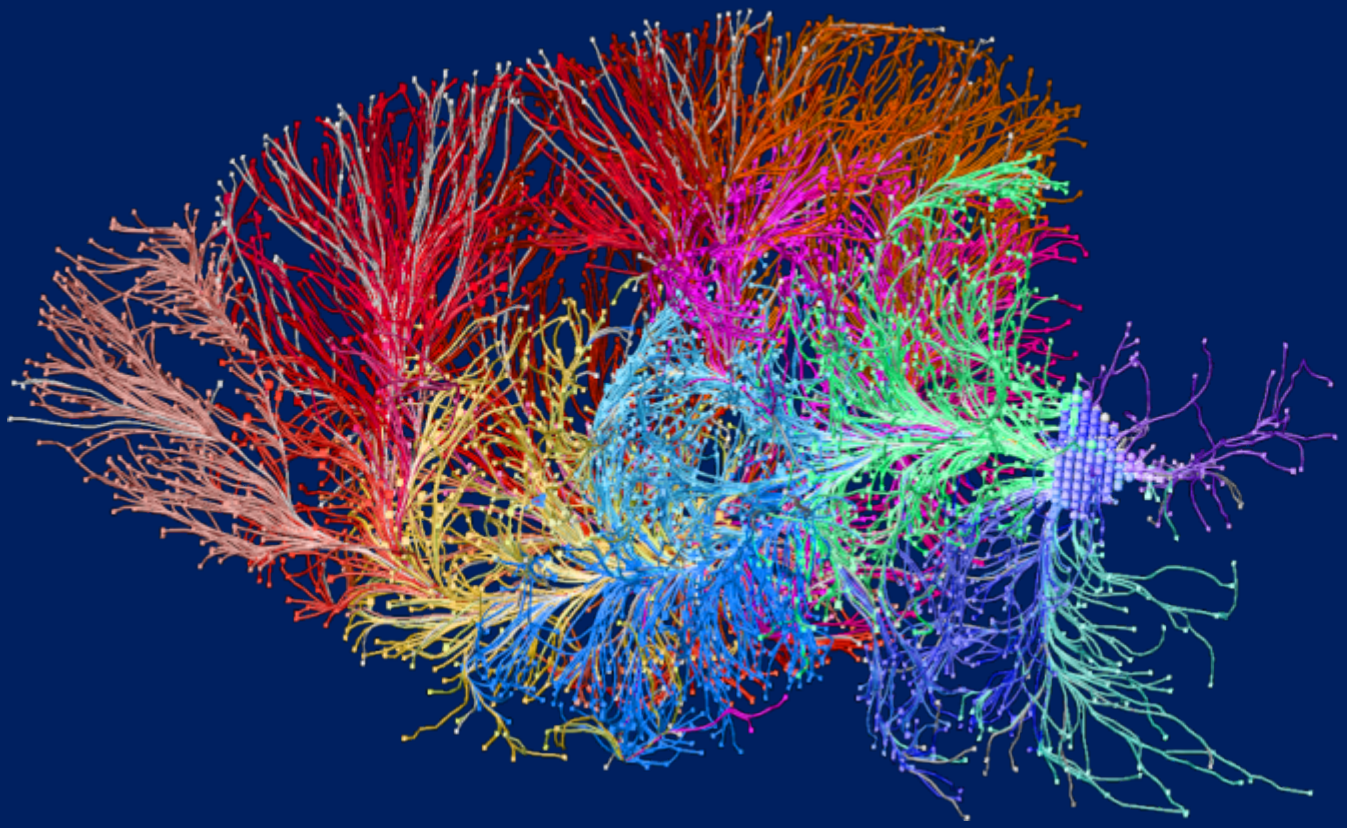

Latoya Stevens

Promotor: Prof. Dr. Kristl Vonck
Co-promotor: Prof. Dr. Robrecht Raedt

UNIVERSITEIT GENT

-2021-

GHENT UNIVERSITY

Faculty of Medicine and Health Sciences

Department of Head and Skin

4BRAIN

Optimization of chemogenetic modulation of the locus coeruleus in rat to study its relation to hippocampal excitability

Latoya Stevens

Promotor: Prof. Dr. Kristl Vonck
Co-Promotor: Prof. Dr. Robrecht Raedt

Thesis submitted to fulfil the requirements for the degree of Doctor (PhD) in health sciences.

-2021-

To refer to this thesis:
Stevens, L. (2021) Optimization of chemogenetic modulation of the locus coeruleus in rat to study its relation to hippocampal excitability. PhD thesis, Ghent University.

Cover: Allen Brain Atlas Connectivity Project Experiment 511971714, TH-Cre_Fl172 mouse

G.S.K.E.
F.M.R.E.

This research was funded by a grant from "Geneeskundige stichting Koningin Elizabeth voor Neurowetenschappen (G.S.K.E)".

Promotor: **Prof. dr. Kristl Vonck**
Ghent University Hospital, Belgium

Co-promotor: **Prof. dr. Robrecht Raedt**
Ghent University, Belgium

Chair: **Prof. dr. Marie-Anne Vanderhasselt**
Ghent University, Belgium

Members of the examination and reading board:

Prof. dr. Apr. Christophe Stove
Ghent University, Belgium

Prof. dr. Ir. Sarah Vergult
Ghent University, Belgium

Dr. Tim van Langenhove
Ghent University Hospital, Belgium

Dr. Benedicte Descamps
Ghent University, Belgium

Dr. Chris Van Den Haute
KU Leuven, Belgium

Publications included in the thesis

Manuscript 1: **Stevens L**, Vonck K, Larsen LE, Van Lysebettens W, Germonpre C, Baekelandt V, Van Den Haute C, Carrette E, Wadman WJ, Boon P, Raedt R. A Feasibility Study to Investigate Chemogenetic Modulation of the Locus Coeruleus by Means of Single Unit Activity. Front Neurosci. 2020;14(March):162, **A1 publication, IF:4.677, Q2 in Neurosciences.**

Manuscript 2: **Stevens L**, Larsen LE, Van Lysebettens W, Carrette E, Boon P, Raedt R, Vonck K. Transducing the locus coeruleus using canine adenovirus type 2 (CAV2) vector in rats for chemogenetic modulation research. Front Neurosci. 2021; 15(April):426, **A1 publication, IF:4.677, Q2 in Neurosciences.**

Preface

Epilepsy is the second most common neurological disorder worldwide, affecting 0.5-1% of the population. Despite currently available anti-epileptic drugs, about 30% of the patients do not respond well to this form of treatment and can be helped by vagus nerve stimulation (VNS). The mechanism of action of VNS is not fully understood but previous research has suggested that the observed seizure-suppressive, memory-enhancing and mood improving effects are mediated by increased locus coeruleus (LC) activity. The LC is a brainstem nucleus with widespread noradrenergic projections throughout the brain affecting brain excitability pathways indicating its possible therapeutic importance in neurological and psychiatric diseases such as epilepsy and major depression disorder. Preclinical studies have proven the anti-epileptic role of noradrenaline (NA) and since the hippocampus, an important structure in encoding memory and seizure generation in temporal lobe epilepsy, is highly innervated by the LC, it is of importance to further investigate the effects of LC-NA output on hippocampal excitability. Previous studies investigating the effect of LC on hippocampal electrophysiology using electrical or chemical stimulation revealed contradictory results. This indicated the need for a selective method to precisely modify LC activity in order to be able to answer the question: how does LC alter brain excitability and what is its role in the observed VNS-induced effects? Therefore, in this thesis, an *in vivo* gene therapy, chemogenetics, is used to express designer receptors exclusively activated by designer drugs (DREADDs) to selectively modify the activity of LC-NA neurons. Chemogenetic activation of LC requires high and cell-specific expression of the excitatory hM3Dq DREADD. Additionally, a dose-response curve of a designer drug, e.g. clozapine, has to be determined to induce selective DREADD-specific modulation of LC neurons after systemic administration. This thesis focused on optimising injection parameters to induce high cell specific DREADD expression in LC-NA neurons with low aspecificity and toxicity. Additionally, the suitability of subclinical doses of clozapine were tested as selective DREADD ligand. These challenges are elaborated in the experimental work section of this thesis followed by the main conclusions and future experimental goals.

Latoya Stevens, Ghent, September 22, 2021

List of abbreviations

AAP:	Assembly Activating Protein
AAV:	Adeno-Associated Virus
ACh:	Acetylcholine
aCSF:	Artificial Cerebrospinal Fluid
AD:	Alzheimer's Disease
AMPA:	α-amino-3-hydroxy-5-methyl-4-isoxazolepropionic acid
ANS:	Autonomic Nervous System
AP:	Anterior-Posterior
ATP:	Adenosine Triphosphate
BB:	Blocking Buffer
BBB:	Blood-Brain-Barrier
CA:	Cornu Ammonis
CamKIIα:	Calmodulin dependent protein Kinase II
cAMP:	Cyclic Adenosine Monophosphate
CAR:	Coxsackie Virus and Adenovirus Receptor
CAV:	Canine Adenovirus
ChR:	Channelrhodopsin
CNO:	Clozapine-N-Oxide
CNS:	Central Nervous System
Cre:	Cre recombinase
CRF:	Corticotropin Releasing Factor
CRH:	Corticotropin-Releasing Hormone
DAG:	Diacylglycerol
DBH:	Dopamine β Hydroxylase
DCZ:	Deschloroclozapine
DG:	Dentate Gyrus
DMSO:	Dimethyl Sulfoxide
DMV:	Dorsal Motor nucleus of the Vagus
DREADD:	Designer Receptor Exclusively Activated by Designer Drugs
DS:	Down Syndrome
DSP-4:	N-(-2- chloroethyl)-N-ethyl-2-bromobenzylamine
DV:	Dorsoventral
EEG:	Electroencephalography
eLGIC:	engineered Ligand Gated Ion Channel
eNpHR:	enhanced Halorhodopsin
EP:	Evoked electrical field Potential
EPSP:	Excitatory Postsynaptic Potential
ER:	Endoplasmatic Reticulum
fEPSP:	field excitatory postsynaptic potential

GABA:	γ-Aminobutyric Acid
GC:	Genome Copies
GFAP:	Glial Fibrillary Acidic Protein
GIRK:	G protein-coupled Inwardly Rectifying potassium channel
GPCR:	G protein-coupled receptor
HF:	Hippocampal Formation
HSPG:	Heparin Sulphate Proteoglycan
HSV:	Herpes Simplex Virus
IEG:	Immediate Early Gene
ILAE:	International League Against Epilepsy
INTENS:	Ionotropic Receptor mediated Neuronal Stimulation
IP3:	Inositol Triphosphate
IPD:	Ion Pore Domain
IPSP:	Inhibitory Postsynaptic Potential
ISO:	Isoproterenol
ITR:	Inverted Terminal Repeat
KORD:	κ-opioid Derived Designer Receptor Exclusively Activated by Designer Drugs
LBD:	Ligand Binding Domain
LC:	Locus Coeruleus
L-DOPA:	L-dihydroxyphenylalanine
LGIC:	Ligand Gated Ion Channel
LTD:	Long Term Depression
LTP:	Long Term Potentiation
MAPK:	Mitogen Activated Protein Kinase
ML:	Mediolateral
MOA:	Mechanism Of Action
MS:	Multiple Sclerosis
MTLE:	Mesial Temporal Lobe Epilepsy
NA:	Noradrenaline
NMDA:	N-Methyl-D-aspartate
NREM:	Non Rapid Eye Movement
NTS:	Nucleus Tractus Solitarius
PA:	Phentolamine
PE:	Phenylephrine
PD:	Parkinson's disease
PIP2:	Phosphatidylinositol 4,5-biphosphate
PKA:	Protein Kinase A
PLC:	Phospholipase C
PNS:	Peripheral Nervous System
PP:	Perforant Path
pp:	physical particles

PS:	Population Spike
PSAM:	Pharmacologically Selective Actuator Molecule
PSEM:	Pharmacologically Selective Effector Molecule
PSP:	Post Synaptic Potential
PVN:	Paraventricular Nucleus
RASSL:	Receptor Activated Solely by Synthetic Ligand
REM:	Rapid Eye Movement
RN:	Raphe Nucleus
RVLM:	Rostroventrolateral Medulla
TH:	Tyrosine Hydroxylase
TLE:	Temporal Lobe Epilepsy
TRE:	Tetracycline Response Element
tTA:	tetracycline Transactivator protein
UHPLC:	Ultra High-Performance Liquid Chromatography
UPR:	Unfolded Protein Response
VLPO:	Ventrolateral Preoptic Area
VNS:	Vagus Nerve Stimulation
WPRE:	Woodchuck hepatitis virus posttranscriptional regulatory element

Table of content

Part I

Background and General Principles

Chapter 1 General principles

1.1 The nervous system

The nervous system comprises the central nervous system (CNS) and peripheral nervous system (PNS). The PNS is defined by all peripheral nerves and ganglia (collections of neurons outside the brain). The PNS has a double role: it carries sensory and motoric commands of the CNS to the peripheral tissues of the body and it transmits peripheral information back to the CNS. The CNS consists of the spinal cord, the brainstem and the cerebral hemispheres. The spinal cord can be divided into a ventral and dorsal part. The ventral spinal cord consists of motor neurons that innervate peripheral muscles. These spinal motor neurons are controlled by cortical neurons allowing consciously controlled movements. The dorsal spinal cord transmits sensory information. Somatic sensory information is picked up at modality specific receptors and transmitted through spinal first order sensory neurons to spinal cord secondary sensory neurons, which will transmit the information to the brain allowing conscious awareness of sensation. The brain consists of the cerebrum, cerebellum and brainstem. The brainstem mainly controls important and vital autonomic functions such as respiration, heart rate, and blood pressure. However, it also innervates the face and organs. The cerebellum coordinates voluntary movements and regulates balance, coordination, and posture, while the cerebrum regulates higher cognitive functions and executive control (1, 2).

The nervous system can also be divided in its autonomic and somatic components. The autonomic nervous system (ANS), also referred to as the involuntary or visceral nervous system, can be divided into an ortho- and parasympathetic part consisting of neurons that control the internal environment via secretory glands and smooth and cardiac muscles. The parasympathetic ANS controls the rest and digest response whereas the orthosympathetic ANS is active during a flight or fight response. In contrast to the ANS which acts without our voluntary control, the somatic nervous system controls our conscious movements (1-3).

1.1.1 Cells of the nervous system

Neurons are the principal cells present in the nervous system and vary both in shape and size. Neurons encode information and transmit it to other neurons, glial cells or non-neural tissue. The typical structure of a neuron, as shown in Figure 1.1, consists of three large components: the cell body or **soma**, which contains the **nucleus** and other cell organelles, and the **dendrites**, which are short outgrowths of the cell body and receive information of other neurons.

Neurons transmit their information to other cells or organs via **axons** also called nerve fibers (Fig 1.1) (2, 4, 5).

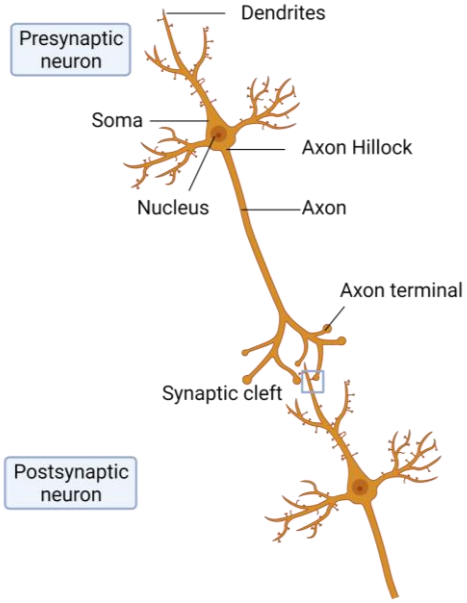

Figure 1.1 Schematic representation of the typical structure of a neuron. Afferent input is received at the dendrites; efferent output is transmitted along the axon to the axon terminal forming the synaptic cleft with the postsynaptic neuron. The soma contains the nucleus and the action potential is formed at the axon hillock. Figure made with Biorender.com.

In most parts of the central nervous system, the somas of neurons are grouped forming grey matter. White matter consists of axons and appears white because of the myelin sheath (2, 5, 6). Classification of neurons can be performed on the basis of their function (for example sensory or motor neurons) and structure (bi- or multipolar and pseudo-unipolar). Bipolar neurons only have one dendrite and axon, whereas multipolar neurons have various dendrites and only one axon. Pseudo-unipolar neurons are characterized by only one process extending from the cell body.

Next to neurons, the nervous system contains more supporting cells or glial cells. Neuroglia cannot conduct action potentials, but they retain the ability to divide. Astrocytes are the largest group of supporting cells in the CNS and form a part of the blood-brain-barrier (BBB) by participating with blood vessel endothelium. Oligodendrocytes are wrapped around the axons in CNS and form the myelin sheat. Schwann cells are the corresponding cells in the PNS and myelinate peripheral nerve fibers. Another neuroglial cell is the ependymal cell which outlines the ventricles (the cavities filled with cerebrospinal fluid). Microglia are the immune cells of the CNS and play a role in protecting the brain from bacteria and debris (1, 2).

1.2 Synaptic neurotransmission

The cell membrane of a neuron is composed of a phospholipid bilayer and separates the intra- from the extracellular medium. It is not permeable for electrically charged molecules and can therefore be considered as an electrical insulator.

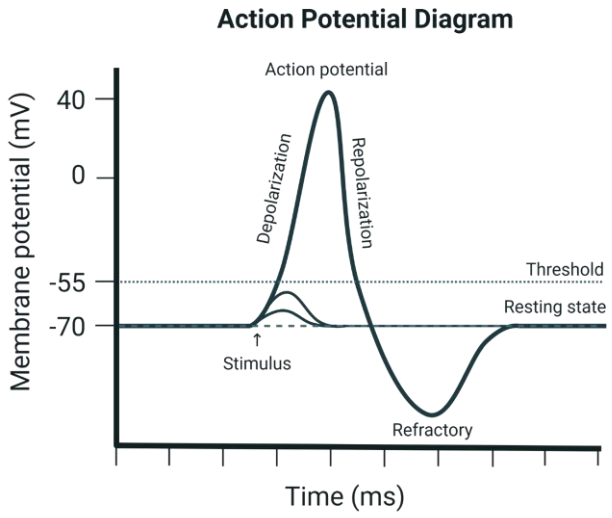

Figure 1.2 Schematic representation of an action potential. When an accumulation of excitatory postsynaptic potentials (EPSPs) (stimulus) reaches the soma, ligand-gated Na^+ channels open followed by an influx of cations and initiation of depolarisation. When the threshold (around -55mV; indicated by the dotted line) is reached, voltage-gated Na^+ channels open increasing the cation influx inducing strong depolarisation. At the peak of the action potential (AP), K^+ channels open resulting in a potassium efflux and simultaneous closure of Na^+ channels. The membrane hyperpolarises as K^+ ions leave the cell. The cell is now unable to generate new APs. Ultimately, K^+ channels close and Na^+/K^+ transporters will restore the membrane potential to its rest potential (-70mV; indicated by the full line). Figure generated with BioRender.com.

The presence of different channels in the membrane allows passage of ions based on the concentration difference between these two media, the difference in voltage (or potential) and the diameter of the pore. Ions, such as Na^+, K^+, Cl^- and Ca^{2+} are separated by the membrane and their concentration differs between the intra- and extracellular environment. The concentration of Na^+ is approximately 10 times higher at the exterior side, whereas K^+ concentration is 30 times higher on the interior side. These concentration differences are maintained by the presence of membrane pumps, such as sodium pumps, which actively pump out Na^+ in exchange for K^+ ions. Furthermore, in resting state K^+ ions leak to the extracellular environment through K^+ channels. Lastly, negatively charged proteins accumulate intracellularly near the cell membrane. This combination creates a voltage difference across the membrane of approximately -70mV referred to as the resting state membrane potential. Charged molecules move across the membrane influenced by both the membrane potential and the concentration gradient, i.e. the electrochemical gradient (2, 5, 6).

Rapid changes in the resting membrane potential due to movement of ions through voltage-gated ion channels can result in the occurrence of action potentials which eventually propagate along the axon and transmit neuronal information.

When the conductance characteristics of the ion channels change by binding of a ligand or changes in voltage, an alteration in the resting membrane potential can occur, which will reduce the voltage-difference between intra and extracellular medium. This is referred to as an initial depolarization (stimulus in Fig 1.2). When a certain threshold is reached (-55mV), as depicted by the dashed line in Fig 1.2, voltage-sensitive sodium channels in the membrane will open, resulting in an even higher influx of Na^+ ions, further depolarizing the membrane. At this point the membrane potential is reversed, where the interior becomes more positive compared to the exterior. When the potential increases up to ± 30 mV, the voltage-gated sodium channels are saturated and become inactive, inhibiting further influx of Na^+ into the cell. Depolarization slows down, voltage-gated potassium channels open and K^+ efflux is induced. This efflux of potassium in combination with the inactivated sodium channels leads to repolarization However, because of the slow closing characteristics of the K^+ channels, potassium remains to flow out of the cell, inducing hyperpolarization leaving the membrane potential below the resting membrane potential. Once these voltage-gated potassium channels are closed, potassium leak channels and the sodium/potassium pump will restore the membrane potential (Fig 1.2) (7).

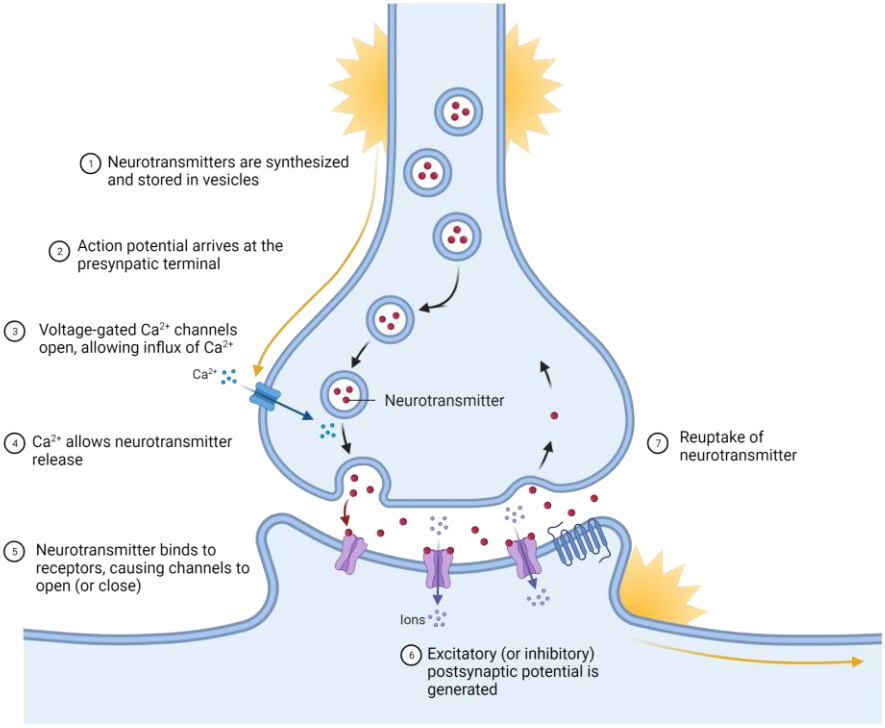

Figure 1.3 Chemical synapse communication. 1) Neurotransmitter is synthesized in the neuron and stored in presynaptic vesicles. 2) After depolarisation, the action potential arrives at the axon terminal and 3) voltage-gated Ca^{2+} channels open, allowing Ca^{2+} influx. 4) Intracellular Ca^{2+} increase induces fusion of the synaptic vesicles with the membrane and release of neurotransmitter in the synaptic cleft. 5) Neurotransmitter binds postsynaptic receptors and 6) induce formation of excitatory or inhibitory postsynaptic potentials. 7) Reuptake of neurotransmitter by the presynaptic neuron occurs. Figure made in Biorender.com.

Action potentials are generated at the axon hillock and will depolarize the neighboring axonal region by opening of voltage-gated Na^+ channels, generating a propagation of the action potential along the axon towards the axonal terminal (2, 5). The **synapse** is the site of neuronal communication and is formed by the axonal termini of the presynaptic neuron and the dendrites of the postsynaptic neuron (Fig 1.1). Although the conduction of neuronal information within the neuron is electrical, the communication between neurons at the synapse is based on the release of chemicals called **neurotransmitters**. Figure 1.3 shows the organization of chemical synapse communication. When the action potential arrives at the axonal terminal, depolarization of the axonal terminus opens voltage-gated Ca^{2+} channels resulting in increased intracellular Ca^{2+} levels. This induces the fusion of presynaptic vesicles filled with synthesized neurotransmitter with the membrane and consequent release of neurotransmitter out of the synaptic vesicles into the inter-neuronal space or synaptic cleft (space between pre- and postsynaptic neuron, Fig.1.3). These neurotransmitters bind receptors present on the surface of the postsynaptic neuron and change the resting membrane potential inducing post synaptic potentials (PSP).

Different neurotransmitters are present of which the activity is mainly determined by the bound receptor characteristics. Glutamate will mostly induce an excitatory response by binding postsynaptic AMPA (α-amino-3-hydroxy-5-methyl-4-isoxazolepropionic acid), NMDA (N-methyl-d-aspartate) and kainate receptors resulting in influx of cations such as Na^+, generating an excitatory postsynaptic potential (EPSP), depolarizing the membrane. On the other hand, γ-aminobutyric acid or GABA can bind $GABA_A$ or $GABA_B$ receptors present on the postsynaptic neuron. Binding of $GABA_A$ receptors leads to the opening of chloride-channels. Extracellular Cl^- is higher than intracellular, which will lead to an influx of Cl^- into the intracellular medium generating an inhibitory postsynaptic potential (IPSP) possibly inducing hyperpolarization (Fig 1.3) (5, 6). Next to electrochemical communication, pure electrical synapses exist, where direct electric communication between neurons is performed through gap junctions (8).

Action potentials are all-or-non-phenomena, they are only generated when the threshold (-55mV) is reached (Fig 1.2), otherwise they do not occur. Since neurons receive multiple presynaptic projections, a summation of postsynaptic potentials occurs at the axon hillock. If more EPSPs than IPSPs are received, depolarization of the membrane potential and subsequent generation of an action potential will occur. Hyperpolarization will be induced when the opposite is true and more IPSPs reach the axon hillock (9).

1.2.1 Neurotransmitter receptors

Neuron to neuron communication is mediated by receptors embedded in the plasma membrane as described above. The cellular response and magnitude of this reaction is defined by the type of receptor present in the membrane, the number of receptors, the state of the receptors and the abundancy of neurotransmitter present in the synaptic cleft. This chemical neurotransmission initiated by the excitation of one neuron can cause both excitation or inhibition in the adjacent postsynaptic neuron mediated by two large classes of receptors: G protein-coupled receptors and ionotropic receptors (10).

1.2.1.1 G protein-coupled receptors

G protein-coupled receptors (GPCRs), the largest group of membrane receptors, can be activated by extracellular molecules and induce neuronal signaling transduction pathways and concurrent de- or hyperpolarization of the cell membrane, regulating the majority of the (neuro)physiological responses such as behavior and mood, vision, immune system regulation and even endocrine functions. A variety of neuroreceptors important for normal functioning of the central nervous system are GPCRs: adenosine, serotonin, adrenergic, acetylcholine, dopamine, cannabinoid, $GABA_B$ and metabotropic glutamate receptors (11, 12).

All GPCRs are structurally characterized by seven transmembrane α-helical segments separated by alternating intracellular and extracellular loops (13). GPCRs occur in an equilibrium between inactive and fully active state. When an agonist binds the extracellular domain of the receptor, the equilibrium is pushed to the active states. The GPCR undergoes conformational changes ultimately leading to the opening of the receptor core. This promotes the binding of the G protein and formation of the signaling complex, which consists of the activated receptor, agonist and heterotrimeric protein (G coupled-protein, α, β and γ G proteins). Binding of the activated receptor with its G protein results in exchanging GDP for GTP and subsequent decoupling of the Gα and Gβγ complex, initiating a specific intracellular signaling pathway (14). However, recent studies have shown that agonist binding is not always enough to shift the equilibrium to the active state, and that binding of the G protein is necessary to stabilize the fully active receptor. Nonetheless, the receptor can undergo a ligand-independent conformational change to the active state, indicating possible constitutive activity (15). GPCRs can be classified in four families based on the Gα subtype, each type activating a different signaling pathway: Gαs, Gαi/o (further referred to as “Gαi”), Gαq/11 (“Gαq”), or Gα12/13. Gα12/13 regulates rho, which controls cytoskeletal events (16).

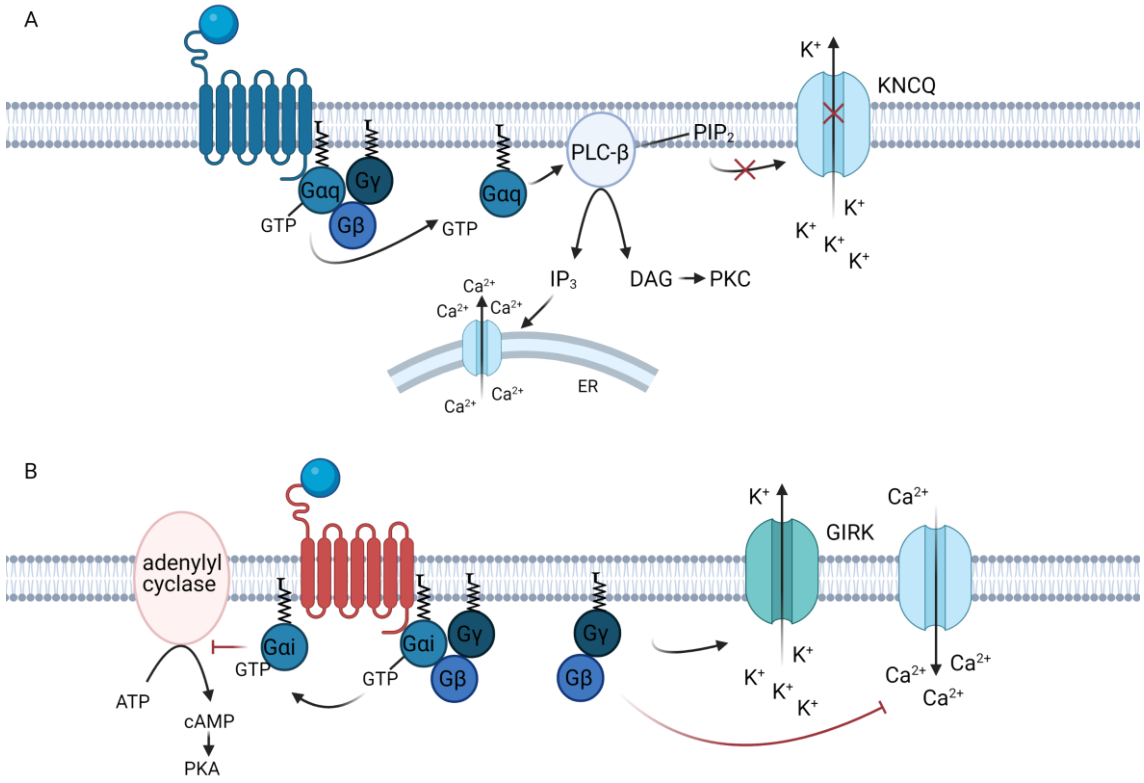

Figure 1.4 Schematic overview of metabotropic G protein-coupled receptors in the cell membrane. Metabotropic G-coupled receptors are known for their slow de- or hyperpolarisation of the cell membrane induced by binding of neurotransmitter released from the presynaptic neuron. **A. The Gαq signalling cascade**. Binding of a ligand (blue circle) to the GPCR (blue), initiates activation of the Gα complex (part of the trimeric G protein) detaches from the Gβγ unit and activates Phospholipase-B (PLC-B), reducing PIP2 and forming inositol triphosphate (IP3) and diacylglycerol (DAG). IP3 induces Ca^{2+} release from the endoplasmatic reticulum (ER), whereas DAG activated PKC. Reduced PIP2 will inhibit K^+ efflux and depolarisation of the cell. **B. The Gαi signalling cascade**. Ligand binding of the GPCR (blue circle) results in Gαi release of the trimeric complex and inhibition of adenylyl cyclase. The Gβγ complex activates GIRK channels inducing leakage of K^+ ions and hyperpolarisation. Simultaneous blockage of the Ca^{2+} influx decreases the intracellular Ca^{2+} concentration. Figure made in Biorender.com.

Gαq- mediated signaling pathway

As depicted in figure 1.4A, in the Gαq-mediated signaling pathway, the Gαq protein activates phospholipase C (PLC-β), which leads to formation of the second messengers diacylglycerol (DAG) and inositol triphosphate (IP3). DAG on its turn activates protein kinase C (PKC) whereas IP3 induces intracellular Ca^{2+} release from the endoplasmatic reticulum (ER) increasing intracellular Ca^{2+} levels. PLC-β also hydrolyses phosphatidylinositol 4,5-biphosphate (PIP_2), reducing its presence, resulting in closing of PIP_2-gated K^+ channels (KNCQ) and inhibition of slowly inactivating outwardly rectifying K^+ currents (M currents). Inhibition of these M currents results in enhanced neuronal excitability (11, 16, 17).

Gαi-mediated signaling pathway

GPCRs coupled to the Gαi evoke the opposite effect and hyperpolarize the cell by decreasing cyclic adenosine monophosphate (cAMP) production from adenosine triphosphate (ATP) by inhibiting adenylyl cyclase. Decreases in cAMP inhibit protein kinase A (PKA) downstream effects. Additionally, the Gβγ subunit induces a K^+ efflux by coupling to inwardly-rectifying potassium channels (GIRK). This decreases the intracellular charge of the cell, inducing hyperpolarization. Depolarization and consequent neurotransmitter release is additionally prevented by blockage of voltage-gated calcium channels, decreasing Ca^{2+} entry (Fig. 1.4 B) (11, 16).

Gαs-mediated signaling pathway

Gαs, like Gαq mediated pathway, also depolarizes the cell by activation of adenylyl cyclase, increasing cAMP production and activation of PKA. PKA induces phosphorylation of proteins carrying a RRXS amino acid sequence, resulting in activation or deactivation depending on the protein type and coupled pathway (11, 16).

β-arrestin-mediated signaling pathways

GPCRs can also bind to β-arrestin complexes, occluding possible binding of a G protein and subsequent G protein signaling. The interaction of β-arrestin mostly occurs when the intracellular elements of the activated GPCR are phosphorylated, initiating internalization of the receptor in a clathrin-mediated manner followed by uptake in an early endosome. In this stage of the pathway, the GPCR can be dephosphorylated and relocated to the cell membrane in its inactive state, or be degraded in lysosomes (14).

1.2.1.2 Ionotropic neurotransmission

In contrast to the slow de- or hyperpolarization of the cell membrane by GPCRs, the activation of ionotropic receptors causes the opening of an ion channel in an all-or-none manner, activating or inhibiting the cell in a faster way. An ionotropic receptor is a large multi-subunit complex composed of four or five proteins that form an ion channel. Unbound ionotropic receptors appear in the closed state and are not permeable for ions. Neurotransmitter binding leads to conformational changes inducing flows of ions relative to their electrochemical gradient changing the membrane potential.

Dissociation of the neurotransmitter or desensitization of the receptor stops the ion flow. Anion or cation selectivity is acquired through the presence of positive or negative charged amino acids located in the ion pore respectively (10). There are two large classes of ionotropic receptors of which one contains the nicotinic acetylcholine (ACh) receptor, γ-aminobutyric acid ($GABA_A$) receptor, a subclass of the serotonin receptors (5-HT3), and the glycine receptor. The other class contains the ionotropic glutamate receptors (1, 10).

1.3 Hippocampal anatomy

The hippocampal formation (HF) is located in the dorsomedial part of the temporal lobe, posterior to the amygdala, and plays an important role in memory, mood and attention, and spatial navigation (10). This structure is often damaged in patients with mesial temporal lobe epilepsy (MTLE). The HF consists of different substructures: the hippocampus proper which contains the cornu ammonis fields and the dentate gyrus, the subiculum, and parasubiculum. The cornu ammonis fields (CA1, CA2, CA3 and CA4 only present in humans) are subdivided in layers differing in connectivity and morphology. The first layer in the dorsal hippocampus is the *stratum oriens*, containing the cell bodies of inhibitory basket cells and horizontal trilaminar cells. The *stratum pyramidale* contains the principal excitatory neurons of CA, the pyramidal cells, and interneurons. The *stratum lucidum* is only present in CA3 and exists of mossy fibers of the dentate gyrus (DG) granule cells. The *stratum radiatum* consists of septal and commissural fibers, Schaffer Collateral (SC) fibers, basket cells and bistratified cells. *Stratum lacunosum* contains SC fibers and perforant path (PP) fibers (18). The PP fibers synaps onto pyramidal cells in the *stratum moleculare* (Fig. 1.5).

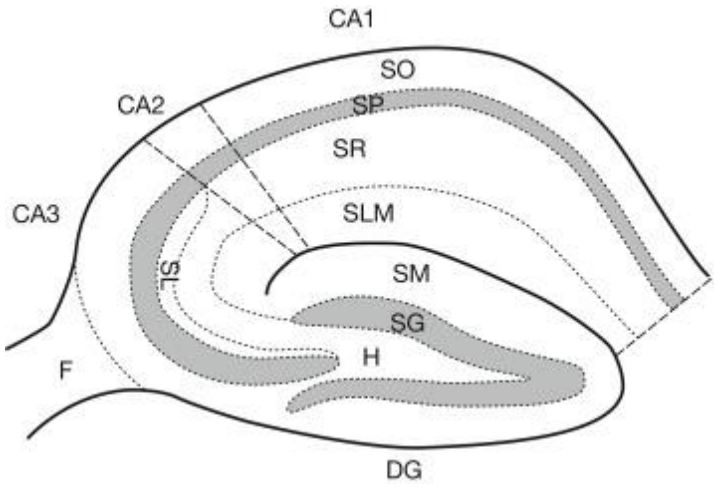

Figure 1.5 Schematic overview of the rat hippocampal formation and different laminae. The Cornu Ammonis (CA) and the Dentate Gyrus (DG) are two sheets of cortex forming the hippocampus. Fimbria (F), Hilus (H), Stratum Oriens (SO), Stratum Pyramidale (SP), Stratum Radiatum (SR), Stratum Lacunosum-Moleculare (SLM), Stratum Lucidum (SL), Stratum Moleculare (SM), Stratum Granulosum (SG). Figure adapted from 'Cellular Migration and Formation of Neuronal Connections, chapter Hippocampal migration' with rights and permission of Elsevier®.

The cornu ammonis forms a cortical sheet that interlocks with the dentate gyrus (DG), a layer of granule cells wrapped around the end of the hippocampus proper. The DG is a trilaminar cortical region with a characteristic semicircle shape. The entorhinal cortex is the major input of the HF, entering through the *perforant path* (PP). The PP projects to the granule cell layer of the dentate gyrus and the dendrites of CA3. Information flows from the DG to the pyramidal cells of the CA3 via the *mossy fiber pathway*. Next to direct synaptic communication between CA3 and CA1 (referred to as *the Schaffer collaterals*), CA2 connects them as well. CA1 cells, which also receive direct input from the entorhinal cortex via the PP, target the subiculum. The cingulum bundle and fornix act as output receivers. These pathways are all unidirectional, meaning that there is no back projection. However, the connectivity of the hippocampus is more complicated as depicted in the trisynaptic circuit as a single hippocampal neuron projects to multiple target neurons and interneurons are abundantly present. The intrinsic connectivity can be seen as a combination of serial and parallel excitatory and inhibitory connections where each neuron is affected by and has effects on other neurons (19). At least three fiber bundles are included in the HF: the angular bundle (connecting to HF to the entorhinal cortex), the dorsal and ventral commissures connecting the hippocampi in both hemispheres, and the fimbria-fornix pathway connecting the hippocampus to other brain regions such as the basal forebrain, hypothalamus, and the brainstem (19).

1.4 Electrophysiology

1.4.1 Unit recording

Unit recording is an electrophysiological recording technique that allows recording of the discharges of a single neuron using a microelectrode system. To record signals from neurons, the electric current flowing through the cell is measured. An action potential propagates through the cell and generates electric currents flowing in and out of the cell, resulting in changes in the voltage potential in and outside the cell. There are two types of unit recording: intracellular and extracellular unit recording. When a recording electrode is placed in the cell, voltage changes across the membrane, during the generation of an action potential, are measured and referred to as intracellular unit recording. Extracellular unit recording is defined by the positioning of a microelectrode close to the cell surface to record voltage changes outside the cell. This technique is often used to determine the effect of pathology or administration of pharmacological agents on neuronal activity in an unbiased manner by quantifying the firing of neurons over an extended period of time (20, 21).

Whereas intracellular unit recording, an invasive recording method, exists in different configurations able to give information in a high temporal and spatial resolution about postsynaptic potentials and currents, input resistance, single channel conductance and synaptic plasticity (21) (22).

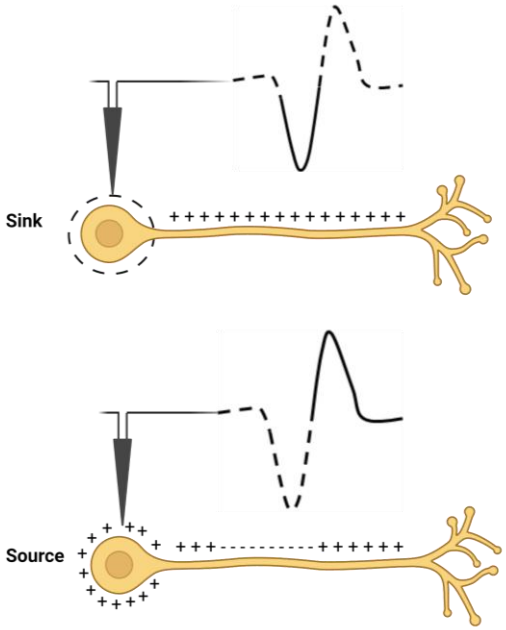

Figure 1.6 Schematic representation of current source and sink. Simplified model of recording action potential at the soma. The membrane under the electrode is first depolarized and acts as a sink, subsequently as the action potential propagates along the axon and away from the soma, the soma becomes a source. This phenomenon results in a biphasic extracellular potential. Often neurons display a more complex spike wave due to electrode positioning, cell morphology, cell excitability and distribution of conductances along the membrane. Figure made in Biorender.

During extracellular recordings, action potentials or spikes are measured. These are the product of a current that flows out to the extracellular space. This outflow of current around the active neuron is explained by volume conductance theory. This theory represents the neuron surrounded by a low resistance medium (volume conductor). When a recording electrode is placed around a single axon, the recorded action potential has a triphasic waveform. At resting membrane potential, the potential is uniform and there is no current flow. During depolarization, a difference in potential between the depolarized and resting regions is created, which results in changes in current. At the depolarized region, current flows into the cell, observed as a negative signal at the electrode, referred to as a *current sink*. Inactive regions around the depolarization act as the *source of current* which results in a positive signal at the electrode (Fig. 1.6). When an action potential is generated and moves along the axon it will approach and move away from the recording electrode.

When it approaches, the electrode is at the place of the current source and will register a positive potential. However, when the action potential reaches the position of the electrode, the depolarized membrane acts like a current sink, and a negative deflection in the signal is observed. As the action potential propagates further, the membrane will repolarize and act again as a source, resulting in a second positive peak. When a recording electrode is placed in the neighborhood of the soma a biphasic extracellular potential is recorded (21).

An action potential at the soma will be reflected as a negative peak. The soma changes subsequently into a source as the action potential moves away to the axon, which leads to a positive peak. This biphasic response with initial negative peak is the general pattern for neurons in the CNS, however it has to be pointed out that in reality this shape is influenced by the conductance at the somatic and dendritic membrane, as well as the location of the electrode relative to the soma, cell excitability and morphology (21).

1.4.2 Electroencephalography

Neurons produce electrical field potentials, as a result of synaptic transmission, which can be measured using electroencephalography (EEG).

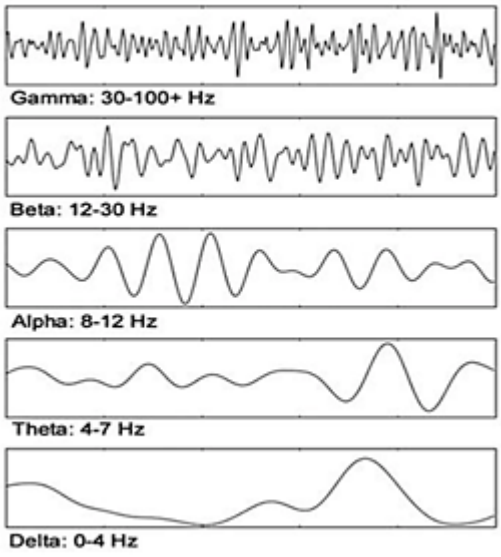

Figure 1.7 Comparison of EEG Bands. EEG is decomposed to functionally distinct EEG bands. With slow wave delta activity (0-4Hz) to theta (4-7Hz), alpha (8-12 Hz) and high frequency activity beta (12-30Hz) and gamma (>30Hz) bands. EEG trace over 1s. Figure with Creative Common License from Chatterjee et al.

The first recordings of EEG were performed by Hans Berger. He observed a rhythmic activity with a 10 Hz oscillation and called it alpha waves (8-13Hz). Other characteristic rhythms were discovered as depicted in Figure 1.7, named delta (<4Hz), theta (4-7Hz), beta (14-30 Hz) and gamma (>30Hz). This classification applies to humans, as it may differ between species (23) (24). Rodent theta rhythms are overall faster (6-10Hz) and more continuous when compared to humans (25). In the awake state, EEG is predominated by beta and gamma waves, theta activity is associated with quiet wakefulness and focused attention. During sleep, EEG slows down and becomes more synchronized showing mostly delta rhythms. During REM sleep, the stage before waking, EEG desynchronizes and shows decreased delta and increased theta activity (26).

The electrical activity or potential differences can be recorded intracranially or through the scalp as mostly performed in the clinic. In contrast to unit recording, where single cell activity is recorded, EEG represents a combination of *current sources* and *current sinks.* Furthermore EEG is a summation of EPSP and IPSP (action potentials contribute to a lesser extent) in the dendrites of the cortical neurons oriented in a perpendicular manner relative to the scalp surface (5).

Source localization of the neurons producing the field potential is hard as neuronal tissue has low resistivity to electrical current flow and there is distortion and attenuation caused by the presence of glial cells, blood vessels, pia and dura mater, the skull, and muscles on the scalp and skin (24, 27). A second disadvantage of scalp EEG is the lack of contribution of activity of deeper structures to the signal. This problem can be resolved using intracranial EEG, performed both in preclinical and clinical settings. In contrast to scalp EEG, where disc electrodes are glued to the skull, depth electrodes are implanted in regions of interest using stereotaxy. These electrodes are made of stainless steel or platinum. The advantage of intracranial recordings is the gain in signal amplitude and signal to noise ratio. These higher quality signals allow more precise source localization, stating the use of this technique in the presurgical evaluation of refractory epilepsy patients (5, 28).

1.4.3 Evoked potentials

Evoked electrical field potentials (EPs) are electrophysiological responses extracellularly recorded in a region of interest in response to a specific stimulus. When an auditory stimulus is presented, this will evoke a response in the auditory cortex, as this stimulus is relevant for the target region. Instead of presenting an extracranial stimulus, electrical stimulation can be applied to afferent nerve fibers to record the evoked response in its projection area. Stimulation of an afferent pathway that synapses with postsynaptic neurons leads to the formation of a field EPSP, which can be recorded near the soma. The response of multiple neurons is recorded when such a bundle of afferents is electrically stimulated (29, 30).

In preclinical research, EPs are often used to unravel the responsiveness of neural circuits, mostly in the hippocampus due to its laminar and neuronal organization. Electrically evoked potentials in the hippocampus include responses measured in the CA1 after Schaffer Collateral stimulation and dentate gyrus EPs after stimulation of the perforant path. Stimulation of the perforant path induces an axonal fiber volley that moves towards the synapse and interacts with the dendrites of the granular cells in the dentate gyrus.

Because the presynaptic fiber volley has a small amplitude, this is not detected with the extracellular recording electrode. The subsequent EPSPs in the postsynaptic dendrites or the population (field) EPSP is recorded. The slope of the field EPSP (fEPSP) is a measure for synaptic transmission, as it is the result of action potentials generated in the stimulation area. When the summation of EPSPs in the postsynaptic neuron is large enough to cross the membrane threshold, inducing a synchronous generation of action potentials, these potentials are referred to as the population spike (PS) (Fig.1.8). To recapitulate: the fEPSP reflects the monosynaptic excitatory synaptic transmission or input, whereas the population spike is the answer and output of the postsynaptic neurons to this input. The relation between the output/input (PS/fEPSP) is a measure for intrinsic excitability and is commonly used in preclinical research (31) (32).

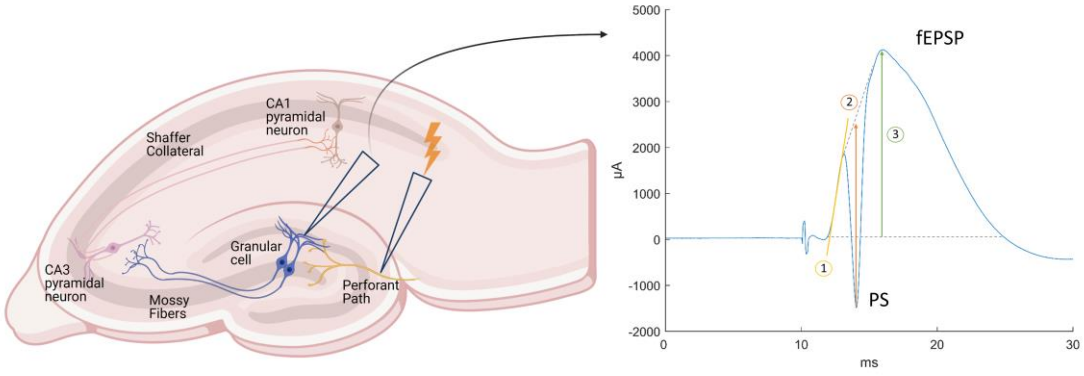

Figure 1.8 Schematic representation of an evoked potential in the dentate gyrus (DG). An electrical pulse is delivered to the perforant path, resulting in a response measured at the granular cells of the DG as depicted. The typical parameters are shown of which 1) fEPSP slope; 2) PS amplitude and 3) fEPSP amplitude. Figure made in Biorender.

1.5 Epilepsy

Epilepsy is the second most common neurological disorder with a prevalence of 0.5-1%, affecting 50 million people worldwide. It is characterized by the occurrence of spontaneous and recurrent epileptic seizures which are the result of an imbalance in excitation and inhibition in the brain causing synchronous and abnormal firing of neurons mostly located in the cortex (33). Epileptic seizures alter the state of the patient in a transient way and present itself as motor, sensory, psychic, or autonomic symptoms. The diagnosis of epilepsy is made when a patients' situation complies to one or more of the criteria set by the International League Against Epilepsy (ILAE): 1) the patient had ≥ 2 unprovoked seizures (24h apart); 2) the patient has had one seizure and a probability of other seizures of minimum 60% (similar to the general recurrence risk after two seizures); the patient is diagnosed with an epilepsy syndrome (34).

1.5.1 Seizure types and etiology

In 2017, the ILAE made a new user friendly classification system for clinicians with a wide variation in resources, allowing different levels of classification depending on the clinical setting available. In the ideal setting a classification should be made at all three levels: seizure type, epilepsy type and epilepsy syndrome, including etiology at each level. A first level of epilepsy classification starts from the seizure type. Here, it is assumed that the clinician was already able to diagnose the seizure as epileptic and distinguished it from non-epileptic events such as syncope, movement disorder, or parasomnias. There are three seizure types: generalized onset, focal onset, and unknown onset seizures. Generalized seizures are characterized by generalized spike-wave activity on EEG with absence, (a)tonic, myoclonic, or tonic-clonic seizures. Focal seizures are restricted to one hemisphere and can be uni- or multifocal. Epilepsy types form the second level of the classification system: generalized epilepsy, focal epilepsy, new category combined generalized and focal epilepsy, and unknown category. The last level includes epilepsy syndrome diagnosis. This refers to a combination of features from seizure types to imaging and EEG characteristics, age-dependent features, and comorbidities (35).

Epilepsy is a multifactorial disease and can originate from structural, genetic, infectious, immune, metabolic, and unknown causes. Structural etiology is diagnosed when structural abnormalities are present during neuroimaging and can be correlated to the electroclinical findings. Patients with genetic epilepsy have a mutation in (un)known genes and seizures as a major symptom of the syndrome. Genetic disorders can lead to metabolic dysfunction associated with epilepsy. In this case, epilepsy is categorized in the metabolic etiology. Infectious etiology is the most common worldwide.

Often patients undergo an infection such as meningitis or encephalitis which leads to seizures. Presence of an auto-immune-mediated central nervous inflammation can lead to seizures and immune epilepsy. When the cause of epilepsy cannot be found in the previously described etiologies (unknown etiology), a specific diagnosis is impossible and is restricted to the basic electroclinical semiology (35). A combination of causes can occur, since the etiologies are not mutually exclusive. It is however important to determine as much etiologies as possible, since it may change the treatment plan. A patient with tuberous sclerosis has both a structural and genetic etiology, where the first etiology is critical to know for epilepsy surgery, the latter can be important to search for more targeted therapies and genetic counselling (35, 36). The prevalence of the different etiologies depends on the timing and place. The type of etiology is not necessarily one-on-one correlated to the seizure or epilepsy type.

In the next paragraph, temporal lobe epilepsy will be discussed in more detail, since it is the most common form of focal epilepsy, with typical hippocampal lesions. Since a large part of patients are refractory, more fundamental research on new treatment possibilities, such as modulating the locus coeruleus, is necessary.

1.5.2 Temporal lobe epilepsy

Temporal lobe epilepsy (TLE) belongs to focal epilepsies of which mesial temporal lobe epilepsy (MTLE) is the most common form characterized by seizure generation in the mesial temporal lobe (hippocampus/amygdala). MTLE can be divided into two subgroups depending on histopathological characteristics: hippocampal sclerosis and paradoxical temporal lobe epilepsy (37). In the majority of patients MTLE is initiated by a traumatic event (febrile seizures, status epilepticus, head trauma) followed by a latency period of 5-10 years in which no symptoms are present but MTLE is developed resulting in the occurrence of spontaneous seizures (38, 39). Focal seizures with or without changes in consciousness, but also generalized seizures are associated with MTLE and are often accompanied by auras, automatisms, motor symptoms and amnesia. Initially, seizures are mostly controlled by anti-epileptic drugs, however when the disease progresses many patients (30%) become untreatable, referred to as refractory (38). Refractory patients can be treated with a ketogenic diet or more invasively respective neurosurgery (38, 40). However, for patients in whom resection is not feasible, neurostimulation techniques can be considered such as deep brain stimulation (DBS) or vagus nerve stimulation (VNS) as explained below (41).

1.6 Vagus nerve stimulation (VNS)

1.6.1 Functional anatomy

Vagus nerve stimulation (VNS) consists of stimulating the vagus nerve (10th cranial nerve) using a helical electrode wrapped around it and connected to a pulse generator implanted subcutaneously in the left upper chest region (Fig 1.9) (42).

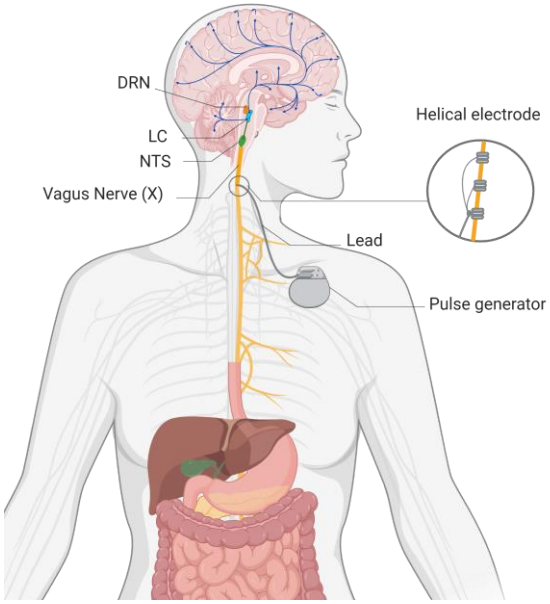

Figure 1.9 Schematic representation of vagus nerve and vagus nerve stimulation device. A subclavicular pulse generator is connected with a helical electrode wind around the vagus nerve (yellow). The vagus nerve sends projections through the nucleus tractus solitarius (NTS, green) to the locus coeruleus (LC, blue), which has widespread projections (dark blue) and the raphe nucleus (DRN, dorsal part, orange). Descending vagus nerve fibers innervate the thoracic and abdominal organs. Figure created with Biorender.com

The vagus nerve originates in the medulla and wanders throughout the body innervating thoracic and abdominal organs controlling a variety of systems such as the autonomic, cardiovascular, respiratory, gastrointestinal, and endocrine systems (43). The vagus nerve consists of different types of afferent (80%) and efferent (20%) nerve fibers, classified as A, B and C fibers based on their diameter and conduction velocity, providing both sensory and motoric innervation (44).

The efferent fibers originate in the nucleus ambiguus and dorsal motor nucleus of the vagus (DMV). Efferents of the nucleus ambiguus provide motoric innervation of the somatic muscles responsible for swallowing and phonation (the pharynx, larynx, soft palate and upper esophagus) and control heart rate (inhibitory projection to the sinoatrial node resulting in lower heart rates). The efferents originating from the DMV are also involved in cardiac control, but less pronounced. The main responsibility is parasympathetic autonomic innervation of the thorax and abdomen, controlling the gastrointestinal systems (6, 45). The nucleus tractus solitarius (NTS) receives most of the afferent fibers. This nucleus sends monosynaptic projections towards different brain regions, of which the parabrachial complex receives the most. The NTS also affects monoaminergic nuclei in a direct and/or indirect manner: the locus coeruleus (LC), the main noradrenergic input in the brain, as well as the raphe nucleus (RN) which has a serotonergic influence (46). The NTS projections to the raphe nucleus are more complex than to the LC because of its more distributed appearance.

The NTS projects via two disynaptic pathways to the LC: an excitatory pathway that synapses in the nucleus paragigantocellularis and an inhibitory pathway forming a synapse at the nucleus prepositus hypoglossi and acting mainly on $GABA_A$ receptors in LC. VNS can affect the LC in an excitatory, inhibitory or neutral manner (47). However, a preclinical study in rats found that VNS leads to an increase in LC firing first and secondly affects RN firing, indicating that VNS facilitates the excitatory pathway and indirectly modulates the RN through LC activation (48). These two brainstem nuclei are known for their anticonvulsant properties and are relevant to the mechanism of action (MOA) of VNS (46, 49). Next to influencing noradrenergic and serotonergic systems, it has been hypothesized that VNS modulates the cholinergic system by secondary activation of the nucleus basalis through LC activation (50) and induce plasticity as described in tinnitus and post-stroke rehabilitation studies by Kilgard et al (51, 52).

1.6.2 The mechanism of action underlying therapeutic effects

This neurostimulation technique is used in clinical setting for refractory epilepsy and depression (53, 54). Clinical research is being performed to identify the therapeutic use of VNS in other mood and cognitive disorders such as anxiety and Alzheimer's disease, and autoimmune diseases such as rheumatoid arthritis (53, 55). Efficacy studies in different centers have demonstrated a mean seizure frequency reduction between 25 and 55% with a large inter-patient variability in efficacy (56, 57). The precise MOA is still unknown and needs to be elucidated. However, there is evidence that the locus coeruleus plays an important role in the therapeutic effects of VNS. Both the anatomical pathway of the vagus nerve to the LC as preclinical animal studies using extracellular unit recordings, microdialysis experiments and LC lesioning techniques give multiple arguments for the hypothesis that VNS induces its effects through modulation of LC activity. Groves et al. was the first to prove that VNS induces an increased LC firing[1] in anesthetized rats (58), supporting the hypothesis that the LC is responsible for the observed VNS-induced noradrenaline (NA) increase in the amygdala (59). Subsequent single unit recording studies in anesthetized rats observed increases of the firing pattern of noradrenergic LC neurons in response to short and long term VNS in a dose dependent manner. Dorr et al. showed a clear increase of the firing rate of LC after both short (1h) and long term (24h or 3days) VNS[2], whereas only long term stimulation affected the activity of the dorsal

[1] VNS (0.5 ms biphasic pulses, 20 Hz, 30-s duration, 0.3 mA) increased LC firing frequency 20-65% above baseline.

[2] 90 days of VNS (30 s on, 5 min off; continuous cycle; 20 Hz, pulse width of 500 µs, 0.25 mA) induced a >2-fold increase in firing frequency compared to control animals.

raphe nucleus (DRN) (49). VNS affects LC activation also in a time dependent manner, where 14 days of VNS increased the number of LC neurons displaying burst activity and the number of spikes per burst while 90 days of VNS led to an even higher increase in the length and number of spikes per burst (indicating an overall increase in the firing rate) (48). A more recent study showed increases in phasic LC firing correlated to the stimulation intensity and pulse width of short trains (0.5s) of VNS (60).

Another argument to state that LC is a key player in the MOA of VNS, is that increased levels of NA are observed in LC projection areas in response to VNS. Our group observed VNS-induced increases in NA in the hippocampus in a rat limbic seizure model. This NA increase is responsible for the anticonvulsant effect as proven by the absence of seizure suppression after blockage of adrenergic receptors (61). Similar increases in NA were observed both in the prefrontal cortex and hippocampus, where the increase was VNS intensity-dependent (62). Manta et al. who previously showed that long term VNS induces increases in the tonic firing pattern of the locus coeruleus, also observed increases in extracellular NA both in prefrontal cortex and hippocampus in response to two weeks of VNS following an approved anti-depressive stimulation paradigm (48, 61).

In addition, it has been shown both by our own group and others that administration of local anesthetics (lidocaine) or selective lesioning through administration of the neurotoxin N-(-2-chloroethyl)-N-ethyl-2-bromobenzylamine (DSP-4), inhibits the VNS-induced anti-seizure and mood stabilizing effects. Krahl et al. locally administered lidocaine or lesioned LC using DSP-4 and observed an absence of the anticonvulsant effects otherwise seen with VNS (63). The anti-depressant effect observed during VNS is also suppressed after DSP-4 administration, emphasizing the importance of LC in VNS mediated effects (64). Next to preclinical findings, a study in epilepsy patients showed a clear effect of VNS on the P300 event related potential sensitive to LC activation, making this a potential biomarker for VNS responders (65).

These preclinical and clinical findings indicate the potential role of the locus coeruleus in altering brain excitability and its importance in neurological and psychiatric diseases such as epilepsy and depression. As the aim of this thesis was to further unravel the role of LC in brain excitability and VNS-induced effects, in the next chapter the anatomy and physiology of the LC are discussed together with previously used electrical and chemical methods to modulate its activity and unravel its effects on hippocampal excitability.

Bibliography

1. Mancall EL, Brock DG. Gray's Clinical Neuroanatomy E-Book: Elsevier Health Sciences; 2011.

2. VanPutte CL, Regan JL, Russo AF. Seeley's essentials of anatomy & physiology: McGraw-Hill; 2013.

3. McCorry LK. Physiology of the autonomic nervous system. American journal of pharmaceutical education. 2007;71(4).

4. Hall JE, Hall ME. Guyton and Hall textbook of medical physiology e-Book: Elsevier Health Sciences; 2020.

5. Cooper R, Binnie CD, Billings R. Techniques in Clinical Neurophysiology: A Practical Manual: Elsevier Churchill Livingstone; 2005.

6. Hall JE, Hall ME. Textbook of Medical Physiology 2011.

7. Raghavan M, Fee D, Barkhaus PE. Generation and propagation of the action potential. Handb Clin Neurol. 2019;160:3-22.

8. Bennett MV. Gap junctions as electrical synapses. J Neurocytol. 1997;26(6):349-66.

9. Lodish H, Berk A, Kaiser C. Molecular cell biology: W.H. Freeman and Company; 2016.

10. Artal P. Handbook of Visual Optics, Two-Volume Set: CRC Press; 2017.

11. Wettschureck N, Offermanns S. Mammalian G proteins and their cell type specific functions. Physiol Rev. 2005;85(4):1159-204.

12. Azam S, Haque ME, Jakaria M, Jo SH, Kim IS, Choi DK. G-Protein-Coupled Receptors in CNS: A Potential Therapeutic Target for Intervention in Neurodegenerative Disorders and Associated Cognitive Deficits. Cells. 2020;9(2).

13. Rosenbaum DM, Rasmussen SGF, Kobilka BK. The structure and function of G-protein-coupled receptors. 2009. p. 356-63.

14. Roth BL. DREADDs for Neuroscientists. 2016. p. 683-94.

15. Calebiro D, Koszegi Z, Lanoiselee Y, Miljus T, O'Brien S. G protein-coupled receptor-G protein interactions: a single-molecule perspective. Physiol Rev. 2021;101(3):857-906.

16. Sladek CD, Song Z. Diverse roles of G-protein coupled receptors in the regulation of neurohypophyseal hormone secretion. J Neuroendocrinol. 2012;24(4):554-65.

17. Alexander GM, Rogan SC, Abbas AI, Armbruster BN, Pei Y, Allen JA, et al. Remote control of neuronal activity in transgenic mice expressing evolved G protein-coupled receptors. Neuron. 2009;63(1):27-39.

18. Valdeolmillos M, Moya F. Leading Process Dynamics During Neuronal Migration. Cellular Migration and Formation of Neuronal Connections: Elsevier; 2013. p. 245-60.

19. Andersen P, Morris R, Amaral D, Bliss T, O 'Keefe J. The Hippocampus Book: Oxford University Press; 2006. 852 p. Andersen P, Morris R, Amaral D, Bliss T, O 'Keefe J. The Hippocampus Book: Oxford University Press; 2006. p. 1-852

20. Ellenbroek B, Abizaid A, Amir S, de Zwaan M, Parylak S, Cottone P, et al. Extracellular Recording. In: Stolerman IP, editor. Encyclopedia of Psychopharmacology. Berlin, Heidelberg: Springer Berlin Heidelberg; 2010. p. 522-5.

21. Heinricher MM. Principles of Extracellular Single-Unit Recording Extracellular Recording: Neuronal Activity in a Functional Context. Journal of Clinical Endocrinology and Metabolism. 1995;80(8):2550-1.

22. Lalley PM. Intracellular Recording. In: Binder MD, Hirokawa N, Windhorst U, editors. Encyclopedia of Neuroscience. Berlin, Heidelberg: Springer Berlin Heidelberg; 2009. p. 2019-26.

23. Chatterjee R, Datta A, DK S. Ensemble Learning Approach to Motor Imagery EEG Signal Classification. Machine Learning in Bio-Signal Analysis and Diagnostic Imaging2019. p. 183-208.

24. Buzsaki G. Rhythms of the Brain: Oxford university press; 2006.

25. Maheshwari A. Rodent EEG: Expanding the Spectrum of Analysis. Epilepsy Curr. 2020;20(3):149-53.

26. Aston-Jones G, Gonzalez M, Doran S. Role of the locus coeruleus-norepinephrine system in arousal and circadian regulation of the sleep-wake cycle. Brain norepinephrine: Neurobiology and therapeutics. New York, NY, US: Cambridge University Press; 2007. p. 157-95.

27. Buzsáki G, Anastassiou CA, Koch C. The origin of extracellular fields and currents—EEG, ECoG, LFP and spikes. Nature reviews neuroscience. 2012;13(6):407-20.

28. Van Loo P, Carrette E, Meurs A, Goossens L, Van Roost D, Vonck K, et al. Surgical successes and failures of invasive video-EEG monitoring. 2011.

29. Eysenck MW, Keane MT. Cognitive psychology : a student's handbook: Psychology Press; 2000. p.1-631.

30. Holdefer RN, MacDonald DB, Skinner SA. Somatosensory and motor evoked potentials as biomarkers for post-operative neurological status. 2015.

31. McNaughton BL, Barnes CA. Physiological identification and analysis of dentate granule cell responses to stimulation of the medial and lateral perforant pathways in the rat. J Comp Neurol. 1977;175(4):439-54.

32. Larsen LE, Wadman WJ, van Mierlo P, Delbeke J, Grimonprez A, Van Nieuwenhuyse B, et al. Modulation of Hippocampal Activity by Vagus Nerve Stimulation in Freely Moving Rats. Brain Stimul. 2016;9(1):124-32.

33. Seino M. Classification criteria of epileptic seizures and syndromes. 2006.

34. Fisher RS, Acevedo C, Arzimanoglou A, Bogacz A, Cross JH, Elger CE, et al. ILAE official report: a practical clinical definition of epilepsy. Epilepsia. 2014;55(4):475-82.

35. Scheffer IE, Berkovic S, Capovilla G, Connolly MB, French J, Guilhoto L, et al. ILAE classification of the epilepsies: Position paper of the ILAE Commission for Classification and Terminology. Epilepsia. 2017;58(4):512-21.

36. Balestrini S, Arzimanoglou A, Blumcke I, Scheffer IE, Wiebe S, Zelano J, et al. The aetiologies of epilepsy. Epileptic Disord. 2021;23(1):1-16.

37. Sharma AK, Reams RY, Jordan WH, Miller MA, Thacker HL, Snyder PW. Mesial temporal lobe epilepsy: pathogenesis, induced rodent models and lesions. Toxicol Pathol. 2007;35(7):984-99.

38. O'Dell CM, Das A, Wallace Gt, Ray SK, Banik NL. Understanding the basic mechanisms underlying seizures in mesial temporal lobe epilepsy and possible therapeutic targets: a review. J Neurosci Res. 2012;90(5):913-24.

39. Tatum WOt. Mesial temporal lobe epilepsy. J Clin Neurophysiol. 2012;29(5):356-65.

40. Mihara T, Usui N, Matsuda K, Tottori T, Kondo A, Terada K, et al. A classification system for verifying the long-term efficacy of resective surgery for drug-resistant seizures. Epilepsy Res. 2018;141:23-30.

41. Gooneratne IK, Green AL, Dugan P, Sen A, Franzini A, Aziz T, et al. Comparing neurostimulation technologies in refractory focal-onset epilepsy. J Neurol Neurosurg Psychiatry. 2016;87(11):1174-82.

42. Howland RH. Vagus Nerve Stimulation. Curr Behav Neurosci Rep. 2014;1(2):64-73.

43. Berthoud HR, Neuhuber WL. Functional and chemical anatomy of the afferent vagal system. Autonomic Neuroscience, 2000, 85.1-3: 1-17.

44. Ruffoli R, Giorgi FS, Pizzanelli C, Murri L, Paparelli A, Fornai F. The chemical neuroanatomy of vagus nerve stimulation. 2011. p. 288-96.

45. Baker E, Lui F. Neuroanatomy, Vagal Nerve Nuclei. 2021.

46. Krahl SE. Vagus nerve stimulation for epilepsy: A review of the peripheral mechanisms. Surg Neurol Int. 2012;3(Suppl 1):S47-52.

47. Henry TR. Therapeutic mechanisms of vagus nerve stimulation. Neurology. 2002;59(6 Suppl 4):S3-14.

48. Manta S, Dong J, Debonnel G, Blier P. Enhancement of the function of rat serotonin and norepinephrine neurons by sustained vagus nerve stimulation. J Psychiatry Neurosci. 2009;34(4):272-80.

49. Dorr AE, Debonnel G. Effect of vagus nerve stimulation on serotonergic and noradrenergic transmission. J Pharmacol Exp Ther. 2006;318(2):890-8.

50. Espana RA, Berridge CW. Organization of noradrenergic efferents to arousal-related basal forebrain structures. J Comp Neurol. 2006;496(5):668-83.

51. Tyler R, Cacace A, Stocking C, Tarver B, Engineer N, Martin J, et al. Vagus Nerve Stimulation Paired with Tones for the Treatment of Tinnitus: A Prospective Randomized Double-blind Controlled Pilot Study in Humans. Sci Rep. 2017;7(1):11960.

52. Khodaparast N, Kilgard MP, Casavant R, Ruiz A, Qureshi I, Ganzer PD, et al. Vagus Nerve Stimulation During Rehabilitative Training Improves Forelimb Recovery After Chronic Ischemic Stroke in Rats. Neurorehabil Neural Repair. 2016;30(7):676-84.

53. Vonck K, Raedt R, Naulaerts J, De Vogelaere F, Thiery E, Van Roost D, et al. Vagus nerve stimulation. . .25 years later! What do we know about the effects on cognition? 2014. p. 63-71.

54. Johnson RL, Wilson CG. A review of vagus nerve stimulation as a therapeutic intervention. J Inflamm Res. 2018;11:203-13.

55. Koopman FA, van Maanen MA, Vervoordeldonk MJ, Tak PP. Balancing the autonomic nervous system to reduce inflammation in rheumatoid arthritis. J Intern Med. 2017;282(1):64-75.

56. Vonck K, Boon P, Goossens L, Dedeurwaerdere S, Claeys P, Gossiaux F, et al. Neurostimulation for refractory epilepsy. Acta Neurol Belg. 2003;103(4):213-7.

57. De Herdt V, Boon P, Ceulemans B, Hauman H, Lagae L, Legros B, et al. Vagus nerve stimulation for refractory epilepsy: a Belgian multicenter study. Eur J Paediatr Neurol. 2007;11(5):261-9.

58. Groves DA, Bowman EM, Brown VJ. Recordings from the rat locus coeruleus during acute vagal nerve stimulation in the anaesthetised rat. Neurosci Lett. 2005;379(3):174-9.

59. Hassert DL, Miyashita T, Williams CL. The effects of peripheral vagal nerve stimulation at a memory-modulating intensity on norepinephrine output in the basolateral amygdala. Behav Neurosci. 2004;118(1):79-88.

60. Hulsey DR, Riley JR, Loerwald KW, Rennaker RL, 2nd, Kilgard MP, Hays SA. Parametric characterization of neural activity in the locus coeruleus in response to vagus nerve stimulation. Exp Neurol. 2017;289:21-30.

61. Raedt R, Clinckers R, Mollet L, Vonck K, El Tahry R, Wyckhuys T, et al. Increased hippocampal noradrenaline is a biomarker for efficacy of vagus nerve stimulation in a limbic seizure model. J Neurochem. 2011;117(3):461-9.

62. Roosevelt RW, Smith DC, Clough RW, Jensen RA, Browning RA. Increased extracellular concentrations of norepinephrine in cortex and hippocampus following vagus nerve stimulation in the rat. Brain Res. 2006;1119(1):124-32.

63. Krahl SE, Clark KB, Smith DC, Browning RA. Locus coeruleus lesions suppress the seizure-attenuating effects of vagus nerve stimulation. Epilepsia. 1998;39(7):709-14.

64. Grimonprez A, Raedt R, Portelli J, Dauwe I, Larsen LE, Bouckaert C, et al. The antidepressant-like effect of vagus nerve stimulation is mediated through the locus coeruleus. J Psychiatr Res. 2015;68:1-7.

65. De Taeye L, Vonck K, van Bochove M, Boon P, Van Roost D, Mollet L, et al. The P3 event-related potential is a biomarker for the efficacy of vagus nerve stimulation in patients with epilepsy. Neurotherapeutics. 2014;11(3):612-22.

Chapter 2 The Locus Coeruleus-Noradrenergic system

2.1 Neurochemistry of noradrenergic neuron

Noradrenaline (NA) is the primary neurotransmitter present in noradrenergic neurons. It is synthesized from the amino acid tyrosine by tyrosine hydroxylase forming L-dihydroxyphenylalanine (L-DOPA), which is further converted to dopamine by L-amino acid decarboxylase. Monoamine transporters will transport dopamine into synaptic vesicles where it is converted to noradrenaline by dopamine-β-hydroxylase (DBH) (Fig 2.1) (1, 2).

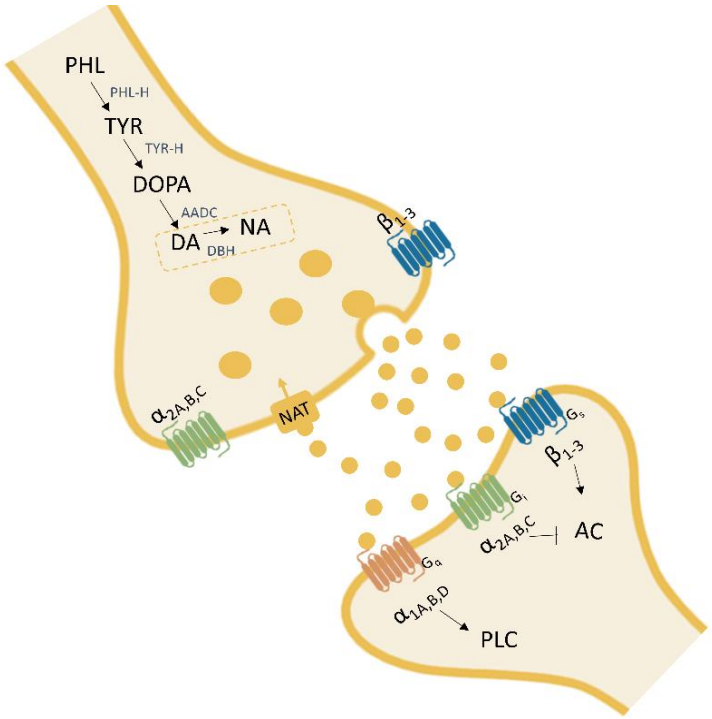

Figure 2.1 Schematic representation of noradrenergic neuron and its synaptic activity. Noradrenaline is synthesized starting from two amino acids phenylalanine and tyrosine and converted to dopamine. DA is transported into vesicles where the conversion to noradrenaline NA takes place (dashed lines). When an action potential is generated synaptic vesicles are transported to the presynaptic membrane and released in the synaptic cleft. Noradrenaline acts on different postsynaptic adrenergic receptors, inducing excitatory or inhibitory postsynaptic potentials depending on the activated secondary messenger cascade. NA also acts on adrenergic autoreceptors on the presynaptic neuron, or is back transported into the neuron for restorage in vesicles. AC: adenylyl cyclase; AADC: L-amino acid decarboxylase; DBH: dopamine β hydroxylase; DOPA: L-dihydroxyphenylalanine; NA: noradrenaline; NAT: noradrenaline transporter; PHL: phenylalanine; PHL-H: phenylalanine hydroxylase; PLC: phospholipase C; TYR: tyrosine; TYR-H: tyrosine hydroxylase.

Noradrenaline modulates the effect of postsynaptic cells through the presence of adrenergic receptors, which are G protein-coupled receptors. Three families can be distinguished, each with different subtypes: α_1-, α_2- and β-receptors. α_1-adrenergic receptors (α_{1A}, α_{1B}, α_{1D}) induce increased excitability due to activation of the Gq-pathway through activation of the PLC-IP3-DAG cascade, resulting in increased intracellular calcium concentrations and a decrease in the

potassium conductance. α_2-adrenergic receptors (α_{2A}, α_{2B}, α_{2C}), which are Gi-coupled receptors, have an opposite effect and have inhibitory effects resulting in decreased firing rate and neurotransmitter release (Fig 2.1). β-adrenergic receptors ($\beta_{1\text{-}3}$) are Gs-coupled receptors and stimulate the cAMP-PKA cascade promoting discharges (1). In the central nervous system all three types of adrenoreceptors are found postsynaptically. The α_2-adrenergic receptors are also present on the noradrenergic neuron itself as autoreceptors. Autoreceptors present on the cell body or dendrites (somatodendritic autoreceptors) inhibit neuronal firing (=impulse-modulating receptors) and are activated by noradrenaline released from the dendrites or recurrent nerve terminals. When located on the axon terminal (presynaptic receptors) they inhibit noradrenaline release (= release-modulating receptors). Next to the release-modulating autoreceptors, synaptic availability of noradrenaline is also regulated by noradrenaline reuptake via presynaptic noradrenaline transporters (NAT) and storage in synaptic vesicles (1, 3). Although LC neurons express multiple types of adrenoreceptors, a radioactive ligand binding study in rats showed that α_2-expressing LC neurons are mostly found in the posterior LC, whereas α_1-adrenergic receptors were more abundantly located in the anterior side (Fig.2.2 B) (2, 4).

Besides noradrenaline, LC neurons release co-transmitters such as adenosine triphosphate (ATP), encephalin, glutamate, neuropeptide Y (NPY) and galanin. The presence of these co-transmitters in LC neurons is linked to their location: galanin-containing neurons are mostly located in the central and dorsal part of LC, whereas NPY positive cells are only present in the ventral part (Fig 2.2 B) (3). Additionally, it has been long hypothesized, since LC neurons produce noradrenaline from dopamine, that dopamine itself is synthesized, stored and co-released with noradrenaline (5). Twenty years ago, a first argument confirmed this hypothesis, detecting cortical dopamine release after pharmacological LC stimulation (6-8). However, one can assume that this is due to indirect effects of LC activation on the ventral tegmental area or dopamine release from dopaminergic terminals through adrenergic receptor stimulation (5, 8). Recent studies using a more selective method, photoactivating LC terminals in the hippocampus, revealed enhanced dopamine and noradrenaline levels resulting in increased spatial memory and novelty associated consolidation, which was absent when noradrenaline was blocked (9-11). These findings indicate that the LC, next to being the noradrenergic center, is also responsible for co-releasing dopamine (5).

2.1.1 Activity of LC neurons

LC neurons have distinct electrophysiological characteristics both in anesthetized and awake animals characterized by broad action potentials, slow and spontaneous firing rates (0-5Hz), and typical phasic bursts followed by periods of inhibition in response to a noxious pinch. Stimulation of noradrenergic axons in the anterior cingulate cortex and olfactory bulb and consecutive recording of antidromic spikes at LC, have shown that LC neurons have conduction velocities ranging from 0.2-0.86m/s, typical for unmyelinated fibers. Additionally, Aston-jones et al. observed that prolonged trains of stimulation decreased the conduction velocity, with cessation of information transmission at long trains of 20Hz (12, 13).

LC neurons display two firing patterns: tonic and phasic, correlating to the state of arousal and attention (14). The presence of phasic activity is correlated to tonic LC activation, where phasic responses are less common and robust in periods of increased tonic activity. Phasic LC firing consists of 2-3 action potentials followed by a typical period of silence (300-700ms) and is induced by salient stimuli, resulting in increased cognitive performance by inducing reorientation to task-relevant cues (15). Tonic discharge modus is state-dependent where LC neurons display the highest firing frequency during active awake periods (>2 Hz), during quiet awake situations the frequency decreases under 2Hz, and even lower rates are observed during slow-wave sleep (1 Hz) to complete silence during Rapid Eye Movement (REM) sleep (12). In contrast to phasic firing where LC neurons synchronize their firing pattern via the presence of gap junctions referred to as electrotonic coupling (12), resulting in an efficient release of noradrenaline followed by a period of silence, tonic discharges lead to the robust release of noradrenaline throughout the brain (14) resulting in uncoupling, playing a “circuit breaker” role allowing reconfiguration of functional networks and disrupting currently ongoing neural activity (16). This is an evolutionary conserved response as it can change behavior in threatening situations and increase survival rate (17).

2.2 Functional anatomy

The locus coeruleus is a small nucleus located in the pontine brainstem and appears as a grey patch on the floor of the fourth ventricle and is known as the most important noradrenergic nucleus of the central nervous system. This nucleus was first identified by the group of Dahlström and Fuxe as the main source of noradrenaline in the brain (2, 3, 18). The LC is one of several noradrenergic nuclei and is composed of a small number of neurons densely packed together (respectively 1500 and 15000 cells per LC in rodents and humans).

The LC (A6) is the largest of 7 noradrenergic nuclei (A1-A7) in rodents. Most of these nuclei are also identified in primates and humans, confirming evolutionary consistency along the mammalian species (19). However, in primates A3 is absent and A4-A7 contains more noradrenergic neurons compared to rodents. These nuclei can be divided into three large groups: caudal, central and rostral. The rostral group is the most important in humans and consists of only one nucleus, the LC. Fiber projections can be divided in two groups arising from the caudal and central group and arising from the LC (or rostral group, A4 is sometimes considered to be part of the coeruleus complex). From the caudal and central nuclear groups (A1, A2, A5, A7) both ascending and descending fibers arise. The ascending fiber bundle or ventral noradrenergic bundle innervates the midbrain reticular formation, hypothalamus and a part of the limbic cortex. These structures are also receiving fibers from the LC. Descending fibers form two bulbospinal bundles projecting to the ventral and intermediate nuclear columns of the spinal cord. The LC itself gives rise to three pathways of fibers: the ascending (or dorsal noradrenergic bundle), the cerebellar, and the descending pathway. The ascending pathway consists of fibers innervating the limbic system (hippocampus, amygdala, and parahippocampal and cingulate gyri) midbrain, thalamus, and the entire neocortex. The descending pathway innervates motor nuclei in the lower brainstem and innervates all columns within the spinal cord (3).

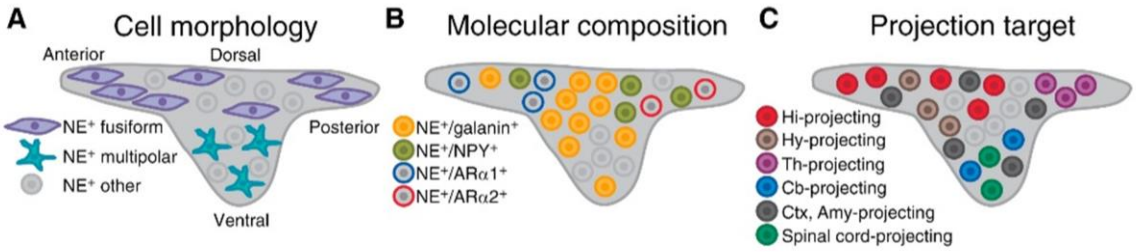

Figure 2.2 Organisation of the locus coeruleus based on cell morphology, molecular composition and anatomical projections. Schematic representation of sagittal view of rat LC. A) Different morphological cells of LC along the dorso-ventral axis, with fusiform cells densely located in dorsal LC, whereas large multipolar cells are mostly found in the central part of LC. B) All LC neurons release noradrenaline, some cells co-release other peptides, linked to their location within the nucleus. Some noradrenergic neurons also express different adrenergic receptors linked to their location. LC neurons containing α_2-receptors are located in the posterior LC, whereas α_1-expressing LC neurons are more found anterior. C) LC neurons projecting to discrete target structures can be found in strict locations along the dorso-ventral axis, with hippocampal projecting neurons mostly found in the dorsal LC. Figure adjusted from Schwarz et al. with permission from Elsevier License.

As depicted in Figure 2.2 A, two types of noradrenergic cells can be distinguished: large multipolar cells (35µm) and smaller fusiform cells (20µm) with a typical distribution over the dorso-ventral axis. Fusiform cells are more dominant in the dorsal part, where cells are more densely packed and aligned in a dorsolateral and ventromedial orientation.

The larger multipolar cells are predominantly located in the ventral LC (3, 20). These cells are characterized by immensely branched axons and varicosities at the terminal fibers giving a string of bead-like appearance. These varicosities are identified as the site of release with many of them making one-to-one contacts with adjacent cells. However, there are varicosities located in the interstitial space without synaptic contact, indicating a hormone-like action referred to as paracrine secretion (3). These fibers connect and modulate neurons, glial cells (astrocytes and oligodendrocytes) and blood vessels in almost the entire brain providing noradrenergic input from the spinal cord to the neocortex, except for the striatum and globus pallidus (1, 3, 12, 20). However, a recent study, exploring the effect of LC activation on functional connectivity networks, observed increased connectivity in the striatum (caudate-putamen) in reaction to chemogenetic LC activation. Staining against a noradrenaline transporter showed expression of noradrenergic axonal LC projections present in striatum confirmed by retrograde labeling using AAV2 injections (16). This result of sparse LC projections to the striatum is in line with an earlier study performing retrograde labeling using horseradish peroxidase by Mason et al. (21).

Apart from the subdivision based on morphological appearance, LC noradrenergic cells can be classified based on their anatomical projections (Fig 2.2C). Neurons located in the dorsal part of LC will mostly project to the hippocampus and septum, whereas ventral LC neurons are mostly projecting to the forebrain and cerebellum. This classification can also be made along the anterior-posterior axis: neurons projecting to the thalamus are located more posterior, whereas the hypothalamus receives projections from neurons located in the anterior LC. Neurons projecting to neocortex and amygdala are located throughout the LC (2).

2.2.1 Afferent and efferent projections of locus coeruleus

Most of the projections to the LC are reciprocal which means that structures that project to LC also receive noradrenergic fibers from this nucleus (indicated by the double arrow in Fig 2.3). The locus coeruleus is involved in different physiological regulatory neural networks such as the autonomic network, sleep-arousal network, pain network and fear and anxiety network (3). The main question is how this brainstem nucleus with widespread projections can affect one network without altering all the other functions. One argument is that the LC consists of subsets of LC neurons with spatially defined projection areas, allowing targeted neuromodulation, counteracting the long-believed hypothesis of a homogenous LC.

Different research groups along the years have shown that there is a correlation between the cell morphology, location within the nucleus (as described above) and the efferent projection area using techniques such as immunohistochemistry, labeled dyes, viral vectors and genetic mapping. Mason and Fibiger were one of the first to describe a difference in efferent topography using horseradish peroxidase injections in different areas along the neuroaxis demonstrating clear LC subdivisions with distinct morphological cells modulating specific target regions (22). Although this supported the hypothesis of a modular LC, Loughlin et al. demonstrated that there is a small portion of LC neurons that innervate multiple cortical areas, which argues for a widespread modulatory effect (23, 24). Recently, a new technology called Mapseq, transducing a neuronal population with a viral library of short RNAs, labeling each neuron with his own RNA code, made it possible to identify the projection pattern on a single-cell level. Mapseq studies supported both the modular organization and widespread arborization hypotheses, identifying LC neurons with a single target area as well as neurons with multiple projection regions (22). Next to projection specificity, the capability of desynchronizing population activity to synchronizing the firing of ensembles is necessary for modular neuromodulation. Totah et al. identified ensembles of LC neurons with distinct spike waveforms and discharge characteristics correlated to their cortical interaction (25, 26).

In mammals, the locus coeruleus projects to the cortex of both hemispheres being the sole source of noradrenaline. Although there is a high distribution of LC projections, a spatial specificity is observed. Chandler et al. used different fluorescent tracers injected in different areas of the prefrontal cortex (PFC) demonstrating that the major part of LC neurons project to a single target area being the medial prefrontal cortex (mPFC) compared to the orbitofrontal cortex (OFC) and the anterior cingulate cortex (ACC). Additionally, they proved that the LC exists of discrete neuron ensembles that innervate discrete cortical areas. These ensembles are characterized by distinct biochemical and electrophysiological properties with a significantly higher noradrenaline release measured in the PFC compared to motor cortex (27, 28). Next to differences in firing and projection distribution, the LC modulates distinct areas by global noradrenaline release affecting postsynaptic receptors with different functional responses distributed with regional differences (22).

It is assumed that the NA-input in the cortex is predominantly excitatory because of the high presence of α_1-adrenergic receptors (29, 30), however in the neocortex a substantial amount of α_2- adrenergic receptors are detected in a layer-specific distribution.

Both in human and in the rodent brain, α_2-adrenergic receptors are densely present in the external neocortical layers (layer I-III)(31). Despite the dense presence and high specific binding of α_2-adrenergic receptors, which are G_i coupled, stimulation in the neocortex leads to overall excitation. This is due to the presence and activation of α_2-adrenergic receptors on the membrane of interneurons, mediating disinhibition of pyramidal cells, ultimately increasing cortical excitability (32). Noradrenergic projections to the cortex are involved in the promotion of wakefulness as it has been found that LC activation results in increased signs of arousal on EEG (33). A study in rats observed that α_1-adrenergic receptor activation in the prefrontal cortex was accompanied by increased cognitive performance in the attentional set shifting task, linked to noradrenaline mediated increase in arousal (34). The LC receives input in a smaller extent from the frontal, parietal, insular, and temporal cortices with a dominant excitatory connection from the prefrontal cortex, which is involved in executive functions (as depicted in Figure 2.3 indicating a reciprocal connection with the cortex) (35). The cerebellum also receives mainly excitatory noradrenergic influence, important for motor performance (30).

Sleep-wakefulness is also regulated through LC connections with the basal forebrain (medial preoptic and septal area, substantia innominata) containing both cholinergic and GABAergic neurons, responsible for wakefulness and sleep respectively through cortical projections (36). LC activates cholinergic neurons through α_1- and β-adrenoreceptors present in the medial preoptic area and acts on α_2-adrenergic receptors present on GABA neurons, resulting in changes in arousal (37, 38). During wakefulness, LC is activated and on its turn activates cholinergic cortical projections. LC is silent during onset of sleep resulting in the absence of disinhibition of GABAergic neurons (36). The role of LC in sleep-wakefulness was confirmed by a study in a human patient, where electrical stimulation of LC resulted in a decrease in slow-wave sleep (30, 39). Next to sleep-wake state, LC is also involved in anxiety, fear, and memory formation and retrieval through connections to the limbic system, more specifically the amygdala and hippocampus. The amygdala, a structure responsible for fear and anxiety responses to threatening stimuli in the environment, has a reciprocal connection to the LC through corticotropin-releasing hormone (CRH) projections (40, 41). Noradrenaline affects amygdala through α_1-adrenergic receptors, increasing the state of anxiety, which in its turn increases LC activity (40). Noradrenergic amygdala activation is also involved in the formation and retrieval of emotional memories (42, 43). To a lesser extent LC-NA fibers act on α_2-adrenergic receptors regulating the autonomic responses to threat (40).

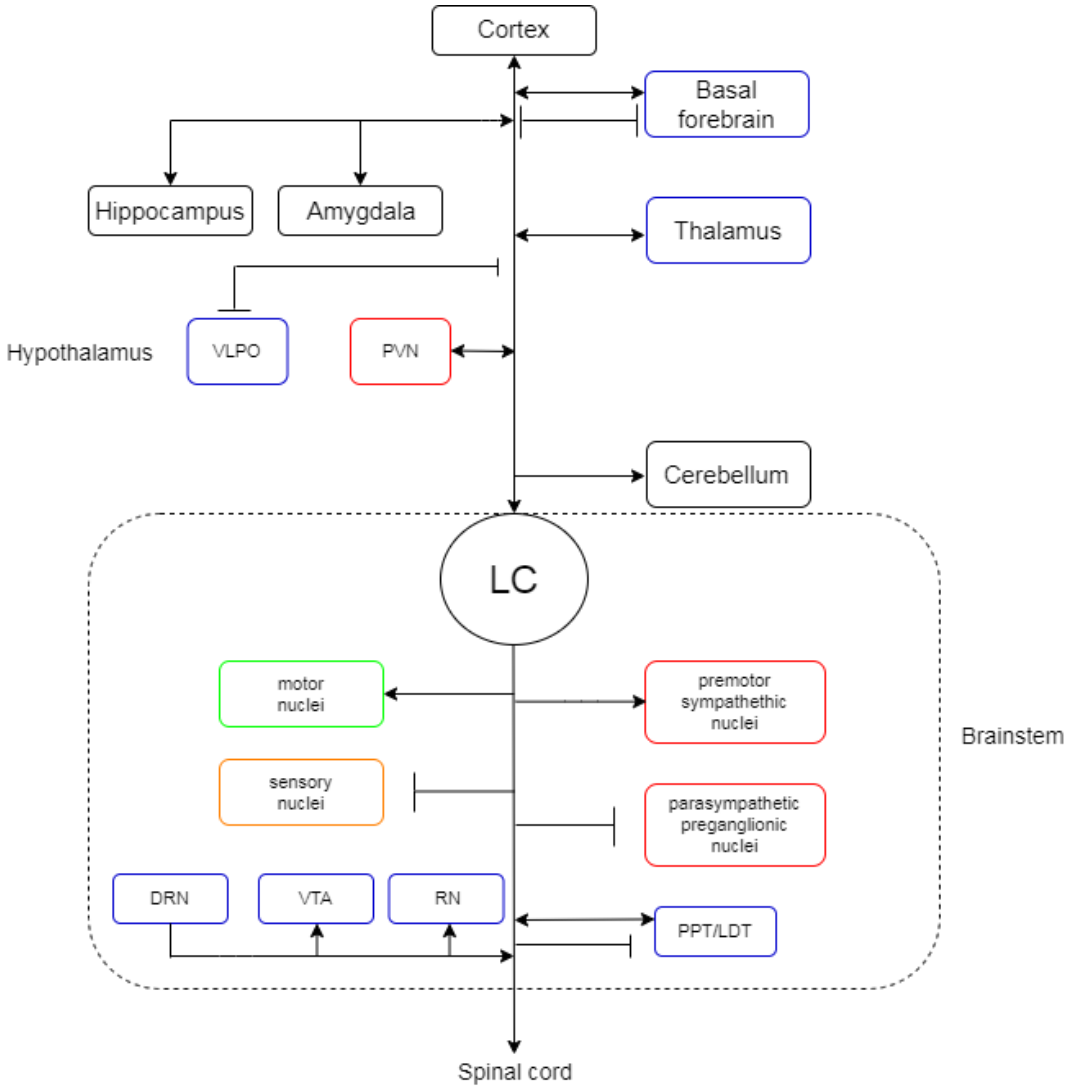

Figure 2.3 Afferents and efferents of the locus coeruleus. Arrows indicate projections, pointed arrow: excitatory projection; flat line: inhibitory projection. Colors indicate function: green: motoric; orange: sensory; blue: sleep-wake; red: autonomic; yellow: endocrine. The dotted line indicated all projections within the brainstem. DRN: Dorsal Raphe Nucleus; LH: Lateral Hypothalamus; PPT/LDT: pedunculopontine/laterodorsal tegmental nuclei; PVN: Paraventricular Nucleus; VLPO: Ventrolateral Preoptic area; VTA: Ventral Tegmental Area.

Because the ultimate aim of this thesis was to determine the effect of chemogenetic LC activation on hippocampal electrophysiology, the projections to the hippocampus are elaborated in more detail in the following section.

2.2.1.1 The hippocampus

Noradrenergic innervation of the hippocampal formation was first described by Blackstad et al. using a fluorescence histochemical method. They observed the presence of very fine NA varicosities mostly in regions rich in dendritic branches and poor in cell bodies, describing axodendritic contacts. In this first study in rats it was already clear that the hilus or subgranular zone of the dentate gyrus has the highest amount of noradrenergic innervations (44). Although immuncytochemical studies in human tissue observed high similarities in distribution of noradrenergic fibers in the hippocampus compared to rodents and monkeys (45), some species-specific adrenergic receptor distributions are observed, with a difference in presence of the adrenergic receptors on dendrites, soma or astrocytes. This indicates the possible variable effect of pharmacological agents (3). Preclinical studies using light microscopy or electron microscopy methodology have shown that there are laminar differences in the presence of both α- and β-adrenergic receptors, where β-adrenergic receptors are present in a uniform way in the dentate gyrus and CA regions, whereas the α_1-adrenergic receptor is more concentrated and corresponding to noradrenergic innervation in the DG (46). In rat labeling studies, subtypes of the α_1-receptor are highly present in both the granular cell layer of DG, as in the pyramidal cell layer of CA1-CA3. A study on human tissue showed a more layer specific presence, with α_{1D} receptors mainly present in the pyramidal cell layers and α_{1A} in the granular cell layer (46, 47). In general, in the rat hippocampus mostly β_1-receptors are observed, whereas in human labeling studies β_2-adrenergic receptors dominate (48). Within the rat DG, the majority of β-adrenergic receptors in the DG are β_1-receptors (present in all layers, most prominent in the molecular layer (49), β_2 is dominant in the granule cell layer) modulating the function of granule cells and parvalbumin expressing interneurons through their postsynaptic presence or indirectly via effects on glial processes. The LC axonal projections in the subgranular layer make contact with dendrites through (a)symmetric synapses or close associations without specializations (46). It is the dorsal LC, and more specifically the large and multipolar cells (23) that projects to the hippocampal formation in an ipsilateral manner (75-90%) via three pathways: the ventral amygdaloid bundle, the cingulum, and the fornix. The hippocampal CA-region receives LC axonal projections mostly via the ventral amygdaloid bundle, whereas the dentate gyrus receives the greatest innervation through the ipsilateral cingulum and equally from the contralateral cingulum, fornix and ventral amygdaloid bundle (50, 51). This NA innervation of the hippocampus seems age-dependent, based on preclinical studies in rodents.

A preclinical study based on electrophysiological and immunohistochemical results stated that a decrease in NA projections is observed with ageing in the dentate gyrus and frontal cortex. However, this is compensated by an increase in axonal branching in these regions. More specifically in the dentate gyrus, a layer specific change in the presence of axonal terminals is observed where a first decline appears in the polymorphic layer and in later stages of ageing this decrease is present in the molecular and granular layer (52). One can assume that an age-dependent change in noradrenergic projections to the hippocampus is also observed in human patients, since cell loss in LC is observed with ageing and in patients with neurodegenerative diseases predominantly in the dorsal hippocampal projecting neurons related to memory impairment (40, 53).

Next to noradrenaline release modulating hippocampal excitability (discussed in more detail in 2.3), recent preclinical studies have shown that LC neurons might also release dopamine in the hippocampal formation, responsible for memory consolidation and spatial learning (9, 10).

2.2.1.2 Diencephalon

As depicted in Fig 2.3, both the thalamus and nuclei of the hypothalamus send and receive projections from the LC, mostly related to sleep-wakefulness functions. The locus coeruleus projects predominantly to the dorsal nuclei of the thalamus promoting wakefulness through activation of α_1-adrenergic receptors inducing single spike firing mode and increasing cortical activity (29, 54). The GABAergic neurons of the ventrolateral preoptic area (VLPO), highly active during slow wave sleep and REM sleep, are inhibited by LC neurons through activation of α_2-adrenergic receptors during the awake state (55). During the awake state, LC thus inhibits the VLPO which in turn disinhibits the inhibitory projections to the tuberomammilary nucleus which has excitatory input to the cortex (56). Reciprocal projections with the lateral hypothalamus containing orexin neurons are also part of the sleep-wakefulness state, as the noradrenergic input inhibits firing, preventing excessive activity during arousal. This part of the hypothalamus has excitatory input to the LC, activating this nucleus and suppressing REM sleep and increasing wakefulness (57). This loop of noradrenaline and orexin is believed to play an important role in narcolepsy, characterized by an imbalance between sleep and wakefulness (56). LC projections to the paraventricular nucleus of the hypothalamus regulates the sympathetic and parasympathetic nervous system, where α_1-adrenergic receptor activation is related to stress responses (58) and α_2-adrenergic receptor activation inhibits GABAergic neurons synapsing with the paraventricular nucleus (PVN) modulating autonomic functions

such as the cardiovascular system (59). The PVN also modulates LC activity through corticotropin-releasing factor (CRF) fibers and forms an indirect pathway to the preganglionic neurons of the peripheral autonomic nervous system (56).

2.2.1.3 Brainstem

LC projects to a variety of brainstem nuclei (dashed box Figure 2.3): the parasympathetic preganglionic nuclei, premotor sympathetic nuclei, pedunculopontine and laterodorsal tegmental nuclei, and the raphe nuclei in the brainstem. Next to cortical and (hypo) thalamic LC projections involved in arousal and sleep-wake state, noradrenergic projections to the pedunculopontine and laterodorsal tegmental nuclei regulate sleep-wake transition. These cholinergic nuclei are active during awake state and REM sleep and project to the thalamus which desynchronizes cortical activity. They consist of two groups of neurons of which one is active during waking and are activated by LC via α_1- adrenergic receptors. The other group of neurons modulates REM sleep initiation and is inhibited by noradrenaline acting on α_2-adrenergic receptors. The pedunculopontine and laterodorsal tegmental nuclei reciprocally send excitatory projections to LC (fig.2.2) and facilitate NA output to the dorsal raphe nucleus and VLPO through activation of nicotinic receptors on noradrenaline terminals (3).

Projections to the parasympathetic preganglionic nuclei are predominantly inhibitory. LC activation attenuates the light reflex response through inhibition of the neurons present in the Edinger-Westphal nucleus via α_2-adrenergic receptor activation, resulting in the absence of light-induced pupil constriction (=pupil dilation). However, there is a species-specific difference in response of the pupil to α2-receptor agonists, since in humans, dogs and rabbits, where the presynaptic α2-receptor predominates, leading to inhibition of LC and consequent pupil constriction, whereas the opposite effect is observed in cats due to dominant postsynaptic effect (30, 40). LC also modulates autonomic functions such as salivatory control by inhibiting salivatory nuclei present in the brainstem. Projections to the dorsal motor nucleus of the vagus (DMV) and nucleus ambiguus (part of the parasympathetic vagal nuclei) are involved in controlling cardiovascular functions. The nucleus ambiguus is involved in heart rate control, responsible for reduction of heart rate in response to baroreceptor stimulation, mediated by an inhibitory connection to the rostroventral medulla. These nuclei have a high presence of α_2-adrenergic receptors, although α_1-adrenergic receptors have been detected in the latter one, which is paradoxal but might be explained by the presence of interneurons clarifying its inhibitory character. Cardiovascular function is also modulated through LC activation of premotor sympathetic nuclei.

The rostroventrolateral medulla (RVLM) projects to the spinal cord in an excitatory way and promotes vasoconstriction. Its activity is synchronized to cardiac activity where environmentally induced changes in blood pressure are sensed by baroreceptors and cardiovascular activity is reduced through the inhibitory projections of the nucleus tractus solitarius to the RVLM. Overall, LC activation leads to a moderate increase of blood pressure and heart rate through these different projections (56).

Next to efferent LC projections, the afferent projections from the dopaminergic ventral tegmental area have an excitatory effect on wakefulness promoting LC neurons, inhibiting sleep, maintaining arousal, and desynchronizing cortical EEG. The neurons of the periaqueductal grey are also involved in wakefulness and fight or flight response through projections to the LC. Reciprocal connections between the dorsal raphe nucleus and LC are also involved in sleep wake transition (as depicted in Fig 2.3) (3).

The caudal raphe nuclei (raphe magnus, pallidus, obscurus) are excited by LC and have sympathetic functions through connections with the spinal cord. Most connections are reciprocal, where LC activation increases the activity of both raphe magnus and pallidus, resulting in an increase of body temperature through its excitatory influence on the intermediolateral cell column of the spinal cord. LC activation also suppresses nociception during opioid analgesia through α_1-adrenergic receptor activation on the caudal raphe nuclei, increasing the firing rate, as proven by pharmacological α_1-adrenergic receptor blockage (60, 61).

Overall, the motor nuclei (green box Fig 2.3) are activated by noradrenaline release due to the presence of α1 adrenergic receptors, whereas the influence of LC on the trigeminal sensory nucleus is inhibitory and important for pain nociception (56).

2.3 Locus coeruleus-noradrenaline system and neurological disorders

Since the LC has widespread projections throughout the brain as discussed above and is important for various functions, pathological changes in LC can result in several neurological and psychiatric disorders (62). For a spectrum of attentional, cognitive, and affective disorders, pharmacologically targeting the noradrenergic system is clinically efficacious, sometimes independent of its etiological role in the disorder. The LC-NA system modulates attention and arousal suggesting it might have a role in the etiology or pharmacological treatment of attention deficit hyperactivity disorder (ADHD). This cognitive disorder characterized by impulsive behavior and inefficient control of attention is treated by alpha-methylphenethylamine (AMPH)-like stimulants of which the mechanism of action is not understood, but is believed to target the noradrenergic system leading to increased extracellular noradrenaline levels. Aston-Jones et al. has observed that increased tonic LC activity is associated with less robust phasic discharges leading to decrease in focused attention, a key symptom of ADHD emphasizing that a dysfunctional LC might be at the basis of this disorder (12). Disturbed LC discharge is suggested to be (partly) responsible for both insomnia and narcolepsy. The LC has major contributions in the sleep-wake cycle, where disturbed PFC and amygdala input can induce imbalanced noradrenaline levels resulting in sleep problems. Narcolepsy is typically characterized by sleepiness, episodes of cataplexy, and cognitive dysfunction. Preclinical and clinical observations have indicated that a reduction in hypocretin neurons, characterized by their wakefulness promoting action through projections to LC, disturb normal LC functioning and therefore induce the above described symptoms. Therefore, the LC-NA system seems to be part of the etiology and pharmacological target strategy.

Hyperreactivity of the LC-NA system is described for post-traumatic stress disorder and panic disorders, contributing not only to the observed panic and anxiety but also imbalanced arousal and attention (10).

Additionally, the LC-NA system is of great importance in the pathophysiology and pharmacological treatment of Major Depressive Disorder, because of its anatomical projections to the limbic system, important in regulation of emotion, cognition, pleasure, and pain. Several studies have shown changes in the presence of adrenergic receptors both in the LC and its frontal lobe projections, indicating a dysfunctional noradrenergic system. Animal studies have shown that increased noradrenaline transmission protects against stress-induced depressive behavior while depletion of NA in patients increases the chances of relapsing into a depressive state.

Therefore, the noradrenergic system is an important pharmacological target when treating patients with depression. NA reuptake inhibitors or NA selective tricyclic antidepressants which increase noradrenaline levels are most effective in treating all symptoms observed with Major Depression Disorder, from emotional distress to loss of appetite and pleasure and fatigue (63).

Clear alterations in LC anatomy and thus function are observed and hypothesized to contribute to major neurodegenerative disorders such as Parkinson's disease and Alzheimer's disease (40, 62, 64). Parkinson's disease (PD) is a progressive neurodegenerative disorder characterized by substantial loss of dopaminergic neurons in substantia nigra. The main symptoms are muscular rigidity, tremor, postural inability, hypokinesia, and bradykinesia. Although the degeneration of dopaminergic neurons is the main pathophysiological characteristic of PD, LC damage plays a substantial role in the manifestation and progression of the disease (65). In patients, loss of LC neurons is observed *post mortem* in a degree which is more severe compared to the neuronal loss in substantia nigra. It is described that this LC neuronal degradation is observed not only more extensively but also prior to the start of dopaminergic damage. Additionally, the remaining LC neurons show anatomical changes in shape of synaptic components, synaptic vesicles, and dendritic arborization. Intracellular changes in mitochondrial health in combination with inclusion of Lewy bodies are observed (40). It is described that the severity of dementia is correlated to the gradation of LC neuron loss (66). The LC projects to the dopaminergic neurons in substantia nigra in an excitatory manner through stimulation of densely expressed α_1-adrenergic receptors (40). Preclinical studies have shown that the LC has both a neuromodulatory role, exciting dopaminergic neurons important for maintaining the nigrostriatal pathway, and a neuroprotective role, since lesioning LC increased dopaminergic cell loss and decreased recovery of motor impairment symptoms in a monkey model for PD (40). It has been described that LC might possess a compensatory role in the early stages of PD, increasing its firing frequency releasing higher levels of NA fulfilling its protective role in maintaining DA functioning (67). LC modulation can have a therapeutic role, where α_2-receptor antagonists are suggested to increase LC activity and relieve some of the symptoms such as motor impairment and even enhance the effects of co-administered L-DOPA as observed in a primate model for PD (68). This form of therapy could also alleviate the depressive, anxiety, and sleep related symptoms (40).

The LC seems to play a similar role in Alzheimer's disease (AD). Pathological characteristics are the presence of β-amyloid plaques and tau containing neurofibrillary tangles combined with degeneration of cholinergic neurons mostly in the nucleus basalis. A variety of symptoms ranging from memory loss to depression and psychosis is observed in patients (64). Similar to PD, a significant cell loss is observed in LC, even more severe than observed in the nucleus basalis, with the remaining neurons showing anatomical changes. LC also plays a role in the development and progression of this neurodegenerative disease, as lesioning the LC in rat models increased the amount of amyloid plaques and memory deficits. Inclusion of neurofibrillary tangles are often first observed within LC neurons, together with increased levels of the monoamine oxidase, a metabolite of noradrenaline, acting as a neurotoxin, decreasing the cellular health (40, 69). Although in general, lower levels of NA are measured, an increase can be detected in the cerebrospinal fluid (70), indicating the compensatory increased activity of the remaining LC neurons, similarly observed in PD. The damage of LC affects the cholinergic transmission, which in its turn gives decreased input to LC exacerbating the decreased cellular health. LC lesions and cell loss have been linked to the cognitive impairment observed with AD, attentional deficits, and correlate to the severity of dementia, similarly to PD (64). Additionally, it has been described that the decrease in LC neurons, decreased NA levels and NA transporters play an important role in the proinflammatory character. Furthermore, decreased clearance of β amyloid plaques showing less microglia infiltration and phagocytosis is observed in the LC projection areas. This indicates the importance of selective LC modulation as a therapeutic target (1, 71).

Next to the common PD and AD pathophysiology, pathological changes and reduction in the number of LC neurons is observed in a plethora of other, less common neurological diseases such as Pick's disease, Down syndrome, Huntington's disease, and amyotrophic lateral sclerosis (ALS), for which often the α_2-antagonist idazoxan is administered to relieve some of the observed symptoms (62).

Since NA has anti-inflammatory effects, mostly through activation of β_2-adrenergic receptors suppressing inflammatory transcription factors (72), it has been demonstrated that the LC-NA system also plays a role in an autoimmune disease of the CNS, multiple sclerosis (MS). Characterized by the presence of white matter plaques and astrocytic gliosis, patients show a plethora of symptoms depending on the location of these pathological signs (73). Both in rodent models and patients, changes in NA levels have been observed, combined with LC damage in rodents (74).

Therapeutic administration of NA reuptake inhibitors and β_2-agonists reduced MS symptoms in animal models and reduced the TNF-α immune response, indicating the anti-inflammatory characteristic of NA and the role of LC within this disease pattern (75).

Epilepsy, one of the most common neurological disorders, is also influenced by the LC-NA system. The majority of studies describe that the LC and its NA release has a protective and anticonvulsant role due to its high affinity for α-adrenergic receptors (76). Although NA has lower affinity for β-adrenergic receptors, the effects are mixed regarding epileptic activity (76, 77). The effect of β-receptor activation in the healthy brain mainly has potentiating effects on hippocampal excitability (described in more detail in section 2.4) (78, 79). NA also plays a role in epileptogenesis.

Our own group has shown that the VNS induced anti-epileptic effects are mediated through increased LC activation and concurrent NA release (80), which resulted in the rationale of this thesis. Can selective LC activation induce anti-epileptic and seizure suppressing effects without confounding effects? However, it is still not clear how different levels of NA can act as anti- or even proconvulsant modulators. Changes in NA are observed in chronic and acute epileptic models. Decreases in NA are observed in genetically predisposed epilepsy models or post-kindling models, indicating its influence on seizure predisposition and kindling epileptogenesis (81, 82). However, it is known that acute epileptic seizures increase LC activity and NA levels in target areas important in epileptic networks as reported both by our own group and others (80, 83). One can hypothesize that the anti- or proconvulsant effect of noradrenaline is correlated to the concentration released in target sites. Possibly, moderate levels of NA will act through activation of α-adrenergic receptors and as an anticonvulsant suppressing excitability. Whether high concentrations, binding β-adrenergic receptors, antagonize the effects induced by α-receptor activation, is not clear (76). Therefore, fundamental experiments are necessary where the effect of selective modulation of LC is evaluated on hippocampal excitability.

2.4 Locus coeruleus-noradrenaline system and hippocampal excitability

Hippocampal excitability, or the responsiveness of principal neurons in the hippocampus to a given stimulus, can be measured to study the possible therapeutic effect of NA on seizures, since seizures are more likely to occur when a hyperexcitable state is present (84).

The effect of LC noradrenergic input in the hippocampus has been extensively studied over the past decades in both *in vitro* and *in vivo* models using different modulation techniques and adrenergic receptor agonists and antagonists (Table 2.1). As described in the paragraphs underneath, previous studies have shown that the firing pattern of LC, duration, location, dose of noradrenaline release, and layer and pathway-specificity play an important role in the effect on hippocampal excitability.

2.4.1 Noradrenaline administration

Neuman and Harley were the first to describe the effect of NA on hippocampal excitability. They observed potentiation of the population spike of the perforant path stimulation evoked potential in the dentate gyrus (DG) 1-8 min after iontophoretic application of NA in the granule cell body layer. In a subset (40%) of experiments, a long-lasting potentiation of the PS was observed. This effect was believed to be β-receptor dependent (85).

2.4.1.1 In vitro NA administration

Most *in vitro* studies applying exogenous NA induced (long-lasting) potentiation of PS of the DG EP with the duration of administration being a key factor, in combination with an overall increase of the EPSP slope (86, 87).

In general, application of a non-specific β-receptor agonist (isoproterenol), induced identical effects as NA: EPSP slope increase, decrease of the latency to spike occurrence and increase of the PS amplitude (as indicated in Table 2.1) (87, 88). These effects were absent when administering β-adrenergic receptor antagonists (timolol or propranolol) (87, 89). An α_1-adrenergic receptor agonist (phenylephrine, PE), failed to mimic the NA-induced effects on DG EPs, and even induced opposite effects at higher concentrations, whereas an α-adrenergic receptor antagonist (phentolamine, PA) could not block NA-induced potentiation of the PS. This supports the hypothesis of Neuman and Harley describing that the effect of NA on hippocampal excitability is mostly β-receptor dependent (85).

Similar effects are observed when recording Schaffer collateral evoked CA1 potentials. β-receptor mediated potentiation of the PS was described by Mueller et al. using bath-applied isoproterenol (77). Protein synthesis inhibitors block NA-induced potentiation of the CA1 EP, indicating the involvement of intracellular plasticity pathways (90).

2.4.1.2 In vivo NA administration

Stanton and Sarvey showed that long-lasting potentiation of the DG PS amplitude is indeed the result of β-receptor activation and subsequent activation of protein synthesis as described in vitro. Administration of protein synthesis inhibitors could differentiate an early and long term phase of NA induced potentiation (89). However, Winson and Dahl observed contrasting results, depending on the location of recording and duration of NA application. Whereas no short term effects of NA iontophoretic application were observed, a delayed long term potentiation after long term NA application was described by Dahl and Winson, in agreement with Neuman and Harley (91).

Chaulk et al. used intracerebroventricular NA application to mimic *in vitro* bath application in an *in vivo* setting, however, more dense innervations and continuous tonic input are present *in vivo,* whereas in the *in vitro* setting probably more receptor sites are reached due to the more targeted approach (92). A clear (long term) potentiation of the PS was observed in a NA dose dependent manner, without uniform effects on the EPSP. However, this potentiating effect was also observed after administration of isoproterenol (β-agonist) or phenylephrine (α-agonist) suggesting a possible role for both types of adrenergic receptors in the potentiating effect *in vivo*. The hypothesis is that binding of NA on α_1-receptors might potentiate the β-receptor effects by enhancing the cAMP cascade coupled to this receptor, however in hippocampal slices this synergistic effect is not fully determined lacking identification of the exact receptor site responsible for this phenomenon (92, 93).

2.4.2 Chemical LC modulation

The above-mentioned studies all applied NA to the hippocampus, but ideally, the physiological release of NA in the hippocampus via LC activation is studied. In general, chemical activation of LC induced potentiation of the PS, as depicted in table 2.1.

Glutamate injections, inducing phasic bursts of LC activity and NA release in the hippocampus, were administered in both anesthetized and awake animals, inducing clear PS potentiation and variable effects on the EPSP (94). Similar as described above, prior administration of propranolol, a non-selective β-receptor antagonist, blocked all potentiating effects, confirming the β-receptor dependent character of NA potentiation (94). Similar effects were observed in awake animals, with a clear potentiation of the population spike, with absence of consistent effects on the EPSP (95).

Systemic injection of idazoxan, an α_2 antagonist, to tonically increase LC firing rate (96) induced PS potentiation in a β-receptor dependent manner (timolol, a non-specific β-receptor antagonist attenuates these effects) (97).

A paired-pulse stimulation paradigm showed next to the increase in PS amplitude, an increase in paired pulse inhibition (feedback inhibition) independent of the response to the first pulse (98), which was later confirmed to be an actual decrease in paired pulse facilitation (97). This indicates that NA modulates hippocampal excitability not merely via its effect on principal cells but also by modulating interneurons as described by Brown et al, who observed that NA can alter the activity of both feedback and feedforward interneurons (97, 99). Because orexinergic projections are detected in the LC, orexin infusion was used to tonically activate LC. In contrast to glutamatergic activation, here gradual long-lasting potentiation of the population spike was observed (100).

2.4.3 Electrical stimulation of LC

The overall increase in the population spike amplitude and differing effects on EPSP are also observed in studies applying electrical stimulation to LC. Here, the timing of the LC stimulation and hippocampal stimulation is an essential factor.

LC activation 40-50ms prior to PP stimulation induced potentiation of the PS and differing or no effects on EPSP and PS latency (101). However, layer specific effects can be observed, similar to some iontophoretic studies (91), with decreases in the EPSP slope at the molecular layer (101). In contrast with previous studies, a β-receptor antagonist (propranolol) did not affect the potentiating effect of LC electrical stimulation, indicating possible contribution of NA-independent pathways, emphasizing the need for selective modulation (102). Electrical stimulation of the LC (1s burst, 100 Hz) paired with low frequency stimulation of Schaffer Collaterals, induced long term depression (LTD) in the CA1 in a N-methyl-D aspartate (NMDA) receptor dependent manner (103).

2.4.4 Optogenetic modulation of LC

Most studies show clear NA induced potentiation of the DG PS, however, some studies show contradictory results both on PS and EPSP in response to LC activation using electrical or chemical stimulation, possibly due to its small size and deep location likely inducing off-target effects. For this reason, opto- or chemogenetics, as used in this thesis, are more favorable since they allow cell-specific modification (see chapter 3). Quinlan and Harley examined the effect of optogenetic LC activation on dentate gyrus EPs, showing a clear potentiation of the population spike in response to single light pulses and delayed NA-induced LTP after 10 min of LC optoactivation (104). This slow onset of potentiation is similar to previously published studies using glutamate (79) or orexin (100).

Another similar finding was that the timing of optoactivation is critical in combination with the pairing of PP electrical stimulation. Light pulses delivered 40-50ms prior to PP stimulation induced PS potentiation, as described by Dahl and Winson using electrical LC activation (101).

These studies emphasize that LC activation and subsequent NA release is necessary to enable long term storage of information and plasticity by changing the excitability threshold of granular cells (103), as confirmed by the absence of potentiation when NA is depleted (105). This NA-induced plasticity is mostly β-receptor dependent, however, a β-receptor antagonist can only inhibit the induction of LTP, once potentiation is initiated, the response is resistant (106). Differences between *in vitro* and *in vivo* studies can be attributed to differences in circuitry as described above (92).

LC modulation can induce different forms of plasticity depending on the dose and duration of NA release (short versus long term potentiation) and timing in relation to concurrent activity present at the DG. The pairing of LC activation and PP stimulation is of importance in the *in vivo* setting to induce long lasting effects, whereas non-paired conditions only induce transient potentiation. Delaying PP stimulation also prevents LTP, possibly due to a lack of high NA levels (103, 107). However this need for pairing is not observed in vitro (87, 108), because of the long-lasting effects of bath applied NA on second messenger systems and endured enhancement of cAMP after NA clearance (107). Additionally, a pathway-specific manner of potentiation in the DG is present where medial perforant path stimulation in combination with NA induces LTP and lateral path stimulation results in the opposite effect (Long Term Depression, LTD) as recorded in hippocampal slices (108).

Additionally, the typical presence of potentiation of PS and the absence of increased EPSP slope are defined as increase in EPSP slope/spike coupling stating that NA increases the response of the granular cells to a given synaptic input, likely due to a lowered K^+ conductance (87, 97, 102).

2.4.5 Effect of LC modulation on EEG

Next to noradrenergic modulation of evoked potentials recorded in the hippocampal formation, the EEG is affected by NA changes. For decades it has been known that the LC-NA system can affect stimuli-induced responses because of its widespread projections throughout the cortex and hippocampus. It has been shown that reducing LC activity using α_2 agonists mediating autoreceptors on the soma of LC neurons, has sedative effects through disinhibition of the VPLO (cfr section 2.2.1) (40). On the other hand, LC activation occurring when presented with arousing stimuli, or by infusion of NA in forebrain sites in experimental settings, increases behavioral activity, arousal, and exploration (109, 110). These findings, together with the observation of LC-NA influencing sleep-wake transition and circadian rhythm shows the correlation of LC activity and EEG activity (38, 111). Studies have been performed under anesthesia where LC is inactivated using local infusions of clonidine, which inhibits LC neuronal firing due to activation of α_2-adrenergic autoreceptor activation. Whereas unilateral LC inactivation had no effect, bilateral silencing induced changes in both neocortical and hippocampal EEG. A shift from low amplitude and high frequency EEG to large amplitude slow wave EEG was observed in the cortex, and the theta dominated EEG typical for the hippocampus was changed to a more mixed frequency EEG (33). The same group of Berridge et al. investigated LC activation as well, by infusing betachenol into the vicinity of LC. There a clear increase in theta frequency was observed in the hippocampal EEG (112). Both findings support the hypothesis and findings of LC-NA modulation of behavioral state.

Table 2.1 Overview of the different types of LC modulation on hippocampal excitability recorded in dentate gyrus or CA1. EPSP: excitatory post synaptic potential; ISO: isoproterenol; LTD: long term depression; LTP: long term potentiation; PA: phentolamine; PE: phenylephrine, PROP: propranolol; PS: population spike.

	Dentate gyrus	**CA1**
NA administration	PS ↗ EPSP↗ (87, 88, 113) PS ↗ (85) LTP (85, 91)	PS ↗ (77) PS ↘ (77)
NA depletion	LTP↘ (113)	
α-receptor agonist	PE: PS↘ EPSP↘ (87) PS↗ EPSP↗ (91) PS↗ (92)	Clonidine: PS (77)
α-receptor antagonist	PA: LTP↘ (92)	
β-receptor agonist	ISO: PS↗ EPSP↗ (87, 88, 92) LTP (114) LTD (91, 114)	ISO: PS↗ (77)
β-receptor antagonist	Timolol: LTP↘ (87, 94, 97, 100) PROP: LTP↘ (79) (94) Metoprolol: LTP↘ (92)	
Electrical modulation	PS ↗ (101, 102, 107) EPSP (101) LTD↘ (115)	LTD (103)
Chemical modulation	Glutamate: PS ↗ (79, 94, 95, 100, 116) Orexin: PS ↗ (100)	Glutamate: PS ↗ (117)
Optogenetic modulation	PS ↗ (104)	

Bibliography

1. Benarroch EE. The locus ceruleus norepinephrine system: functional organization and potential clinical significance. Neurology. 2009;73(20):1699-704.

2. Schwarz LA, Luo L. Organization of the locus coeruleus-norepinephrine system. 2015. p. R1051-R6.

3. Szabadi E. Functional neuroanatomy of the central noradrenergic system. J Psychopharmacol. 2013;27(8):659-93.

4. Chamba G, Weissmann D, Rousset C, Renaud B, Pujol JF. Distribution of alpha-1 and alpha-2 binding sites in the rat locus coeruleus. Brain Res Bull. 1991;26(2):185-93.

5. Ranjbar-Slamloo Y, Fazlali Z. Dopamine and Noradrenaline in the Brain; Overlapping or Dissociate Functions? Front Mol Neurosci. 2019;12:334.

6. Devoto P, Flore G, Brodie BB. On the Origin of Cortical Dopamine: Is it a Co-Transmitter in Noradrenergic Neurons? Current Neuropharmacology. 2006;4:115-25.

7. Devoto P, Flore G, Saba P, Fa M, Gessa GL. Stimulation of the locus coeruleus elicits noradrenaline and dopamine release in the medial prefrontal and parietal cortex. J Neurochem. 2005;92(2):368-74.

8. Kawahara H, Kawahara Y, Westerink BH. The noradrenaline-dopamine interaction in the rat medial prefrontal cortex studied by multi-probe microdialysis. Eur J Pharmacol. 2001;418(3):177-86.

9. Kempadoo KA, Mosharov EV, Choi SJ, Sulzer D, Kandel ER. Dopamine release from the locus coeruleus to the dorsal hippocampus promotes spatial learning and memory. Proc Natl Acad Sci U S A. 2016;113(51):14835-40.

10. Takeuchi T, Duszkiewicz AJ, Sonneborn A, Spooner PA, Yamasaki M, Watanabe M, et al. Locus coeruleus and dopaminergic consolidation of everyday memory. Nature. 2016;537(7620):357-62.

11. McNamara CG, Dupret D. Two sources of dopamine for the hippocampus. Trends Neurosci. 2017;40(7):383-4.

12. Berridge CW, Waterhouse BD. The locus coeruleus-noradrenergic system: Modulation of behavioral state and state-dependent cognitive processes. 2003. p. 33-84.

13. Aston-Jones G, Segal M, Bloom FE. Brain aminergic axons exhibit marked variability in conduction velocity. Brain Res. 1980;195(1):215-22.

14. Ramos BP, Arnsten AFT. Adrenergic pharmacology and cognition: Focus on the prefrontal cortex. 2007.

15. Aston-Jones G, Cohen JD. An integrative theory of locus coeruleus-norepinephrine function: adaptive gain and optimal performance. Annu Rev Neurosci. 2005;28(1):403-50.

16. Zerbi V, Floriou-Servou A, Markicevic M, Vermeiren Y, Sturman O, Privitera M, et al. Rapid Reconfiguration of the Functional Connectome after Chemogenetic Locus Coeruleus Activation. Neuron. 2019;103(4):702-18 e5.

17. Roeder T. Tyramine and octopamine: ruling behavior and metabolism. Annu Rev Entomol. 2005;50:447-77.

18. Schwarz LA, Miyamichi K, Gao XJ, Beier KT, Weissbourd B, DeLoach KE, et al. Viral-genetic tracing of the input-output organization of a central noradrenaline circuit. Nature. 2015;524(7563):88-92.

19. Foote SL, Bloom FE, Aston-Jones G, Vining A. Nucleus Locus Ceruleus: New Evidence of Anatomical and Physiological Specificity. Physiological reviews, 1983, 63.3: 844-914.

20. Swanson LW. The locus coeruleus: a cytoarchitectonic, Golgi and immunohistochemical study in the albino rat. Brain Res. 1976;110(1):39-56.

21. Mason ST, Fibiger HC. Regional topography within noradrenergic locus coeruleus as revealed by retrograde transport of horseradish peroxidase. J Comp Neurol. 1979;187(4):703-24.

22. Chandler DJ, Jensen P, McCall JG, Pickering AE, Schwarz LA, Totah NK. Redefining Noradrenergic Neuromodulation of Behavior: Impacts of a Modular Locus Coeruleus Architecture. J Neurosci. 2019;39(42):8239-49.

23. Loughlin SE, Foote SL, Grzanna R. Efferent projections of nucleus locus coeruleus: Morphologic subpopulations have different efferent targets. Neuroscience. 1986;18(2):307-19.

24. Loughlin SE, Foote SL, Fallon JH. Locus coeruleus projections to cortex: topography, morphology and collateralization. Brain Res Bull. 1982;9(1-6):287-94.

25. Totah NK, Neves RM, Panzeri S, Logothetis NK, Eschenko O. The Locus Coeruleus Is a Complex and Differentiated Neuromodulatory System. Neuron. 2018;99(5):1055-68 e6.

26. Totah NKB, Logothetis NK, Eschenko O. Noradrenergic ensemble-based modulation of cognition over multiple timescales. Brain Res. 2019;1709(December):50-66.

27. Chandler DJ, Gao WJ, Waterhouse BD. Heterogeneous organization of the locus coeruleus projections to prefrontal and motor cortices. Proc Natl Acad Sci U S A. 2014;111(18):6816-21.

28. Chandler DJ, Lamperski CS, Waterhouse BD. Identification and distribution of projections from monoaminergic and cholinergic nuclei to functionally differentiated subregions of prefrontal cortex. Brain Res. 2013;1522:38-58.

29. Day HE, Campeau S, Watson SJ, Jr., Akil H. Distribution of alpha 1a-, alpha 1b- and alpha 1d-adrenergic receptor mRNA in the rat brain and spinal cord. J Chem Neuroanat. 1997;13(2):115-39.

30. Samuels ER, Szabadi E. Functional neuroanatomy of the noradrenergic locus coeruleus: its roles in the regulation of arousal and autonomic function part I: principles of functional organisation. Curr Neuropharmacol. 2008;6(3):235-53.

31. Pascual J, del Arco C, Gonzalez AM, Pazos A. Quantitative light microscopic autoradiographic localization of alpha 2-adrenoceptors in the human brain. Brain Res. 1992;585(1-2):116-27.

32. Andrews GD, Lavin A. Methylphenidate increases cortical excitability via activation of alpha-2 noradrenergic receptors. Neuropsychopharmacology. 2006;31(3):594-601.

33. Berridge CW, Page ME, Valentino RJ, Foote SL. Effects of locus coeruleus inactivation on electroencephalographic activity in neocortex and hippocampus. Neuroscience. 1993;55(2):381-93.

34. Lapiz MD, Morilak DA. Noradrenergic modulation of cognitive function in rat medial prefrontal cortex as measured by attentional set shifting capability. Neuroscience. 2006;137(3):1039-49.

35. Cedarbaum JM, Aghajanian GK. Activation of locus coeruleus neurons by peripheral stimuli: modulation by a collateral inhibitory mechanism. Life Sci. 1978;23(13):1383-92.

36. Aston-Jones G, Zhu Y, Card JP. Numerous GABAergic afferents to locus ceruleus in the pericerulear dendritic zone: possible interneuronal pool. J Neurosci. 2004;24(9):2313-21.

37. Berridge CW, Foote SL. Enhancement of Behavioral and Electroencephalographic Indices of Waking following Stimulation of Noradrenergic β-Receptors within the Medial Septal Region of the Basal Forebrain. The Journal of Neuroscience. 1996;16(21):6999-7009.

38. Berridge CW, Isaac SO, Espana RA. Additive wake-promoting actions of medial basal forebrain noradrenergic alpha1- and beta-receptor stimulation. Behav Neurosci. 2003;117(2):350-9.

39. Samuels ER, Szabadi E. Functional neuroanatomy of the noradrenergic locus coeruleus: its roles in the regulation of arousal and autonomic function part II: physiological and pharmacological manipulations and pathological alterations of locus coeruleus activity in humans. Curr Neuropharmacol. 2008;6(3):254-85.

40. Samuels ER, Szabadi E. Functional Neuroanatomy of the Noradrenergic Locus Coeruleus: Its Roles in the Regulation of Arousal and Autonomic Function Part II: Physiological and Pharmacological Manipulations and Pathological Alterations of Locus Coeruleus Activity in Humans. 2008.

41. McCall JG, Al-Hasani R, Siuda ER, Hong DY, Norris AJ, Ford CP, et al. CRH Engagement of the Locus Coeruleus Noradrenergic System Mediates Stress-Induced Anxiety. Neuron. 2015;87(3):605-20.

42. Ferry B, Roozendaal B, McGaugh JL. Involvement of α1-adrenoceptors in the basolateral amygdala in modulation of memory storage. European Journal of Pharmacology. 1999;372(1):9-16.

43. Chen FJ, Sara SJ. Locus coeruleus activation by foot shock or electrical stimulation inhibits amygdala neurons. Neuroscience. 2007;144(2):472-81.

44. Blackstad TW, Fuxe K, Hokfelt T. Noradrenaline nerve terminals in the hippocampal region of the rat and the guinea pig. Z Zellforsch Mikrosk Anat. 1967;78(4):463-73.

45. Powers RE, Struble RG, Casanova MF, O'Connor DT, Kitt CA, Price DL. Innervation of human hippocampus by noradrenergic systems: normal anatomy and structural abnormalities in aging and in Alzheimer's disease. Neuroscience. 1988;25(2):401-17.

46. Harley CW. Norepinephrine and the dentate gyrus. Prog Brain Res. 2007;163(February 2007):299-318.

47. Szot P, White SS, Greenup JL, Leverenz JB, Peskind ER, Raskind MA. Alpha1-adrenoreceptor in human hippocampus: binding and receptor subtype mRNA expression. Brain Res Mol Brain Res. 2005;139(2):367-71.

48. Duncan GE, Little KY, Koplas PA, Kirkman JA, Breese GR, Stumpf WE. Beta-adrenergic receptor distribution in human and rat hippocampal formation: marked species differences. Brain Res. 1991;561(1):84-92.

49. Milner TA, Shah P, Pierce JP. beta-adrenergic receptors primarily are located on the dendrites of granule cells and interneurons but also are found on astrocytes and a few presynaptic profiles in the rat dentate gyrus. Synapse. 2000;36(3):178-93.

50. Loy R, Koziell DA, Lindsey JD, Moore RY. Noradrenergic innervation of the adult rat hippocampal formation. J Comp Neurol. 1980;189(4):699-710.

51. Haring JH, Davis JN. Differential distribution of locus coeruleus projections to the hippocampal formation: anatomical and biochemical evidence. Brain Res. 1985;325(1-2):366-9.

52. Ishida Y, Shirokawa T, Miyaishi O, Komatsu Y, Isobe K. Age-dependent changes in projections from locus coeruleus to hippocampus dentate gyrus and frontal cortex. Eur J Neurosci. 2000;12(4):1263-70.

53. Marcyniuk B, Mann DM, Yates PO. The topography of nerve cell loss from the locus caeruleus in elderly persons. Neurobiol Aging. 1989;10(1):5-9.

54. McCormick DA, Pape HC, Williamson A. Actions of norepinephrine in the cerebral cortex and thalamus: implications for function of the central noradrenergic system. Prog Brain Res. 1991;88(C):293-305.

55. Szymusiak R, Alam N, Steininger TL, McGinty D. Sleep-waking discharge patterns of ventrolateral preoptic/anterior hypothalamic neurons in rats. Brain Res. 1998;803(1-2):178-88.

56. Samuels ER, Szabadi E. Functional neuroanatomy of the noradrenergic locus coeruleus: its roles in the regulation of arousal and autonomic function part I: principles of functional organisation. Curr Neuropharmacol. 2008;6(3):235-53.

57. Bourgin P, Huitró N-Resé S, Spier AD, Ronique Fabre V, Morte B, Criado JR, et al. Hypocretin-1 Modulates Rapid Eye Movement Sleep through Activation of Locus Coeruleus Neurons. 2000.

58. Stone EA, Quartermain D, Lin Y, Lehmann ML. Central alpha1-adrenergic system in behavioral activity and depression. Biochem Pharmacol. 2007;73(8):1063-75.

59. Li DP, Atnip LM, Chen SR, Pan HL. Regulation of synaptic inputs to paraventricular-spinal output neurons by alpha2 adrenergic receptors. J Neurophysiol. 2005;93(1):393-402.

60. Nakamura S, Iwama T. Antidromic activation of the rat locus ooeruleus neurons from hippocampus, cerebral and cerebellar cortices.

61. Couto LB, Moroni CR, dos Reis Ferreira CM, Elias-Filho DH, Parada CA, Pela IR, et al. Descriptive and functional neuroanatomy of locus coeruleus-noradrenaline-containing neurons involvement in bradykinin-induced antinociception on principal sensory trigeminal nucleus. J Chem Neuroanat. 2006;32(1):28-45.

62. Marien MR, Colpaert FC, Rosenquist AC. Noradrenergic mechanisms in neurodegenerative diseases: a theory. Brain Res Brain Res Rev. 2004;45(1):38-78.

63. Moret C, Briley M. The importance of norepinephrine in depression. Neuropsychiatr Dis Treat. 2011;7(Suppl 1):9-13.

64. Singh S. Noradrenergic pathways of locus coeruleus in Parkinson's and Alzheimer's pathology. Int J Neurosci. 2020;130(3):251-61.

65. Bari BA, Chokshi V, Schmidt K. Locus coeruleus-norepinephrine: basic functions and insights into Parkinson's disease. Neural Regen Res. 2020;15(6):1006-13.

66. Zweig RM, Cardillo JE, Cohen M, Giere S, Hedreen JC. The locus ceruleus and dementia in Parkinson's disease. Neurology. 1993;43(5):986-91.

67. Wang T, Zhang QJ, Liu J, Wu ZH, Wang S. Firing activity of locus coeruleus noradrenergic neurons increases in a rodent model of Parkinsonism. Neurosci Bull. 2009;25(1):15-20.

68. Henry B, Fox SH, Peggs D, Crossman AR, Brotchie JM. The alpha2-adrenergic receptor antagonist idazoxan reduces dyskinesia and enhances anti-parkinsonian actions of L-dopa in the MPTP-lesioned primate model of Parkinson's disease. Mov Disord. 1999;14(5):744-53.

69. Betts MJ, Kirilina E, Otaduy MCG, Ivanov D, Acosta-Cabronero J, Callaghan MF, et al. Locus coeruleus imaging as a biomarker for noradrenergic dysfunction in neurodegenerative diseases. Brain. 2019;142(9):2558-71.

70. Elrod R, Peskind ER, DiGiacomo L, Brodkin KI, Veith RC, Raskind MA. Effects of Alzheimer's disease severity on cerebrospinal fluid norepinephrine concentration. Am J Psychiatry. 1997;154(1):25-30.

71. Puranik N, Yadav D, Chauhan PS, Kwak M, Jin JO. Exploring the Role of Gene Therapy for Neurological Disorders. Curr Gene Ther. 2021;21(1):11-22.

72. Braun D, Madrigal JL, Feinstein DL. Noradrenergic regulation of glial activation: molecular mechanisms and therapeutic implications. Curr Neuropharmacol. 2014;12(4):342-52.

73. Hellings N, Raus J, Stinissen P. Insights into the immunopathogenesis of multiple sclerosis. Immunol Res. 2002;25(1):27-51.

74. Polak PE, Kalinin S, Feinstein DL. Locus coeruleus damage and noradrenaline reductions in multiple sclerosis and experimental autoimmune encephalomyelitis. Brain. 2011;134(Pt 3):665-77.

75. Laureys G, Gerlo S, Spooren A, Demol F, De Keyser J, Aerts JL. beta(2)-adrenergic agonists modulate TNF-alpha induced astrocytic inflammatory gene expression and brain inflammatory cell populations. J Neuroinflammation. 2014;11:21.

76. Ghasemi M, Mehranfard N. Mechanisms underlying anticonvulsant and proconvulsant actions of norepinephrine. Neuropharmacology. 2018;137:297-308.

77. Mueller AL, Hoffer BJ, Dunwiddie TV. Noradrenergic responses in rat hippocampus: Evidence for mediation by α and β receptors in the in vitro slice. Brain Research. 1981;214(1):113-26.

78. Harley CW, Lalies MD, Nutt DJ. Estimating the synaptic concentration of norepinephrine in dentate gyrus which produces β-receptor mediated long-lasting potentiation in vivo using microdialysis and intracerebroventricular norepinephrine. Brain Research. 1996;710(1-2):293-8.

79. Walling SG, Harley CW. Locus ceruleus activation initiates delayed synaptic potentiation of perforant path input to the dentate gyrus in awake rats: a novel beta-adrenergic- and protein synthesis-dependent mammalian plasticity mechanism. J Neurosci. 2004;24(3):598-604.

80. Raedt R, Clinckers R, Mollet L, Vonck K, El Tahry R, Wyckhuys T, et al. Increased hippocampal noradrenaline is a biomarker for efficacy of vagus nerve stimulation in a limbic seizure model. J Neurochem. 2011;117(3):461-9.

81. Bengzon J, Kalen P, Lindvall O. Evidence for long-term reduction of noradrenaline release after kindling in the rat hippocampus. Brain Res. 1990;535(2):353-7.

82. Dailey JW, Mishra PK, Ko KH, Penny JE, Jobe PC. Noradrenergic abnormalities in the central nervous system of seizure-naive genetically epilepsy-prone rats. Epilepsia. 1991;32(2):168-73.

83. Jimenez-Rivera CA, Weiss GK. The effect of amygdala kindled seizures on locus coeruleus activity. Brain Res Bull. 1989;22(4):751-8.

84. Queiroz CM, Gorter JA, Lopes da Silva FH, Wadman WJ. Dynamics of evoked local field potentials in the hippocampus of epileptic rats with spontaneous seizures. J Neurophysiol. 2009;101(3):1588-97.

85. Neuman RS, Harley CW. Long-lasting potentiation of the dentate gyrus population spike by norepinephrine. Brain Res. 1983;273(1):162-5.

86. Sarvey JM. Blockade of Norepinephrine-Induced Long-Lasting Potentiation in the Hippocampal Dentate Gyrus by an Inhibitor of Protein Synthesis. Brain research, 1985, 361.1-2: 276-283.

87. Lacaille JC, Harley CW. The action of norepinephrine in the dentate gyrus: beta-mediated facilitation of evoked potentials in vitro. Brain Res. 1985;358(1-2):210-20.

88. Haas HL, Rose GM. Noradrenaline blocks potassium conductance in rat dentate granule cells in vitro. Neurosci Lett. 1987;78(2):171-4.

89. Stanton PK, Sarvey JM. Blockade of norepinephrine-induced long-lasting potentiation in the hippocampal dentate gyrus by an inhibitor of protein synthesis. Brain Res. 1985;361(1-2):276-83.

90. Stanton PK, Sarvey JM. Blockade of long-term potentiation in rat hippocampal CA1 region by inhibitors of protein synthesis. J Neurosci. 1984;4(12):3080-8.

91. Winson J, Dahl D. Action of norepinephrine in the dentate gyrus. II. Iontophoretic studies. Exp Brain Res. 1985;59(3):497-506.

92. Chaulk PC, Harley CW. Intracerebroventricular norepinephrine potentiation of the perforant path-evoked potential in dentate gyrus of anesthetized and awake rats: A role for both α- and β-adrenoceptor activation. Brain Research. 1998;787(1):59-70.

93. Pedarzani P, Storm JF. Interaction between alpha- and beta-adrenergic receptor agonists modulating the slow Ca(2+)-activated K+ current IAHP in hippocampal neurons. Eur J Neurosci. 1996;8(10):2098-110.

94. Harley CW, Milway JS. Glutamate ejection in the locus coeruleus enhances the perforant path-evoked population spike in the dentate gyrus. Exp Brain Res. 1986;63(1):143-50.

95. Klukowski G, Harley CW. Locus coeruleus activation induces perforant path-evoked population spike potentiation in the dentate gyrus of awake rat. Exp Brain Res. 1994;102(1):165-70.

96. Richter-Levin G, Segal M, Sara S, Sara S. An a2 antagonist, idazoxan, enhances EPSP-spike coupling in the rat dentate gyrus. Brain research, 1991, 540.1-2: 291-294 991.

97. Knight J, Harley CW. Idazoxan increases perforant path-evoked EPSP slope paired pulse inhibition and reduces perforant path-evoked population spike paired pulse facilitation in rat dentate gyrus. Brain Res. 2006;1072(1):36-45.

98. Sara SJ, Bergis O. Enhancement of excitability and inhibitory processes in hippocampal dentate gyrus by noradrenaline: a pharmacological study in awake, freely moving rats. Neurosci Lett. 1991;126(1):1-5.

99. Brown RA, Walling SG, Milway JS, Harley CW. Locus ceruleus activation suppresses feedforward interneurons and reduces beta-gamma electroencephalogram frequencies while it enhances theta frequencies in rat dentate gyrus. J Neurosci. 2005;25(8):1985-91.

100. Walling SG, Nutt DJ, Lalies MD, Harley CW. Orexin-A infusion in the locus ceruleus triggers norepinephrine (NE) release and NE-induced long-term potentiation in the dentate gyrus. J Neurosci. 2004;24(34):7421-6.

101. Dahl D, Winson J. Action of norepinephrine in the dentate gyrus. I. Stimulation of locus coeruleus. Exp Brain Res. 1985;59(3):491-6.

102. Harley C, Milway JS, Lacaille JC. Locus coeruleus potentiation of dentate gyrus responses: evidence for two systems. Brain Res Bull. 1989;22(4):643-50.

103. Lemon N, Aydin-Abidin S, Funke K, Manahan-Vaughan D. Locus coeruleus activation facilitates memory encoding and induces hippocampal LTD that depends on beta-adrenergic receptor activation. Cereb Cortex. 2009;19(12):2827-37.

104. Quinlan MAL, Strong VM, Skinner DM, Martin GM, Harley CW, Walling SG. Locus Coeruleus Optogenetic Light Activation Induces Long-Term Potentiation of Perforant Path Population Spike Amplitude in Rat Dentate Gyrus. Front Syst Neurosci. 2018;12:67.

105. Dahl D, Bailey WH, Winson J. Effect of norepinephrine depletion of hippocampus on neuronal transmission from perforant pathway through dentate gyrus. J Neurophysiol. 1983;49(1):123-33.

106. Harley CW, Evans S. Locus-Coeruleus-Induced Enhancement of the Perforant-Path Evoked Potential. In: Woody C.D. ADL, McGaugh J.L., editor. Cellular Mechanisms of Conditioning and Behavioral Plasticity. Boston, MA: Springer; 1988. p. 415-23.

107. Reid AT, Harley CW. An associativity requirement for locus coeruleus-induced long-term potentiation in the dentate gyrus of the urethane-anesthetized rat. Exp Brain Res. 2010;200(2):151-9.

108. Dahl D, Sarvey JM. Norepinephrine induces pathway-specific long-lasting potentiation and depression in the hippocampal dentate gyrus (long-term potentiation/synaptic plasticity/catecholamines). 1989.

109. Flicker C, Geyer MA. Behavior during hippocampal microinfusions. I. Norepinephrine and diversive exploration. Brain Res. 1982;257(1):79-103.

110. Segal DS, Mandell AJ. Behavioral activation of rats during intraventricular infusion of norepinephrine. Proc Natl Acad Sci U S A. 1970;66(2):289-93.

111. Gonzalez MM, Aston-Jones G. Circadian regulation of arousal: role of the noradrenergic locus coeruleus system and light exposure. Sleep. 2006;29(10):1327-36.

112. Berridge CW, Foote SL. Effects of Locus Coeruleus Activation on Electroencephalographic Activity in Neocortex and Hippocampus. 1991.

113. Stanton PK, Sarvey JM. Norepinephrine Regulates Long-Term Potentiation of Both the Population Spike and Dendritic Epsp in Hippocampal Dentate Gyrus. Brain Research Bulletin. 1987;18(1):115-9.

114. Lethbridge RL, Walling SG, Harley CW. Modulation of the perforant path-evoked potential in dentate gyrus as a function of intrahippocampal beta-adrenoceptor agonist concentration in urethane-anesthetized rat. Brain Behav. 2014;4(1):95-103.

115. Hansen N, Manahan-Vaughan D. Locus Coeruleus Stimulation Facilitates Long-Term Depression in the Dentate Gyrus That Requires Activation of beta-Adrenergic Receptors. Cereb Cortex. 2015;25(7):1889-96.

116. Harley CW, Sara SJ. Locus coeruleus bursts induced by glutamate trigger delayed perforant path spike amplitude potentiation in the dentate gyrus. Exp Brain Res. 1992;89(3):581-7.

117. Olpe HR, Laszlo J, Pozza MF, De Herdt P, Waldmeier PC, Jones RS. Glutamate-induced activation of rat locus coeruleus increases CA1 pyramidal cell excitability. Neurosci Lett. 1986;65(1):11-6.

Chapter 3 Chemo- and optogenetics

Chemo- and optogenetics are research tools used in the field of neuroscience where cell-specific transduction is performed to induce expression of membrane proteins. Activation of these proteins, either receptors or ion channels/pumps, can lead to excitation or inhibition of the target cells. A transgene cassette carrying the gene of interest can be incorporated in the target cells of interest using transgenic technology or viral vectors. Since this thesis focuses on optimization of chemogenetic modulation of LC, the chemogenetic approach using viral vectors will be discussed in more detail. However, since optogenetics is an interesting tool with high temporal resolution for investigating LC functioning we will highlight the background and current state-of-the art in the field.

3.1 Optogenetics

Optogenetic tools combine optical and genetic methods to induce fast and specific modulation of cells within neural tissue. The optogenetic toolbox consists of a targeting method to induce opsin expression and precisely timed light delivery (1). A photoreceptor protein or rhodopsin exists of an opsin, a seven-transmembrane protein, encoded by opsin genes, and a light-isomerizable chromophore all-trans-retinal. Retinal serves as a co-factor and undergoes a conformational change upon light administration inducing opsin activation. There are two families: microbial opsins (type I) and animal opsins (type II). Similar to the chemogenetic tools, opsins are coupled either to ion channels or GPCRs. Microbial opsins are photo-sensitive ion channels whereas type II opsins belong to the GPCR group. The first microbial opsins were generated in 2005: channelrhodopsin-1(ChR1) and channelrhodopsin-2(ChR2) derived from *Chlamydomonas reinhardtii* (green algae), both nonspecific cation channels activated by blue light (2, 3). Light administration in the vicinity of ChR2 will lead to conformational changes inducing the influx of cations resulting in depolarization of the target cell (Fig 3.1) (2) as described in hippocampal neurons, where they achieved high temporal control over the spiking pattern (4). Next to excitatory opsins, enhanced halorhodopsin (eNpHR) was created to induce neuronal inhibition. This opsin derived from *Natronomonas pharaonis* is activated by light from the yellow spectrum and hyperpolarizes the neuron through influx of Cl^- ions (Fig 3.1) (5). Next to type I opsins, which are the most extensively used in the field of neuroscience, type II opsins are developed to control neuronal activity through G protein-coupled signaling pathways. These mammalian opsins are known as optoXRs, activated by green light and induce de- or hyperpolarization of the cell depending on the G-coupled pathway (Fig 3.1 right panel).

Since the first opsins were introduced, multiple modifications have been performed to optimize their function, resulting in a variety of tools with their own kinetics, conductance properties, and activation wavelength (3).

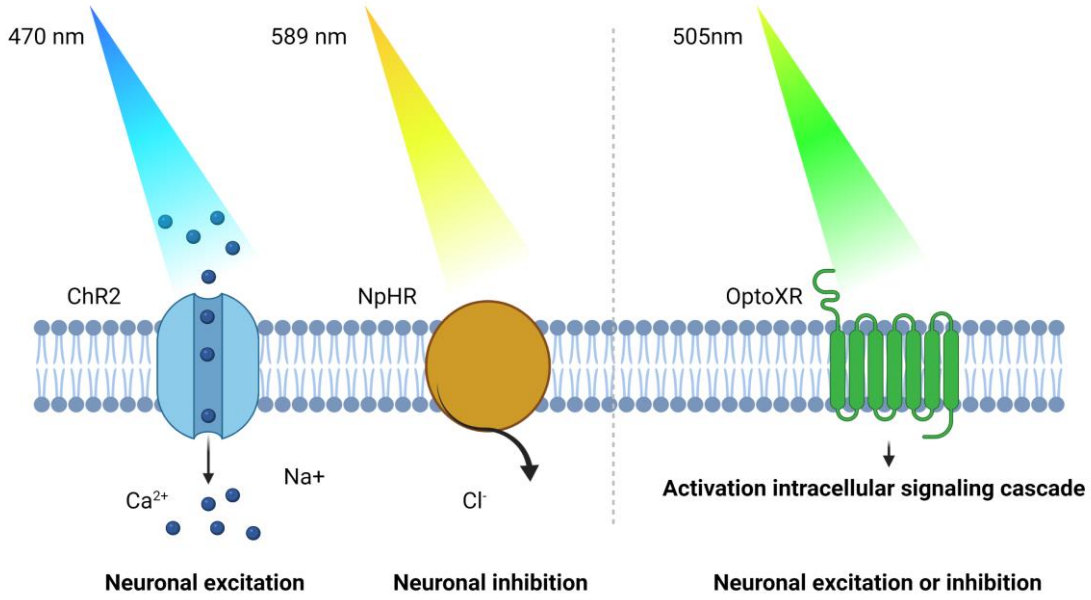

Figure 3.1 Two types of opsins used for optogenetics. Type I opsins are photo-sensitive ion channels: Channelrhodopsin (ChR) and halorhodopsin (NpHR) are excited by blue or yellow light respectively, resulting in the exchange of cations or anions through the cell membrane inducing neuronal excitation or inhibition (left panel). Type II opsins, OptoXR are activated by green light and change cell excitability through G-protein coupled signalling pathways (right panel). Figure created with BioRender.com

3.2 Chemogenetics

Chemogenetics is a research tool that uses genetically engineered proteins made unresponsive to their endogenous molecules and only respond to small chemical actuators, which are otherwise considered biologically inert. There are different groups of genetically engineered proteins: kinases, non-kinase enzymes and the most commonly used ligand gated ion channels (LGICs) and G protein-coupled receptors (GPCRs) (6, 7). For this thesis, the main focus was to introduce a genetically modified GPCR.

3.2.1 Chemogenetic tools interfering with ion conductance

Engineered ion channels are able to de- or hyperpolarize the cell in a fast modus. Different types of ligand gated ion channels (LGICs) are present with invertebrate or mammalian origin (7). The glutamate-gated chloride channel derived from the roundworm is a high conductance chloride channel that can be activated by the administration of an antiparasite drug (ivermectin) and suppresses neuronal activity (8). TRPV1 is a nonselective cation channel activated by capsaicin, resulting in depolarization of the cell (7, 9). The combination of limited characterization of these channels and the need to knock down endogenous ion channel genes gave rise to the development of engineered ligand gated ion channels (eLGIC).

Engineered ligand gated ion channels (eLGICs) can alter activity of genetically targeted cells. eLGICs are made of different combinations of the genetically modified ligand binding domain (LBD) of the α7-nicotinic acetylcholine receptor coupled, (= pharmacologically selective actuator molecule, PSAM), to an ion pore domain (IPD)of the cys-loop ion channel receptor family (Fig 3.2). The LBD can be combined with the IPD of the 5-HT3 serotonin receptor to induce depolarization after binding of the agonist (pharmacologically selective effector molecule, PSEM), whereas coupling to the chloride-selective glycine receptor IPD will lead to Cl^- influx and hyperpolarization (7, 10).

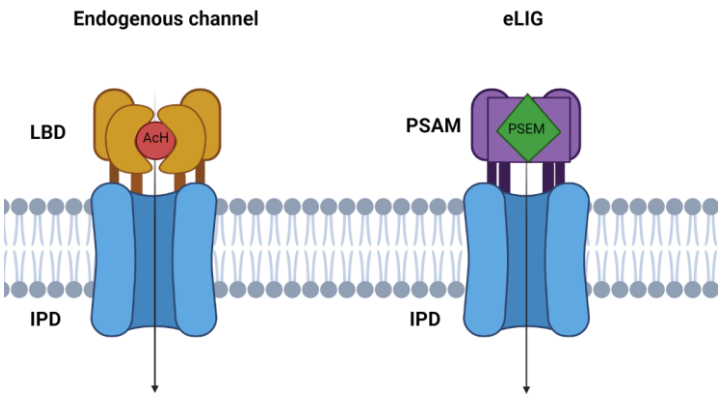

Figure 3.2 Schematic representation of engineered ligand gated ion channel. An endogenous ligand gated ion channel consists of two parts: the ligand binding domain (LBD) and the ion pore domain (IPD). Engineering of the LBD domain of the α_7-nicotinic acetylcholine receptor forms a pharmacologically selective actuator molecule (PSAM) which inhibits binding of acetylcholine (AcH), and can only be activated by binding of a pharmacologically selective effector molecule (PSEM). Depending on the character of the IPD, influx of cations or anions will occur which can de- or hyperpolarise the cell membrane. Figure created with BioRender.com

Recently a new type of eLGIC, the insect ionotropic receptor-mediated neuronal stimulation (INTENS), was used to modulate LC neurons. This is derived from an olfactory ionotropic receptor from *Drosophila melanogaster* which mediates chemical detection. This ionotropic receptor is a heteromeric complex which consists of two subunits: IR84a and IR8a and responds to odorants such as phenylacetaldehyde and phenylacetic acid in an excitatory manner. Administration of the ligands leads to an influx of cations such as Na^+ and K^+, depolarizing the membrane potential and increasing firing frequency, but also small currents of Ca^{2+} are detected. In LC neurons it was described that the Ca^{2+} influx leads to sustained NA release probably due to activation of the Ca-calmodulin complex, protein kinase C mediated trafficking of glutamate receptors, TH gene expression, and sustained NA biosynthesis (11).

3.2.2 Chemogenetic tools based on G protein coupled receptors

A first study using a pioneer chemogenetic tool was published in 1990, describing a mutated β_2-adrenergic receptor that was no longer responsive to NA but was activated by a chemical substance L-185.870 (12). Although the potency of the compound for this initial genetically engineered receptor was low, this was the first proof of concept for the chemogenetic approach. It was at the end of the 20th century that the first family of genetically engineered receptors was created: The Receptors Activated Solely by Synthetic Ligand (RASSLs). The first receptor in this class was a modified κ-opioid receptor that was designed to be insensitive to its endogenous ligand but responsive to a synthetic agonist (spiradoline)(13).

Different RASSLs were designed but the disadvantage of these first trials was the presence of high levels of constitutive activity in combination with low ligand specificity (7).

Armbuster and Roth tried to overcome these hurdles by generating a new family of genetically engineered receptors. They subjected the human muscarinic M3 receptor to random mutagenesis which gave rise to the most commonly used chemogenetic receptor: The Designer Receptors Exclusively Activated by Designer Drugs (DREADDs). Since DREADDs are the main modified receptors used in this thesis we will further elaborate on this subgroup (14). Today an entire group of DREADD-based muscarinic receptors are used, all of them are insensitive to their native ligand acetylcholine and can be activated by designer drugs.

3.2.2.1 Designer Receptors Exclusively activated by designer drugs (DREADDs)

DREADDs are currently the most commonly used chemogenetic platform and an entire group of DREADD-based muscarinic receptors are used. The implementation of two point mutations was enough to make the M3 muscarinic receptor insensitive to its native ligand acetylcholine and sensitive to a designer drug. Genetic modification of the other muscarinic receptors arised rapidly creating two large groups depending on the G protein-coupled signaling cascade: M2, M4 DREADDs and a κ-opioid-derived DREADD (KORD) and DREADDs derived from M1,M3 and M5 (14). Up till now, hM3D(G)q and hM4D(G)i DREADDs are mostly used and described in neuroscientific research.

Inhibitory DREADD receptors

Upon binding of a designer drug or DREADD agonist, neuronal inhibition will be induced through initiation of the Gαi-coupled pathway. G-protein coupled inwardly rectifying potassium (GIRK) channels will be activated in combination with inhibition of voltage-gated Ca^{2+} channels, resulting in hyperpolarization and decreased neurotransmitter release (described in more detail in 1.2.1). This inhibitory DREADD has been used and validated to silence neuronal activity (15), where our own group has proven it to be efficient to reduce the activity of excitatory pyramidal cells in the hippocampus of both rats and mice reducing excitability and epileptic seizures (16, 17). The κ-opioid derived DREADD (KORD) is activated by the inert ligand salvinorin B and couples to the Gi cascade reducing neuronal excitability (Fig.3.3 right panel).

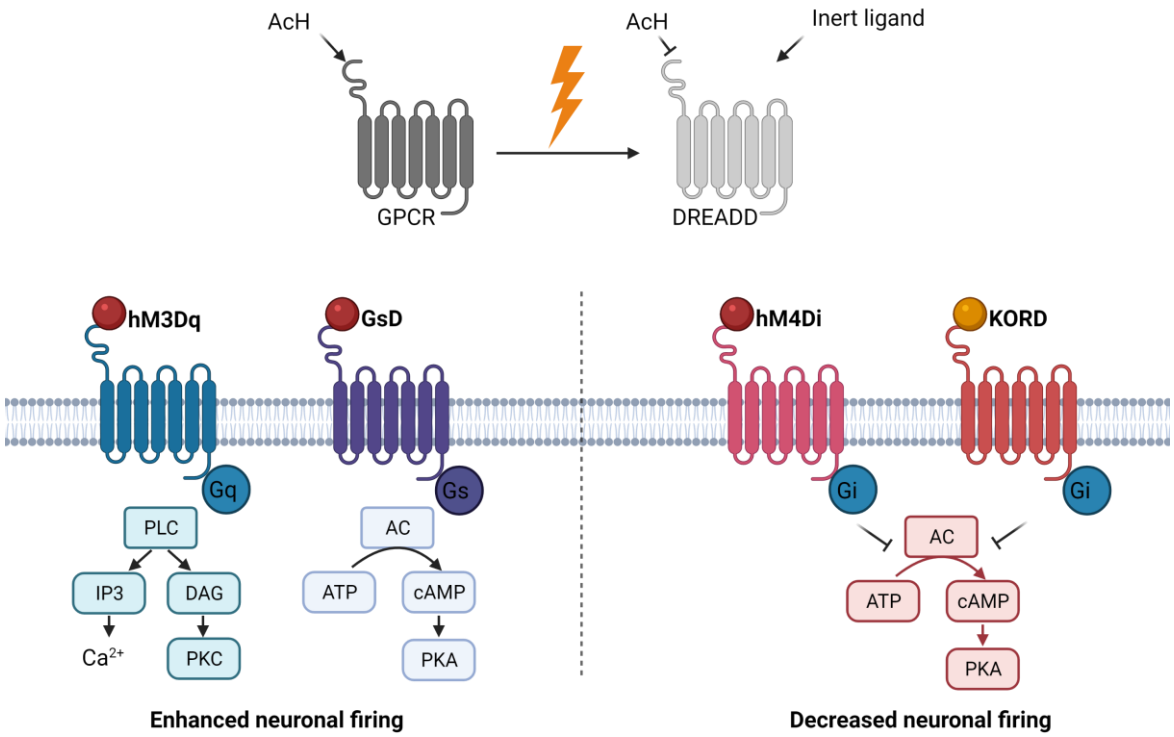

Figure 3.3 Chemogenetic tools based on modified GPCRs. DREADD receptors are genetically modified muscarinic receptors that have become inert for their native ligand acetylcholine, and can be activated by a designer drug (inert ligand). DREADDs influence cell excitability in a slow manner by activating G-coupled pathways. Two large classes can be distinguished: 1) DREADDs that increase cell excitability and induce enhanced neuronal firing through the Gq- or Gs-pathway, the hM3Dq and GsD receptor respectively (left) and 2) DREADDs that decrease cell excitability by decreasing cAMP production, i.e. hM4Di and KORD coupled to the Gi pathway (right). Red dots represent the inert ligand; yellow dot represents salvinorin B. Figure created with BioRender.com

Excitatory DREADD receptors

Binding of an agonist to the hM3D(G)q receptor induces the opposite effect of the hM4Di receptor and results in neuronal excitation due to activation of the Gαq coupled pathway due to inhibition of KCNQ channels, decreasing K^+ efflux and subsequent longer depolarization, enhancing the change of increased neuronal firing (Fig 3.3). This DREADD receptor has been validated for enhancing neuronal excitability since 2009 and is widely used in the field of neuroscience (15, 18).

Subsequently an additional DREADD (GsD, a chimeric muscarinic-adrenergic receptor) was produced by coupling the intracellular loops of a β_1-adrenergic receptor to the ligand binding domain of an M3 receptor (19). Binding of an agonist activates the Gαs pathway and induces neuronal excitation by cAMP-mediated signaling (19) (Fig.3.3).

3.2.2.2 Designer Drugs

The goal of using DREADDs is to modulate specific target cells by inducing cell-specific expression of the modified GPCR in combination with the use of synthetic selective agonists. DREADD-specific agonists should have two main characteristics: 1) be pharmacologically inert (avoiding DREADD-independent effects due to binding of endogenous receptors); 2) have a high bioavailability after systemic administration. Currently a list of different DREADD actuators is available.

Clozapine-N-Oxide (CNO)

Clozapine-N-Oxide (CNO) was the prototype of an inert chemogenetic ligand and was believed to fulfil the two criteria: inert character and a high bioavailability and potency for DREADDs(14). It was believed to easily cross the blood-brain-barrier (BBB) with a fast distribution and long-lasting effect, however it was recently discovered that CNO is not able to penetrate the BBB and has only moderate affinity for DREADDs (20-22). Additionally, many groups have shown that a small portion of CNO can be back metabolized to clozapine in different species (f.e. guinea pigs, primates and humans), which led to the hypothesis that CNO exerts its effect on DREADD receptors through to the back-metabolized clozapine (6, 20, 23-25).

CNO is mostly used in doses ranging from 1-20 mg/kg, although in studies investigating DREADD-specific modulation of LC, this varies between 0.03 and 10 mg/kg. Although these low doses should not induce effects in control animals, MacLaren et al. observed DREADD-independent effects in behavioral tasks performed by rodents after administration of 1 mg/kg (23).

Clozapine

A recent study by Gomez et al. showed that CNO is converted to clozapine, which is able to cross the BBB and induce DREADD activation more easily when compared to CNO. Its high potency and permeability led to the suggestion of using subclinical doses of clozapine as DREADD actuator (20). *In vivo* doses of 0.1 mg/kg clozapine, which resembles plasma levels of converted 10 mg/kg CNO, have been used to activate DREADDs and decrease locomotor activity, whereas a 10 times higher concentration led to similar findings in control animals, possibly due to the sedative effect of clozapine induced by binding endogenous receptors (20).

Clozapine has a rather low specificity profile with affinity for a broad range of endogenous neuroreceptors such as serotonergic, muscarinic, noradrenergic, dopaminergic and histaminergic receptors (26). This increases the risk of possible DREADD-independent physiological effects. In studies reporting chemogenetic modulation of the locus coeruleus, doses of 0.03-10 mg/kg CNO are used without any off-target effects, suggesting that clozapine doses up to 0.1 mg/kg should be safe to use. In general, clozapine has the advantage of being an approved drug for human patients with schizophrenia, however, doses should be carefully titrated to avoid off-target effects or side-effects reported with higher concentrations (27).

New generation DREADD agonists

Since the ideal key to fit the lock has not been found, other approved drugs or new compounds have been tested to act as selective and inert DREADD agonists. Olanzapine, similar to clozapine, is an approved drug for patients suffering from schizophrenia and bipolar disorder. Although doses of 0.1 mg/kg are used for DREADD activation, and induced no effects on locomotion in rats, it did affect working memory in non-human primates (28, 29). Perlapine, shortly used as a sleep-promoting drug for human patients, has been suggested as DREADD actuator. Although *in vitro* good agonist characteristics were observed, it has a rather low specificity profile with known affinity for dopaminergic and serotonergic receptors (6). Compound 21, known for its affinity for hM3Dq and hM4Di DREADDs, easy brain penetration and long-lasting effect has been suggested as DREADD agonist. Although it shows less off target effects compared to clozapine and doses up to 3 mg/kg have no effects on behavior, it tends to have a lower potency (6, 21, 30). Two newer compounds are JHU37107 and JHU37152, with promising characteristics for DREADD activation, but with a selectivity profile comparable to clozapine, showing lower affinity for serotonin receptors but higher affinity for muscarinic receptors (31). These components are relatively new, and not much is reported yet, however they seem to be efficient to use in rodents and monkeys at doses between 0.01 and 0.3 mg/kg (32). The youngest addition to the DREADD agonist family is deschloroclozapine. It has a 100 times higher affinity and potency for DREADDs compared to CNO or compound 21. It has been reported that very low doses of 0.001-0.003 mg/kg can be used to activate the hM3Dq DREADD receptor, and due to the absence of off-target effects at doses that are 100 times higher combined with its high penetrative characteristic, it seems to be the most promising DREADD actuator thus far (29, 33).

3.3 DREADD expression systems

3.3.1 Transgene expression cassette

Typically, a viral vector contains a transgene expression cassette containing the main elements necessary for targeted gene expression: a promoter, transgene of interest, regulatory elements and a protein tag useful for localization during fundamental research (as depicted in fig.3.4 for the used viral vectors in this thesis). Engineering this expression cassette in coherence with the serotype of the viral vector is necessary to tailor and achieve high cell-specific transgene expression for fundamental neural circuit studies and future translational therapeutic use (34).

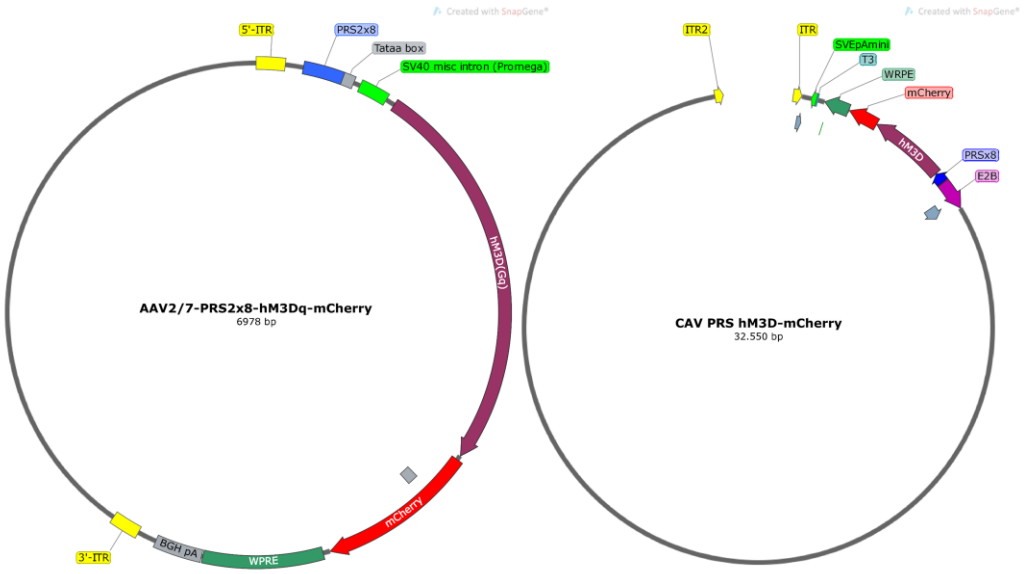

Figure 3.4 Gene expression cassette of the AAV and CAV viral vector. Each expression cassette consists of a promoter sequence (PRSx8, blue), the transgene (hM3Dq, purple) and a red fluorescent tag fused to it (mCherry, red), the inverted terminal repeats (yellow) and the Woodchuck hepatitis virus post-transcriptional regulatory element (WPRE, dark green) to enhance transduction efficiency. Figure created in SnapGene.

3.3.1.1 Promoter

The serotype of the viral vector has an influence on the tropism of the cell, however to ensure gene expression in a certain neuron or glial population the capsid proteins are not enough. To prevent off-target expression due to possible leakage of viral particles, a promoter sequence is added to the transgene expression cassette (35). This promoter sequence is necessary for the initiation of the transcription process. Choosing the correct promoter sequence for an experiment is part of the transcriptional targeting strategy and is one of the main necessities for chemo- or optogenetic studies. To increase the cell-type specificity using viral technology a specific promoter (gene regulatory element) can drive cell-type specific transgene expression due to the presence of specific transcription factors which activate the promoter sequence only present in the target cells. One could hypothesize that strong ubiquitous promoters are necessary (36).

Although promoters derived from viral genomes (f.e. Cytomegalovirus CMV promoter) are stronger in driving gene expression (37), the choice of a mammalian derived promoter is safer, since the sequence is less likely to be recognized by host defense cells. However, these mammalian promoters could compromise the high expression levels necessary for neuroscientific research, which is then often counteracted by increasing the viral titer. To avoid this, promoter engineering is performed to increase transcription efficiency and consequent expression levels using lower viral titers (36).

LC specific promoter

Multimerization of cis-acting elements has been performed to produce the synthetic dopamine-β-hydroxylase (DBH) promoter, PRSx8 (Fig 3.4). The PRSx8 promoter consists of eight copies of a promoter sequence from the cis-regulatory region of the DBH gene that binds the Phox2a/b transcription factors. This promoter sequence has proven to successfully drive gene expression in noradrenergic neurons expressing the Phox2a/b transcription factors with higher specificity compared to the human DBH promoter (36, 38, 39). However, due to the multimerization of binding spots for the Phox2a transcription factors, possible sequestration of these transcription factors is possible. This might disturb the normal physiology of the NA neurons. Therefore, another way of promoter engineering was created. Point mutations were made in the transcription binding sites PRS2 and PRS3 of the human DBH promoter to increase affinity for the Phox2 transcription factors. Hwang et al. showed that this increased promoter strength up to 20 times without loss of cell-specificity. This indicates that when creating modified receptors, it is useful to use the backbone of naturally occurring promoters (40).

A variety of cell-specific promoters is already used and validated to restrict gene expression in neurons and glial cells, next to the above described promoters to induce expression in noradrenergic neurons. The human synapsin 1 gene (hSyn) promoter is used to restrict expression in neurons (41), whereas the calmodulin dependent protein kinase II (CamKIIα) promoter can be used to target excitatory neurons as used in our own lab for genetic modification of hippocampal pyramidal neurons (16, 17). Astrocyte specific expression can be achieved using the glial fibrillary acidic protein (GFAP) promoter (36, 37).

3.3.1.2 Transgene of interest

Inserting a gene of interest with mammalian origin is often not a problem, since the sequence resembles the sequences of the host species. However, a wild-type gene sequence or adapted version does not necessarily induce high and robust protein translation (34). It has been reported that guanine-cytosine content and termination signals can impact transgene expression. Secondly, the codon sequence can influence the yield of protein translation. Codon optimization is widely used in gene therapy studies to enhance gene expression. Here, a certain nucleotide sequence is replaced by the preferential sequence in the host without changing the translated protein. DREADDs could be adapted using the preferential codons for each host species, to induce faster protein translation. Although codon optimization is a widely used technique, even for therapeutic goals in clinical therapy (vaccines), one should take into account that faster and more robust translation is not necessarily an advantage, since the translational machinery could be depleted, leading to misfolded proteins (42, 43). To avoid this, the proportion of optimal and rare codons should be determined to obtain a codon optimization strategy where the number of natural codons in the host is maintained. Codon harmonization is already an optimized method, however, studies report that risks of rate-limiting translation and safety issues are of concern (43). Because of these risks, optimization is necessary especially when expressing mammalian derived proteins.

3.3.1.3 Regulatory elements, introns and polyadenylation signals

Transgene expression can be enhanced using several additional elements present in the cassette acting post-transcriptionally. Many cassettes contain a Woodchuck hepatitis virus Post-transcriptional Regulatory Element (WPRE) (Fig 3.4) , which facilitates cytoplasmatic accumulation and translation of mRNA, increasing transgene expression both *in vitro* as *in vivo* (37, 44). However, one has to be careful when high specificity is important, since this posttranscriptional enhancer can facilitate translation also in off-target cells (35). Additionally, introns are added to the expression cassette, often between the promoter and the transgene. A variety of introns exists, such as the SV40 intron, with the ability to increase transgene expression up to 80-fold (44). Since the polyadenylation of a transcript is not only necessary for nuclear export but also for translation and stabilizing mRNA, different boosting polyadenylation signals can be added to the expression cassette to optimize transgene expression. Most studies report the use of SV40 late or bovine growth hormone polyA signal sequences which increase transgene expression both *in vitro* and *in vivo*.

This is often combined with a SV40 late polyA signal enhancer placed upstream of the polyadenylation signal, facilitating this process even more (44).

3.3.1.4 Protein tag

When introducing a novel receptor or ion channel into target cells, one should be able to characterize the exact expression levels and location. Therefore, DREADDs, opsins or eLGICs are mostly fused to a fluorescent protein tag for visualization (45).

In most fundamental studies, intrinsically fluorescent protein tags are used since they become fluorescent after folding and no additional endogenous or exogenous fluorophore ligand is necessary. The most widely used fluorescent tag is Green Fluorescent Protein (GFP), isolated from the jellyfish *Aequorea Victoria*. GFP engineering led to the enhanced GFP, with improved brightness. Adjustments to the chromophore gave rise to fluorescent tags in the blue and yellow spectrum (46, 47). In this thesis, the mCherry tag was used. This is a monomeric red fluorescent protein (mRFP) initially derived from the naturally DsRed. mRFP has been engineered to produce fluorophores of different spectra with the mOrange and tdTomato being some commonly used examples (48). Although these fluorescent tags are widely used in both chemo- and optogenetic research, studies have been describing possible toxic effects due to subcellular localization and aggregation. Subretinal injections of the AAV-CAV-GFP viral vector induced toxicity due to overexpression of GFP (49). Similar toxicity was observed when administering plasmids carrying mCherry to HeLa cells or Xenopus embryos. The monomeric FusionRed seems to be equally efficient but has less tendency to aggregate and induce cytotoxicity (50). Next to the well described fluorophores, recently HA or FLAG tags are used. These epitopes are smaller in size which is beneficial as they leave more space available for the transgene and reduce the risk of disrupting the protein folding process (51).

3.3.2 Gene delivery approaches

3.3.2.1 Transgenic approaches

One transgenic technique uses the Tet-off system where a tetracycline transactivator protein (tTA) binds the tetracycline response element (TRE) which will induce expression of the transgene. Administration of tetracycline which binds tTA and inhibits its binding to TRE, will inhibit transgene expression. Practically, two transgenic lines are used. A transgenic mouse line that expresses the gene of interest under control of a TRE promoter is crossed with a transgenic line that expresses tTA under control of a cell-specific promoter.

This will lead to tTA binding to TRE, resulting in expression of the gene of interest only in the target cells (due to the use of the cell-specific promoter) (6, 18, 52). Another technique uses the combination of a transgenic line and a viral vector approach (described below), the Flip-excision (FLEX)-switch viral vector based on the Cre-lox recombination system. In this technique, the viral vector contains a construct where the transgene is reverse orientated and flanked by two pairs of heterotypic antiparallel LoxP recombination sites. This viral vector is injected in transgenic animals expressing Cre recombinase under control of a cell-type specific promoter. In the presence of Cre recombinase, the LoxP sites are removed and the transgene acquires the correct orientation (6, 53).

3.3.2.2 Viral vector approach

For gene delivery, different types of viral vectors can be used derived from modified herpes simplex viruses (HSV), lentiviral vectors and more commonly used adeno-associated virus (AAV) vectors and canine adenovirus (CAV) vectors (6).

The advantage of using HSV is its large packaging capacity (20kb), however it has been reported that the duration of transgene expression is insufficient. Lentiviral vectors are also commonly used in intracerebral gene therapy studies, with the ability of genome-integration as its main characteristic (54). Since both the AAV and CAV are used in this thesis, these two types of viral vectors will be discussed in more detail.

Using a viral vector approach to introduce a transgene is more translatable to human patients, and even in the setting of preclinical research more practical when compared to the labor-intensive use of transgenic lines. Depending on the research goal, different administration routes can be selected. Most research focused on targeting the CNS is using a direct intraparenchymal delivery of viral vector. Expression of the transgene is influenced by the serotype, volume, and even purification method of the viral vector. Some serotypes (AAV9, AAV.Rh10 and AAV.Rh8) have the ability to cross the BBB, and can be delivered intravenously to obtain a wide distribution pattern in CNS. Additionally, viral vectors can be injected in the cerebrospinal fluid (CSF) by administration in the lateral ventricle, intrathecal, subpial, or via the cisterna magna. In the last two described administration routes, age plays an important role, where injection in the neonate phase might induce a more widespread gene delivery(45).

Adeno-associated virus (AAV) vector

The wild-type adeno-associated virus (AAV) was discovered in the 1960s. Six different types of AAV (1-6) are present in primates, with AAV2 being isolated from human patients. Studying its biology, scientists were able to clone the AAV2 sequence into a plasmid, without knowing that the derived viral vector would become one of the most important platforms for gene therapy today. AAV is a virus from the *Parvoviridae* family (genus Dependoviridae) and consists of single stranded DNA (4.7 kb) flanked by two inverted terminal repeats (ITR). Additionally, the non-enveloped icosahedral capsid contains Rep genes required for replication and Cap genes necessary for the formation of the different subunits of the capsid and an assembly activating protein (AAP) for virion assembly. In its wild-type form, the AAV is dependent on a helpervirus (Adenovirus or Herpesvirus) to start a lytic productive pathway for replication and encapsidation. Lysis of the host cell by the helpervirus will lead to release of the AAV virions. In absence of a helper virus, the AAV will integrate in a site-specific manner in the host genome (AAVS1 on the human chromosome 19).

To form an AAV viral vector, the AAV protein coding sequences are removed to insert the transgene expression cassette (max 5kb) between the two inverted terminal repeats (ITR), necessary for guiding genome replication and packaging during manufacturing of AAV viral vector. The viral genes responsible for replication and integration are removed, reducing cytotoxicity, immune response and the chance of genome integration (34). AAVs are widely used for intracerebral gene delivery because of its long-term gene expression lasting up to months or even years (55). In comparison to other viral vectors, the AAV viral vector is very resistant to heat, pH changes, and is safe to use in the CNS. Low toxicity is reported with little activation of astrocytes or immune response although a humoral response can be present as neutralizing antibodies have been reported, even in human patients (55-57). Different serotypes are characterized with every one of them having certain advantages (e.g. AAV5 will transduce neurons in a wider area compared to AAV2). AAV2 is highly characterized and used in the field of neuroscience because of its preference for neurons (56). The serotype of an AAV determines the capsid protein sequence and affects the receptor-mediated entry of the viral particle into the target cell due to receptor interactions. Often cross-packaging of different AAV genomes into different AAV serotypes is used to optimize the tropism (cell type selective infection ability) and in this way increase cell-type specific expression (55, 58-60).

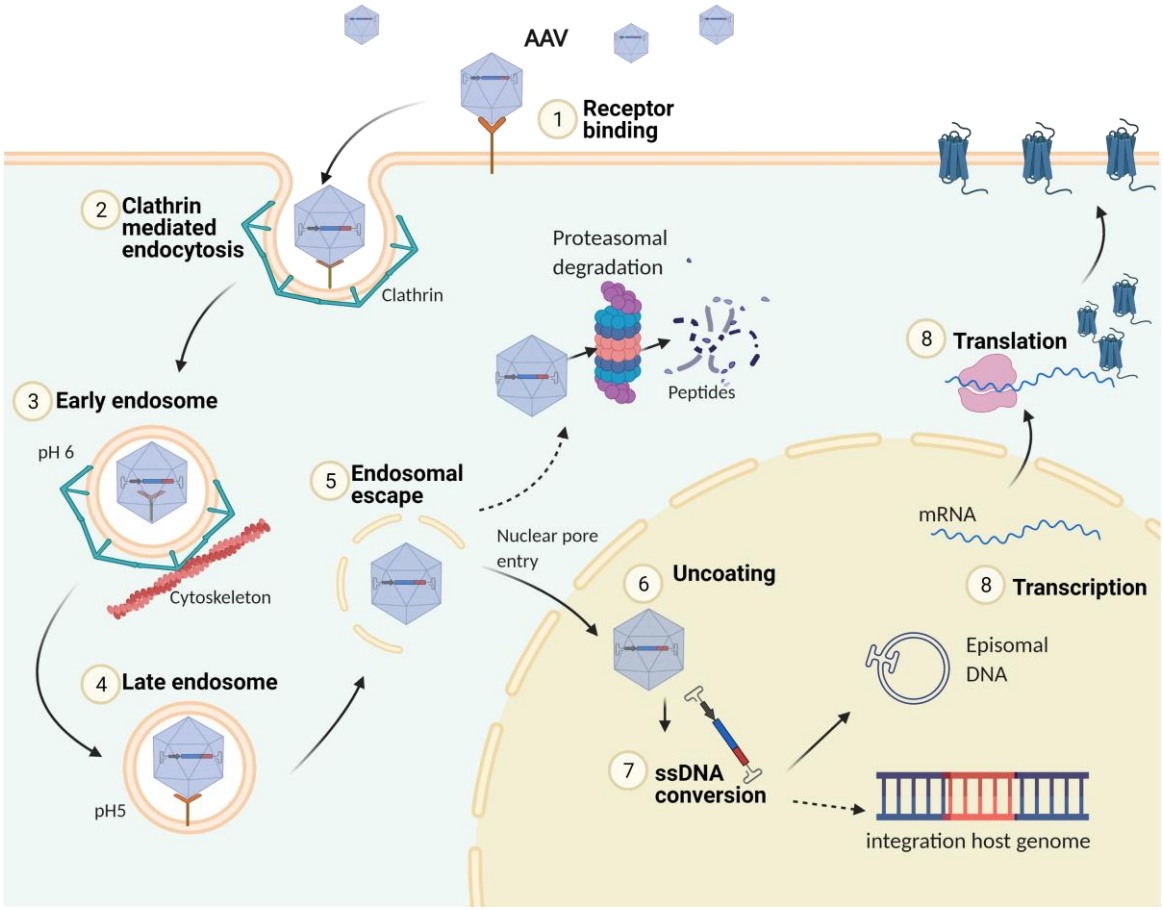

Figure 3.5 Representation of the transduction pathway of AAV vector particle. (1) The AAV virion will bind cell surface receptors followed by clathrin-mediated endocytosis (2). The endosome containing the AAV virion traffics through the cytosol and undergoes maturation under low pH conditions (3-4). Conformational changes induce endosomal escape (5), from which the virion enters the nucleus through the nuclear pore followed by uncoating (6) and conversion of the single stranded DNA to double stranded DNA (7). Transcription is followed by translation (8-9) and transport to the membrane depending on signalling sequences. Only a small percentage of the DNA can integrate in the host genome DNA. Some viral particles undergo proteolysis after endosomal escape, breaking down the particle into particles which can be recognised by the host immune cells. Figure created with BioRender.com

Fig 3.5 shows the transduction pathway of an AAV viral vector particle starting with the entry to the cell, mediated by binding of the particle to receptors present on the surface of the host cell, mainly heparin sulfate proteoglycan (HSPG) receptors (58). Co-factors such as αvβ5 integrins present on the target cells are responsible for endocytosis of the viral particle (59). Endocytosis takes place and the viral particles are transported along the cytoskeletal network to the nucleus. The viral particle escapes and enters the cytosol through acidification of the endosome. Accumulation in the perinuclear zone is either followed by entry in the nucleus through the nuclear pore complex followed by uncoating or by proteolysis by the proteasome forming peptides which can be recognized by the immune system (60).

Single stranded DNA is converted to double stranded DNA, which is a rate-limiting step, followed by circularization and formation of concatemers to stabilize the genome as episomal DNA and achieve persisting gene expression in (post)mitotic cells. However as described above, a small portion of the AAV genome can integrate in the genome (34) (Fig.3.5). Unfortunately, liver studies in mice reported AAV genome insertion leading to chromosomal deletions and loss-of-function mutagenesis (61-63).

Canine adenovirus type 2 (CAV2) vector

At the end of the 20th century, scientists were searching for viral technology of non-human origin to circumvent potential immune-related side-effects as observed when using adenovirus viral vectors. The Canine adenovirus type 2 (CAV2) viral vector was the first non-human viral vector that was sequenced and produced, initially as a vaccine for domestic dogs. However, during this production process it was discovered that CAV2 viral vectors have a high affinity for neurons after administration in the olfactory region of rats and even after intramuscular administration. Because of this preferential affinity for neurons and weak recognition by the innate immune response in human patients and the adaptive immune response in rats, it quickly became clear that this viral vector tool would be commonly used (64, 65). The CAV2, a non-human adenoviridae virus with double-stranded DNA, contains a non-enveloped capsid and to make it replication defective, the early gene region 1 (E1) is removed. CAV2 viral vectors, with a packaging capacity of 30kb, can transduce neurons both at the site of injection (cell body entry) or induce transduction through retrograde axonal transport (66) after intracerebral injection in rodents (65).

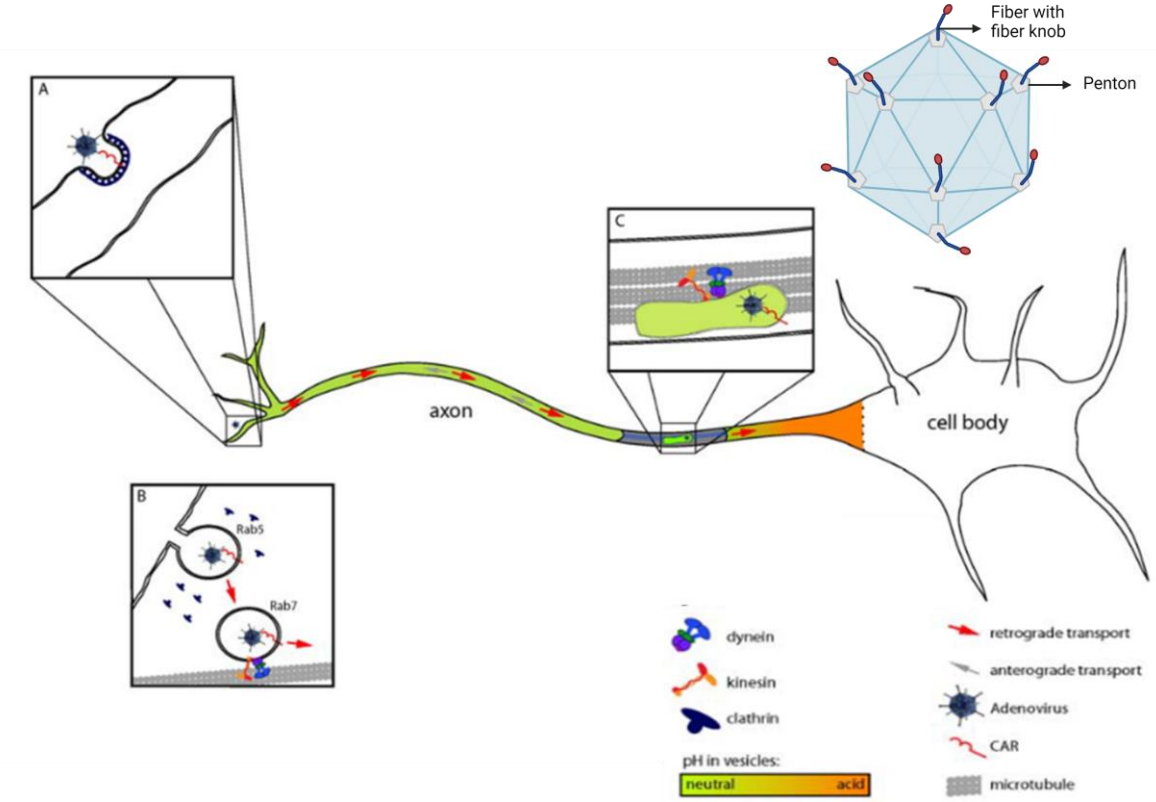

Figure 3.6 Schematic representation of CAV2 viral particle entry and retrograde transport. CAV2 particle graphic in top right corner, characterised by icosahedral shape and penton base with fiber and fiber knob. A. Binding of particle on CAR receptor. B. Clathrin-mediated endocytosis of viral particle and CAR receptor, with maturation of Rab5 to Rab7 endosome initiating transport along the axon. C. Transport is mediated through dynein and kinesin, with a favour for retrograde transport to the nucleus. Figure adjusted from Bru et al., with permission of the Creative Common License.

As shown in Figure 3.6, CAV2 particles have, similar to the AAV, an icosahedral capsid with on its surface a hexon, penton base, and fiber. These particles enter the cell through binding of its C-fiber on the coxsackievirus and adenovirus receptor (CAR) on the axons of neurons. Upon CAV2 particle binding of CAR, the receptor is co-internalized via lipid rafts, dynamin and actin, important factors for lysosome targeting and degradation. Post-translational modifications present on the CAR cytoplasmatic tail are important for CAV2 internalization and engagement. Internalization and permeabilization occurs in clathrin-coated pits. Entry in the cell and further transport occurs in endosomes with neutral pH, maturation of the endosome from Rab5 to Rab7 starts the pathway of axonal transport. The viral particles recruit dynein, a microtubules element responsible for retrograde transport from the nerve terminal to the cell body to start the transport to the nucleus (67).

3.4 Chemogenetic and optogenetic modulation of locus coeruleus

Chemogenetics can be used to selectively modulate the activity of the LC and assess its modulatory effects on different functions such as memory, pain and learning behavior. Vazey et al. was one of the first to describe the effect of chemogenetic modulation of the LC in anesthetized rats investigating its wakefulness promoting character. An AAV2/9 viral vector carrying the noradrenergic specific PRSx8 promoter to induce high and specific expression of the excitatory hM3Dq DREADD receptor (98% $DBH^+/mCherry^+$) was used to determine the effect of CNO administration on LC firing frequency and cortical EEG under isoflurane anesthesia. Both local and systemic application of CNO (0.1 or 1 and 10 mg/kg respectively) increased LC activity up to 200% above baseline levels (as confirmed by extracellular unit recording), resulting in clear cortical arousal defined by decreased delta and increased theta activity and increased emergence from general anesthesia. No effect on general locomotion was observed, indicating a DREADD-specific effect (39). Because of its high transduction efficiency, the AAV2/9-PRSx8-hM3Dq-mCherry viral vector, first described by Vazey and Aston-Jones, is used in multiple studies investigating the modulatory effect of LC on memory and behavior. However not in all studies the same transduction levels were observed, possibly explained by the difficult position of LC in the deep brainstem.

Multiple studies describe the effect of chemogenetic modulation of LC on behavior both in rat and mice. McCall et al. has shown that LC activation is necessary to induce stress-induced anxiety in mice by transducing LC with an AAV5 viral vector carrying the inhibitory hM4Di DREADD (68). A defensive response is observed in stressful threat situations due to LC-mediated modulation of the amygdala and colliculus superior. Chemogenetic inhibition of LC induced by injection of AAV2/9-DIO-hM4Di viral vector in Th:Cre mice leads to lower looming responses in stress animals after systemic administration of CNO (0.3 mg/kg) by modulation of the colliculi superiori (69, 70). An enhanced freezing response is observed in rats expressing the excitatory hM3Dq DREADD in LC after administration of CNO, due to its effect on the central amygdala (71). These effects are noradrenergic as confirmed by application of adrenergic receptor agonists or antagonists, stating α_2- and β-adrenoreceptor dependent mechanisms.

Chemogenetic LC modulation has also been used to define anxiety and pain. It is known that pain activates LC which in its turn activates the basolateral amygdala in a β-receptor dependent manner, leading to anxiety and hypersensitivity to aversive experiences. Chemogenetic inhibition of LC reverses this anxiety response in animals with pain as observed by longer times spent in the center of an open field test (72).

Hirschberg et al. uses a CAV viral vector to induce the expression of an engineered ligand gated ion channel PSAM in LC using the same PRSx8 promoter as Vazey and Aston-Jones. Chemogenetic LC axonal activation in the spinal cord by systemic PSEM administration induces analgesic effects in a rat model for neuropathic pain (73).

Because of the high noradrenergic innervation of the hippocampus, the effect of LC modulation on memory is widely studied. Chemogenetic activation of LC axonal projections in the mPFC has led to enhanced performance in the attentional set shifting task because increased tonic LC activity increases exploratory behavior (74). This increase in exploratory behavior and enhancement of disengagement from current behavior also leads to impaired behavior in the foraging task (75). These chemogenetic studies prove that tonic LC activity can modulate behavior and memory depending on the hippocampal-dependent task that is presented. Fukabori et al. used the INTENS technology to chemogenetically activate LC by application of odor ligands to increase LC firing frequency by influx of cations, and induce a sustained increase in NA release in the amygdala due to Ca^{2+} influx and consecutive activation of the Ca-calmodulin complex and protein kinase C mediated trafficking mediating TH gene expression and sustained NA biosynthesis (11).

3.4.1 Modulation of LC and memory

LC plays an important role in memory and disorders such as Alzheimer's disease and Down syndrome. Chemogenetic LC modulation is explored to further determine the pathophysiological characteristics and possible future therapeutic approaches. In a mouse model for Down syndrome (DS), chemogenetic LC activation using hM3Dq expression and CNO (0.03 mg/kg) administration, increased the performance in the novel object recognition task, a hippocampal-dependent memory task (76). The group of Hamlett et al. proved by chemogenetic inhibition of LC, that LC degeneration and dysregulation of adrenergic receptors in the hippocampus, induces microglia activation and inflammation, and that intact LC signaling is important for learning in this DS model (77). Rorabaugh et al. restored reversal learning of rats with Alzheimer's disease pathology by chemogenetically activating LC neurons. Due to the increased tonic LC activity, the behavioral flexibility increases which improves this type of learning, however, the acquisition decreased because of the increase in exploration and lack of focus on the current task (78).

3.4.2 Modulation of LC and pain

Other studies have explored the effect of optogenetic modulation of LC neurons *in vitro* and *in vivo* on nociception, memory encoding, behavior and modulation of cardiac vagal neurons. Optoactivation of LC using CAV viral vectors has defined a module of pontospinal projecting LC neurons with specific electrophysiological characteristics (slower afterdischarge and shorter action potential) that play a role in nociception and have analgesic properties (79). Optogenetic activation of LC during the hindpaw thermal withdrawal response characterized discrete subpopulations of LC-NA neurons with a bidirectional response on thermal nociception: pro and antinociceptive responses (80).

3.4.3 Modulation of LC in learning behavior

Xiang et al. used optogenetics as an identification tool in a behavioral study. Opto-identification and optoactivation of LC neurons was performed during a T maze task, describing an acceleration in task related efforts and increased performance. This reflects that LC activity is necessary for mobilization of resources and responding to challenging situations by inducing a network reset (81). Different studies show the positive effect of LC optoactivation and memory consolidation. Increased LC activity during sleep interferes with non-rapid eye movement (NREM) and REM related EEG signatures important for induction of synaptic plasticity and incorporation of new information into existing memory circuits, impairing hippocampal spatial encoding. Vazey et al. shows that phasic optoactivation of LC neurons induces event-related potentials in the cortex necessary for cortical encoding of salient stimuli (82). It is clear that optogenetic modulation of LC allows determination of dynamics in types of memory and learning processes. Glennon et al. paired LC activation with previously unrewarded tones and observed an accelerated rate of learning and response in the perceptual task. Increased LC activity enhances perceptual performance of rats in a tactile discrimination task due to increased thalamic sensory processing in response to LC-NA modulation of intrathalamic circuit dynamics (83). Optogenetic silencing of LC impaired reversal learning and extra dimensional set shifting in the attentional set shifting task, describing the modulatory effect of LC-NA neurons on prefrontal cortex activity affecting cognitive flexibility (84). Optoactivation of LC neurons in mice showed that increased LC activity is necessary for the acceleration of defensive responses, as confirmed by chemogenetic inhibition (described above) (69). Wang et al described the effect of ChR2-mediated LC activation on cardiac vagal neurons, where increased LC depolarization leads to increased inhibitory transmission to these neurons which generate parasympathetic activity to the heart inducing bradycardia (85).

3.5 Validation of transduction efficiency and DREADD functionality

As the functionality of the expressed receptor is partly defined by the expression level, the transduction efficiency and functional expression can be assessed using different techniques both *in vitro* as *in vivo*, awake and under anesthesia, or *post mortem*.

3.5.1 Histology

3.5.1.1 Immunohistochemical detection of transgene

A first phase in chemogenetic studies is to optimize the expression levels. To achieve high transduction efficiency, pilot trials are often performed to titrate the volume and titer of the viral vector. To examine the expression levels, animals are in general sacrificed 2-3 weeks after viral vector administration to isolate the brains. Subsequently, immunohistochemistry (immunofluorescence stainings) is performed using primary and secondary antibodies against the target cells and genetically modified receptor coupled to a fluorescent tag. Commonly a cell count is performed to determine the expression level and specificity, but also projection areas of the targeted cells can be examined.

3.5.1.2 C-Fos staining

To molecularly validate chemo- or optoactivation of LC neurons, the expression of the neural activity marker c-Fos in LC-NA neurons can be assessed *post mortem* using immunohistochemistry. C-Fos is an immediate early gene (IEG) and functions as a transcription factor to regulate downstream target genes. However, c-Fos is mostly used in neuroscience research as a marker of neural activity in response to stimuli. The expression of IEG's is fast and due to low basal levels, the signal-to-noise ratio in response to a given stimulus is high (86). The expression of c-Fos localized in LC neurons, in response to administration of a ligand to activate chemogenetic receptors or to light in case of opsins, is commonly used as a validation step in literature. In studies performing chemogenetic or optogenetic modulation of LC, the ligand or light train is administered between 75 and 120 min before transcardial perfusion and collection of the brain (68, 69, 71, 72, 75, 78, 87), (88). An immunofluorescence staining is performed to colocalize the c-Fos expression with TH or DBH^+ LC-NA neurons or with the mCherry or eGFP tag coupled to the transduced receptor.

3.5.2 Electrophysiological recordings

3.5.2.1 Patch clamp technique

In vitro voltage clamp techniques are used to validate the functionality and safety of the expression of modified receptors or opsins. Li and Pickering first injected rats with CAV-PRS-hM3Dq-mCherry viral vector to induce the expression of ChR2 in LC-NA neurons. To test for possible toxicity of the viral vector, the expression of the opsin, and optoactivation, voltage clamp experiments were performed 2 weeks after transduction. No changes in the intrinsic properties of the neurons were observed compared to control animals and a clear one-to-one action potential was observed after light stimulation with frequency of up to 40 Hz (79).

3.5.2.2 In vivo extracellular unit recording

A direct method to validate the functionality of the expressed receptor or ion channel, is *in vivo* extracellular unit recording, where the effect of receptor/channel activation on the firing frequency of a single neuron is measured. Vazey et al. tested the effect of multiple doses of CNO (0.1-10 mg/kg) and different administration routes (systemic i.p. versus local) on the firing frequency of LC-NA neurons transduced with the excitatory DREADD receptor under isoflurane anesthesia. A clear increase in firing frequency was observed in hM3Dq expressing animals compared to baseline activity, whereas this effect was absent in control animals (39). *In vivo* extracellular unit recording of LC neurons was also performed to test the functionality of systemic administration of PSEM to activate eLGIC PSAM expressed in noradrenergic neurons of rats under anesthesia. A 10-fold increase in firing frequency was observed compared to baseline (73). As the group of Fukabori et al. is the first to describe the use of INTENS to modify LC activity, unit recording was performed to assess the functional response to local or systemic administration PhAc in mice (11).

In vivo extracellular unit recording is also used in preclinical studies optogenetically modifying LC activity to assess the functional expression. Different light paradigms (tonic versus phasic, continuous versus pulsed) were tested to determine whether they can drive LC activity across physiological relevant frequencies and reproduce innate firing patterns (79, 80, 82).

3.5.3 Pupillometry

The LC has inhibitory connections with the Edinger-Westphal nucleus, responsible for pupil constriction. When LC is activated, NA will be released and acts on α_2-adrenergic receptors leading to pupil dilatation (89). LC-mediated pupil dilatation is being used as an indirect measurement of increased LC activity in human patients (90), but also in preclinical studies performing chemogenetic activation of LC.

Zerbi et al. increased LC activity by administering clozapine, which binds hM3Dq DREADD receptors expressed in LC of mice and used pupillometry as a first validation step to ensure that their chemogenetic approach indeed activated LC neurons (87). This technique has the possibility to be used both in combination with chemo- or optogenetics, as the animal is anesthetized and the pupil diameter is recorded using a camera and post-processed in tools such as Matlab (87).

3.5.4 Behavioral tests

3.5.4.1 Emergence test

The emergence test is used as a functional outcome test to indirectly measure LC activation. As described in section 2.3, the LC is known to promote wakefulness through its influence on other structures involved in sleep-wake transitioning (89). To assess in *in vivo* animals whether chemo- or optoactivation after transduction of LC is successful enough to activate LC neurons and induce increased firing frequencies, the emergence test can be performed. Here, animals are first deeply anesthetized and chemo- or optogenetically activated after 20 minutes. Twenty minutes after this activation, anesthesia is stopped and it is expected that chemo- or optogenetically activated animals expressing an excitatory modified GPCR, eLGIC or opsin, have a faster emergence from anesthesia. This validation technique has been used by Vazey et al. who chemogenetically activated the LC of rats injected with the AAV2/9-PRSx8-hM3Dq-mCherry using systemic administration of CNO (1 mg/kg, i.p.) and observed an acceleration in emergence (39). The same test was performed to validate whether optoactivation of LC neurons expressing ChR2 is able to induce changes in behavior. A brief sleep to wake transition was observed in response to brief unilateral light pulses with clear loss of delta power in the EEG up to 6 months after viral vector injection confirming a stable functional ChR2 expression pattern (79, 80, 82).

3.5.4.2 Open field test (OFT)

An indirect behavioral response of LC activation is increased anxiety. This can be tested in an open field test, where animals with high anxiety spend less time in the center of the open field. This is again an indirect measure of LC activation and can be performed in animals where the LC is chemo- or optogenetically modified. In literature, a variety of studies use this behavioral test to validate the functionality of the DREADD expression. Chemogenetic activation of LC by systemic administration of the ligand (i.e. clozapine) leads to increased anxiety and decreased locomotor activity compared to control animals that do not express the hM3Dq receptor.

Often this test is combined with a rotarod test, where the DREADD ligand or saline is injected to test motor impairment and confirm that the decreased locomotor activity in the OFT is due to increased LC activity (87). Janitzky et al. performed an OFT before the experiment to assess whether unilateral optogenetic inactivation of LC leads to behavioral changes or increased anxiety (84).

3.5.5 Noradrenaline detection

3.5.5.1 Microdialysis

To measure extracellular noradrenaline levels in projection areas of LC, microdialysis, an invasive technique both used for delivery and sampling, can be used. A microdialysis probe is implanted in the target area and perfused with artificial cerebrospinal fluid (aCSF) which exits the tube of the probe through the semipermeable membrane. Small molecules will pass the semipermeable membrane via the principle of passive diffusion between the dialysate and the extracellular environment. The flow of molecules is determined by the concentration gradient, as noradrenaline is not present in the perfusion fluid, molecules will move across the semipermeable membrane and can be collected. Typically, a few baseline samples are collected before LC activation to compare changes in NA concentration relative to baseline levels (91). This technique can be used both in combination with chemo- or optomodulation of the locus coeruleus. Activation of LC neurons using an odor sensitive eLGIC (INTENS) and determination of changes in NA levels in the anterior cingulate cortex and amygdala was performed in mice after administration of different concentrations of Phac delivered in the LC through a cannula or through systemic administration, where the highest concentration (0.6%) increased NA levels in a sustained manner up to 233% above baseline levels (11). Microdialysis was used to sample extracellular fluid in the prefrontal cortex after delivery of high-frequency light pulses in the LC to activate noradrenergic neurons, resulting in a decreased NA level compared to baseline, stating that this non-physiological stimulation depleted NA in the noradrenergic terminals. The disadvantage of this sampling technique, especially in combination with optogenetic modulation of the LC, is the low temporal resolution of several minutes. In the study of Carter et al. they were unable to detect NA changes over 10-15s of LC-stimulation to correspond this to the observed behavioral arrest. They hypothesized that due to the temporal resolution an initial rapid increase in NA was not detected as it was followed by a decrease due to local breakdown at the synapse or the inability of LC to restore NA while firing at frequencies above baseline levels.

An alternative for microdialysis is voltammetry which has a higher temporal resolution but lacks good distinction between the different catecholamines (92).

3.5.5.2 Ultra-high-performance liquid chromatography (UHPLC)

To indirectly measure increases/decreases in NA levels in LC target structures after chemo- or optogenetic modulation of LC neurons, UHPLC coupled with electrochemical detection can be used. After modulation of LC neurons using the appropriate ligand or light pulse, animals are sacrificed and brains are collected on ice. Target structures of interest such as hippocampus or cortex can be isolated to determine NA level changes in response to LC activation. This approach mainly determines neurotransmitter turnover, thus neuronal activity, as measurement in whole tissue cannot make a differentiation between intra- or extracellular neurotransmitter levels. Zerbi et al. used this approach to determine NA and dopamine turnover in target regions such as the hippocampus and its relation to observed increases in interconnectivity measured using fMRI, in response to chemogenetic LC activation (87).

Bibliography

1. Deisseroth K. Optogenetics: 10 years of microbial opsins in neuroscience. Nat Neurosci. 2015;18(9):1213-25.

2. Nagel G, Szellas T, Huhn W, Kateriya S, Adeishvili N, Berthold P, et al. Channelrhodopsin-2, a directly light-gated cation-selective membrane channel. Proceedings of the National Academy of Sciences, 2003, 100.24: 13940-13945.

3. Fenno L, Yizhar O, Deisseroth K. The development and application of optogenetics. Annu Rev Neurosci. 2011;34(1):389-412.

4. Boyden ES, Zhang F, Bamberg E, Nagel G, Deisseroth K. Millisecond-timescale, genetically targeted optical control of neural activity. Nat Neurosci. 2005;8(9):1263-8.

5. Gradinaru V, Thompson KR, Deisseroth K. eNpHR: a Natronomonas halorhodopsin enhanced for optogenetic applications. Brain Cell Biol. 2008;36(1-4):129-39.

6. Roth BL. DREADDs for Neuroscientists. *Neuron*, 2016, 89.4: 683-694.

7. Sternson SM, Roth BL. Chemogenetic tools to interrogate brain functions. Annu Rev Neurosci. 2014;37(1):387-407.

8. Slimko EM, McKinney S, Anderson DJ, Davidson N, Lester HA. Selective Electrical Silencing of Mammalian Neurons In Vitro by the Use of Invertebrate Ligand-Gated Chloride Channels. Journal of Neuroscience, 2002, 22.17: 7373-7379.

9. Zemelman BV, Nesnas N, Lee GA, Miesenbö G. Photochemical gating of heterologous ion channels: Remote control over genetically designated populations of neurons. Proceedings of the National Academy of Sciences, 2003, 100.3: 1352-1357.

10. Magnus CJ, Lee PH, Atasoy D, Su HH, Looger LL, Sternson SM. Chemical and genetic engineering of selective ion channel-ligand interactions. Science. 2011;333(6047):1292-6.

11. Fukabori R, Iguchi Y, Kato S, Takahashi K, Eifuku S, Tsuji S, et al. Enhanced emotional memory retrieval by chemogenetic activation of locus coeruleus norepinephrine neurons. bioRxiv. 2020:831313.

12. Straders CD, Gaffneysb T, Suggn EE, Candelores R, Keysll R, Patchettn AA, et al. Allele-specific Activation of Genetically Engineered Receptors. The Journal of Biological Chemistry. 1991;266(1).

13. Coward P, Wada HG, Falk MS, Chan SDH, Meng F, Akil H, et al. Controlling signaling with a specifically designed G i-coupled receptor. Proceedings of the National Academy of Sciences, 1998, 95.1: 352-357.

14. Armbruster BN, Li X, Pausch MH, Herlitze S, Roth BL. Evolving the lock to fit the key to create a family of G protein-coupled receptors potently activated by an inert ligand. Proc Natl Acad Sci U S A. 2007;104(12):5163-8.

15. Urban DJ, Roth BL. DREADDs (designer receptors exclusively activated by designer drugs): chemogenetic tools with therapeutic utility. Annu Rev Pharmacol Toxicol. 2015;55(1):399-417.

16. Goossens MG, Boon P, Wadman W, Van den Haute C, Baekelandt V, Verstraete AG, et al. Long-term chemogenetic suppression of seizures in a multifocal rat model of temporal lobe epilepsy. Epilepsia. 2021;62(3):659-70.

17. Desloovere J, Boon P, Larsen LE, Merckx C, Goossens MG, Van den Haute C, et al. Long-term chemogenetic suppression of spontaneous seizures in a mouse model for temporal lobe epilepsy. Epilepsia. 2019;60(11):2314-24.

18. Zhu H, Roth BL. DREADD: a chemogenetic GPCR signaling platform. Int J Neuropsychopharmacol. 2014;18(1):1-6.

19. Guettier JM, Gautam D, Scarselli M, Ruiz de Azua I, Li JH, Rosemond E, et al. A chemical-genetic approach to study G protein regulation of beta cell function in vivo. Proc Natl Acad Sci U S A. 2009;106(45):19197-202.

20. Gomez JL, Bonaventura J, Lesniak W, Mathews WB, Sysa-Shah P, Rodriguez LA, et al. Chemogenetics revealed: DREADD occupancy and activation via converted clozapine. Science. 2017;357(6350):503-7.

21. Jendryka M, Palchaudhuri M, Ursu D, van der Veen B, Liss B, Katzel D, et al. Pharmacokinetic and pharmacodynamic actions of clozapine-N-oxide, clozapine, and compound 21 in DREADD-based chemogenetics in mice. Sci Rep. 2019;9(1):4522.

22. Mahler SV, Aston-Jones G. CNO Evil? Considerations for the Use of DREADDs in Behavioral Neuroscience. Neuropsychopharmacology. 2018;43(5):934-6.

23. MacLaren DA, Browne RW, Shaw JK, Krishnan Radhakrishnan S, Khare P, Espana RA, et al. Clozapine N-Oxide Administration Produces Behavioral Effects in Long-Evans Rats: Implications for Designing DREADD Experiments. eNeuro. 2016;3(5):219-16.

24. Manvich DF, Webster KA, Foster SL, Farrell MS, Ritchie JC, Porter JH, et al. The DREADD agonist clozapine N-oxide (CNO) is reverse-metabolized to clozapine and produces clozapine-like interoceptive stimulus effects in rats and mice. Sci Rep. 2018;8(1):3840.

25. Raper J, Morrison RD, Daniels JS, Howell L, Bachevalier J, Wichmann T, et al. Metabolism and Distribution of Clozapine-N-oxide: Implications for Nonhuman Primate Chemogenetics. ACS Chem Neurosci. 2017;8(7):1570-6.

26. Ilg AK, Enkel T, Bartsch D, Bahner F. Behavioral Effects of Acute Systemic Low-Dose Clozapine in Wild-Type Rats: Implications for the Use of DREADDs in Behavioral Neuroscience. Front Behav Neurosci. 2018;12:173.

27. Wenthur CJ, Lindsley CW. Classics in chemical neuroscience: clozapine. ACS Chem Neurosci. 2013;4(7):1018-25.

28. Weston M, Kaserer T, Wu A, Mouravlev A, Carpenter JC, Snowball A, et al. Olanzapine: A potent agonist at the hM4D(Gi) DREADD amenable to clinical translation of chemogenetics. Sci Adv. 2019;5(4):eaaw1567.

29. Upright NA, Baxter MG. Effect of chemogenetic actuator drugs on prefrontal cortex-dependent working memory in nonhuman primates. Neuropsychopharmacology. 2020;45(11):1793-8.

30. Thompson KJ, Khajehali E, Bradley SJ, Navarrete JS, Huang XP, Slocum S, et al. DREADD Agonist 21 Is an Effective Agonist for Muscarinic-Based DREADDs in Vitro and in Vivo. ACS Pharmacol Transl Sci. 2018;1(1):61-72.

31. Goutaudier R, Coizet V, Carcenac C, Carnicella S. DREADDs: The Power of the Lock, the Weakness of the Key. Favoring the Pursuit of Specific Conditions Rather than Specific Ligands. eNeuro. 2019;6(5):171-90.

32. Bonaventura J, Eldridge MAG, Hu F, Gomez JL, Sanchez-Soto M, Abramyan AM, et al. High-potency ligands for DREADD imaging and activation in rodents and monkeys. Nat Commun. 2019;10(1):4627.

33. Nagai Y, Miyakawa N, Takuwa H, Hori Y, Oyama K, Ji B, et al. Deschloroclozapine, a potent and selective chemogenetic actuator enables rapid neuronal and behavioral modulations in mice and monkeys. Nat Neurosci. 2020;23(9):1157-67.

34. Wang D, Tai PWL, Gao G. Adeno-associated virus vector as a platform for gene therapy delivery. Nat Rev Drug Discov. 2019;18(5):358-78.

35. Castle MJ, Turunen HT, Vandenberghe LH, Wolfe JH. Controlling AAV Tropism in the Nervous System with Natural and Engineered Capsids. Methods Mol Biol. 2016;1382:133-49.

36. Boulaire J, Balani P, Wang S. Transcriptional targeting to brain cells: Engineering cell type-specific promoter containing cassettes for enhanced transgene expression. Adv Drug Deliv Rev. 2009;61(7-8):589-602.

37. Fitzsimons HL, Bland RJ, During MJ. Promoters and regulatory elements that improve adeno-associated virus transgene expression in the brain. Methods. 2002;28(2):227-36.

38. Hwang DY, Carlezon WA, Jr., Isacson O, Kim KS. A high-efficiency synthetic promoter that drives transgene expression selectively in noradrenergic neurons. Hum Gene Ther. 2001;12(14):1731-40.

39. Vazey EM, Aston-Jones G. Designer receptor manipulations reveal a role of the locus coeruleus noradrenergic system in isoflurane general anesthesia. Proc Natl Acad Sci U S A. 2014;111(10):3859-64.

40. Hwang DY, Hwang MM, Kim HS, Kim KS. Genetically engineered dopamine beta-hydroxylase gene promoters with better PHOX2-binding sites drive significantly enhanced transgene expression in a noradrenergic cell-specific manner. Mol Ther. 2005;11(1):132-41.

41. Sjulson L, Cassataro D, DasGupta S, Miesenbock G. Cell-Specific Targeting of Genetically Encoded Tools for Neuroscience. Annu Rev Genet. 2016;50:571-94.

42. Fath S, Bauer AP, Liss M, Spriestersbach A, Maertens B, Hahn P, et al. Multiparameter RNA and codon optimization: a standardized tool to assess and enhance autologous mammalian gene expression. PLoS One. 2011;6(3):e17596.

43. Mauro VP, Chappell SA. A critical analysis of codon optimization in human therapeutics. Trends Mol Med. 2014;20(11):604-13.

44. Powell SK, Rivera-Soto R, Gray SJ. Viral expression cassette elements to enhance transgene target specificity and expression in gene therapy. Discov Med. 2015;19(102):49-57.

45. Haery L, Deverman BE, Matho KS, Cetin A, Woodard K, Cepko C, et al. Adeno-Associated Virus Technologies and Methods for Targeted Neuronal Manipulation. Front Neuroanat. 2019;13:93.

46. Thorn K. Genetically encoded fluorescent tags. Mol Biol Cell. 2017;28(7):848-57.

47. Crivat G, Taraska JW. Imaging proteins inside cells with fluorescent tags. Trends Biotechnol. 2012;30(1):8-16.

48. Shaner NC, Campbell RE, Steinbach PA, Giepmans BN, Palmer AE, Tsien RY. Improved monomeric red, orange and yellow fluorescent proteins derived from Discosoma sp. red fluorescent protein. Nat Biotechnol. 2004;22(12):1567-72.

49. Khabou H, Cordeau C, Pacot L, Fisson S, Dalkara D. Dosage Thresholds and Influence of Transgene Cassette in Adeno-Associated Virus-Related Toxicity. Hum Gene Ther. 2018;29(11):1235-41.

50. Shemiakina, II, Ermakova GV, Cranfill PJ, Baird MA, Evans RA, Souslova EA, et al. A monomeric red fluorescent protein with low cytotoxicity. Nat Commun. 2012;3:1204.

51. Brizzard B. Epitope tagging. Biotechniques. 2008;44(5):693-5.

52. Alexander GM, Rogan SC, Abbas AI, Armbruster BN, Pei Y, Allen JA, et al. Remote control of neuronal activity in transgenic mice expressing evolved G protein-coupled receptors. Neuron. 2009;63(1):27-39.

53. Urban DJ, Roth BL. DREADDs (designer receptors exclusively activated by designer drugs): chemogenetic tools with therapeutic utility. Annu Rev Pharmacol Toxicol. 2015;55:399-417.

54. Simonato M, Bennett J, Boulis NM, Castro MG, Fink DJ, Goins WF, et al. Progress in gene therapy for neurological disorders. Nat Rev Neurol. 2013;9(5):277-91.

55. Lai CM, Lai YK, Rakoczy PE. Adenovirus and adeno-associated virus vectors. DNA Cell Biol. 2002;21(12):895-913.

56. McCown TJ. Adeno-associated virus (AAV) vectors in the CNS. Curr Gene Ther. 2005;5(3):333-8.

57. Xiao W, Chirmule N, Berta SC, McCullough B, Gao G, Wilson JM. Gene therapy vectors based on adeno-associated virus type 1. J Virol. 1999;73(5):3994-4003.

58. Summerford C, Samulski RJ. Membrane-associated heparan sulfate proteoglycan is a receptor for adeno-associated virus type 2 virions. J Virol. 1998;72(2):1438-45.

59. Asokan A, Hamra JB, Govindasamy L, Agbandje-McKenna M, Samulski RJ. Adeno-associated virus type 2 contains an integrin alpha5beta1 binding domain essential for viral cell entry. J Virol. 2006;80(18):8961-9.

60. Douar AM, Poulard K, Stockholm D, Danos O. Intracellular trafficking of adeno-associated virus vectors: routing to the late endosomal compartment and proteasome degradation. J Virol. 2001;75(4):1824-33.

61. Nakai H, Wu X, Fuess S, Storm TA, Munroe D, Montini E, et al. Large-scale molecular characterization of adeno-associated virus vector integration in mouse liver. J Virol. 2005;79(6):3606-14.

62. Nakai H, Montini E, Fuess S, Storm TA, Grompe M, Kay MA. AAV serotype 2 vectors preferentially integrate into active genes in mice. Nat Genet. 2003;34(3):297-302.

63. Deyle DR, Russell DW. Adeno-associated virus vector integration. Curr Opin Mol Ther. 2009;11(4):442-7.

64. Kremer EJ, Boutin S, Chillon M, Danos O. Canine adenovirus vectors: an alternative for adenovirus-mediated gene transfer. J Virol. 2000;74(1):505-12.

65. Del Rio D, Beucher B, Lavigne M, Wehbi A, Gonzalez Dopeso-Reyes I, Saggio I, et al. CAV-2 Vector Development and Gene Transfer in the Central and Peripheral Nervous Systems. Front Mol Neurosci. 2019;12:71.

66. Junyent F, Kremer EJ. CAV-2--why a canine virus is a neurobiologist's best friend. Curr Opin Pharmacol. 2015;24:86-93.

67. Bru T, Salinas S, Kremer EJ. An update on canine adenovirus type 2 and its vectors. Viruses. 2010;2(9):2134-53.

68. McCall JG, Al-Hasani R, Siuda ER, Hong DY, Norris AJ, Ford CP, et al. CRH Engagement of the Locus Coeruleus Noradrenergic System Mediates Stress-Induced Anxiety. Neuron. 2015;87(3):605-20.

69. Li L, Feng X, Zhou Z, Zhang H, Shi Q, Lei Z, et al. Stress Accelerates Defensive Responses to Looming in Mice and Involves a Locus Coeruleus-Superior Colliculus Projection. Curr Biol. 2018;28(6):859-71 e5.

70. Li L, Wang L. Modulation of Innate Defensive Responses by Locus Coeruleus-Superior Colliculus Circuit. 2018.

71. Gu Y, Piper WT, Branigan LA, Vazey EM, Aston-Jones G, Lin L, et al. A brainstem-central amygdala circuit underlies defensive responses to learned threats. Mol Psychiatry. 2020;25(3):640-54.

72. Llorca-Torralba M, Suarez-Pereira I, Bravo L, Camarena-Delgado C, Garcia-Partida JA, Mico JA, et al. Chemogenetic Silencing of the Locus Coeruleus-Basolateral Amygdala Pathway Abolishes Pain-Induced Anxiety and Enhanced Aversive Learning in Rats. Biol Psychiatry. 2019;85(12):1021-35.

73. Hirschberg S, Li Y, Randall A, Kremer EJ, Pickering AE. Functional dichotomy in spinal- vs prefrontal-projecting locus coeruleus modules splits descending noradrenergic analgesia from ascending aversion and anxiety in rats. Elife. 2017;6(Lc):e29808-e.

74. Cope ZA, Vazey EM, Floresco SB, Aston Jones GS. DREADD-mediated modulation of locus coeruleus inputs to mPFC improves strategy set-shifting. Neurobiol Learn Mem. 2019;161:1-11.

75. Kane GA, Vazey EM, Wilson RC, Shenhav A, Daw ND, Aston-Jones G, et al. Increased locus coeruleus tonic activity causes disengagement from a patch-foraging task. Cogn Affect Behav Neurosci. 2017;17(6):1073-83.

76. Fortress AM, Hamlett ED, Vazey EM, Aston-Jones G, Cass WA, Boger HA, et al. Designer receptors enhance memory in a mouse model of Down syndrome. J Neurosci. 2015;35(4):1343-53.

77. Hamlett ED, Ledreux A, Gilmore A, Vazey EM, Aston-Jones G, Boger HA, et al. Inhibitory designer receptors aggravate memory loss in a mouse model of down syndrome. Neurobiol Dis. 2020;134:104616.

78. Rorabaugh JM, Chalermpalanupap T, Botz-Zapp CA, Fu VM, Lembeck NA, Cohen RM, et al. Chemogenetic locus coeruleus activation restores reversal learning in a rat model of Alzheimer's disease. Brain. 2017;140(11):3023-38.

79. Li Y, Hickey L, Perrins R, Werlen E, Patel AA, Hirschberg S, et al. Retrograde optogenetic characterization of the pontospinal module of the locus coeruleus with a canine adenoviral vector. 2016. p. 274-90.

80. Hickey L, Li Y, Fyson SJ, Watson TC, Perrins R, Hewinson J, et al. Optoactivation of locus ceruleus neurons evokes bidirectional changes in thermal nociception in rats. J Neurosci. 2014;34(12):4148-60.

81. Xiang L, Harel A, Gao H, Pickering AE, Sara SJ, Wiener SI. Behavioral correlates of activity of optogenetically identified locus coeruleus noradrenergic neurons in rats performing T-maze tasks. Sci Rep. 2019;9(1):1361.

82. Vazey EM, Moorman DE, Aston-Jones G. Phasic locus coeruleus activity regulates cortical encoding of salience information. Proc Natl Acad Sci U S A. 2018;115(40):E9439-E48.

83. Rodenkirch C, Liu Y, Schriver BJ, Wang Q. Locus coeruleus activation enhances thalamic feature selectivity via norepinephrine regulation of intrathalamic circuit dynamics. Nat Neurosci. 2019;22(1):120-33.

84. Janitzky K, Lippert MT, Engelhorn A, Tegtmeier J, Goldschmidt J, Heinze HJ, et al. Optogenetic silencing of locus coeruleus activity in mice impairs cognitive flexibility in an attentional set-shifting task. Front Behav Neurosci. 2015;9(NOVEMBER):286.

85. Wang X, Pinol RA, Byrne P, Mendelowitz D. Optogenetic stimulation of locus ceruleus neurons augments inhibitory transmission to parasympathetic cardiac vagal neurons via activation of brainstem alpha1 and beta1 receptors. J Neurosci. 2014;34(18):6182-9.

86. Duman RS, Adams DH, Simen BB. Transcription factors as modulators of stress responsivity. Handbook of Stress and the Brain - Part 1: The Neurobiology of Stress. Techniques in the Behavioral and Neural Sciences. 15: Academic Press; 2005. p. 679-98.

87. Zerbi V, Floriou-Servou A, Markicevic M, Vermeiren Y, Sturman O, Privitera M, et al. Rapid Reconfiguration of the Functional Connectome after Chemogenetic Locus Coeruleus Activation. Neuron. 2019;103(4):702-18 e5.

88. Uematsu A, Tan BZ, Ycu EA, Cuevas JS, Koivumaa J, Junyent F, et al. Modular organization of the brainstem noradrenaline system coordinates opposing learning states. Nat Neurosci. 2017;20(11):1602-11.

89. Samuels ER, Szabadi E. Functional Neuroanatomy of the Noradrenergic Locus Coeruleus: Its Roles in the Regulation of Arousal and Autonomic Function Part I: Principles of Functional Organisation. 2008.

90. Joshi S, Li Y, Kalwani RM, Gold JI. Relationships between Pupil Diameter and Neuronal Activity in the Locus Coeruleus, Colliculi, and Cingulate Cortex. Neuron. 2016;89(1):221-34.

91. Chefer VI, Thompson AC, Zapata A, Shippenberg TS. Overview of brain microdialysis. Current protocols in neuroscience,47(1), 7-1.

92. Carter ME, Yizhar O, Chikahisa S, Nguyen H, Adamantidis A, Nishino S, et al. Tuning arousal with optogenetic modulation of locus coeruleus neurons. Nat Neurosci. 2010;13(12):1526-33.

Chapter 4 Rationale and Research aims

The locus coeruleus-noradrenaline (LC-NA) system modulates neuronal circuits throughout the brain, influencing different functions such as sleep, cognition, memory, and neuroplasticity. It is studied for its role in brain excitability and different neurological and psychiatric diseases such as epilepsy. Epilepsy is the second most common neurological disorder, characterized by the occurrence of spontaneous and recurrent epileptic seizures. Epilepsy affects 0.5-1% of the population and only 30% of these patients can be adequately treated with the currently available anti-seizure drugs (1). In patients with recurrent seizures, cognitive disorders and depression are common comorbidities affecting the quality of life enlarging the disease burden of epilepsy. Vagus nerve stimulation (VNS) is an approved neuromodulatory therapy for patients with refractory epilepsy and Major Depressive Disorder (2). Efficacy studies have shown a mean seizure frequency reduction between 25 and 55% with the presence of high inter-patient variability in efficacy (3), emphasizing the need for optimization and the lack of knowledge concerning the mechanism of action (MOA).

Experimental animal studies and anatomical arguments obtained by both our own group and others support the finding that the locus coeruleus (LC), might be (partly) responsible for the seizure and mood stabilizing effects observed with VNS. The LC is a small nucleus in the brainstem with widespread noradrenergic projections throughout the brain and receives a large portion of the vagal afferents (4). Animal experiments under anesthesia have revealed that short trains of VNS induce phasic bursts of LC neurons which increase in an intensity and duration dependent manner (5). Long-term VNS also increased the firing rate of LC neurons in a dose and time dependent manner (6, 7). Next to elevation of LC activity, an elevation in NA was observed using microdialysis after acute (8, 9) and chronic (7) VNS administration in LC projection areas such as the hippocampus and cortex. Selective lesioning of LC using neurotoxin DSP-4 negated the VNS-induced seizure suppressing and mood stabilizing effects (10, 11), emphasizing the role of LC in the MOA of the therapeutic effects of VNS. This positive correlation was also found in a patient study, recording P3 event related potentials as a measure for LC activation and its relation to VNS responders (12). Despite these arguments emphasizing the importance of LC activation in the MOA of VNS, it is still unclear how increased LC activation induces changes in hippocampal excitability and suppresses epileptic seizures and depressive symptoms. Our group has investigated the effect of VNS on hippocampal excitability extensively, indicating clear effects on evoked potentials in the dentate gyrus and hippocampal EEG (13, 14).

However, a clear conclusion about the underlying mechanism responsible for the therapeutic effects remained elusive, especially because of the recently discovered presence of VNS-induced hypothermia in freely moving rats, not present in human patients, making it hard to translate these findings to the clinic (15, 16).

Other groups have used direct modulation techniques to modulate LC activity and NA release to study its effect on hippocampal excitability, using electrical (17-21) or chemical stimulation (22-27) both *in vivo* and *in vitro*. These studies revealed an overall NA-induced long term potentiation of the population spike of hippocampal evoked potentials, which is mostly β-receptor mediated. However, depression of the excitability of the granular cells of the dentate gyrus was also observed, indicating the presence of contradictory results possibly due to the differences in specificity of the methods used to modulate a small brainstem nucleus enabling possible off-target effects. This highlights the need for a selective method to modulate LC activity to further unravel its role in brain excitability, more specifically hippocampal excitability and its role in the MOA of VNS.

Based on these findings, we aimed to use chemogenetics, a technique able to modulate specific brain structures with high cellular specificity using Designer Receptors Exclusively Activated by Designer Drugs (DREADD), to modify LC activity to further unravel its role in brain excitability, more specifically hippocampal excitability and other neurological diseases. In order to chemogenetically modulate LC, there are two requirements:

1) High cell-specific DREADD expression is achieved in LC-NA neurons;
2) Identification of an agonist (inert) ligand to induce DREADD-specific modulation.

To achieve high-cell specific DREADD expression in noradrenergic neurons, the titer of a viral vector needs to be optimized to achieve high levels of expression combined with low levels of aspecificity and possible viral vector-induced toxicity. In a first experiment we investigated the possibility of using an adeno-associated virus (AAV) vector to induce high and specific expression of the hM3Dq DREADD in LC-NA neurons. Subclinical doses of clozapine were administered in anesthetized healthy animals expressing hM3Dq in LC using single unit recording, to validate the suitability of this ligand as selective agonist. The results of this experiment are presented in **chapter 5**, emphasizing the difficulty of targeting a brainstem nucleus and the need for optimization of the transduction efficiency and clozapine dose.

A second experiment, presented in **chapter 6**, was performed to optimize the expression and specificity of hM3Dq expression in LC neurons, using a different type of viral vector, canine adenovirus type 2 (CAV2) vector.

Both volume and absolute number of viral particles were titrated to achieve a condition of high cell-specific expression and low aspecificity. DREADD expression was assessed by immunofluorescence stainings followed by post-processing image analysis on confocal images. Ideal parameters for high numbers of cell-specific expression were determined, however, signs of toxicity were observed when undiluted and high titers of CAV were injected in LC.

The discrepancy in transduction efficiency between AAV2/7 and CAV2, the observed aspecific hM3Dq expression despite using a validated specific promoter, and the signs of toxicity are discussed in more detail in **chapter 7** listing the main conclusions and future perspectives of this thesis.

Bibliography

1. Kwan P PK, Brodie M MJ. EARLY IDENTIFICATION OF REFRACTORY EPILEPSY Background More than 30 percent of patients with. The New England Journal of Medicine. 2000;342(5):314-9.

2. Kanner AM. Depression in epilepsy: prevalence, clinical semiology, pathogenic mechanisms, and treatment. Biol Psychiatry. 2003;54(3):388-98.

3. Vonck K, Raedt R, Naulaerts J, De Vogelaere F, Thiery E, Van Roost D, et al. Vagus nerve stimulation. . .25 years later! What do we know about the effects on cognition? 2014. p. 63-71.

4. Szabadi E. Functional neuroanatomy of the central noradrenergic system. J Psychopharmacol. 2013;27(8):659-93.

5. Hulsey DR, Riley JR, Loerwald KW, Rennaker RL, 2nd, Kilgard MP, Hays SA. Parametric characterization of neural activity in the locus coeruleus in response to vagus nerve stimulation. Exp Neurol. 2017;289:21-30.

6. Dorr AE, Debonnel G. Effect of vagus nerve stimulation on serotonergic and noradrenergic transmission. J Pharmacol Exp Ther. 2006;318(2):890-8.

7. Manta S, El Mansari M, Debonnel G, Blier P. Electrophysiological and neurochemical effects of long-term vagus nerve stimulation on the rat monoaminergic systems. Int J Neuropsychopharmacol. 2013;16(2):459-70.

8. Raedt R, Clinckers R, Mollet L, Vonck K, El Tahry R, Wyckhuys T, et al. Increased hippocampal noradrenaline is a biomarker for efficacy of vagus nerve stimulation in a limbic seizure model. J Neurochem. 2011;117(3):461-9.

9. Roosevelt RW, Smith DC, Clough RW, Jensen RA, Browning RA. Increased extracellular concentrations of norepinephrine in cortex and hippocampus following vagus nerve stimulation in the rat. Brain Res. 2006;1119(1):124-32.

10. Krahl SE, Clark KB, Smith DC, Browning RA. Locus coeruleus lesions suppress the seizure-attenuating effects of vagus nerve stimulation. Epilepsia. 1998;39(7):709-14.

11. Grimonprez A, Raedt R, Portelli J, Dauwe I, Larsen LE, Bouckaert C, et al. The antidepressant-like effect of vagus nerve stimulation is mediated through the locus coeruleus. J Psychiatr Res. 2015;68:1-7.

12. De Taeye L, Vonck K, van Bochove M, Boon P, Van Roost D, Mollet L, et al. The P3 event-related potential is a biomarker for the efficacy of vagus nerve stimulation in patients with epilepsy. Neurotherapeutics. 2014;11(3):612-22.

13. Larsen LE, Wadman WJ, van Mierlo P, Delbeke J, Grimonprez A, Van Nieuwenhuyse B, et al. Modulation of Hippocampal Activity by Vagus Nerve Stimulation in Freely Moving Rats. Brain Stimul. 2016;9(1):124-32.

14. Larsen LE, Wadman WJ, Marinazzo D, van Mierlo P, Delbeke J, Daelemans S, et al. Vagus Nerve Stimulation Applied with a Rapid Cycle Has More Profound Influence on Hippocampal Electrophysiology Than a Standard Cycle. Neurotherapeutics. 2016;13(3):592-602.

15. Larsen LE, Lysebettens WV, Germonpre C, Carrette S, Daelemans S, Sprengers M, et al. Clinical Vagus Nerve Stimulation Paradigms Induce Pronounced Brain and Body Hypothermia in Rats. Int J Neural Syst. 2017;27(5):1750016.

16. Van Lysebettens W, Vonck K, Larsen LE, Sprengers M, Carrette E, Bouckaert C, et al. Hypothermia Masks Most of the Effects of Rapid Cycling VNS on Rat Hippocampal Electrophysiology. Int J Neural Syst. 2019;29(9):1950008.

17. Dahl D, Winson J. Action of norepinephrine in the dentate gyrus. I. Stimulation of locus coeruleus. Exp Brain Res. 1985;59(3):491-6.

18. Harley C, Milway JS, Lacaille JC. Locus coeruleus potentiation of dentate gyrus responses: evidence for two systems. Brain Res Bull. 1989;22(4):643-50.

19. Reid AT, Harley CW. An associativity requirement for locus coeruleus-induced long-term potentiation in the dentate gyrus of the urethane-anesthetized rat. Exp Brain Res. 2010;200(2):151-9.

20. Hansen N, Manahan-Vaughan D. Locus Coeruleus Stimulation Facilitates Long-Term Depression in the Dentate Gyrus That Requires Activation of beta-Adrenergic Receptors. Cereb Cortex. 2015;25(7):1889-96.

21. Lemon N, Aydin-Abidin S, Funke K, Manahan-Vaughan D. Locus coeruleus activation facilitates memory encoding and induces hippocampal LTD that depends on beta-adrenergic receptor activation. Cereb Cortex. 2009;19(12):2827-37.

22. Lacaille JC, Harley CW. The action of norepinephrine in the dentate gyrus: beta-mediated facilitation of evoked potentials in vitro. Brain Res. 1985;358(1-2):210-20.

23. Walling SG, Nutt DJ, Lalies MD, Harley CW. Orexin-A infusion in the locus ceruleus triggers norepinephrine (NE) release and NE-induced long-term potentiation in the dentate gyrus. J Neurosci. 2004;24(34):7421-6.

24. Harley CW, Milway JS. Glutamate ejection in the locus coeruleus enhances the perforant path-evoked population spike in the dentate gyrus. Exp Brain Res. 1986;63(1):143-50.

25. Olpe HR, Laszlo J, Pozza MF, De Herdt P, Waldmeier PC, Jones RS. Glutamate-induced activation of rat locus coeruleus increases CA1 pyramidal cell excitability. Neurosci Lett. 1986;65(1):11-6.

26. Chaulk PC, Harley CW. Intracerebroventricular norepinephrine potentiation of the perforant path-evoked potential in dentate gyrus of anesthetized and awake rats: A role for both α- and β-adrenoceptor activation. Brain Research. 1998;787(1):59-70.

27. Lethbridge RL, Walling SG, Harley CW. Modulation of the perforant path-evoked potential in dentate gyrus as a function of intrahippocampal beta-adrenoceptor agonist concentration in urethane-anesthetized rat. Brain Behav. 2014;4(1):95-103.

Part II

Experimental work

Chapter 5 A feasibility study to investigate chemogenetic modulation of the locus coeruleus by means of single unit activity

Latoya Stevens[1], Kristl Vonck[1], Lars Emil Larsen[1], Wouter Van Lysebettens[1], Charlotte Germonpré[1], Veerle Baekelandt[2], Chris Van Den Haute[2,3], Evelien Carrette[1], Wytse Jan Wadman[1], Paul Boon[1], Robrecht Raedt[1*]

[1] 4BRAIN, Institute for Neuroscience, Department Head and Skin, Ghent University, Ghent, Belgium

[2] Laboratory for Neurobiology and Gene therapy, Center for Molecular Medicine and Leuven Brain Institute, KU Leuven, Leuven, Belgium

[3] Leuven Viral Vector Core, Centre for Molecular Medicine, KU Leuven, Leuven, Belgium

Published in Frontiers in Neuroscience, 14th of March 2020, 14(162): doi: 10.3389/fnins.2020.00162

Abstract

Aim: Selective chemogenetic modulation of locus coeruleus (LC) neurons would allow dedicated investigation of the role of the LC-NA pathway in brain excitability and disorders such as epilepsy. This study investigated the feasibility of an experimental set-up where chemogenetic modification of the brainstem locus coeruleus NA neurons is aimed at and followed by LC unit activity recording in response to clozapine.

Methods: The LC of male Sprague-Dawley rats was injected with 10nl of adeno-associated viral vector AAV2/7-PRSx8-hM3Dq-mCherry (n=19, DREADD group) or AAV2/7-PRSx8-eGFP (n=13, Controls). Three weeks later, LC unit recordings were performed in anesthetized rats. We investigated whether clozapine, a drug known to bind to modified neurons expressing hM3Dq receptors, was able to increase the LC firing rate. Baseline unit activity was recorded followed by subsequent administration of 0.01 mg/kg and 0.1 mg/kg of clozapine in all rats. hM3Dq-mCherry expression levels were investigated using immunofluorescence staining of brainstem slices at the end of the experiment.

Results: Unit recordings could be performed in 12 rats and in a total of 12 neurons (DREADDs: n=7, controls: n=5). Clozapine 0.01 mg/kg did not affect the mean firing rate of recorded LC-neurons; 0.1 mg/kg induced an increased firing rate, irrespective whether neurons were recorded from DREADD or control rats (p=0.006). Co-labeling of LC neurons and mCherry-tag showed that 20.6 ± 2.3% LC neurons expressed the hM3Dq receptor. Aspecific expression of hM3Dq-mCherry was also observed in non-LC neurons (26.0 ± 4.1%).

Conclusions: LC unit recording is feasible in an experimental set-up following manipulations for DREADD induction. A relatively low transduction efficiency of the used AAV was found. In view of this finding, the effect of injected clozapine on LC-NA could not be investigated as a reliable outcome parameter for activation of chemogenetically modified LC neurons. The use of AAV2/7, a vector previously applied successfully to target dopaminergic neurons in the substantia nigra, leads to insufficient chemogenetic modification of the LC compared to transduction with AAV2/9.

5.1 Introduction

The Locus coeruleus (LC)-noradrenaline (NA) pathway is believed to play an important role in the development and treatment of epilepsy (1). Different preclinical studies demonstrated the anti-epileptic role of endogenous NA since lesioning LC accelerates the rate of amygdala kindling (1) and attenuates seizure-suppressing effects of Vagus Nerve Stimulation (VNS) (2). In general, it is known that the LC-NA pathway modulates brain excitability, which is evident based on hippocampal evoked potentials (EP) and electro-encephalography (EEG). Activation of the LC-NA system induces synaptic plasticity in the form of long term depression or long term potentiation depending on simultaneous activation of the neural target and glutamate release. These paradoxal effects could be explained by the 'hot spot theory' referring to the hypothesis that the local increase in NA concentration is depending on the initial activation of the neural target, where local glutamate increases lead to NA increase of LC-varicosities (3-8).

To further unravel the precise role of the LC-NA pathway in modulation of brain excitability and eventually even in the mechanism of action of VNS, selective LC modulation is desirable. Chemogenetics is a technique able to modulate specific brain structures with high cellular specificity using Designer Receptors Exclusively Activated by Designer Drugs (DREADD). DREADDs are muscarinic metabotropic receptors (hM3Dq for excitation, hM4Di for inhibition) that are genetically engineered to be inert for the endogenous ligand acetylcholine but are known to respond to so called 'designer drugs' such as Clozapine-N-Oxide (CNO) (9). CNO is a major metabolite of clozapine, a clinically used antipsychotic drug. Activation of Gq-coupled hM3Dq by CNO was previously shown to activate neurons through phospholipase C (PLC) dependent mechanisms (10). Activation of hM3Dq-NA neurons under isoflurane anesthesia by systemic CNO administration was demonstrated to enhance recovery of arousal from anesthesia by Aston-Jones et al. (11).

Frequently used techniques for *in vivo* transduction of LC neurons consist of an intracerebral injection of a viral vector, such as adeno-associated viral vector (AAV) or canine adeno-associated viral vector (CAV), in the vicinity of LC. To achieve LC specific expression of the DREADD, a selective promoter is used such as PRSx8, a synthetic dopamine-β-hydroxylase (DBH) promoter (11, 12). Alternatively, site-specific recombinase technology can be used which consists of injecting a Cre-dependent AAV vector in TH-Cre transgenic mice. Previous research groups using AAVs mostly used an AAV2/9, which resulted in successful transduction of LC (11, 13-17).

In this study we examined the feasibility of injecting AAV2/7, carrying the PRSx8-hM3Dq-mCherry construct, to induce LC-specific expression of the excitatory hM3Dq DREADD. To achieve this, an AAV2/7 was injected in the rat LC. This AAV serotype was used because it has proven efficiency in transducing high numbers of dopaminergic neurons in the substantia nigra (18).

We also aimed to determine the effects of systemic administration of two different subclinical doses of clozapine (0.01 and 0.1 mg/kg). Earlier evidence showed that CNO, upon systemic injection in rats, is back-converted to clozapine (19). In contrast to CNO, clozapine easily crosses the blood-brain barrier. Since clozapine has high affinity for DREADDs, activation of DREADDs in the brain by systemic CNO is mainly caused by its metabolite clozapine (9). Importantly, at therapeutic doses, i.e. 1-10 mg/kg, clozapine binds to a broad range of neuroreceptors including dopamine $D_{2\text{-}4}$, serotonin 5-HT_{2A}, 5-HT_{2C}, muscarinic M_1, M_2, M_3, M_4, adrenergic α_1 and α_2, as well as histamine H_1 receptors (20). Some of these receptors are expressed in LC (21-24).

The aim of our study was to design an experimental approach where selective modulation of neurons of the LC through chemogenetic stimulation would allow us to investigate the noradrenergic pathway in the regulation of brain excitability. The aim was to use the hM3DQ DREADD approach, systemic administration of subclinical doses of clozapine and recording of LC neuronal firing modulation with the ultimate aim of performing this in awake epileptic rats in the future.

5.2 Materials and Methods

5.2.1 Animals

Thirty-two adult male Sprague-Dawley rats (Envigo, The Netherlands) were used in this study and treated according to European guidelines (directive 2010/63/EU). The study protocol was approved by the local Ethical Committee on Animal Experiments of Ghent University (ECD 16/31). Animals were kept under environmentally controlled conditions: 12h light/dark cycles with artificially dimmed light, temperature and relative humidity at 20-23°C and 40-60%, respectively, with food (Rats and Mice Maintenance, Carfil, Belgium) and water ad libitum. All animals were housed individually in type III H cages (Tecniplast, Australia) on wood-based bedding (Carfil, Belgium). Cages were enriched with paper nesting material (Nestil, Carfil, Belgium).

5.2.2 Viral vector administration

Animals (n=32; 9-10 weeks old; 309±15g body weight) were anesthetized with a mixture of medical oxygen and isoflurane (5% for induction, 2% for maintenance, Isoflo, Zoetis, UK); body temperature was controlled using a heating pad. Rats were placed in a stereotaxic frame (Stoelting, USA) and the skull was exposed. Bregma was lowered 2mm relative to lambda (15° head angle) to target the LC and avoid the transverse sinus. Using a Neuro-Syringe (Hamilton model 7001 point style 3, Hamilton company, Nevada, USA) and Quintessential Stereotaxic Injection system (flow rate 2nl/min, Stoelting, USA), injections of 10nl of an adeno-associated viral vector (AAV) serotype 2/7 containing a PRSx8-hM3Dq-mCherry plasmid (5.99E+12 GC/ml) (n=19; 11 unilateral and 8 bilateral) or AAV2/7-PRSx8-eGFP plasmid as a control (n=13; 5 unilateral and 8 bilateral) were performed in the LC (3.9 AP, 1.15 ML relative to lambda, -5.7 DV from dura). After injection the syringe was left in place for an additional 5min and was then slowly withdrawn to avoid backflow. Following surgery, animals were subcutaneously (s.c.) injected with the nonsteroidal anti-inflammatory drug meloxicam (NSAID, 1mg/kg metacam, Boehringer Ingelheim, Germany) and lidocaine (5% Xylocaine gel, Astrazeneca, UK) was applied to the incision site to minimize discomfort. All animals recovered three weeks in their home cage to allow for optimal viral vector expression (25).

5.2.3 Electrophysiology: *in vivo* extracellular unit recording in locus coeruleus neurons

At least three weeks after viral vector injection animals (387 ± 26g body weight) were used for LC unit recordings. Rats were anesthetized with a mixture of medical oxygen and isoflurane (5% for induction, 1.5% for maintenance, n=18) or were induced with 5% isoflurane followed

by an intraperitoneal injection of urethane (1.5 g/kg, n=14). Rats were placed in the stereotaxic frame as described in 2.2. For unit recording, a tungsten microelectrode (.008"/200 µm shank diameter, impedance ≥ 1.5 MΩ, FHC, USA) was implanted under electrophysiological control and audio monitoring to target LC neurons. As a reference and ground, two custom made epidural scalp electrodes, consisting of an insulated copper wire attached to a stainless steel microscrew (1.75mm diameter; Plastics One, USA) were placed above the left and right frontal cortex. Electrophysiological recordings were amplified (x10 000), filtered (300Hz-3kHz) and digitized at 31 kHz using a 1401 micro and Spike2 software (Cambridge Electronic Design, UK) for online visualization of action potentials and storage for post-processing. Action potentials are detected as input signals crossing a trigger level set by the researcher. LC neurons can be visually identified online as they are characterized by the occurrence of a typical pattern called 'a phasic burst inhibition' following a foot pinch (11, 26). After identification of LC neurons, a stable baseline period of 300s was recorded followed by subsequent subcutaneous injections of clozapine into the loose skin of the neck, starting with the lowest dose of 0.01 mg/kg and followed by 0.1 mg/kg (dissolved in 3% DMSO in saline). Action potentials were recorded for at least 650s after each clozapine injection. After the recording period following 0.1 mg/kg clozapine administration, clonidine (0.04 mg/kg), an α_2 agonist which inhibits the spontaneous firing of LC-NA neurons, was injected subcutaneously to confirm the LC identity of recorded neurons (20). Recording was stopped when a decrease in the firing frequency at least to baseline levels was observed.

5.2.4 Histology

At the end of the unit recording sessions, animals were deeply anesthetized with an overdose of sodium pentobarbital (200 mg/kg, i.p.) and transcardially perfused with phosphate-buffered saline (PBS) followed by paraformaldehyde (4%, pH 7.4). The brains were post fixed in paraformaldehyde (4%, pH 7.4) for 24h and subsequently cryoprotected in a sucrose solution of 10-20-30% at 4°C, snap-frozen in isopentane and stored in liquid nitrogen at -196°C. After 1 hour on -20°C, coronal cryosections of 40µm were made using a cryostat (Leica, Germany). The sections were rinsed twice for 5min in distilled water (dH_2O) followed by incubation in 0.5% and 1% H_2O_2 for 30 and 60min respectively to block endogenous peroxidase activity. After washing twice for 5min in PBS, sections were incubated in blocking buffer (BB) made of PBS containing 0.4% Fish Skin Gelatin (FSG) and 0.2% Triton X for 45min to block non-specific antibody binding sites. The sections were then incubated in primary antibodies to visualize noradrenergic LC neurons and GFP or mCherry tag respectively with mouse anti-

DBH (1:1000, Merck, clone 4F10.2) and chicken anti-green fluorescent protein (1:1000, Abcam, ab13970) or rabbit anti-red fluorescent protein (targeting mCherry, 1:1000, Rockland, ROCK600-901-379) diluted in BB for 1 hour at room temperature and subsequently overnight at 4°C. On the next day the sections were washed twice in blocking buffer for 10 min followed by incubation in secondary antibodies Alexa Fluor goat anti-mouse 488 nm (1:1000, Abcam, Ab 150113) or Alexa Fluor goat anti-mouse 594 nm (1:1000, Abcam, ab150176) against DBH^+ cells and Alexa goat anti-rabbit 594 nm or Alexa fluor goat-anti chicken 488 nm (against mCherry or GFP tag) diluted in BB for 1 hour at room temperature in darkness. After washing twice in PBS for 5 min, a nuclear DAPI staining was performed and subsequent rinsing in PBS (2x5 min). Sections were mounted on glass slides and cover slipped using Vectashield H1000 mounting medium (Vector Laboratories, USA) to prevent photo bleaching.

The viral vector expression levels were determined using a fluorescence microscope (Carl Zeiss, Axiovert 200M and Nikon Eclipse TE2000-E, Germany). Pictures of DAPI, DBH and GFP or mCherry were taken with the AxioVision Microscope Software (6D acquisition) connected to the Carl Zeiss fluorescence microscope on the 10x magnification. For each animal that underwent successful unit recording, images were taken from three slices along the anterior-posterior axis of the LC and exported as TIFF files before being analyzed in Fiji-ImageJ software. To determine hM3Dq-DBH colocalization, three sections containing LC per animal were used to quantify the number of DBH^+ LC cells by placing virtual markers on a merged image of DBH^+/DAPI. These markers were then copied on the merged image of DBH^+/mCherry to determine the number of LC cells expressing hM3Dq-mCherry. To quantify aspecific hM3Dq-mCherry expression, cells that were $DBH^-/mCherry^+$ were counted and divided by the total number of $mCherry^+$ cells.

5.2.5 Electrophysiological data analysis

Units which responded with a typical phasic bursting/tonic inhibition pattern after foot pinch, of which the activity could be stably recorded upon the administration of both clozapine dosages and whose activity was inhibited by administration of clonidine were included in the analysis. Units were offline identified in Spike2 and confirmed as independent using principal component and autocorrelation (27). The mean firing frequency per 10 second bins was calculated for an episode of 300 seconds during baseline (30 data points) and 300 seconds after injection of both clozapine dosages (30 data points before the next injection covering the maximum effect of each dose). DREADD and control group averages of baseline and clozapine (0.01 and 0.1 mg/kg) epochs were calculated.

To determine the effect of group (DREADD vs control), treatment (baseline, clozapine 0.01 mg/kg and clozapine 0.1 mg/kg) and their interaction a two-way repeated measures ANOVA was performed, followed by post-hoc Bonferroni test for comparing individual conditions. All data are presented as mean ± standard error of mean (SEM). Statistical analysis was performed in SPSS for windows (version 25). Graphs were made in GraphPad Prism 6.

5.3 Results

5.3.1 Effect of systemic clozapine administration on LC firing frequency

Successful electrophysiological recordings were performed in 12 animals. A total of 12 neurons were recorded, 7 in DREADD-injected animals and 5 in control animals, all characterized by foot pinch elicited phasic bursting and decreased firing frequency after clonidine administration. A two-way repeated measures ANOVA showed no interaction between treatment and group ($F=0.212$, $p=0.655$). No significant effect of group was reported ($F=1.429$, $p=0.259$) although treatment has a significant effect on the firing frequency ($F=14.623$, $p=0.003$). Systemic administration of the 0.01 mg/kg clozapine had no significant effect on the mean firing frequency (2.72 ± 0.48 Hz, $p=0.468$) of recorded LC neurons compared to baseline (2.34 ± 0.30 Hz) whereas an increased firing rate was observed after 0.1 mg/kg clozapine (3.57 ± 0.54 Hz, $p=0.006$), irrespective whether recordings were performed in DREADD or control animals. A significant difference between the two doses of clozapine on the firing frequency was observed ($p=0.003$) (fig 5.1). In all LC neurons, firing frequency was reduced to baseline levels or completely inhibited after clonidine administration confirming LC identity.

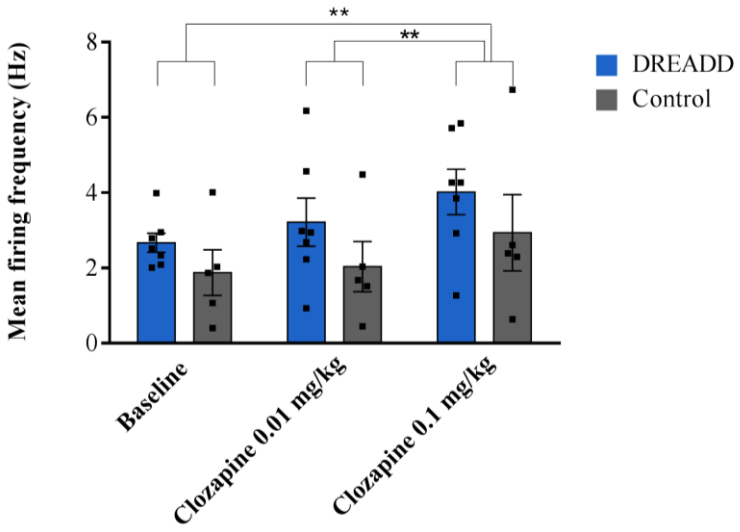

Figure 5.1 The effect of systemic administration of different doses of clozapine on the mean firing frequency of LC neurons in DREADD and control injected animals. Electrophysiological recordings were performed in 12 animals (DREADD group n = 7; control n = 5), in each animal one neuron was recorded for a stable baseline period (300 s) followed by subsequent injections of clozapine (0.01 and 0.1 mg/kg, s.c.). No difference in the effect of clozapine on the firing frequency of neurons recorded in DREADD-injected or control animals was observed ($F = 14.623$, $p = 0.003$). The highest dose of clozapine (0.1 mg/kg) increased the firing frequency compared to baseline ($p = 0.006$) whereas the lowest dose of clozapine (0.01 mg/kg) showed no effect ($p = 0.312$). A significant difference between the two doses of clozapine on the mean firing frequency was observed ($p = 0.003$). Each bar represents the mean firing frequency ±SEM (firing frequencies from individual neurons represented by black

5.3.2 Viral vector expression

Double label immunostaining for the mCherry tag coupled to the hM3Dq receptor and DBH was used to quantify the transduction efficiency of the viral vector in LC-NA neurons and its specificity (fig.2A). All animals that underwent successful unit recording at least three weeks after viral vector administration showed expression of hM3Dq in LC-NA cells and adjacent axons although there was variability in the fraction of LC cells expressing hM3Dq (fig.2A-C). HM3Dq expression was evident in 20.6 ± 2.3% LC neurons (21 sections; three sections/animal; range 11-32%). Aspecific expression of hM3Dq-mCherry was also observed in cells outside the LC (26.0 ± 4.1% of mCherry positive cells was DBH negative) (fig 5.2C).

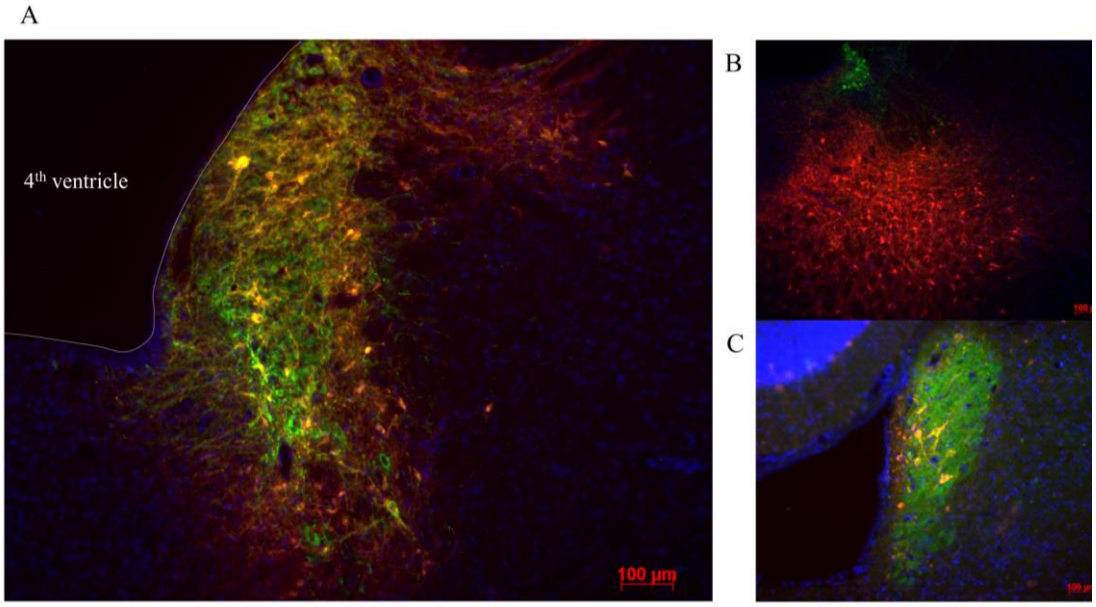

Figure 5.2 Visualization of hM3Dq-mCherry expression in LC injected with PRSx8-driven AAV. (A–C) LC-NA neurons are visualized using primary anti-DBH antibody (green) and expression of hM3Dq DREADD is visualized with the mCherry tag (red). (B) Aspecific hM3Dq expression (red) in DBH- non LC neurons. (C) Only a low number of transduced neurons are observed in some animals. Scale bar 100 µm.

5.4 Discussion

In this study we tested the feasibility of an experimental approach where LC neurons were transduced with AAV vectors for induction of DREADD expression, followed by LC unit recording and subcutaneous clozapine injections to investigate the potential to selectively modulate LC-NA neurons. This approach could ultimately be used in the context of investigating the role of the LC-NA pathway in regulating cortical excitability in awake epileptic rats.

For chemogenetic modification we used the adeno-associated viral vector (AAV2/7), previously used in the substantia nigra (18), to selectively express the excitatory hM3Dq DREADD in LC neurons using the PRSx8 promoter. *Post mortem* analysis of hM3Dq presence in the brainstem revealed low levels of expression in LC in combination with the presence of aspecific expression in surrounding non-LC neurons.

The transduction efficiency of specific cells is defined by the AAV serotype, promoter and injection site (28). Our observed transduction levels were in contrast with high specificity and expression levels of >95% in previous studies using AAV2/9-PRSx8-hM3Dq-mCherry to transduce the LC (11). The serotype of the viral vector may be one of the primary reasons for the poor expression levels and aspecificity.

The transduction efficiency of an AAV is determined by AAV entry in the target cell (29) which is controlled by the AAV capsid with its proteins on the surface that determine the binding specificity and entry of the virion to cells (30, 31). In contrast to other groups who use the AAV2/9 and achieve high expression levels, in this study AAV2/7 was used, which means that the genome of serotype 2 is encapsulated in a viral capsid formed by serotype 7 (11, 16). Probably the presence of different surface proteins presented on the capsid in comparison to AAV2/9 leads to lower binding affinity for the surface receptors on LC-NA cells and possible affinity for non-LC cells, explaining both low expression levels and aspecificity. Although previous research has proven that AAV2/7 is as effective as AAV2/9 in transducing dopaminergic neurons in substantia nigra, this might be different when targeting noradrenergic LC cells due to their different receptors and co-receptors (18, 29).

Next to the AAV serotype, expression specificity is also defined by the promoter. The PRSx8 promoter is a synthetic DBH promoter which consist of eight copies of a promoter sequence from the cis-regulatory region of the DBH gene that binds the Phox2a/b transcription factors. This promoter sequence has proven to successfully drive gene expression in catecholaminergic neurons expressing the Phox2a/b transcription factors (12) as described by other groups using AAV2/9-PRSx8 construct observing high expression levels (11). Because of these observations, it is less likely that the observed aspecific expression in our study is due to promoter characteristics. However, it is possible that due to the affinity of the capsid for receptors present on non-LC cells, Phox2 transcription factors present in these non-catecholaminergic cells (32) activate gene expression. Another possible explanation might be the presence of transactivator activity in the AAV inverted terminal repeats. Terminal repeats (TR) contain sequences necessary for replication and packaging of recombinant DNA and cannot be deleted. Haberman et al. have shown that an AAV TR construct without a promoter can initiate gene expression, indicating its transcriptional and promoter ability, resulting in a loss of tissue-specific expression (33). When the number of viral vector virions at the injection site is high (= high multiplicity of infection (MOI)) the amount of TR mediated transcription can increase or promoter leakage can occur, which means that the promoter will be active in non-specific cells, resulting in detectable aspecific expression (32).

Finally we cannot exclude the inadequate delivery of the adeno-associated viral vector in the vicinity of LC as we were not able to localize the exact injection site using *post mortem* immunohistochemical analysis (34).

However, we used a validated technique to target LC and observed expression in all injected animals supporting the conclusion that the injection was performed correctly (13, 16).

The ultimate aim of the experiment was to determine whether presumed subtherapeutic doses of clozapine could be used to specifically activate DREADD expressing LC neurons in anesthetized rats.

We found that LC unit recording is feasible following manipulations to induce DREADD expression although the yield is relatively low as we were only able to perform successful electrophysiological recordings in 35% of the animals. This is similar to other research groups targeting locus coeruleus with success rates around 45% and is possibly due to the small size and location of the nucleus in the pontine brainstem (35). In the current experimental setting, we were not able to draw conclusions on the feasibility to chemogenetically increase LC neuronal activity with clozapine. Since only a limited fraction of LC neurons showed expression of the DREADD upon AAV injection, we could not claim that we recorded from DREADD positive LC neurons in the DREADD group. In fact, this study showed that 0.1 mg/kg clozapine increases the firing rate of LC neurons even in the control group and is thus independent of DREADD expression. We can thus conclude that 0.1 mg/kg clozapine does significantly activate non-DREADD neuroreceptors influencing the firing rate of LC neurons. This dose is thus less suitable for future experiments to selectively activate DREADD-expressing LC neurons (9, 36).

These DREADD-independent effects of low doses of clozapine were not expected as previous studies using 0.1-10 mg/kg CNO were without effects on LC firing frequency in control animals (11). These doses correspond or are even higher than the doses of clozapine used in this study keeping in mind that 10 mg/kg CNO ~ 0.1mg/kg clozapine described by Gomez et al. (9). A previous study in healthy animals showed an increased firing frequency of LC and ventral tegmental area neurons after intravenous administration clozapine (0.078 mg/kg – 10 mg/kg) (37, 38). Pretreatment with a selective antagonist at the glycine site of the NMDA receptor inhibited the activation of LC neurons after administration of the highest dose of clozapine but cannot solely explain the increased firing frequency as administration of a selective partial agonist of the glycine/NMDA receptor did not increase the LC activity. However it has been shown that clozapine is able to increase extracellular glutamate levels (39). These findings suggest that a combination of activating the glycine site of the NMDA receptor and increased glutamatergic release, as a result of activation of clozapine sensitive receptors located on glutamatergic afferents to LC, might be responsible for activation of LC noradrenergic neurons

after administration of the highest dose of clozapine (38). Local delivery of clozapine as performed by Vazey et al. (11), instead of systemic administration (s.c.) could possibly rule out major effects of activated glutamatergic afferents to LC, although activation of presynaptic axons would still be possible. However, we chose in our study to subcutaneously inject our animals, knowing that clozapine has proven to cross the blood-brain-barrier easily and to have a high affinity for DREADDs (9). Due to the absence of differences in effects on LC firing frequency after administration of CNO locally or systemically (11) and with the future prospect of performing experiments in awake animals, subcutaneous administration of clozapine was preferred.

Next to activation of endogenous NMDA receptors, recent studies suggest that low doses of clozapine, result in occupancy of endogenous receptors in the brain and significant changes in neurometabolite levels and effects on locomotion, anxiety and cognitive flexibility (25, 40). Clozapine has affinity for D2, M2, 5-HT1a, α1 and histamine receptors present in LC which can also lead to excitation and increased firing frequency (21-24).

From our results and sequence of experimental steps, we conclude that the use of AAV2/7 is less desirable to specifically induce DREADD expression in LC neurons in comparison to previously used approaches. A different AAV serotype such as the AAV2/9 as discussed above leads to higher transduction levels. Other groups have even used a different type of viral vector (i.e. CAV) to induce the expression of opsins or engineered ligand gated ion channels in the noradrenergic neurons resulting in high expression patterns after direct injection in LC or administration in LC projection areas (11, 13-17, 26). These more successful approaches of induction of genetic modifications in LC-NA neurons may be due to higher affinity of the virion for the LC-NA surface receptors. An alternative for increasing transduction efficiency and selectivity is the use of a Cre-Lox system for hM3Dq expression in LC (41). The group of Harley and Walling et al. used a TH:Cre rat line to induce expression of an opsin in LC by injecting a Cre-dependent AAV with the promoter and gene of interest between loxP sites, assuring selective expression in LC cells that contain Cre recombinase (35). Because of these findings we believe that for further optimization of the experimental approach studied in this work, transduction efficiency studies with different viral vector serotypes are required when targeting a new brain structure such as a brainstem nucleus, even when a similar type of neurons ie. noradrenergic neurons are the primary content of the nucleus. An experimental setup with higher transduction efficiency and selectivity is required in combination with a technique to ensure that unit recording was performed in transduced cells to validate the effect of clozapine

as a possible selective DREADD ligand. We propose future viral vector experiments with: 1) a different serotype (e.g. AAV2/9 or CAV) to achieve more efficient transduction of LC-NA neurons; 2) a lower titer to avoid aspecific expression due to possible promoter leakage resulting from high MOI and/or 3) higher injected volumes to cover more LC cells (11, 32). To allow confirmation on the transduction characteristics of the recorded LC neurons in anesthetized rats juxtacellular labelling with neurobiotin can be performed as proven by other groups performing LC unit recording (42-45).

Although this feasibility study demonstrated that our approach is suboptimal to selectively modulate LC, we still believe that chemogenetics, a technique which allows cell-specific modulation is needed to further investigate the role of this brainstem nucleus in brain excitability. A viral vector approach with high transduction efficiency in combination with LC-selective expression of DREADDs and a selective ligand will enable us to study the effect of LC in the epileptic brain and its role in attenuating seizures as observed during VNS (46). So far, experiments that used electrical stimulation or infusion of chemicals to modulate LC function gave ambiguous results concerning its role in modulating hippocampal excitability. Electrical stimulation in LC induced β-receptor-dependent long term depression (LTD) while glutamate injection in LC induced long term potentiation (LTP) in hippocampus (4, 8). Some LC activation studies show increased hippocampal responses to afferent input (7, 47-51) while others demonstrate reduced gamma power reflecting decreased activity of local hippocampal neurons (3, 52). These contradictory results might be the result of the small size and deep location of the LC, making the risk of off-target effects by non-selective electrical and chemical stimulation techniques likely.

These findings emphasize that further research using chemogenetics is necessary in the field of LC research, allowing cell-specific modulation and defining its function in brain excitability and confirming its role in the mechanism of action of VNS.

Funding

Latoya Stevens is supported by a PhD-grant from the Queen Elisabeth Medical Foundation for Neurosciences (G.S.K.E) and the Ghent Institute for Neuroscience. Prof. Dr. K. Vonck and Prof. Dr. R. Raedt are supported by the Special Research Funds (BOF) of Ghent University. Prof. Dr. P. Boon is supported by research grants from FWO, BOF and Ghent University. Prof. Dr. V. Baekelandt is supported by FWO Neuro-TRAFFIC and ERA-NET Cofund REACT NSCs (SBO/S006617N) and KU Leuven (IOF C32/15/031).

Author contributions

LS, KV, LL, WVL, CG, EC, WW, PB, and RR contributed to the study design and analysis plan. LS and WVL obtained the data. LS, KV, and RR analyzed the data and prepared the manuscript. VB and CV designed and provided the viral vectors. All authors reviewed the manuscript.

Bibliography

1. Giorgi FS, Pizzanelli C, Biagioni F, Murri L, Fornai F. The role of norepinephrine in epilepsy: from the bench to the bedside. Neurosci Biobehav Rev. 2004;28(5):507-24.

2. Krahl SE, Clark KB, Smith DC, Browning RA. Locus coeruleus lesions suppress the seizure-attenuating effects of vagus nerve stimulation. Epilepsia. 1998;39(7):709-14.

3. Brown RA, Walling SG, Milway JS, Harley CW. Locus ceruleus activation suppresses feedforward interneurons and reduces beta-gamma electroencephalogram frequencies while it enhances theta frequencies in rat dentate gyrus. J Neurosci. 2005;25(8):1985-91.

4. Hansen N, Manahan-Vaughan D. Locus Coeruleus Stimulation Facilitates Long-Term Depression in the Dentate Gyrus That Requires Activation of beta-Adrenergic Receptors. Cereb Cortex. 2015;25(7):1889-96.

5. Lacaille JC, Harley CW. The action of norepinephrine in the dentate gyrus: beta-mediated facilitation of evoked potentials in vitro. Brain Res. 1985;358(1-2):210-20.

6. Mather M, Clewett D, Sakaki M, Harley CW. Norepinephrine ignites local hotspots of neuronal excitation: How arousal amplifies selectivity in perception and memory. Behav Brain Sci. 2016;39:e200.

7. Reid AT, Harley CW. An associativity requirement for locus coeruleus-induced long-term potentiation in the dentate gyrus of the urethane-anesthetized rat. Exp Brain Res. 2010;200(2):151-9.

8. Walling SG, Harley CW. Locus ceruleus activation initiates delayed synaptic potentiation of perforant path input to the dentate gyrus in awake rats: a novel beta-adrenergic- and protein synthesis-dependent mammalian plasticity mechanism. J Neurosci. 2004;24(3):598-604.

9. Gomez JL, Bonaventura J, Lesniak W, Mathews WB, Sysa-Shah P, Rodriguez LA, et al. Chemogenetics revealed: DREADD occupancy and activation via converted clozapine. Science. 2017;357(6350):503-7.

10. Alexander GM, Rogan SC, Abbas AI, Armbruster BN, Pei Y, Allen JA, et al. Remote control of neuronal activity in transgenic mice expressing evolved G protein-coupled receptors. Neuron. 2009;63(1):27-39.

11. Vazey EM, Aston-Jones G. Designer receptor manipulations reveal a role of the locus coeruleus noradrenergic system in isoflurane general anesthesia. Proc Natl Acad Sci U S A. 2014;111(10):3859-64.

12. Hwang DY, Carlezon WA, Jr., Isacson O, Kim KS. A high-efficiency synthetic promoter that drives transgene expression selectively in noradrenergic neurons. Hum Gene Ther. 2001;12(14):1731-40.

13. Rorabaugh JM, Chalermpalanupap T, Botz-Zapp CA, Fu VM, Lembeck NA, Cohen RM, et al. Chemogenetic locus coeruleus activation restores reversal learning in a rat model of Alzheimer's disease. Brain. 2017;140(11):3023-38.

14. Fortress AM, Hamlett ED, Vazey EM, Aston-Jones G, Cass WA, Boger HA, et al. Designer receptors enhance memory in a mouse model of Down syndrome. J Neurosci. 2015;35(4):1343-53.

15. Zerbi V, Floriou-Servou A, Markicevic M, Vermeiren Y, Sturman O, Privitera M, et al. Rapid Reconfiguration of the Functional Connectome after Chemogenetic Locus Coeruleus Activation. Neuron. 2019;103(4):702-18 e5.

16. Cope ZA, Vazey EM, Floresco SB, Aston Jones GS. DREADD-mediated modulation of locus coeruleus inputs to mPFC improves strategy set-shifting. Neurobiol Learn Mem. 2019;161:1-11.

17. Kane GA, Vazey EM, Wilson RC, Shenhav A, Daw ND, Aston-Jones G, et al. Increased locus coeruleus tonic activity causes disengagement from a patch-foraging task. Cogn Affect Behav Neurosci. 2017;17(6):1073-83.

18. Van der Perren A, Toelen J, Carlon M, Van den Haute C, Coun F, Heeman B, et al. Efficient and stable transduction of dopaminergic neurons in rat substantia nigra by rAAV 2/1, 2/2, 2/5, 2/6.2, 2/7, 2/8 and 2/9. Gene Ther. 2011;18(5):517-27.

19. MacLaren DA, Browne RW, Shaw JK, Krishnan Radhakrishnan S, Khare P, Espana RA, et al. Clozapine N-Oxide Administration Produces Behavioral Effects in Long-Evans Rats: Implications for Designing DREADD Experiments. eNeuro. 2016;3(5):219-16.

20. Svensson TH, Bunney BS, Aghajanian GK. Inhibition of both noradrenergic and serotonergic neurons in brain by the a-adrenergic agonist clonidine. Brain Research. 1975;92:291-306.

21. Baerentzen S, Casado-Sainz A, Lange D, Shalgunov V, Tejada IM, Xiong M, et al. The Chemogenetic Receptor Ligand Clozapine N-Oxide Induces in vivo Neuroreceptor Occupancy and Reduces Striatal Glutamate Levels. Front Neurosci. 2019;13:187.

22. Korotkova TM, Sergeeva OA, Ponomarenko AA, Haas HL. Histamine excites noradrenergic neurons in locus coeruleus in rats. Neuropharmacology. 2005;49(1):129-34.

23. Egan TM, North RA. Acetylcholine acts on m2-muscarinic receptors to excite rat locus coeruleus neurones. Br J Pharmacol. 1985;85(4):733-5.

24. Szabo ST, Blier P. Functional and pharmacological characterization of the modulatory role of serotonin on the firing activity of locus coeruleus norepinephrine neurons. Brain Res. 2001;922(1):9-20.

25. Smith KS, Bucci DJ, Luikart BW, Mahler SV. DREADDs: Use and application in behavioral neuroscience. 2016. p. 137-55.

26. Hirschberg S, Li Y, Randall A, Kremer EJ, Pickering AE. Functional dichotomy in spinal- vs prefrontal-projecting locus coeruleus modules splits descending noradrenergic analgesia from ascending aversion and anxiety in rats. Elife. 2017;6(Lc):e29808-e.

27. Chaijale NN, Curtis AL, Wood SK, Zhang XY, Bhatnagar S, Reyes BA, et al. Social stress engages opioid regulation of locus coeruleus norepinephrine neurons and induces a state of cellular and physical opiate dependence. Neuropsychopharmacology. 2013;38(10):1833-43.

28. Martin KRG, Klein RL, Quigley HA. Gene delivery to the eye using adeno-associated viral vectors. Methods. 2002;28(2):267-75.

29. Lai CM, Lai YK, Rakoczy PE. Adenovirus and adeno-associated virus vectors. DNA Cell Biol. 2002;21(12):895-913.

30. Delbeke J, Hoffman L, Mols K, Braeken D, Prodanov D. And Then There Was Light: Perspectives of Optogenetics for Deep Brain Stimulation and Neuromodulation. Front Neurosci. 2017;11(December):663.

31. Rabinowitz JE, Rolling F, Li C, Conrath H, Xiao W, Xiao X, et al. Cross-packaging of a single adeno-associated virus (AAV) type 2 vector genome into multiple AAV serotypes enables transduction with broad specificity. J Virol. 2002;76(2):791-801.

32. Bruinstroop E, Cano G, Vanderhorst VG, Cavalcante JC, Wirth J, Sena-Esteves M, et al. Spinal projections of the A5, A6 (locus coeruleus), and A7 noradrenergic cell groups in rats. J Comp Neurol. 2012;520(9):1985-2001.

33. Haberman RP, McCown TJ, Samulski RJ. Novel Transcriptional Regulatory Signals in the Adeno-Associated Virus Terminal Repeat A/D Junction Element. 2000.

34. Sara SJ, Herve-Minvielle A. Inhibitory influence of frontal cortex on locus coeruleus neurons. Proc Natl Acad Sci U S A. 1995;92(13):6032-6.

35. Quinlan MAL, Strong VM, Skinner DM, Martin GM, Harley CW, Walling SG. Locus Coeruleus Optogenetic Light Activation Induces Long-Term Potentiation of Perforant Path Population Spike Amplitude in Rat Dentate Gyrus. Front Syst Neurosci. 2018;12:67.

36. Mahler SV, Aston-Jones G. CNO Evil? Considerations for the Use of DREADDs in Behavioral Neuroscience. Neuropsychopharmacology. 2018;43(5):934-6.

37. Schwieler L, Linderholm KR, Nilsson-Todd LK, Erhardt S, Engberg G. Clozapine interacts with the glycine site of the NMDA receptor: electrophysiological studies of dopamine neurons in the rat ventral tegmental area. Life Sci. 2008;83(5-6):170-5.

38. Nilsson LK, Schwieler L, Engberg G, Linderholm KR, Erhardt S. Activation of noradrenergic locus coeruleus neurons by clozapine and haloperidol: involvement of glutamatergic mechanisms. Int J Neuropsychopharmacol. 2005;8(3):329-39.

39. Daly DA, Moghaddam B. Actions of clozapine and haloperidol on the extracellular levels of excitatory amino acids in the prefrontal cortex and striatum of conscious rats. Neurosci Lett. 1993;152(1-2):61-4.

40. Bouret S, Duvel A, Onat S, Sara SJ. Phasic activation of locus ceruleus neurons by the central nucleus of the amygdala. J Neurosci. 2003;23(8):3491-7.

41. Witten IB, Steinberg EE, Lee SY, Davidson TJ, Zalocusky KA, Brodsky M, et al. Recombinase-driver rat lines: tools, techniques, and optogenetic application to dopamine-mediated reinforcement. Neuron. 2011;72(5):721-33.

42. Dempsey B, Turner AJ, Le S, Sun QJ, Bou Farah L, Allen AM, et al. Recording, labeling, and transfection of single neurons in deep brain structures. Physiol Rep. 2015;3(1):1-13.

43. Bangasser DA, Zhang X, Garachh V, Hanhauser E, Valentino RJ. Sexual dimorphism in locus coeruleus dendritic morphology: a structural basis for sex differences in emotional arousal. Physiol Behav. 2011;103(3-4):342-51.

44. Hajos M, Allers KA, Jennings K, Sharp T, Charette G, Sik A, et al. Neurochemical identification of stereotypic burst-firing neurons in the rat dorsal raphe nucleus using juxtacellular labelling methods. Eur J Neurosci. 2007;25(1):119-26.

45. Allers KA, Sharp T. Neurochemical and anatomical identification of fast- and slow-firing neurones in the rat dorsal raphe nucleus using juxtacellular labelling methods in vivo. Neuroscience. 2003;122(1):193-204.

46. Raedt R, Clinckers R, Mollet L, Vonck K, El Tahry R, Wyckhuys T, et al. Increased hippocampal noradrenaline is a biomarker for efficacy of vagus nerve stimulation in a limbic seizure model. J Neurochem. 2011;117(3):461-9.

47. Haas HL, Rose GM. Noradrenaline blocks potassium conductance in rat dentate granule cells in vitro. Neurosci Lett. 1987;78(2):171-4.

48. Dahl D, Sarvey JM. Norepinephrine induces pathway-specific long-lasting potentiation and depression in the hippocampal dentate gyrus (long-term potentiation/synaptic plasticity/catecholamines). 1989.

49. Edison HT, Harley CW. Medial and lateral perforant path evoked potentials are selectively modulated by pairing with glutamatergic activation of locus coeruleus in the dentate gyrus of the anesthetized rat. Hippocampus. 2012;22(3):501-9.

50. Knight J, Harley CW. Idazoxan increases perforant path-evoked EPSP slope paired pulse inhibition and reduces perforant path-evoked population spike paired pulse facilitation in rat dentate gyrus. Brain Res. 2006;1072(1):36-45.

51. Sara SJ, Bergis O. Enhancement of excitability and inhibitory processes in hippocampal dentate gyrus by noradrenaline: a pharmacological study in awake, freely moving rats. Neurosci Lett. 1991;126(1):1-5.

52. Walling SG, Brown RA, Milway JS, Earle AG, Harley CW. Selective tuning of hippocampal oscillations by phasic locus coeruleus activation in awake male rats. Hippocampus. 2011;21(11):1250-62.

Chapter 6 Optimized parameters for transducing the locus coeruleus using canine adenovirus type 2 (CAV2) vector in rats for chemogenetic modulation research

Latoya Stevens[1], Lars Emil Larsen[1,2], Wouter Van Lysebettens[1], Evelien Carrette[1], Paul Boon[1], Robrecht Raedt[1*†], Kristl Vonck[1†]

[1]4BRAIN, Institute for Neuroscience, Department Head and Skin, Ghent University, Ghent, Belgium
[2] Medical Imaging and Signal Processing, Department of Electronics and Information Systems, Ghent University, Ghent, Belgium

Published in Frontiers in Neuroscience, 13h of April 2020, 15(426): doi: 10.3389/fnins.2021.663337

Abstract

Introduction The locus coeruleus noradrenergic (LC-NA) system is studied for its role in various neurological and psychiatric disorders such as epilepsy and Major Depression Disorder. Chemogenetics is a powerful technique for specific manipulation of the LC to investigate its functioning. Local injection of AAV2/7 viral vectors has limitations with regards to efficiency and specificity of the transduction, potentially due to low tropism of AAV2/7 for LC neurons. In this study we used a canine adenovirus type 2 (CAV2) vector with different volumes and viral particle numbers to achieve high and selective expression of hM3Dq, an excitatory Designer Receptor Exclusively Activated by Designer Drugs (DREADD), for chemogenetic modulation of LC neurons.

Methods Adult male Sprague-Dawley rats were injected in the LC with different absolute numbers of CAV2-PRSx8-hM3Dq-mCherry physical particles (0.1E9, 1E9, 5E9 ,10E9 or 20E9 pp) using different volumes (LowV=3x300nl, MediumV=3x600nl, HighV=3x1200nl). Two weeks post-injection, double-labelling immunohistochemistry for dopamine β hydroxylase (DBH) and mCherry was performed to determine hM3Dq expression and its specificity for LC neurons. The size of the transduced LC was compared to the contralateral LC to identify signs of toxicity.

Results Administration of Medium volume (3x600nl) and 1E9 particles resulted in high expression levels with 87.3±9.8% of LC neurons expressing hM3Dq, but low selectivity with 36.2±17.3% of hM3Dq expression in non-LC neurons. The most diluted conditions (Low volume_0.1Epp and Medium Volume_0.1Epp) presented similar high transduction of LC neurons (70.9±12.7% and 77.2± 9.8%) with lower aspecificity (5.5±3.5% and 4.0±1.9%

respectively). Signs of toxicity were observed in all undiluted conditions as evidenced by a decreased size of the transduced LC.

Conclusion

This study identified optimal conditions (Low and Medium Volume with 0.1E9 particles of CAV2-PRSx8-hM3Dq-mCherry) for safe and specific transduction of LC neurons with excitatory DREADDs to study the role of the LC-NA system in health and disease.

6.1 Introduction

Through its widespread projections, the locus coeruleus (LC)-noradrenaline (NA) system modulates cortical, subcortical, cerebellar, brainstem, and spinal cord neuronal circuits influencing important physiological functions such as sleep, attention, memory, cognitive control and neuroplasticity (1-3). The LC-NA system is studied for its role in various neurological disorders such as depression, Parkinson's disease, Alzheimer's disease and epilepsy (4-7). Chemogenetics is a technique to specifically modulate brain structures and/or neuronal phenotypes using Designer Receptors Exclusively Activated by Designer Drugs (DREADDs) and greatly facilitates studying their contribution to behavior and disease. DREADDs are genetically modified G protein-coupled receptors inert for the endogenous ligand acetylcholine and activated by 'designer drugs' such as Clozapine-N-Oxide (CNO), clozapine, deschloroclozapine (DCZ), compound 21 or JHU37152 and JHU37160 (8-11).

A frequently used method to induce expression of DREADDs in LC neurons consists of injecting a viral vector, such as the adeno-associated virus (AAV) vector or canine adenovirus type 2 (CAV2) vector, in the LC region or its projection targets (12, 13). Using PRSx8, a synthetic dopamine-β-hydroxylase (DBH) promoter, LC-specific DREADD expression is achieved (12, 14). Apart from the type of viral vector and the promoter sequence, parameters such as injection site, volume and the amount of viral vector particles define cell-specific expression and specificity (15, 16).

In this study, we compared different conditions for injecting CAV2-PRSx8-hM3Dq-mCherry viral vector in the LC to induce expression of the excitatory DREADD, hM3Dq, specifically in LC neurons. Our previous results demonstrated low cell-specific expression and specificity using the AAV2/7-PRSx8-hM3Dq-mCherry. We hypothesized that this is due to low tropism of the AAV2/7 viral particle for LC noradrenergic cells (17). The CAV2 viral vector has been proven to efficiently transduce neurons by uptake both at the cell body and at the axonal terminals (18-21) and is validated to target the LC (13, 22, 23).

Pickering et al. demonstrated that CAV2 vectors containing the PRSx8 promoter can transduce LC neurons with high efficiency via direct or retrograde administration for opto-activation experiments (23). However, Hayat et al. observed a substantial lower level of GtACR2 expression when compared to ChR2 using identical injection parameters. This indicates that transduction efficiency is amongst other factors dependent on the transgene itself (22). Additionally, to our knowledge no study describes the use of CAV2 carrying a plasmid to express the excitatory hM3Dq DREADD receptor. Since the transgene sequence itself can influence transduction efficiency, a reliable viral vector administration protocol is required when introducing a novel genetically modified receptor (24). When injecting a novel viral vector into a target area, safety of the administration has to be assessed, since viral vectors can induce toxicity with consequent cell loss (25).

By testing different injection volumes and numbers of CAV2-PRSx8-hM3Dq-mCherry viral vector particles to obtain optimal transduction efficiency with minimal aspecificity and toxicity in the LC of adult rats, we aim to achieve a condition where cell-specific modulation of the LC is feasible to study its role in regulating excitability of neural pathways.

6.2 Material and Methods

6.2.1 Animals

Adult male Sprague-Dawley rats (Envigo, The Netherlands) were used in this study and treated according to European guidelines (directive 2010/63/EU). The local Ethical Committee on Animal Experiments of Ghent University (ECD 16/31) approved the study protocol. Animals were kept under environmentally controlled conditions: 12h light/dark cycles with artificially dimmed light, temperature and relative humidity at 20-23°C and 40-60% respectively with food (Rats and Mice Maintenance, Carfil, Belgium) and water ad libitum. All animals were group-housed in Type IV cages (Tecniplast, Australia) on wood-based bedding (Carfil, Belgium). Cages were enriched with paper nesting material and cardboard tunnels (Carfil, Belgium).

6.2.2 Viral vector administration

Animals (n=43; 10-11 weeks old; 371 ± 72 g body weight) were anesthetized with a mixture of medical oxygen and isoflurane (5% for induction, 2% for maintenance, Isoflo, Zoetis, UK); body temperature was controlled using a heating pad. Rats were placed in a stereotaxic frame (Stoelting, USA) and the skull was exposed. Bregma was lowered 2mm relative to lambda (15° head angle) to target the LC and avoid the transverse sinus. Using a

Hamilton Neuros Syringe (Hamilton company, Nevada, USA) and Quintessential Stereotaxic Injection system (flowrate 150nl/min, Stoelting, USA), three injections of CAV2-PRSx8-hM3Dq-mCherry vector solutions ($5.9x10^9$ pp/µl undiluted, in PBS) were performed along the dorsoventral axis in the LC (3.9 AP, 1.15 ML relative to lambda, -5.8, -5.5, -5.3 DV from dura). The following injection conditions were tested: 3x300 nl containing 5E9 pp of CAV2 (LowV_5E9, n=7, unilateral), 3x600nl containing 10E9pp CAV2 (MediumV_10E9, n=8, unilateral), 3x1200nl containing 20E9 pp CAV2 (HighV_20E9, n=5, unilateral), 3x300 nl containing $1E^9$ pp of CAV2 (LowV_1E9, n=8, bilateral n=5), 3x600nl containing 1E9 pp CAV2 (MediumV_1E9, n=6, unilateral), 3x300 nl containing 0.1E9 pp CAV2 (LowV_0.1E9, n=4, bilateral) and 3x600 nl containing 0.1E9 pp of CAV2 (MediumV_0.1E9, n=5, bilateral) (Table 6.1).

Table 6.1 Overview of the different conditions: volume and number of physical viral particles. The number of animals included in the analysis, without the four animals showing no clear hM3Dq expression (LowV_0.1E9 group, n=1; LowV_1E9, n=1; MediumV_10E9 group, n=1; MediumV_1E9 group, n=1).

Group ID	# animals	Volume	# viral particles	Titer
LowV_0.1E9	3	3x300nl	$0.1x10^9$	~$0.55x10^8$ pp/µl
MediumV_0.1E9	5	3x600nl	$0.1x10^9$	~$1.1x10^8$ pp/µl
LowV_1E9	7	3x300nl	$1x10^9$	~$0.55x10^9$pp/µl
MediumV_1E9	5	3x600nl	$1x10^9$	~ $1.1x10^9$pp/µl
LowV_5E9	7	3x300nl	$5x10^9$	~$5.9x10^9$ pp/µl
MediumV_10E9	7	3x600nl	$10x10^9$	~$5.9x10^9$ pp/µl
HighV_20E9	5	3x1200nl	$20x10^9$	~$5.9x10^9$ pp/µl

After each injection the syringe was left in place for an additional 5 min and then slowly retracted to avoid backflow. Two-component silicone gel (Kwik-Sil; World Precision Instruments, FL, USA) was applied to the craniotomy to protect the brain surface. After surgery, animals were subcutaneously (s.c.) injected with the nonsteroidal anti-inflammatory drug meloxicam (1mg/kg metacam, Boehringer Ingelheim, Germany) and lidocaine (5% Xylocaine gel, Astrazeneca, UK) was applied to the incision site to minimize discomfort. All animals recovered two weeks in their home cage to allow for optimal viral vector expression (26).

6.2.3 Histology

6.2.3.1 Tissue collection and fixation

Animals were euthanized two weeks after viral vector injections with an overdose of sodium pentobarbital (200 mg/kg, i.p.) followed by a transcardial perfusion with phosphate-buffered saline (PBS) and subsequent paraformaldehyde (4%, pH 7.4). The brains were post-fixed in paraformaldehyde for 24h and subsequently cryoprotected in a sucrose solution of 10 % (1day),

20 % (±2 days) and 30% (±3 days) at 4°C until saturation was achieved, snap-frozen in isopentane and stored in liquid nitrogen at -196°C. After 1 hour at -20°C, tissue was transferred to a Cryostat (Leica, Germany) and coronal cryosections of 40µm were made.

6.2.3.2 Immunofluorescence staining

Double label immunostaining for DBH and the mCherry tag fused to the hM3Dq receptor was performed to quantify specificity of hM3Dq expression, and evaluate possible damage to the LC. Twelve histological sections were selected per animal starting approximately 10.5 mm posterior to Bregma, and keeping every third section (80 µm apart), towards anterior. Selected sections were rinsed twice for 5min in distilled water (dH_2O) followed by incubation in 0.5% and 1% H_2O_2 for 30 and 60min respectively to block endogenous peroxidase activity. After washing twice for 5 min in PBS, sections were incubated for 45min in blocking buffer (BB; 0.4% Fish Skin Gelatin (FSG) and 0.2% Triton X in PBS). For one hour at room temperature and subsequently overnight at 4°C, sections were incubated in BB with primary antibodies to visualize noradrenergic LC neurons (mouse anti-DBH, 1:1000, clone 4F10.2, Merck,) and mCherry tag (rabbit anti-red fluorescent protein, 1:1000, ROCK600-901-379, Rockland). The next day, sections were washed twice in BB for 10 min followed by one hour incubation in BB with the secondary antibodies Alexa Fluor goat anti-mouse 488 nm (1:1000, Ab 150113, Abcam) and Alexa goat anti-rabbit 594 nm (1:1000, Ab 150176, Abcam) diluted in BB for 1 hour. After washing twice in PBS for 5 min, a nuclear DAPI stain was performed. After two additional washing steps in PBS (2x5 min), sections were mounted on glass slides and cover slipped using Vectashield H1000 mounting medium (Vector Laboratories, USA) to prevent photobleaching.

6.2.3.3 Fluorescence microscopy and image analysis

Glass slides were scanned using a Pannoramic 250 slide scanner equipped with a Plan Apochromat 40X objective and a pco.edge 4.2 4MP camera to have overview images of all sections. Detailed images of the LC sections were acquired using the Olympus IX81 confocal microscope using Olympus Fluoview FV1000 software or a Nikon A1R confocal laser scanning microscope (Nikon Benelux, Brussels, Belgium) equipped with a Plan Apo VC 20X, 0.75 NA objective lens (Nikon). Images were exported as .nd2 and tiff files for post-processing.

For each rat, images of three tissue sections containing a clear LC nucleus were selected to qualitatively identify the presence and location of the hM3Dq expression. In bilaterally injected animals, both hemispheres were checked for expression and the first injected hemisphere was selected for further analysis, since this resembles the unilateral injected conditions. To assess possible signs of toxicity, in unilaterally injected animals, the injected LC was compared to the contralateral non-injected LC.

Quantitative analysis in bilaterally injected animals was only performed in animals showing unilateral expression of the DREADD, to be able to compare the size of the DREADD-expressing versus the non-expressing LC. Bilaterally DREADD expressing animals were qualitatively assessed for signs of toxicity. Post-processing analysis was performed in Fiji ImageJ Software.

To determine cell-specific expression levels, hM3Dq-DBH colocalization was quantified by placing virtual markers on merged DBH^+/DAPI images to identify the LC cells. These markers were then copied on the merged DBH^+/mCherry images to determine the fraction of LC cells expressing hM3Dq-mCherry. To determine % aspecific hM3Dq expression, the total number of $mCherry^+$ pixels were counted (# of white pixels after "selection of all pixels" and "invert" command on the 8-bit trict TIFF file), minus the ones present in the manually encircled LC and then divided by the total number of $mCherry^+$ pixels.

To assess potential damage induced by the administration of the CAV2 viral vector and subsequent transduction, differences in DBH expression and LC size were compared between transduced and non-transduced hemispheres, since viral vector-induced toxicity can induce cell loss. The DBH^+ image (8-bit tiff file) was split into a transduced- and contralateral non-transduced site, followed by contrast enhancing using "autothreshold – default". "Convert to mask" and "invert" commands to achieve a black background with white pixels. "Analyze particles tool" was used to select and encircle a cluster of white pixels and calculate the total area in $pixels^2$ representing the size of both transduced and contralateral non-transduced LC. The size of both transduced and contralateral non-transduced LC was normalized to the average of the contralateral non-transduced LC within the animal (three sections) (%). Significant decreases in the size of the transduced LC compared to its contralateral non-transduced LC due to cell loss were interpreted as signs of toxicity (25, 27, 28).

6.2.4 Statistical analysis

Statistical analysis was performed using SPSS statistics 27 (IBM corporation, Armonk, New York, USA) and Graphs were made in Graphpad Prism 6. To compare LC-specific expression between conditions, the fraction of DBH^+ cells expressing hM3Dq were fitted into a random effects linear mixed model as dependent variable with injection condition as fixed factor. The individual sections were selected as random intercept and variance components as covariance structure. Since the aspecific expression data is unbound and overdispersion is present, a generalized mixed model with negative binomial log link and with random intercept for animal ID was fitted to the data.

The number of aspecific mCherry pixels was set as dependent variable with the log transformed all $mCherry^+$ pixels as offset and the injection condition as fixed effect. To determine whether there was a significant difference in size of the transduced LC compared to the contralateral non-transduced LC per condition, a linear mixed model was performed with the normalized size as dependent variable, the condition and the side (transduced or non-transduced) and interaction as fixed factors and individual section as intercept. A significant decrease in transduced LC compared to its contralateral non-transduced LC was interpreted as toxicity. All data are represented as mean ± standard error of the mean. A p-value of <0.05 was required for rejection of the null hypothesis.

6.3 Results

6.3.1 Viral vector expression

In all but four animals (n=1 of LowV_0.1E9 group, n=1 of LowV_1E9, n=1 of MediumV_10E9 group, n=1 of MediumV_1E9 group), clear hM3Dq expression was present in the soma and axonal projections of LC neurons (Figure 6.1). In only 6/13 (46%) of the bilaterally injected animals, bilateral expression of hM3Dq expression was observed, possibly due to off-target administration (Supplementary figure 6.1, injection tract visible)(29).

The fraction of LC neurons expressing hM3Dq was highest in the MediumV_1E9 condition (87.3 ± 9.8%) and significantly different from the LowV_5E9 (44.9 ± 8.3%, p=0.002), MediumV_10E9 (59.8 ± 8.3%, p=0.041) and HighV_20E9 group (45.5 ± 9.8%, p=0.005). MediumV_0.1E9 group (77.2 ±5.9%) has significant higher expression compared to the LowV_5E9 (44.9 ± 8.3%, p=0.018) and HighV_20E9 group (45.5 ± 9.8%, p=0.029) (Figure 6.2A).

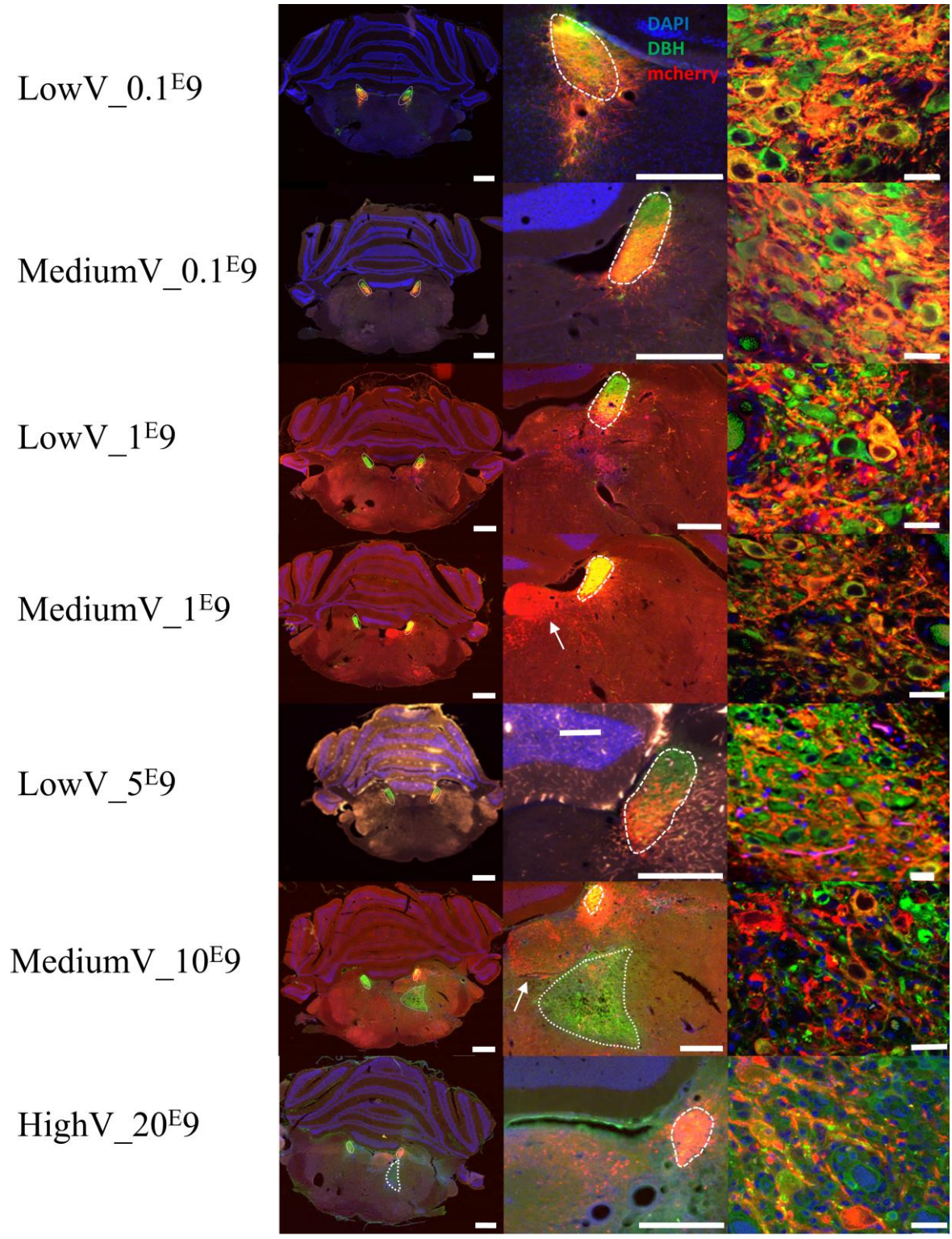

Figure 6.1 Representative visualization of hM3Dq expression pattern in LC after injection of CAV2-PRSx8-hM3Dq-mCherry in LC for each condition. Each row represents a condition. The first column represents an overview of an LC containing tissue section; the second column shows a more detailed view of hM3Dq expression in the region of LC. The last column shows a confocal image of DBH+/hM3Dq+ cells. LC is encircled with a dashed line. Aspecific hM3Dq expression is indicated by a white arrow. Ectopic DBH expression is indicated by the dotted line. LC-NA neurons and projections are visualized using primary anti-DBH antibody (green, AF 488nm) and expression of hM3Dq DREADD is visualized using anti-RFP (red, AF 594nm), cell nuclei are stained with DAPI (blue). Scale bar is represented at each image, left column 1000µm, middle column 500µm and right column 25µm.

A generalised mixed negative binomial model estimates the rate of aspecific hM3Dq expression in the LowV_1E9(18.9 ± 7.6%) and MediumV_1E9 condition (36.2 ± 17.3%) to be 4.8 times (95%CI 1.4-16.4, p=0.014) and 9.1 times (95%CI 2.4-34.7, p=0.001) higher compared to the MediumV_0.1E9 condition (4.0 ± 1.9%), showing the lowest levels of aspecificity. The aspecific expression in the MediumV_10E9 condition (15.5 ± 6.3%) is estimated to be 3.9 times higher (95% CI 1.1 -13.5, p = 0.031) compared to the MediumV_0.1E9 condition (4.0 ± 1.9%) (Figure 6.2B; Supplementary Table 6.1 Fixed coefficients).

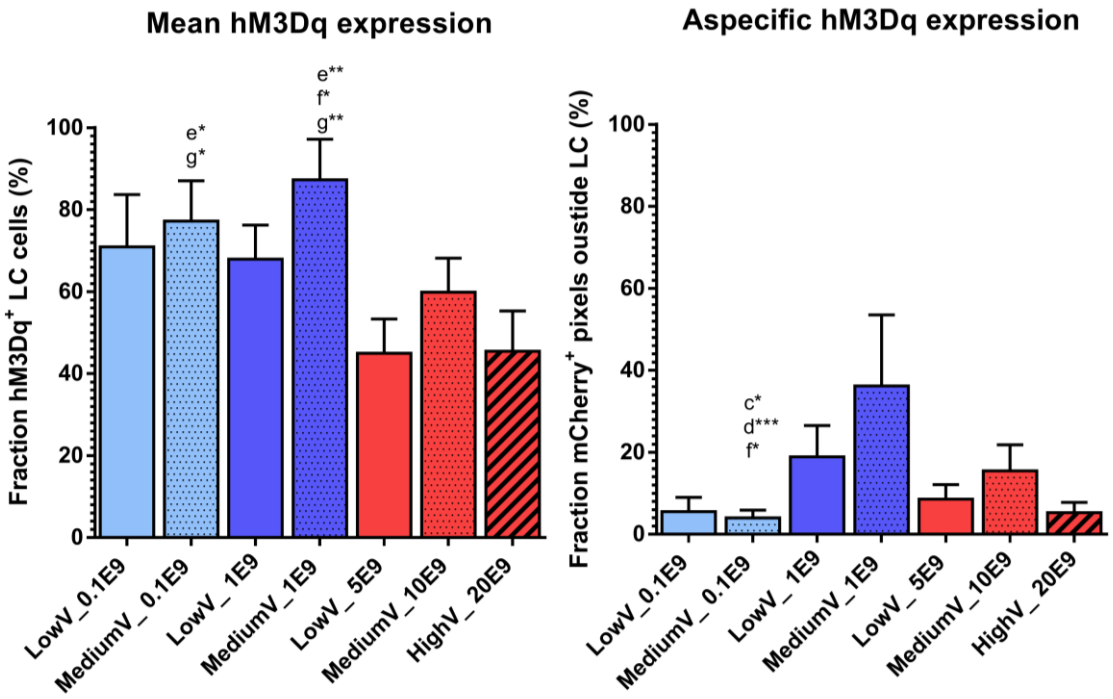

Figure 6.2 Transduction efficiency of CAV2-PRSx8-hM3Dq-mCherry viral vector to express hM3Dq in LC. (A) Mean hM3Dq expression in DBH positive cells after manual cell count. MediumV_1E9 induces the highest level of hM3Dq expression compared to LowV_5E9, MediumV_10E9 and HighV_20E9. MediumV_0.1E9 condition shows similar levels, significantly higher compared to LowV_5E9 and HighV_20E9. (B) Mean aspecific hM3Dq expression. In the MediumV_0.1E9 condition the lowest level of aspecific expression is observed compared to LowV_1E9, MediumV_1E9 and MediumV_10E9. GLM negative binomial statistical analysis showed that the chance of an mCherry+ pixels detected outside LC is respectively 4.8, 9.1 and 3.9 times higher in the LowV_1E9, MediumV_1E9 and MediumV_10E9 condition compared to HighV_20E9. Bars represent the mean ± SEM per condition. Pattern inside the bars represent the injected volume: low, 3x300nl=no pattern; medium, 3x600nl=dotted pattern; high, 3x1200nl=striped pattern. Colours of the bars represent the dilution: undiluted (5,10,20E9 pp) =red; diluted to 1E9pp =dark blue; diluted to 0.1E9pp =light blue. Letters above the bar represent significant difference with the corresponding condition (a: the first bar from the left, in alphabetical order with the last bar being g). Stars added to the letters indicate the level of significance (*p<0.05; **p<0.01, ***p<0.001).

6.3.2 Signs of toxicity

Conditions with the highest number of viral particles were associated with a clear difference in DBH expression and size of the transduced LC compared to the contralateral LC. Quantitative comparison of transduced versus contralateral non-transduced LC size showed a significant size reduction in these conditions. Toxicity was significantly high in the MediumV_10E9 condition ($p<0.001$), showing a significant decrease in the size of the transduced LC compared to its contralateral LC. The size of injected LC was 38.5 ± 6.7% of the contralateral LC volume. A significant reduction in size of transduced LC was also observed in the LowV_5E9 (77.2 ± 6.7%; $p=0.002$) and HighV_20E9 (66.4 ±7.9%; $p<0.001$) conditions compared to the contralateral non-transduced LC (Fig 6.3).

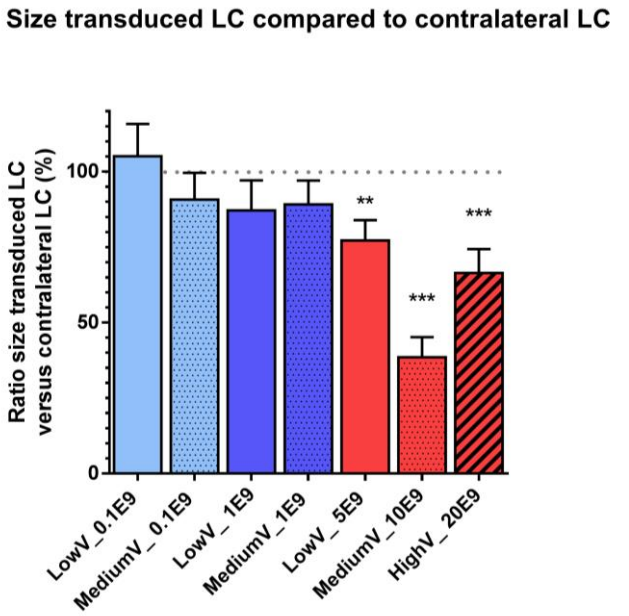

Figure 6.3 Graphical representation of the size of the transduced LC compared to the contralateral non-transduced LC. A significant decrease in size was observed in all undiluted conditions with the highest decrease in the MediumV_10E9 condition (transduced LC was 38.5 ± 6.7% of the contralateral LC size, $p<0.001$). A significant decrease in size of transduced LC was also observed in the LowV_5E9 (77.2 ± 6.7, $p=0.002$) and HighV_20E9(66.4 ± 7.9$p<0.001$) condition. Bars represent the mean difference in LC size ± SEM per condition normalised to the contralateral non-transduced LC (represented by dotted line). Pattern inside the bars represent the injected volume: low, 3x300nl=no pattern; medium, 3x600nl=dotted pattern; high, 3x1200nl=striped pattern. Colours of the bars represent the dilution: undiluted (5,10,20E9 pp) =red; diluted to 1E9pp =dark blue; diluted to 0.1E9pp =light blue. (**$p<0.01$, ***$p<0.001$).

Qualitative analysis of tissue sections from the MediumV_10E9 and HighV_20E9 condition showed additionally to decreased LC size, ectopic DBH expression in the transduced brainstem and clear lesions in the injected LC (Figure 6.1A-B MediumV_10E9, HighV_20E9; Fig 6.4).

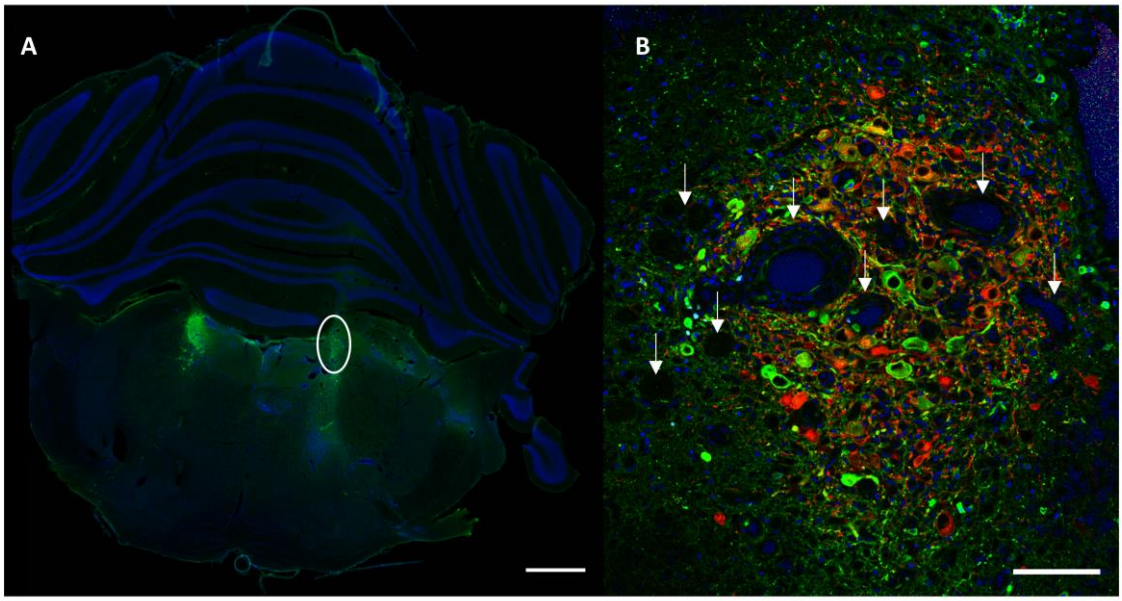

Figure 6.4 Representative section visualizing signs of toxicity. (A) A clear difference in size of the transduced LC (right, encircled) compared to contralateral in animal injected with MediumV_10E9 condition. Only cell nuclei (DAPI, blue) and DBH^+ neurons (primary antibody anti-DBH, AF 488, green) are visualized in this image. **(B)** A clear decrease in number of LC neurons, in combination with the presence of lesions and vacuoles (indicated by the white arrows). LC-NA neurons and projections are visualized using primary anti-DBH antibody (green, AF 488nm) and expression of hM3Dq DREADD is visualized using anti-RFP (red, AF 594nm), cell nuclei are stained with DAPI (blue). Scale bar left image 1000µm and right image 100µm.

Qualitative analysis of the bilaterally hM3Dq expressing animals did not show clear visible signs of toxicity in the LowV_0.1E9, LowV_1E9 and MediumV_0.1E9 condition as confirmed by quantitative analysis of the unilateral expressing animals of these groups (Representative image Supplementary Fig. 6.2).

6.4 Discussion

This study evaluated different conditions for injection of CAV2 viral vector to obtain expression of hM3Dq DREADD in a high number of LC neurons with limited aspecific expression and toxicity.

All conditions resulted in hM3Dq expression in LC noradrenergic neurons but differences in expression specificity and toxicity were observed. Transduction levels are the highest when diluted conditions, 0.1E9 pp and 1E9 pp of CAV2-PRSx8-hM3Dq-mCherry at the target site, are used with average expression ranging from 67.9 ±8.3% to 87.3± 9.8%. This is much higher

compared to our previous AAV2/7 approach (20.6 ± 2.3%; 5.99x10^9 GC/µl) (17) and similar to other groups using the CAV2 viral vector to induce expression of Channelrhodopsin under control of a PRSx8 promoter at conditions similar to ours (3 injections of 400nl, a total of 10^9 viral particles at the target site) observing expression levels of 83 ± 3.4% (22). Low expression levels of hM3Dq were observed with the highest numbers of viral particles (> 1E9 pp). A similar decrease in expression levels associated with increasing titers have been described upon pontospinal injections of AAV for retrograde labelling of noradrenergic neurons (30) and after injections of an adenovirus vector in striatum (27). Injection of high viral vector titers can result in blood-brain barrier changes and leakage of viral particles in systemic circulation as observed after AAV injection in the substantia nigra of mice, resulting in lower expression levels (31). Injecting more than 1E9 CAV2 particles also resulted in signs of toxicity with decreased size of LC, ectopic DBH expression and the presence of lesions. Excess load of viral particles can induce cellular stress and disrupt the homeostasis of the endoplasmatic reticulum (ER). Once ER stress is induced, and proteins do not properly fold, the unfolded protein response (UPR) pathways are activated to restore the cellular machinery. This includes activation of immune pathways with recruitment of macrophages, astrocytes and microglia and infiltration of antigen nonspecific T cells. This immune response can result in clearance of viral particles as well as substantial loss of astrocytes and neurons (27, 28). Additionally, when a point of no return is reached, UPR will induce apoptosis and autophagy leading to cell loss (25). Next to high presentation of viral proteins and transgene, high levels of the PRSx8 promoter might also induce changes in LC-NA physiology due to sequestration of Phox2 proteins at the multiple Phox2 binding sites in the promoter sequence. These proteins are necessary for maintaining normal NA phenotype, possibly explaining changes in DBH expression and even cell loss (32). Although the ectopic DBH expression was only observed in animals injected with high titer conditions, we cannot rule out that this phenomenon is possibly due to non-specific binding of the antibody to compromised cells (33).
The CAV2 viral vector, a non-human derived viral vector, is described to be safer in use for long-term experiments and eventual translation to the clinic, due to the absence of a pre-existing immune response (19, 20), however our observations indicate that the use of high titers of CAV2-PRSx8-hM3Dq-mCherry can induce signs of toxicity with tissue damage and concurrent lower transduction efficiency potentially due to a combination of innate immune responses, cellular stress and phox2 protein sequestration (25, 27, 32).

Although injecting 1E9 CAV2 particles (MediumV_1E9 condition) did not result in LC damage, a significant presence of aspecific hM3Dq expression (36.2 ± 17.3%) was observed.

By further reducing the number of injected CAV2 particles to 0.1E9, efficient transduction of LC neurons was preserved (>70%) while aspecific expression was significantly reduced to levels below 5% in the MediumV_0.1E9 and LowV_0.1E9 condition. Previous studies using the CAV2 viral vector to induce PRSx8-driven expression of ChR2, PSAM and GtACR2 reported comparably low levels of aspecific expression (0-2%) (13, 22, 34, 35). Viral vectors (both AAV and CAV2) containing PRSx8 driven plasmids are widely used and validated to induce selective transduction in noradrenergic neurons both in mice and rats (12, 13, 22, 23, 29, 35-39). In a previous study, using AAV2/7 viral vector to transduce cells with the PRSx8-hMD3q-mCherry construct, we observed low levels of hM3Dq expression in LC (20.6 ± 2.3%) with high levels of aspecific expression (26.0 ± 4.1%) outside the LC (17). These observations indicate that CAV2 is a more efficient tool than AAV2/7 to introduce genes in LC neurons and that PRSx8 can result in important leakage of expression in non-catecholaminergic neurons. The latter effect is thought to be (partially) mediated by Phox2 regulatory elements in the promoter sequence activated by Phox2 transcription factors also present in non-catecholaminergic neurons (14, 40). In our study, off-target hM3Dq expression was assessed using pixel values instead of manually counting $mCherry^+/DBH^-$ cells. To quantify aspecific expression levels in a similar fashion as the cell-specific hM3Dq levels quantification, confocal images of the entire section should be acquired to detect any possible off-target expression and provide the ability for manual cell counting. As aspecific expression was not the primary hypothesis of this study resulting in the lack of confocal image data outside of the LC region, quantification of the DBH^-/ $mCherry^+$ pixels of the epifluorescence whole section images served as a valid proxy for off-target expression.

In a subset of the injected animals no expression was observed (four in total) and in a subset of bilaterally injected animals unilateral expression was observed, possibly due to off-target administration, similar to other studies describing the difficulties of targeting a small brainstem nucleus and observing unilateral expression after bilateral LC administration of the viral vector (29, 38). Animals with bilateral hM3Dq expression could not be included for quantitative analysis of toxicity. In these animals of the LowV_0.1E9, LowV_1E9 and MediumV_0.1E9 conditions qualitative analysis did not show major signs of toxicity as observed with the high titer conditions.

Our results indicate that introducing a new genetic product into a target region using viral vectors should be approached with caution and thorough titration with control for toxicity. A few papers describe these phenomena after injection of adenoviral or adeno-associated viral

vectors, however not much is reported about CAV2 (25, 27, 28). Since the use of CAV2 viral vectors in future clinical trials is considered because of its known advantages such as high tropism for neurons, ability for retrograde transport and lack of existing immune response in patients (19-21), further research including its safety at higher titers is necessary.

We conclude that direct injection of 0.1E9 CAV2-PRSx8-hM3Dq-mCherry viral vector particles in LC of adult rats is a suitable approach for near complete transduction of LC neurons while keeping aspecific expression and toxicity low. This will allow future chemogenetic modulating of LC to unravel its role in regulating the excitability of brain networks and in specific neurological diseases.

6.5 Supplementary material

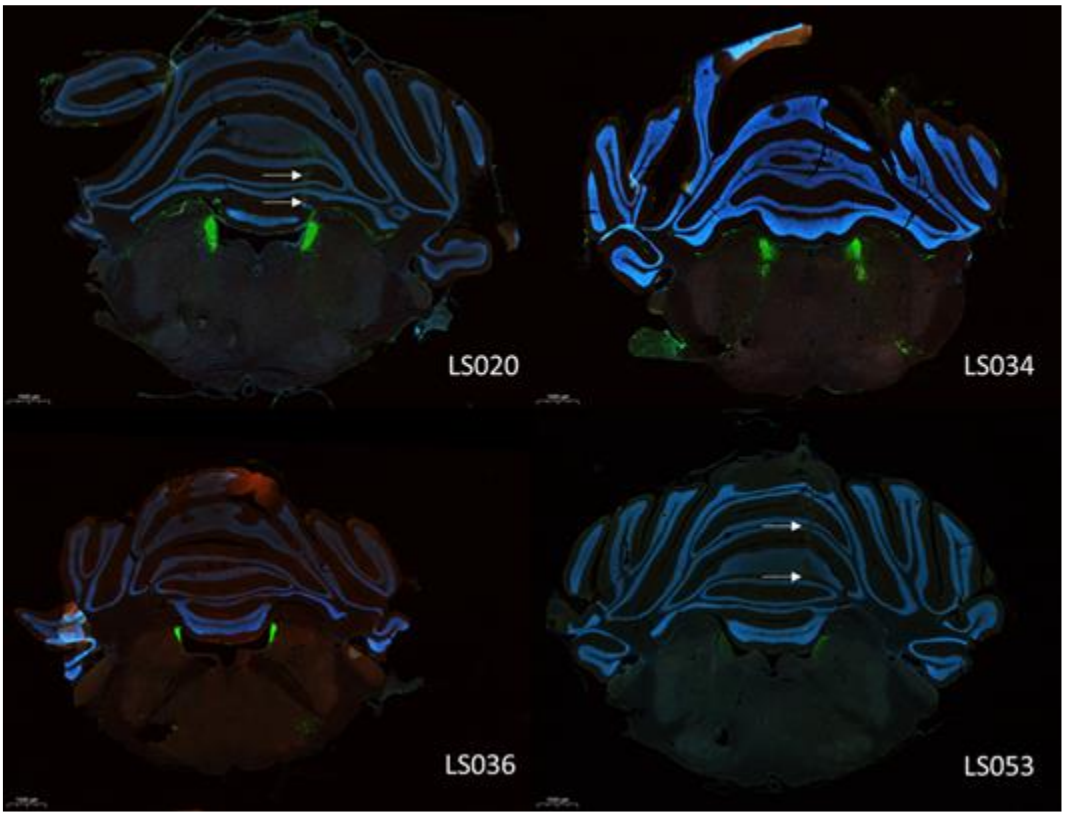

Supplementary Figure 6.1 Overview of animals without clear hM3Dq expression. LS020 (MediumV_10E9), LSO34(LowV_1E9), LSO36(MediumV_1E9) and LSO53 (LowV_0.1E9) show no hM3Dq expression probably due to off target injection. The injection tract (indicated by white arrow) is visible in LSO20 and LSO53 and indicates the injection to be medial from LC, possibly ending in the fourth ventricle explaining absence of hM3Dq expression.

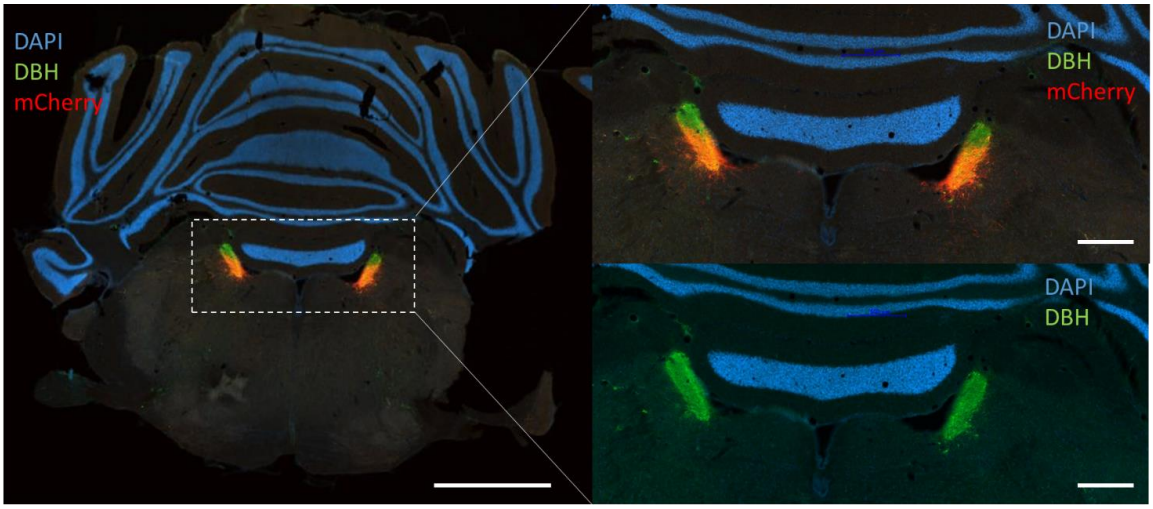

Supplementary Figure 6.2 Representative image of bilaterally injected animal bilaterally expressing hM3Dq DREADD. Left panel. Overview of section (LowV_0.1E9). Right upper panel gives an overview of bilateral hM3Dq expression. Right lower panel showing LC without hM3Dq, indicating no clear signs of toxicity. Qualitative analysis reveals identical size, no cell loss or lesions. Scale bar left 2000µm, right 500µm.

Supplementary Table 6.1. Fixed coefficients of the generalized mixed model with negative binomial log link analysis of the aspecific expression dataset.

Fixed Coefficients[a]

Model Term	Coefficient	Std. Error	t	Sig.	95% Confidence Interval		Exp(Coefficient)	95% Confidence Interval for Exp(Coefficient)	
					Lower	Upper		Lower	Upper
Intercept	-3,228	,4770	-6,767	,000	-4,173	-2,282	,040	,015	,102
Low_u	,780	,6245	1,248	,215	-,458	2,017	2,180	,632	7,518
Low_d	1,562	,6245	2,501	,014	,324	2,799	4,766	1,383	16,432
Low_D	,330	,7923	,416	,678	-1,240	1,900	1,391	,289	6,687
Medium_u	1,366	,6245	2,187	,031	,128	2,604	3,920	1,137	13,513
Medium_d	2,213	,6745	3,281	,001	,876	3,550	9,140	2,401	34,797
High_u	,295	,6749	,437	,663	-1,043	1,632	1,343	,352	5,116
Medium_D	0[b]	.	.	.	.	.	.	.	.
NegativeBinomial	1,286	.	.	.	.	.			

Funding

Latoya Stevens was supported by a Ph.D. grant from the Queen Elisabeth Medical Foundation for Neurosciences (G.S.K.E) and the Ghent Institute for Neuroscience. Profs. Dr. Kristl Vonck and Dr. Robrecht Raedt are supported by the Special Research Funds (BOF) of Ghent University. Prof. Dr. Paul Boon was supported by research grants from FWO, BOF, and Ghent University.

Author contributions

LS, WVL, RR, and KV contributed to the study design and analyzed plan. LS performed the experimental work and obtained histological data. LS and WVL performed data and statistical analysis. LS, RR, and KV prepared the manuscript. All authors reviewed the manuscript.

Bibliography

1. Szabadi E. Functional neuroanatomy of the central noradrenergic system. J Psychopharmacol. 2013;27(8):659-93.

2. Samuels ER, Szabadi E. Functional Neuroanatomy of the Noradrenergic Locus Coeruleus: Its Roles in the Regulation of Arousal and Autonomic Function Part I: Principles of Functional Organisation. 2008.

3. Samuels ER, Szabadi E. Functional Neuroanatomy of the Noradrenergic Locus Coeruleus: Its Roles in the Regulation of Arousal and Autonomic Function Part II: Physiological and Pharmacological Manipulations and Pathological Alterations of Locus Coeruleus Activity in Humans. 2008.

4. Bari BA, Chokshi V, Schmidt K. Locus coeruleus-norepinephrine: basic functions and insights into Parkinson's disease. Neural Regen Res. 2020;15(6):1006-13.

5. Mather M, Harley CW. The Locus Coeruleus: Essential for Maintaining Cognitive Function and the Aging Brain. Trends Cogn Sci. 2016;20(3):214-26.

6. Grimonprez A, Raedt R, Portelli J, Dauwe I, Larsen LE, Bouckaert C, et al. The antidepressant-like effect of vagus nerve stimulation is mediated through the locus coeruleus. J Psychiatr Res. 2015;68:1-7.

7. Raedt R, Clinckers R, Mollet L, Vonck K, El Tahry R, Wyckhuys T, et al. Increased hippocampal noradrenaline is a biomarker for efficacy of vagus nerve stimulation in a limbic seizure model. J Neurochem. 2011;117(3):461-9.

8. Gomez JL, Bonaventura J, Lesniak W, Mathews WB, Sysa-Shah P, Rodriguez LA, et al. Chemogenetics revealed: DREADD occupancy and activation via converted clozapine. Science. 2017;357(6350):503-7.

9. Bonaventura J, Eldridge MAG, Hu F, Gomez JL, Sanchez-Soto M, Abramyan AM, et al. High-potency ligands for DREADD imaging and activation in rodents and monkeys. Nat Commun. 2019;10(1):4627.

10. Jendryka M, Palchaudhuri M, Ursu D, van der Veen B, Liss B, Katzel D, et al. Pharmacokinetic and pharmacodynamic actions of clozapine-N-oxide, clozapine, and compound 21 in DREADD-based chemogenetics in mice. Sci Rep. 2019;9(1):4522.

11. Nagai Y, Miyakawa N, Takuwa H, Hori Y, Oyama K, Ji B, et al. Deschloroclozapine, a potent and selective chemogenetic actuator enables rapid neuronal and behavioral modulations in mice and monkeys. Nat Neurosci. 2020;23(9):1157-67.

12. Vazey EM, Aston-Jones G. Designer receptor manipulations reveal a role of the locus coeruleus noradrenergic system in isoflurane general anesthesia. Proc Natl Acad Sci U S A. 2014;111(10):3859-64.

13. Hirschberg S, Li Y, Randall A, Kremer EJ, Pickering AE. Functional dichotomy in spinal- vs prefrontal-projecting locus coeruleus modules splits descending noradrenergic analgesia from ascending aversion and anxiety in rats. Elife. 2017;6(Lc):e29808-e.

14. Hwang DY, Carlezon WA, Jr., Isacson O, Kim KS. A high-efficiency synthetic promoter that drives transgene expression selectively in noradrenergic neurons. Hum Gene Ther. 2001;12(14):1731-40.

15. Delbeke J, Hoffman L, Mols K, Braeken D, Prodanov D. And Then There Was Light: Perspectives of Optogenetics for Deep Brain Stimulation and Neuromodulation. Front Neurosci. 2017;11(December):663.

16. Castle MJ, Turunen HT, Vandenberghe LH, Wolfe JH. Controlling AAV Tropism in the Nervous System with Natural and Engineered Capsids. Methods Mol Biol. 2016;1382:133-49.

17. Stevens L, Vonck K, Larsen LE, Van Lysebettens W, Germonpre C, Baekelandt V, et al. A Feasibility Study to Investigate Chemogenetic Modulation of the Locus Coeruleus by Means of Single Unit Activity. Front Neurosci. 2020;14(March):162.

18. Soudais C, Boutin S, Hong SS, Chillon M, Danos O, Bergelson JM, et al. Canine adenovirus type 2 attachment and internalization: coxsackievirus-adenovirus receptor, alternative receptors, and an RGD-independent pathway. J Virol. 2000;74(22):10639-49.

19. Kremer EJ, Boutin S, Chillon M, Danos O. Canine adenovirus vectors: an alternative for adenovirus-mediated gene transfer. J Virol. 2000;74(1):505-12.

20. Del Rio D, Beucher B, Lavigne M, Wehbi A, Gonzalez Dopeso-Reyes I, Saggio I, et al. CAV-2 Vector Development and Gene Transfer in the Central and Peripheral Nervous Systems. Front Mol Neurosci. 2019;12:71.

21. Junyent F, Kremer EJ. CAV-2--why a canine virus is a neurobiologist's best friend. Curr Opin Pharmacol. 2015;24:86-93.

22. Hayat H, Regev N, Matosevich N, Sales A, Paredes-Rodriguez E, Krom AJ, et al. Locus coeruleus norepinephrine activity mediates sensory-evoked awakenings from sleep. Sci Adv. 2020;6(15):eaaz4232.

23. Li Y, Hickey L, Perrins R, Werlen E, Patel AA, Hirschberg S, et al. Retrograde optogenetic characterization of the pontospinal module of the locus coeruleus with a canine adenoviral vector. 2016. p. 274-90.

24. Wang D, Tai PWL, Gao G. Adeno-associated virus vector as a platform for gene therapy delivery. Nat Rev Drug Discov. 2019;18(5):358-78.

25. Sen D, Balakrishnan B, Jayandharan GR. Cellular unfolded protein response against viruses used in gene therapy. Front Microbiol. 2014;5:250.

26. Smith KS, Bucci DJ, Luikart BW, Mahler SV. DREADDs: Use and application in behavioral neuroscience. 2016. p. 137-55.

27. Thomas CE, Birkett D, Anozie I, Castro MG, Lowenstein PR. Acute direct adenoviral vector cytotoxicity and chronic, but not acute, inflammatory responses correlate with decreased vector-mediated transgene expression in the brain. Mol Ther. 2001;3(1):36-46.

28. Reimsnider S, Manfredsson FP, Muzyczka N, Mandel RJ. Time course of transgene expression after intrastriatal pseudotyped rAAV2/1, rAAV2/2, rAAV2/5, and rAAV2/8 transduction in the rat. Mol Ther. 2007;15(8):1504-11.

29. Rorabaugh JM, Chalermpalanupap T, Botz-Zapp CA, Fu VM, Lembeck NA, Cohen RM, et al. Chemogenetic locus coeruleus activation restores reversal learning in a rat model of Alzheimer's disease. Brain. 2017;140(11):3023-38.

30. Howorth PW, Teschemacher AG, Pickering AE. Retrograde adenoviral vector targeting of nociresponsive pontospinal noradrenergic neurons in the rat in vivo. J Comp Neurol. 2009;512(2):141-57.

31. Van der Perren A, Toelen J, Carlon M, Van den Haute C, Coun F, Heeman B, et al. Efficient and stable transduction of dopaminergic neurons in rat substantia nigra by rAAV 2/1, 2/2, 2/5, 2/6.2, 2/7, 2/8 and 2/9. Gene Ther. 2011;18(5):517-27.

32. Hwang DY, Hwang MM, Kim HS, Kim KS. Genetically engineered dopamine beta-hydroxylase gene promoters with better PHOX2-binding sites drive significantly enhanced transgene expression in a noradrenergic cell-specific manner. Mol Ther. 2005;11(1):132-41.

33. Buchwalow I, Samoilova V, Boecker W, Tiemann M. Non-specific binding of antibodies in immunohistochemistry: fallacies and facts. Sci Rep. 2011;1:28.

34. Hickey L, Li Y, Fyson SJ, Watson TC, Perrins R, Hewinson J, et al. Optoactivation of locus ceruleus neurons evokes bidirectional changes in thermal nociception in rats. J Neurosci. 2014;34(12):4148-60.

35. Xiang L, Harel A, Gao H, Pickering AE, Sara SJ, Wiener SI. Behavioral correlates of activity of optogenetically identified locus coeruleus noradrenergic neurons in rats performing T-maze tasks. Sci Rep. 2019;9(1):1361.

36. Fortress AM, Hamlett ED, Vazey EM, Aston-Jones G, Cass WA, Boger HA, et al. Designer receptors enhance memory in a mouse model of Down syndrome. J Neurosci. 2015;35(4):1343-53.

37. Cope ZA, Vazey EM, Floresco SB, Aston Jones GS. DREADD-mediated modulation of locus coeruleus inputs to mPFC improves strategy set-shifting. Neurobiol Learn Mem. 2019;161:1-11.

38. Kane GA, Vazey EM, Wilson RC, Shenhav A, Daw ND, Aston-Jones G, et al. Increased locus coeruleus tonic activity causes disengagement from a patch-foraging task. Cogn Affect Behav Neurosci. 2017;17(6):1073-83.

39. Vazey EM, Moorman DE, Aston-Jones G. Phasic locus coeruleus activity regulates cortical encoding of salience information. Proc Natl Acad Sci U S A. 2018;115(40):E9439-E48.

40. Bruinstroop E, Cano G, Vanderhorst VG, Cavalcante JC, Wirth J, Sena-Esteves M, et al. Spinal projections of the A5, A6 (locus coeruleus), and A7 noradrenergic cell groups in rats. J Comp Neurol. 2012;520(9):1985-2001.

Part III
Discussion, general conclusion and future perspectives

Chapter 7 Discussion and future perspectives

7.1 Conclusions

The locus coeruleus-noradrenergic system is believed to play an important role in key functions such as cognition, attention, sleep-wake cycle, and neuroplasticity through its widespread projections throughout the brain (1-3). More recently, (pre)clinical studies have emphasized the potential therapeutic role of the LC-NA system in neurological disorders such as Alzheimer's disease, Parkinson's', Major Depressive Disorder, and epilepsy (4-7). Since 30% of epileptic patients are not helped with the current anti-epileptic drugs, neuromodulation techniques such as vagus nerve stimulation (VNS) are applied. Despite its proven efficacy in a subset of refractory patients, the mechanism of action is still not fully understood. (Pre)clinical studies have proven a role for the LC-NA system in the VNS-induced anti-epileptic and mood-enhancing effects through increases of noradrenaline in the hippocampus (6-8). To elucidate the exact relation between the LC and hippocampal excitability, a neuromodulation technique is needed with higher specificity compared to electrical and chemical modulation techniques. Chemogenetics, a technique to induce cell-specific expression of an excitatory hM3Dq DREADD receptor (9), is desirable to selectively modify the activity of the LC neurons and determine their role in modulating hippocampal excitability. High and specific hM3Dq expression is needed in order to selectively activate LC neurons in response to systemic administration of the agonistic ligand. In this thesis, optimization of the hM3Dq DREADD in LC-NA neurons was performed using different types of viral vectors. A first step was made to chemogenetically modify the genetically transduced LC neurons using systemic injections of different doses of clozapine. From this thesis we can conclude that:

- AAV2/7-PRSx8-hM3Dq-mCherry approach is suboptimal to induce hM3Dq expression in LC-NA neurons in high and specific levels (**Chapter 5**).
- Presumed subclinical doses of clozapine (0.1 mg/kg, s.c.) induced modulatory effects in control animals doubting its applicability as selective ligand for chemogenetic activation of LC (**Chapter 5**).
- More than $1x10^9$ physical particles (pp) of CAV2-PRSx8-hM3Dq-mCherry at the injection site induced signs of toxicity with decreased LC size, cell loss and lesions (**Chapter 6**).
- Titrating the number of physical particles of CAV2-PRSx8-hM3Dq-mCherry below $1x10^9$ induced high levels of cell-specific hM3Dq expression in LC-NA neurons and low aspecificity. No signs of toxicity were observed (**Chapter 6**).

7.2 General Discussion

7.2.1 Difference in transduction efficiency of AAV2/7 and CAV2 viral vector approach

Analysis of the immunofluorescence stainings performed on brain sections containing LC was necessary to both qualitatively and quantitatively assess the hM3Dq expression levels after AAV2/7 or CAV2 viral vector administration. To achieve selective chemogenetic activation of LC-NA neurons, high cell-specific hM3Dq expression is required.

In the first manuscript described in chapter 5, a small volume of undiluted AAV2/7-PRSx8-hM3Dq-mCherry viral vector was injected in LC of healthy rats, resulting in overall low cell-specific expression (21%) and presence of hM3Dq in non-catecholaminergic neurons (26%) in the vicinity of LC. Whereas in the second manuscript using a different type of viral vector, CAV2, carrying the same construct, induced high levels of cell-specific expression (up to 87%) and low levels of aspecific expression (<5%), however only when less than $1x10^9$ physical viral particles were administered. The discrepancy in transduction efficiency of both viral vector approaches can have different causes. Due to different methodology strategies (as discussed below in more detail) and intrinsic characteristics of the viral vectors, one cannot strictly compare the outcome parameters of both approaches. Although optimization of the injection strategy of CAV2 induced higher transduction efficiency compared to AAV2/7, some conditions resulted in higher levels of aspecificity. This emphasizes the importance of titration experiments, and that one injection condition cannot be seen as the golden standard for each research question.

Expression of a transgene (hM3Dq) in a target cell (LC neuron) upon viral vector administration depends on different steps starting from the administration (route, volume, dose) to binding and internalisation of the viral particle, followed by a series of intracellular events that can be stopped at every step, inhibiting transcription and/or translation (10-12). Since both viral vectors were locally administered to achieve focal hM3Dq expression, and show high tropism for neurons, the discrepancy in transduction efficiency must have another reason (13, 14).

7.2.1.1 Compatibility of the viral particle and the target cell

AAV2/7 seems suboptimal when compared to other serotypes of AAV (e.q AAV2/9), where with the same promoter construct >97% of LC neurons express hM3Dq after local injection (15-17). However, we have to approach this comparison with the necessary nuance, since we never tested the AAV2/9 viral vector in our own lab, and based on literature there are some

differences present in administration strategy. Not only a different injection procedure is used (glass pipette versus Neurosyringe), also a larger volume (1.4µl versus 10nl) is injected with a functional titer that cannot be compared to our AAV2/7 expressed in number of genome copies, due to a different assay method. However, the low transduction efficiency of the AAV2/7 viral vector condition might also be due to other factors, such as an intrinsic lower compatibility of the AAV2/7 viral particle and the surface receptors present on LC neurons. In general, tropism is mainly controlled by the serotype of the viral vector, which defines the characteristics of the capsid proteins (pentons, hexons and fibers) (18, 19). Both AAV and CAV have non-enveloped icosahedral shaped capsids, however the shape, length and bends of the fiber and fiber knob at the distal end responsible for binding target cell receptors will differ between serotypes (13, 14, 20-25). AAV2/7 is an engineered viral vector where the genome of serotype 2 is encapsulated in a viral capsid with the characteristics of serotype 7 (18). Although AAV2/7 was as effective as AAV2/9 in transducing dopaminergic neurons in substantia nigra (26), the difference in capsid proteins compared to AAV2/9 can lead to a lower affinity for the surface receptors on LC-NA neurons, resulting in lower expression levels when compared to studies using the AAV2/9 approach (15-17).

In general, AAV internalisation is depending primarily on the binding of HSPG receptors and secondary on the presence of $\alpha_v\beta5$ integrins who act as facilitators in the internalisation process (27-29). Inhibition of these integrins using the chelating agent EDTA led to inefficient transduction, indicating the importance of integrins as co-receptors (27, 28, 30). Receptor and co-receptor types preferentially bound by different AAV serotypes have been identified. The AAV2/9 has high affinity for laminin receptors. However, the exact receptor preference of AAV2/7 is still unknown (19, 31), despite extensive array studies containing more than 600 glycans and natural or synthetic heparins (32). Considering the low transduction efficiency observed with AAV2/7 in our study (33), we hypothesise that either low levels of the primary receptors or co-receptors ($\alpha_v\beta5$integrins) are present in LC neurons, resulting in not only a low attachment profile, but perhaps also low internalisation capacity. Since the receptor affinity of AAV2/7 is unknown, it is hard to solve this problem. In order to tackle this problem, the receptor affinity of AAV2/7 should be further explored.

Recently a study described the use of a receptor complementation strategy, genetically modifying the target cells first to express a large amount of CAR receptors in order to optimise the binding and transduction of CAV particles (34). Nevertheless, more research is being conducted to identify and map the different capsid formations to optimise the interaction of viral particles with the host cells (32).

Our titration study, injecting different volumes and number of viral particles of the CAV2 viral vector in the LC of healthy rats led to an optimised protocol (0.1x10e9 pp at site) for high cell-specific expression (>70%) and low aspecificity (<5%). Despite the unknown distribution of CAR receptors (21), we can assume that CAR receptors are abundantly present on the surface of LC neurons, since both our own group and other studies reported high transduction efficiency using CAV2 to target LC (35-38). CAV viral vectors use similar internalisation pathways compared to AAV, however through binding of another type of primary receptor. Secondly, binding of the β-domain of $\alpha_v\beta5$ integrins is the most common (13, 20-22). However, there have been cases of CAR- and integrin-independent transduction, indicating that CAV2 viral particles can internalise cells lacking CAR receptors or this specific type of integrin (20), increasing its ability to bind and internalise cells and increase its chances of transduction.

Another possible reason for the discrepancy in transduction efficiency of AAV2/7 versus different injection conditions of CAV2 can be the net charge of the virions. The external loops of the proteins forming the capsid are charged and influence attachment. If the net charge of the viral particle is more neutral, the level of repulsion between the capsid and the cell surface is lower, permitting easier attachment. Studies have been modelling these charges, based on the presence of external loops and EM structure, showing that CAV viral particles are more neutral when compared to adenoviral particles (20), possibly explaining its higher affinity and transduction efficiency for LC neurons compared to AAV2/7 observed in our studies.

As described above, also here a critical approach to the observed difference in transduction efficiency between AAV and CAV is necessary. Although we were able to substantially increase the transduction efficiency by titrating the injection parameters of CAV, we cannot compare it completely to the AAV results, since no identical experimental approach was used. Firstly, larger volumes (3x300nl, 3x600nl and 3x1200nl) were injected spread over three coordinates along the dorsoventral axis (-5.3, -5.5 and -5.7 DV), which might partially explain the increased coverage of LC with hM3Dq expression, in contrast to a single AAV injection of 10nl at -5.7DV.

Since it was never our primary goal to perform a comparative study of different viral vectors, caveats in the methodology hinder strict differentiation. Nevertheless, in preliminary studies we injected larger volumes of AAV at a single stereotactic location in LC, which did not result in higher levels of cell-specific expression (these larger volumes are summerized in Appendix Table B.1).

7.2.1.2 Production and purification method influencing transduction efficiency

As described above, the viral vector solution itself can influence the transduction efficiency. Production and purification methods have been optimised by viral vector cores to produce pure and high yields of viral vector for (pre)clinical studies. Despite the validated purification methods, differences in purity and presence of empty viral particles could explain the differences in transduction efficiency observed in this thesis between AAV2/7 and CAV. In this thesis, the AAV and CAV viral vectors have been purified using iodaxinol and Caesium chloride (CsCl) gradient chromatography respectively. The iodaxinol gradient chromatography used for purification of the AAV2/7 viral vector used in the first manuscript, has the ability to achieve highly purified viral vectors in a short time. Despite the low level of impurities, this method leaves more empty particles in the viral vector solution when compared to the purification of AAV on a CsCl gradient chromatography (39). Since already a low titer was injected in LC, the exact number of viral particles could be even lower due to the presence of empty particles explaining the observed low levels of cell-specific expression. High amounts of empty particles could bind the target cells inhibiting fully packed particles from binding. In contrast, the CsCl gradient chromatography method for purification of the CAV2 viral vector used in this thesis, is characterised by low levels of empty particles (<1%) but a higher level of impurities. These residual proteins, nucleic acids, excess viral capsid and consequent induced toxicity could in high numbers reduce transduction efficiency, which could explain the decreases in gene expression observed when undiluted CAV2-PRS-hM3Dq-mCherry was injected. However, diluted viral vector decreasing the number of viral particles to less than $1x10^9$ pp induced high levels of expression, possibly due to the low amount of empty particles when compared to the AAV, resulting in an actual number of viral particles observably higher compared to AAV2/7 (27, 39-42).

7.2.1.3 Other factors influencing transduction efficiency

Although we were able to optimise hM3Dq expression in LC of healthy rats using CAV2 viral vector, the expression levels (70.9±12.7% and 77.2± 9.8% in the most diluted conditions) are still lower when compared to other studies introducing ChR2 in LC (>95%) (43). However, Hayat et al. observed lower expression levels when introducing GtACR2 in LC neurons (35%), using identical injection parameters (36). This indicates that the transgene itself, amongst other factors, influences expression efficiency (44).

We are aware that although in literature both AAV and CAV lead to high cell-specific expression of genetically modified receptors and ion channels in LC-NA neurons, variability in efficiency can still be present due to the small size of LC and possible off-target injection.

The AAV2/9-PRSx8-hM3Dq-mCherry viral vector is described to be highly effective to transduce LC neurons in rat, however, Rorabaugh et al. observed in a subset of bilaterally injected animals unilateral expression of the transgene (45). We also observed unilateral hM3Dq expression in bilaterally CAV2 injected animals. Next to off-target administration as described in literature (36, 45), we hypothesise that inflammation (as described below in detail) could be responsible for this observation, which has to be confirmed by additional experiments injecting at different time points combined with immunohistochemistry to assess the presence and distribution of microglial infiltration as described by Thomas et al. (46).

The location and small size of LC results in almost inevitable variability in observed expression levels and remains to be one of the hurdles in the chemogenetic approach of LC.

We suggest two possible administration strategies to deal with the difficulty of targeting a small nucleus. First, using the CAV viral vector has the advantage that it has high retrograde transport capacity. More specifically, for our studies, the viral vector could be injected in the hippocampus, greatly innervated by noradrenergic neurons in order to transduce LC neurons at the axonal location, with the advantage that the hippocampal region is easier to target in rodents. This approach has been successfully used to transduce the pontospinal projecting LC neurons. Nevertheless, one should take into account that optimization of the injection parameters is necessary and in general higher titers (100 times) are necessary to obtain similar expression levels compared to local administration (43). Secondly, in case of AAV, there are serotypes (AAV9,AAV.Rh8 and AAV.Rh10) that can cross the blood-brain-barrier and are described to transduce neurons or glial cells in the CNS after intravenous injection (10). A recently published paper characterising AAV serotype capsid structures found that the residues present in

AAV.Rh10 mediating the BBB passage are partially preserved in the AAV7 (47). Additionally, a study by Zhang et al. described GFP expression in neurons of neonatal mice after administration of AAV7 in the temporal vein, indicating its capability of crossing the BBB (48). However, this approach is mostly used to target widespread regions of the CNS. Additionally, vascular injection increases the risk of antibody recognition and elimination of viral particles (10).

7.2.2 Aspecific hM3Dq expression

Cell-specific hM3Dq expression is required to achieve selective modulation of LC-NA cells after systemic administration of a DREADD ligand. In both our studies, hM3Dq expression was observed in non-noradrenergic neurons in the vicinity of LC. The AAV2/7 viral vector induced aspecific expression levels of 26% ± 4.1%, whereas the CAV2 showed variable results depending on the injected titer, with the highest levels (36.2 ± 17.3%) in the condition injected with Medium_1x10e9 particles and the lowest aspecificity observed in Medium_0.1x10e9 particles (4.0 ±.1.9%).

Specificity is mainly controlled by the serotype and promoter (49, 50). However, administration route, volume, and dose (number of particles) can also influence the specificity of transgene expression (11, 14). In both experimental studies, a local intraparenchymal injection of viral vector was performed to achieve focal expression. Increasing the number of viral particles and/or volume can lead to more widespread and off-target expression since more particles are being endocytosed in the vicinity of the injection site (14). Preliminary experiments injecting higher volumes (50, 125nl) of undiluted AAV2/7, administering higher number of physical particles, induced immense widespread off-target expression (indicated in Table B.1 Appendix B), with similar expression levels in LC. Decreasing the volume to 10nl resulted in less spreading of the hM3Dq expression, although significant expression of hM3Dq was still present in non-LC neurons. Lowering the number of viral particles by diluting the AAV2/7 viral vector in sterile PBS however, decreased the total amount of transgene expression, leading to almost no visible hM3Dq expression (Table B1 Appendix B). The observed aspecificity was in great contrast with previous research groups using local injection of higher volumes of AAV2/9-PRSx8-hM3Dq-mCherry (1-1.5µl) in LC of rats and mice to induce DREADD expression, experiencing low to absent levels of aspecific expression (16, 17, 51).

However, carefull comparisation is necessary due to the above mentioned differences in methodology which can affect transduction efficiency and tropism.

In the CAV2 study we observed a similar phenomenon. Injection of $1x10^9$ particles of CAV2-PRSx8-hM3Dq-mCherry induced high levels of hM3Dq receptor (38.1 ± 6.3%) in the vicinity of LC. This level of hM3Dq expression in non-noradrenergic neurons is even higher than observed using the AAV2/7 approach, indicating that the injected number of particles is a key factor. Additionally, we have to point out that a different methodology to asses aspecificity was used in both our studies.

In the first manuscript, aspecific DREADD expression upon AAV administration was assessed using a manual cell count method, whereas a proxy for aspecifity was used by calculating the $mCherry^+$ pixels to identify aspecific hM3Dq expression with the CAV approach. This is clearly a methological caveat due to practical reasons, complicating a strict comparison between the two studies. For future studies, we would advise to use a standardised manual cell count when comparing different types of viral vector concerning cell-specific and aspecificity outcome parameters (as described in Appendix B).

Nevertheless, decreasing the number of viral particles presented at the injection site, significantly reduced aspecificity levels below 5%. Previous research groups using CAV2 viral vector to induce PRSx8-driven expression of GtACR2, ChR2 and PSAM reported similar low levels of aspecific expression (0-2%) (36, 38, 52, 53). One could hypothesize that these studies used similar titers and number of physical particles at the target site, however we cannot claim this for certain since the undiluted titers are presented in different units (40).

Aspecificity in both our studies could be due to affinity of the viral particles for non-catecholaminergic neurons as described above. Since both viral vectors, AAV2/7 and CAV2, used in this thesis contain PRSx8 driven plasmids, and the promoter sequence is driving cell-specific gene expression, one could hypothesize that this synthetic DBH promoter is not as specific as previously claimed. However, these PRSx8 driven constructs are validated and used to induce selective gene expression in noradrenergic neurons in both rats and mice (15-17, 36, 43, 45, 51-54). Therefore, we believe that it is less likely that the observed aspecific expression is merely due to promoter characteristics. Nonetheless, promoter leakage can occur, inducing gene expression in non-catecholaminergic neurons due to the presence of Phox2 transcription factors activating the PRSx8 promoter as described by Bruinstroop et al. after injection of AAV-

PRSx8-GFP in LC, A5 and A7, observing GFP expression in non DBH^+ neurons (55, 56). The same observation was made by Card et al., injecting a lentiviral vector carrying a PRSx8-GFP plasmid into the ventrolateral medulla, indicating non-DBH neurons expressing GFP(57). Since promoter activation is depending on binding of specific and regular transcription factors, sequence optimization of the transcription binding sites could decrease off-target expression by allowing only certain combinations of TFs to bind the promoter sequence (58).

Another possible explanation for the observed aspecificity, might be the presence of transactivator activity in the viral vector inverted terminal repeats (ITR). ITRs contain sequences necessary for replication and packaging of recombinant DNA and cannot be deleted (23). Haberman et al. have shown that an AAV TR construct without promoter can initiate gene expression, indicating its transcriptional and promoter ability, resulting in a loss of tissue-specific expression (59). We cannot exclude off-target administration of the viral vector, resulting in high numbers of viral particles (high multiplicity of infection) presented in the vicinity of LC. This could lead to endocytosis in non-catecholaminergic neurons due to affinity of the particles for non-LC neurons. This would result in aspecific hM3Dq expression due to the above described phenomena: promoter leakage and intrinsic promoter activity of ITR.

7.2.3 Toxicity

Decreased size of LC and lesions were observed after histological analysis of tissue sections when animals were injected with more than $1x10^9$ particles of the CAV2-PRSx8-hM3Dq-mCherry. These signs of toxicity were absent in animals injected with diluted CAV2 viral vector or AAV2/7 viral vector (33, 60), nor is it reported by other groups using the CAV2 viral vector to induce expression of a transgene in LC (36, 43, 52). Viral vector induced toxicity is reported before, also after administration into immune privileged sites (10). It is clear from our results, that the observed signs of toxicity are related to the high titer, since lowering the number of viral particles did not induce decreased LC size or lesions.

Cellular stress and disruption of homeostasis of the endoplasmatic reticulum (ER) can be induced by excess load of viral particles. ER stress and an overload of the translation machinery results in improperly folded proteins which activates the unfolded protein response (UPR) pathways to restore the intracellular machinery (44). Activation of immune pathways recruiting astrocytes, macrophages, microglia and even infiltration of antigen nonspecific T cells are a consequence of this UPR response (46, 61). When a point of no return is reached, cell loss is induced through activation of apoptosis and autophagy pathways (44).

Increased doses of adenoviral vector (>10^8 iu) injected in the mouse striatum induce an innate immune reaction with substantial loss of neurons and astrocytes (46, 62) probably due to an upregulation of chemokines and interferon genes inducing local cytotoxicity (63). This inflammatory reaction was dose-dependent, where below a certain threshold the acute response was resolved after 30 days, not influencing transgene expression, whereas with high doses permanent damage and reduced expression was observed (46, 61).

However, we cannot differentiate between damage induced by an overexpression of the membrane bound hM3Dq DREAD (phenotoxicity), an induced immune response (immunotoxicity) against capsid proteins, the transgene or the fluorescent tag as reported for GFP expression in substantia nigra after AAV administration (64).

Thomas et al. used heat inactivated adenoviral vector and observed no toxicity or leukocyte infiltration indicating that intact viral particles (and not viral proteins or transgene) were responsible for cell damage (46). It is possible that in our study, not only an acute inflammatory response is elicited by the high amount of foreign viral protein, but that the overload of the cellular machinery not only for translation but also for transport of the receptor to the membrane and/or the presence of the cytosolic mCherry tag causes cell toxicity as described *in vitro* (65, 66). Overexpression and even ectopic expression of a transgene are correlated with signs of toxicity (64). To our knowledge, no study describes neurotoxicity induced by DREADD expression. However, a study published by our own group injecting AAV2/7 carrying a plasmid to induce hM4Di, the inhibitory DREADD, into the excitatory cells of the hippocampus, observed clear and progressive neurotoxicity when hM4Di was overexpressed. Cell damage was absent when a control viral vector or vector with a different fluorescent tag was used, pointing out the origin of cytotoxicity (67). Other studies using a viral vector approach to induce expression of opsins, observed changes in electrophysiological characteristics and the formation of opsin aggregates in the cytosol indicating possible cell toxicity (19, 68). Additional experiments controlling for the transgene or fluorescent tag should be performed to identify the exact cause of toxicity.

Additionally, high levels of the PRSx8 promoter could explain the changes in LC-NA neuron physiology observed in the CAV2 study. The PRSx8 promoter is a validated synthetic DBH promoter which consist of eight to twelve copies of a promoter sequence from the cis-regulatory region of the DBH gene that binds the Phox2a/b transcription factors (56). Sequestration of Phox2 transcription factors, necessary for maintaining normal DBH expression and LC-NA phenotype, could lead to disturbed DBH production and cell loss (58).

The CAV2 viral vector, a non-human derived viral vector, is described to be safer in use for long-term experiments and eventual translation to the clinic, due to the absence of a pre-existing immune response (13, 21). However, we have shown that cell damage might occur, in contrast to other groups never observing lesions or toxicity. It is hard to compare these results since the titer was expressed in viral genomic copies which does not give information about the number of viral particles. As described above, the purification method and number of empty particles may influence this process. High levels of impurity (CpG, nucleic acids), as observed with the CsCl gradient chromatography used for CAV purification, might induce immune responses and toxicity (39, 40, 69).

Whereas empty particles, occurring more in iodaxinol purified vectors (e.g. AAV2/7) (39), were first thought to be immunotoxic due to higher number of viral proteins (70), they are now believed to have high advantages for clinical use since they are not capable to undergo conformational changes and present antigens. Moreover, empty particles can act as decoy to overcome pre-existing immune responses (71, 72).

Since the use of CAV2 viral vectors in future clinical trials is considered because of its known advantages such as high tropism for neurons, ability for retrograde transport and lack of existing immune response in patients (13, 21, 22), further research including its safety at higher titers is necessary. Secondly, control viral vectors should be administered to identify the components responsible for the observed toxicity. A lot of research is investigating possible modifications to decrease immune responses elicited by the host. Modifying the tyrosine residues at the surface viral capsid inhibits degradation by proteasomes leading to less peptides being presented to the immune cells and increased transduction efficiency since more genomes can enter the nuclear pore (73). Similar studies reported that proteasome inhibitors decreased the peptide presentation resulting in higher expression levels and lower toxicity (74). Codon optimization could be performed, where the optimal nucleic acids for the hosts are used, although careful approach is recommended (described in 3.3.1) (75). Viral capsid engineering and optimization of the quantification and purification methods should be applied to achieve conditions of high transgene expression and safety applicable for human patients in the future (25, 49, 71, 72, 76).

7.2.4 Suitability of clozapine as ligand for chemogenetic validation

To selectively activate the genetically engineered LC neurons, an inert ligand or designer drug is necessary which upon administration selectively binds the expressed DREADD receptors. The first and most extensively described ligand in chemogenetic research is Clozapine-N-Oxide (CNO). Earlier evidence showed that CNO, upon systemic injection in rats, is back-converted to clozapine (77). Gomez et al. has proven that in contrast to CNO, clozapine easily crosses the blood-brain barrier and that activation of DREADDs in the brain by systemic CNO is mainly caused by its metabolite clozapine (78).

In our study, we therefore systemically administered low doses of clozapine as selective ligand to selectively bind hM3Dq receptors and increase LC activity performing single unit recording under anaesthesia.

However, we were not able to make a conclusion about the suitability of presumed subclinical doses of clozapine as selective agonist, since we observed low expression levels. This made it almost impossible to validate whether the recorded neurons were actually transduced. An increased firing rate of LC-NA neurons was observed after administration of the highest dose of clozapine (0.1 mg/kg; s.c.), however this was also observed in control animals lacking hM3Dq, indicating a DREADD-independent effect of clozapine (33). We did not expect this effect, since previous studies chemogenetically activating LC, both in rats and mice in awake and anesthetised state, used 0.1-10 mg/kg CNO, observing no effects in control animals (15-17, 45, 51, 79, 80). These are similar or even higher doses compared to our 0.01-0.1mg/kg clozapine, since 10 mg/kg CNO corresponds to 0.1 mg/kg clozapine following the study of Gomez et. al (78). Only one study could be found performing chemogenetic modulation of LC under anaesthesia in mice, however, no measurements on neuron level were performed. Clozapine 0.03 mg/kg did not induce effects in control animals on behavioural level, indicating that this might be a more suitable dose of clozapine to use as “inert” ligand (81).

Clozapine is known to have a relative high affinity for DREADDs, however, it is a compound with affinity for a broad range of neuroreceptors including serotonin, dopamine, muscarinic, adrenergic, and histamine receptors (82). Some of these receptors are expressed in LC-NA neurons, indicating a possible mechanism explaining the clozapine-induced increased LC firing frequencies through endogenous receptor activation (83-86).

Additionally, off-target effects using clozapine have been observed in other studies targeting different nuclei. In rats, doses of 0.05-0.1 mg/kg had no effect on working memory or social interaction, but significantly affected locomotion, cognitive flexibility and anxiety (87), whereas Cho et al. reported these DREADD-independent effects only when doses of 1 mg/kg were used (88). A similar dose in mice did not alter locomotion(89), indicating the need for well controlled experimental designs due to the low specificity of clozapine. It has been reported that administering clozapine (0.078-10 mg/kg, intravenously) in healthy naive rats increased LC firing frequencies (90).

Clozapine can also modulate LC activity through binding of the glycine site of the NMDA receptor as reported by Schwieler et al. However, this could not solely explain the clozapine-induced increase in LC firing frequency, since no increase was observed after administration of a partial agonist of this glycine site (91). A combination of NMDA receptor activation(90) and increased extracellular glutamate release through binding of clozapine sensitive neuroreceptors present on glutamatergic afferents (92) could explain the DREADD-independent increased LC activity in control animals. This is, to our knowledge, not reported before in LC-hM3Dq expressing animals, especially not in studies describing unit recording. We have to point out that our study has some caveats, such as low expression levels and the use of single tungsten electrodes, making it hard to record and impossible to identify the transduction character of a recorded neuron. However, in animals injected with the CAV2 achieving high and specific hM3Dq expression it would be possible to achieve a dose-response curve for clozapine and juxtacellular labelling with neurobiotin, which could give confirmation about the transduction characteristics of the recorded neurons as described by multiple other groups performing unit recording in LC (93-96).

7.3 Future research perspectives

This thesis pointed out that chemogenetic modulation of LC is a complex technique mostly because of the small size and location in the brainstem. Injection of a viral vector and recording of LC neurons is challenging when targeting a nucleus of 1500 neurons in rodents. Secondly, to achieve selective modulation, a dose-response characterisation of a designer drug should be performed in an extremely controlled manner to avoid DREADD-independent effects.

In this thesis we show that the first hurdle is overcome, and that an optimal condition for the injection of CAV2-PRSx8-hM3Dq-mCherry viral vector is achieved which induces high levels of hM3Dq expression in LC-NA neurons. This condition gives the opportunity to further examine and elaborate the effect of LC-NA system in hippocampal excitability and epilepsy.

7.3.1 Choice of ligand

To achieve chemogenetic modulation of a genetically modified LC, a suitable designer drug needs to be characterised which induces selective agonistic effects upon systemic administration. When scanning the current literature, all studies performing LC research used CNO (15-17, 45, 51, 79, 80). Whether clozapine, used in our study, is the most ideal ligand available is still debatable, since only one study in mice using clozapine 0.03 mg/kg to selectively modulate LC could be found (81). Additionally, clozapine is known for its high affinity profile for endogenous receptors, also present in LC, indicating the need for well-controlled experiments to find a selective dose. Due to its approved use as antipsychotic drug it would be easy to use for future translational research, however severe side-effects such as agranulocytosis, myocarditis and decreasing seizure threshold at therapeutic doses are reported (97).

This emphasizes the need for other compounds to be explored. The last few years compound 21 and perlapine have been tested, and show next to high affinity for DREADDs also affinity for endogenous receptors, increasing the risk of off target effects (89, 98, 99). Recently, olanzapine has been proven to be an efficient agonist for hM4Di receptors, also in our lab, however like clozapine it has proconvulsant characteristics (67).

Newer DREADD agonists such as JHU 37152, JHU37160 and deschloroclozapine are currently arising in literature indicating high affinity profiles for hM3Dq and hM4Di receptors (100, 101).

JHU is validated in our own lab for DREADD-related seizure supressing studies and expresses relative high affinity for hM3Dq DREADDs, this could be a reasonable option (78, 100).

However, deschloroclozapine, the newest addition to the DREADD agonists, seems to be the most promising compound since it has an affinity for DREADDs a hundred times higher compared to clozapine and no off-target effects could be reported when used in monkeys (101). Therefore, we suggest to perform a well-controlled experiment to characterise a dose-response curve of deschloroclozapine to determine its suitability as DREADD ligand by performing unit recording of LC neurons in animals expressing high levels of hM3Dq and control animals. Not only side-effects due to activation of endogenous receptors should be controlled, but also the injection procedure itself, since LC is known for its typical increase in firing frequency in response to arousing painful stimuli. Instead of using a single tungsten electrode as described in chapter 5, we suggest the use of 32-multichannel silicon probes to increase data output (36). Next to this direct measurement of the functionality as DREADD agonist by recording the effect on LC firing frequency, one should take into account that controlled setting in further research is necessary especially in behavioural experiments. It seems that more and more studies are pointing out that finding the correct ligand parameters is more than finding the correct dose, keeping in mind that species, strain and even gender might play a role in the response (99).

7.3.2 Chemogenetic activation of LC and its relation to hippocampal excitability and epileptic seizures

When the functional validation of the hM3Dq receptors in LC neurons is performed and the correct dose of designer drug is determined, the ultimate goal of this research project can be pursued. What is the effect of chemogenetically and thus selective LC activation on hippocampal excitability? Does chemogenetic LC activation have a possible therapeutic role in epilepsy?

7.3.2.1 Chemogenetic LC modulation and hippocampal excitability

In a preliminary experiment, we investigated the effect of chemogenetic activation of LC using low doses of clozapine on hippocampal excitability by recording dentate gyrus evoked potentials (DG EPs) under anesthesia in animals injected with the CAV-PRSx8-hM3Dq-mCherry viral vector and control animals (See appendix). A similar experiment has already been performed by Quinlan and Harley et al. using optoactivation of LC in order to study its effect on hippocampal EPs under anaesthesia. They reported delayed LTP of the population spike recorded in dentate gyrus which seemed less robust compared to previous studies using chemical LC activation (102).

However, a train of optogenetic activation induced a short period of increased LC activity, whereas we expect to induce a more tonic long-lasting increase in LC firing frequency in response to chemogenetic modulation.

In our experiment, animals showing high levels of bilateral hM3Dq expression were included for EP pre-processing and data analysis looking at the fEPSP slope (measurement for the efficiency of presynaptic neurotransmission), fEPSP amplitude (resembles the postsynaptic depolarisation) and PS amplitude (measurement for postsynaptic action potentials). The averages of these EP parameters were compared between DREADD and control animals, showing subtle differences after DREADD activation. Although based on literature (described in 2.4) we expected to find a clear potentiation of the population spike, a trend to a decreased fEPSP slope and amplitude was observed in DREADD animals already after the lowest dose of clozapine (0.01 mg/kg), whereas no decrease in presynaptic neurotransmission or postsynaptic depolarisation was found in the control animals. However, this discrepancy in effect was not observed for the PS amplitude, where both in DREADD and control animals a decrease was observed, indicating a DREADD-independent effect. Although these recordings were made in animals expressing high levels of hM3Dq, this experiment should be repeated using deschloroclozapine as described above in a well-controlled setting. One has to take into account, when recording effects of LC modulation on hippocampal excitability, that a stable baseline recording is important. Several studies both *in vitro* as *in vivo* have reported plasticity induced by the stimulation protocol itself (103-105), interfering with the drug-induced responses. Therefore, we suggest that the stimulation protocol is first tested in control animals using a stimulation interpulse interval of 40s as described by Managhan-Vaughan, characterised as being stable for recordings over several hours (106).

A key feature in these experiments will be to determine changes in noradrenaline measured in the hippocampus and control with other adrenergic agonists and antagonists to completely assess the mechanism of action (7).

7.3.2.2 Chemogenetic LC modulation and its therapeutic role

Once the effects of selective LC activation on hippocampal excitability are established in healthy animals by recording both DG EPs as spontaneous EEG activity, the potential therapeutic effects can be explored. Therefore, chemogenetic LC modulation can be performed to study its effect on epileptic seizures as our VNS studies have shown that indirect LC activation has anticonvulsant effects (6, 7).

For this, an intrahippocampal pilocarpine model can be used to acutely induce epileptic seizures, a model validated in our lab and proven to be sensitive to changes in noradrenaline (7). In this model, the effect of tonic chemogenetic LC activation can be studied on the convulsive patterns induced by pilocarpine administration together with simultaneous microdialysis to correlate the noradrenaline change to the effect on seizures. Based on previous work in our lab, we expect that chronic LC activation induced by chemogenetic modulation might decrease seizure duration and severity (7). Nevertheless, as pointed out before it is hard to predict to which extent noradrenaline changes can work pro- or anticonvulsive, emphasizing the importance of such experimental work to confidently state the therapeutic role of selective LC modulation.

We also believe that chemogenetic LC modulation has a role in fundamental and translational experiments regarding other neurological diseases such as Parkinson's and Alzheimer's disease. These diseases are characterised by a plethora of symptoms of which a lot are coupled back to the LC-NA system. As described in the introduction of this thesis, there are studies reporting the pathological changes in LC is often the first subclinical symptom (4, 5). It has been reported that in the early stage, the LC shows an increased firing rate to compensate for the disturbance in the neural circuit (107), indicating that chemogenetic LC activation might have a therapeutic function, trying to restore the network and associated symptoms.

In this thesis we emphasized the importance of a selective modulation technique to target LC. Overall, the use of chemogenetics to specifically modulate the LC-NA system is an interesting tool to investigate its role in the etiology and pathology and therapy of several neurological, neurodegenerative and psychiatric diseases. However, given the complex nature of the LC-NA system, it is clear that well-designed preclinical research needs to be performed in order to establish its potential clinical use.

Bibliography

1. Szabadi E. Functional neuroanatomy of the central noradrenergic system. J Psychopharmacol. 2013;27(8):659-93.

2. Samuels ER, Szabadi E. Functional Neuroanatomy of the Noradrenergic Locus Coeruleus: Its Roles in the Regulation of Arousal and Autonomic Function Part I: Principles of Functional Organisation. 2008.

3. Samuels ER, Szabadi E. Functional Neuroanatomy of the Noradrenergic Locus Coeruleus: Its Roles in the Regulation of Arousal and Autonomic Function Part II: Physiological and Pharmacological Manipulations and Pathological Alterations of Locus Coeruleus Activity in Humans. 2008.

4. Bari BA, Chokshi V, Schmidt K. Locus coeruleus-norepinephrine: basic functions and insights into Parkinson's disease. Neural Regen Res. 2020;15(6):1006-13.

5. Mather M, Harley CW. The Locus Coeruleus: Essential for Maintaining Cognitive Function and the Aging Brain. Trends Cogn Sci. 2016;20(3):214-26.

6. Grimonprez A, Raedt R, Portelli J, Dauwe I, Larsen LE, Bouckaert C, et al. The antidepressant-like effect of vagus nerve stimulation is mediated through the locus coeruleus. J Psychiatr Res. 2015;68:1-7.

7. Raedt R, Clinckers R, Mollet L, Vonck K, El Tahry R, Wyckhuys T, et al. Increased hippocampal noradrenaline is a biomarker for efficacy of vagus nerve stimulation in a limbic seizure model. J Neurochem. 2011;117(3):461-9.

8. De Taeye L, Vonck K, van Bochove M, Boon P, Van Roost D, Mollet L, et al. The P3 event-related potential is a biomarker for the efficacy of vagus nerve stimulation in patients with epilepsy. Neurotherapeutics. 2014;11(3):612-22.

9. Roth BL. DREADDs for Neuroscientists. 2016. p. 683-94.

10. Wang D, Tai PWL, Gao G. Adeno-associated virus vector as a platform for gene therapy delivery. Nat Rev Drug Discov. 2019;18(5):358-78.

11. Haery L, Deverman BE, Matho KS, Cetin A, Woodard K, Cepko C, et al. Adeno-Associated Virus Technologies and Methods for Targeted Neuronal Manipulation. Front Neuroanat. 2019;13:93.

12. Douar AM, Poulard K, Stockholm D, Danos O. Intracellular trafficking of adeno-associated virus vectors: routing to the late endosomal compartment and proteasome degradation. J Virol. 2001;75(4):1824-33.

13. Kremer EJ, Boutin S, Chillon M, Danos O. Canine adenovirus vectors: an alternative for adenovirus-mediated gene transfer. J Virol. 2000;74(1):505-12.

14. Castle MJ, Turunen HT, Vandenberghe LH, Wolfe JH. Controlling AAV Tropism in the Nervous System with Natural and Engineered Capsids. Methods Mol Biol. 2016;1382:133-49.

15. Kane GA, Vazey EM, Wilson RC, Shenhav A, Daw ND, Aston-Jones G, et al. Increased locus coeruleus tonic activity causes disengagement from a patch-foraging task. Cogn Affect Behav Neurosci. 2017;17(6):1073-83.

16. Cope ZA, Vazey EM, Floresco SB, Aston Jones GS. DREADD-mediated modulation of locus coeruleus inputs to mPFC improves strategy set-shifting. Neurobiol Learn Mem. 2019;161:1-11.

17. Vazey EM, Aston-Jones G. Designer receptor manipulations reveal a role of the locus coeruleus noradrenergic system in isoflurane general anesthesia. Proc Natl Acad Sci U S A. 2014;111(10):3859-64.

18. Rabinowitz JE, Rolling F, Li C, Conrath H, Xiao W, Xiao X, et al. Cross-packaging of a single adeno-associated virus (AAV) type 2 vector genome into multiple AAV serotypes enables transduction with broad specificity. J Virol. 2002;76(2):791-801.

19. Delbeke J, Hoffman L, Mols K, Braeken D, Prodanov D. And Then There Was Light: Perspectives of Optogenetics for Deep Brain Stimulation and Neuromodulation. Front Neurosci. 2017;11(December):663.

20. Soudais C, Boutin S, Hong SS, Chillon M, Danos O, Bergelson JM, et al. Canine adenovirus type 2 attachment and internalization: coxsackievirus-adenovirus receptor, alternative receptors, and an RGD-independent pathway. J Virol. 2000;74(22):10639-49.

21. Del Rio D, Beucher B, Lavigne M, Wehbi A, Gonzalez Dopeso-Reyes I, Saggio I, et al. CAV-2 Vector Development and Gene Transfer in the Central and Peripheral Nervous Systems. Front Mol Neurosci. 2019;12:71.

22. Junyent F, Kremer EJ. CAV-2--why a canine virus is a neurobiologist's best friend. Curr Opin Pharmacol. 2015;24:86-93.

23. May Lai C, Lai YKY, Elizabeth Rakoczy P. Adenovirus and Adeno-Associated Virus Vectors. 2002.

24. Darr S, Madisch I, Hofmayer S, Rehren F, Heim A. Phylogeny and primary structure analysis of fiber shafts of all human adenovirus types for rational design of adenoviral gene-therapy vectors. J Gen Virol. 2009;90(Pt 12):2849-54.

25. Kotterman MA, Schaffer DV. Engineering adeno-associated viruses for clinical gene therapy. Nat Rev Genet. 2014;15(7):445-51.

26. Van der Perren A, Toelen J, Carlon M, Van den Haute C, Coun F, Heeman B, et al. Efficient and stable transduction of dopaminergic neurons in rat substantia nigra by rAAV 2/1, 2/2, 2/5, 2/6.2, 2/7, 2/8 and 2/9. Gene Ther. 2011;18(5):517-27.

27. Summerford C, Bartlett JS, Samulski RJ. AlphaVbeta5 integrin: a co-receptor for adeno-associated virus type 2 infection. Nat Med. 1999;5(1):78-82.

28. Summerford C, Samulski RJ. Membrane-associated heparan sulfate proteoglycan is a receptor for adeno-associated virus type 2 virions. J Virol. 1998;72(2):1438-45.

29. Asokan A, Hamra JB, Govindasamy L, Agbandje-McKenna M, Samulski RJ. Adeno-associated virus type 2 contains an integrin alpha5beta1 binding domain essential for viral cell entry. J Virol. 2006;80(18):8961-9.

30. Kwon I, Schaffer DV. Designer gene delivery vectors: molecular engineering and evolution of adeno-associated viral vectors for enhanced gene transfer. Pharm Res. 2008;25(3):489-99.

31. Agbandje-McKenna M, Kleinschmidt J. AAV capsid structure and cell interactions. Methods Mol Biol. 2011;807:47-92.

32. Mietzsch M, Broecker F, Reinhardt A, Seeberger PH, Heilbronn R. Differential adeno-associated virus serotype-specific interaction patterns with synthetic heparins and other glycans. J Virol. 2014;88(5):2991-3003.

33. Stevens L, Vonck K, Larsen LE, Van Lysebettens W, Germonpre C, Baekelandt V, et al. A Feasibility Study to Investigate Chemogenetic Modulation of the Locus Coeruleus by Means of Single Unit Activity. Front Neurosci. 2020;14(March):162.

34. Li SJ, Vaughan A, Sturgill JF, Kepecs A. A Viral Receptor Complementation Strategy to Overcome CAV-2 Tropism for Efficient Retrograde Targeting of Neurons. Neuron. 2018;98(5):905-17 e5.

35. Hirschberg S, Li Y, Randall A, Kremer EJ, Pickering AE. Functional dichotomy in spinal- vs prefrontal-projecting locus coeruleus modules splits descending noradrenergic analgesia from ascending aversion and anxiety in rats. Elife. 2017;6.

36. Hayat H, Regev N, Matosevich N, Sales A, Paredes-Rodriguez E, Krom AJ, et al. Locus coeruleus norepinephrine activity mediates sensory-evoked awakenings from sleep. Sci Adv. 2020;6(15):eaaz4232.

37. Sales AC, Friston KJ, Jones MW, Pickering AE, Moran RJ. Locus Coeruleus tracking of prediction errors optimises cognitive flexibility: An Active Inference model. PLoS Comput Biol. 2019;15(1):e1006267.

38. Hickey L, Li Y, Fyson SJ, Watson TC, Perrins R, Hewinson J, et al. Optoactivation of locus ceruleus neurons evokes bidirectional changes in thermal nociception in rats. J Neurosci. 2014;34(12):4148-60.

39. Strobel B, Miller FD, Rist W, Lamla T. Comparative Analysis of Cesium Chloride- and Iodixanol-Based Purification of Recombinant Adeno-Associated Viral Vectors for Preclinical Applications. Hum Gene Ther Methods. 2015;26(4):147-57.

40. Ayuso E, Mingozzi F, Montane J, Leon X, Anguela XM, Haurigot V, et al. High AAV vector purity results in serotype- and tissue-independent enhancement of transduction efficiency. Gene Ther. 2010;17(4):503-10.

41. Summerford C, Samulski RJ. Viral receptors and vector purification: new approaches for generating clinical-grade reagents. Nat Med. 1999;5(5):587-8.

42. Segura MM, Kamen AA, Garnier A. Overview of current scalable methods for purification of viral vectors. Methods Mol Biol. 2011;737:89-116.

43. Li Y, Hickey L, Perrins R, Werlen E, Patel AA, Hirschberg S, et al. Retrograde optogenetic characterization of the pontospinal module of the locus coeruleus with a canine adenoviral vector. 2016. p. 274-90.

44. Sen D, Balakrishnan B, Jayandharan GR. Cellular unfolded protein response against viruses used in gene therapy. Front Microbiol. 2014;5:250.

45. Rorabaugh JM, Chalermpalanupap T, Botz-Zapp CA, Fu VM, Lembeck NA, Cohen RM, et al. Chemogenetic locus coeruleus activation restores reversal learning in a rat model of Alzheimer's disease. Brain. 2017;140(11):3023-38.

46. Thomas CE, Birkett D, Anozie I, Castro MG, Lowenstein PR. Acute direct adenoviral vector cytotoxicity and chronic, but not acute, inflammatory responses correlate with decreased vector-mediated transgene expression in the brain. Mol Ther. 2001;3(1):36-46.

47. Mietzsch M, Jose A, Chipman P, Bhattacharya N, Daneshparvar N, McKenna R, et al. Completion of the AAV Structural Atlas: Serotype Capsid Structures Reveals Clade-Specific Features. Viruses. 2021;13(1).

48. Zhang H, Yang B, Mu X, Ahmed SS, Su Q, He R, et al. Several rAAV vectors efficiently cross the blood-brain barrier and transduce neurons and astrocytes in the neonatal mouse central nervous system. Mol Ther. 2011;19(8):1440-8.

49. Powell SK, Rivera-Soto R, Gray SJ. Viral expression cassette elements to enhance transgene target specificity and expression in gene therapy. Discov Med. 2015;19(102):49-57.

50. Fitzsimons HL, Bland RJ, During MJ. Promoters and regulatory elements that improve adeno-associated virus transgene expression in the brain. Methods. 2002;28(2):227-36.

51. Fortress AM, Hamlett ED, Vazey EM, Aston-Jones G, Cass WA, Boger HA, et al. Designer receptors enhance memory in a mouse model of Down syndrome. J Neurosci. 2015;35(4):1343-53.

52. Hirschberg S, Li Y, Randall A, Kremer EJ, Pickering AE. Functional dichotomy in spinal- vs prefrontal-projecting locus coeruleus modules splits descending noradrenergic analgesia from ascending aversion and anxiety in rats. Elife. 2017;6(Lc):e29808-e.

53. Xiang L, Harel A, Gao H, Pickering AE, Sara SJ, Wiener SI. Behavioral correlates of activity of optogenetically identified locus coeruleus noradrenergic neurons in rats performing T-maze tasks. Sci Rep. 2019;9(1):1361.

54. Vazey EM, Moorman DE, Aston-Jones G. Phasic locus coeruleus activity regulates cortical encoding of salience information. Proc Natl Acad Sci U S A. 2018;115(40):E9439-E48.

55. Bruinstroop E, Cano G, Vanderhorst VG, Cavalcante JC, Wirth J, Sena-Esteves M, et al. Spinal projections of the A5, A6 (locus coeruleus), and A7 noradrenergic cell groups in rats. J Comp Neurol. 2012;520(9):1985-2001.

56. Hwang DY, Carlezon WA, Jr., Isacson O, Kim KS. A high-efficiency synthetic promoter that drives transgene expression selectively in noradrenergic neurons. Hum Gene Ther. 2001;12(14):1731-40.

57. Card JP, Sved JC, Craig B, Raizada M, Vazquez J, Sved AF. Efferent projections of rat rostroventrolateral medulla C1 catecholamine neurons: Implications for the central control of cardiovascular regulation. J Comp Neurol. 2006;499(5):840-59.

58. Hwang DY, Hwang MM, Kim HS, Kim KS. Genetically engineered dopamine beta-hydroxylase gene promoters with better PHOX2-binding sites drive significantly enhanced transgene expression in a noradrenergic cell-specific manner. Mol Ther. 2005;11(1):132-41.

59. Haberman RP, McCown TJ, Samulski RJ. Novel Transcriptional Regulatory Signals in the Adeno-Associated Virus Terminal Repeat A/D Junction Element. 2000.

60. Stevens L, Larsen LE, Van Lysebettens W, Carrette E, Boon P, Raedt R, et al. Optimized Parameters for Transducing the Locus Coeruleus Using Canine Adenovirus Type 2 (CAV2) Vector in Rats for Chemogenetic Modulation Research. Frontiers in Neuroscience. 2021;15(426).

61. Lowenstein PR, Mandel RJ, Xiong WD, Kroeger K, Castro MG. Immune responses to adenovirus and adeno-associated vectors used for gene therapy of brain diseases: the role of immunological synapses in understanding the cell biology of neuroimmune interactions. Curr Gene Ther. 2007;7(5):347-60.

62. Reimsnider S, Manfredsson FP, Muzyczka N, Mandel RJ. Time course of transgene expression after intrastriatal pseudotyped rAAV2/1, rAAV2/2, rAAV2/5, and rAAV2/8 transduction in the rat. Mol Ther. 2007;15(8):1504-11.

63. Zirger JM, Barcia C, Liu C, Puntel M, Mitchell N, Campbell I, et al. Rapid upregulation of interferon-regulated and chemokine mRNAs upon injection of 108 international units, but not lower doses, of adenoviral vectors into the brain. J Virol. 2006;80(11):5655-9.

64. Khabou H, Cordeau C, Pacot L, Fisson S, Dalkara D. Dosage Thresholds and Influence of Transgene Cassette in Adeno-Associated Virus-Related Toxicity. Hum Gene Ther. 2018;29(11):1235-41.

65. Kintaka R, Makanae K, Moriya H. Cellular growth defects triggered by an overload of protein localization processes. Sci Rep. 2016;6:31774.

66. Wagner S, Baars L, Ytterberg AJ, Klussmeier A, Wagner CS, Nord O, et al. Consequences of membrane protein overexpression in Escherichia coli. Mol Cell Proteomics. 2007;6(9):1527-50.

67. Goossens MG, Boon P, Wadman W, Van den Haute C, Baekelandt V, Verstraete AG, et al. Long-term chemogenetic suppression of seizures in a multifocal rat model of temporal lobe epilepsy. Epilepsia. 2021;62(3):659-70.

68. Gradinaru V, Thompson KR, Deisseroth K. eNpHR: a Natronomonas halorhodopsin enhanced for optogenetic applications. Brain Cell Biol. 2008;36(1-4):129-39.

69. Xiong W, Wu DM, Xue Y, Wang SK, Chung MJ, Ji X, et al. AAV cis-regulatory sequences are correlated with ocular toxicity. Proc Natl Acad Sci U S A. 2019;116(12):5785-94.

70. Gao K, Li M, Zhong L, Su Q, Li J, Li S, et al. Empty Virions In AAV8 Vector Preparations Reduce Transduction Efficiency And May Cause Total Viral Particle Dose-Limiting Side-Effects. Mol Ther Methods Clin Dev. 2014;1(9):20139.

71. Mingozzi F, High KA. Immune responses to AAV vectors: overcoming barriers to successful gene therapy. Blood. 2013;122(1):23-36.

72. Mingozzi F, Anguela XM, Pavani G, Chen Y, Davidson RJ, Hui DJ, et al. Overcoming preexisting humoral immunity to AAV using capsid decoys. Sci Transl Med. 2013;5(194):194ra92.

73. Zhong L, Li B, Mah CS, Govindasamy L, Agbandje-McKenna M, Cooper M, et al. Next generation of adeno-associated virus 2 vectors: point mutations in tyrosines lead to high-efficiency transduction at lower doses. Proc Natl Acad Sci U S A. 2008;105(22):7827-32.

74. Finn JD, Hui D, Downey HD, Dunn D, Pien GC, Mingozzi F, et al. Proteasome inhibitors decrease AAV2 capsid derived peptide epitope presentation on MHC class I following transduction. Mol Ther. 2010;18(1):135-42.

75. Fath S, Bauer AP, Liss M, Spriestersbach A, Maertens B, Hahn P, et al. Multiparameter RNA and codon optimization: a standardized tool to assess and enhance autologous mammalian gene expression. PLoS One. 2011;6(3):e17596.

76. Colella P, Ronzitti G, Mingozzi F. Emerging Issues in AAV-Mediated In Vivo Gene Therapy. Mol Ther Methods Clin Dev. 2018;8:87-104.

77. MacLaren DA, Browne RW, Shaw JK, Krishnan Radhakrishnan S, Khare P, Espana RA, et al. Clozapine N-Oxide Administration Produces Behavioral Effects in Long-Evans Rats: Implications for Designing DREADD Experiments. eNeuro. 2016;3(5):219-16.

78. Gomez JL, Bonaventura J, Lesniak W, Mathews WB, Sysa-Shah P, Rodriguez LA, et al. Chemogenetics revealed: DREADD occupancy and activation via converted clozapine. Science. 2017;357(6350):503-7.

79. McCall JG, Al-Hasani R, Siuda ER, Hong DY, Norris AJ, Ford CP, et al. CRH Engagement of the Locus Coeruleus Noradrenergic System Mediates Stress-Induced Anxiety. Neuron. 2015;87(3):605-20.

80. Llorca-Torralba M, Suarez-Pereira I, Bravo L, Camarena-Delgado C, Garcia-Partida JA, Mico JA, et al. Chemogenetic Silencing of the Locus Coeruleus-Basolateral Amygdala Pathway Abolishes Pain-Induced Anxiety and Enhanced Aversive Learning in Rats. Biol Psychiatry. 2019;85(12):1021-35.

81. Zerbi V, Floriou-Servou A, Markicevic M, Vermeiren Y, Sturman O, Privitera M, et al. Rapid Reconfiguration of the Functional Connectome after Chemogenetic Locus Coeruleus Activation. Neuron. 2019;103(4):702-18 e5.

82. Svensson TH, Bunney BS, Aghajanian GK. Inhibition of both noradrenergic and serotonergic neurons in brain by the a-adrenergic agonist clonidine. Brain Research. 1975;92:291-306.

83. Egan TM, North RA. Acetylcholine acts on m2-muscarinic receptors to excite rat locus coeruleus neurones. Br J Pharmacol. 1985;85(4):733-5.

84. Szabo ST, Blier P. Functional and pharmacological characterization of the modulatory role of serotonin on the firing activity of locus coeruleus norepinephrine neurons. Brain Res. 2001;922(1):9-20.

85. Korotkova TM, Sergeeva OA, Ponomarenko AA, Haas HL. Histamine excites noradrenergic neurons in locus coeruleus in rats. Neuropharmacology. 2005;49(1):129-34.

86. Baerentzen S, Casado-Sainz A, Lange D, Shalgunov V, Tejada IM, Xiong M, et al. The Chemogenetic Receptor Ligand Clozapine N-Oxide Induces in vivo Neuroreceptor Occupancy and Reduces Striatal Glutamate Levels. Front Neurosci. 2019;13:187.

87. Ilg AK, Enkel T, Bartsch D, Bahner F. Behavioral Effects of Acute Systemic Low-Dose Clozapine in Wild-Type Rats: Implications for the Use of DREADDs in Behavioral Neuroscience. Front Behav Neurosci. 2018;12:173.

88. Cho J, Ryu S, Lee S, Kim J, Kim HI. Optimizing clozapine for chemogenetic neuromodulation of somatosensory cortex. Sci Rep. 2020;10(1):6001.

89. Jendryka M, Palchaudhuri M, Ursu D, van der Veen B, Liss B, Katzel D, et al. Pharmacokinetic and pharmacodynamic actions of clozapine-N-oxide, clozapine, and compound 21 in DREADD-based chemogenetics in mice. Sci Rep. 2019;9(1):4522.

90. Nilsson LK, Schwieler L, Engberg G, Linderholm KR, Erhardt S. Activation of noradrenergic locus coeruleus neurons by clozapine and haloperidol: involvement of glutamatergic mechanisms. Int J Neuropsychopharmacol. 2005;8(3):329-39.

91. Schwieler L, Linderholm KR, Nilsson-Todd LK, Erhardt S, Engberg G. Clozapine interacts with the glycine site of the NMDA receptor: electrophysiological studies of dopamine neurons in the rat ventral tegmental area. Life Sci. 2008;83(5-6):170-5.

92. Daly DA, Moghaddam B. Actions of clozapine and haloperidol on the extracellular levels of excitatory amino acids in the prefrontal cortex and striatum of conscious rats. Neurosci Lett. 1993;152(1-2):61-4.

93. Allers KA, Sharp T. Neurochemical and anatomical identification of fast- and slow-firing neurones in the rat dorsal raphe nucleus using juxtacellular labelling methods in vivo. Neuroscience. 2003;122(1):193-204.

94. Hajos M, Allers KA, Jennings K, Sharp T, Charette G, Sik A, et al. Neurochemical identification of stereotypic burst-firing neurons in the rat dorsal raphe nucleus using juxtacellular labelling methods. Eur J Neurosci. 2007;25(1):119-26.

95. Bangasser DA, Zhang X, Garachh V, Hanhauser E, Valentino RJ. Sexual dimorphism in locus coeruleus dendritic morphology: a structural basis for sex differences in emotional arousal. Physiol Behav. 2011;103(3-4):342-51.

96. Dempsey B, Turner AJ, Le S, Sun QJ, Bou Farah L, Allen AM, et al. Recording, labeling, and transfection of single neurons in deep brain structures. Physiol Rep. 2015;3(1):1-13.

97. Wenthur CJ, Lindsley CW. Classics in chemical neuroscience: clozapine. ACS Chem Neurosci. 2013;4(7):1018-25.

98. Goutaudier R, Coizet V, Carcenac C, Carnicella S. Compound 21, a two-edged sword with both DREADD-selective and off-target outcomes in rats. PLoS One. 2020;15(9):e0238156.

99. Goutaudier R, Coizet V, Carcenac C, Carnicella S. DREADDs: The Power of the Lock, the Weakness of the Key. Favoring the Pursuit of Specific Conditions Rather than Specific Ligands. eNeuro. 2019;6(5):171-90.

100. Bonaventura J, Eldridge MAG, Hu F, Gomez JL, Sanchez-Soto M, Abramyan AM, et al. High-potency ligands for DREADD imaging and activation in rodents and monkeys. Nat Commun. 2019;10(1):4627.

101. Nagai Y, Miyakawa N, Takuwa H, Hori Y, Oyama K, Ji B, et al. Deschloroclozapine, a potent and selective chemogenetic actuator enables rapid neuronal and behavioral modulations in mice and monkeys. Nat Neurosci. 2020;23(9):1157-67.

102. Quinlan MAL, Strong VM, Skinner DM, Martin GM, Harley CW, Walling SG. Locus Coeruleus Optogenetic Light Activation Induces Long-Term Potentiation of Perforant Path Population Spike Amplitude in Rat Dentate Gyrus. Front Syst Neurosci. 2018;12:67.

103. Harris EW, Lasher SS, Steward O. Analysis of the habituation-like changes in transmission in the temporodentate pathway of the rat. Brain Res. 1979;162(1):21-32.

104. Harris EW, Lasher SS, Steward O. Habituation-like decrements in transmission along the normal and lesion-induced temporodentate pathways in the rat. Brain Res. 1978;151(3):623-31.

105. Reid AT, Harley CW. An associativity requirement for locus coeruleus-induced long-term potentiation in the dentate gyrus of the urethane-anesthetized rat. Exp Brain Res. 2010;200(2):151-9.

106. Manahan-Vaughan D. Handbook of in Vivo Neural Plasticity Techniques2018. 1-540 p.

107. Wang T, Zhang QJ, Liu J, Wu ZH, Wang S. Firing activity of locus coeruleus noradrenergic neurons increases in a rodent model of Parkinsonism. Neurosci Bull. 2009;25(1):15-20.

English Summary

The locus coeruleus-noradrenaline (LC-NA) system modulates neuronal circuits throughout the brain, influencing different functions such as sleep, cognition, memory and neuroplasticity. It is studied for its role in brain excitability and different neurological and psychiatric diseases such as Parkinson's disease, Alzheimer's disease, major depression disorder and epilepsy. Epilepsy is one of the most common neurological disorder worldwide, affecting 0.5-1% of the population.Vagus nerve stimulation (VNS) has been used for patients suffering from refractory epilepsy whom are not being helped with the current anti-epileptic drugs. Although the exact mechanism of action of VNS is not fully understood, there is evidence that the LC-NA system is a key player, since lesioning the LC attenuates the seizure-suppressing and mood enhancing induced effects.

To unravel the role of the LC-NA system in hippocampal excitability and its possible therapeutic effect, selective modulation of the LC is necessary. In the past, electrical and chemical LC stimulation resulted in variable effects on excitability, probably due to the aselectivity of the method and complexity of the LC-NA modulatory system.

These findings highlighted the need for a cell-specific method to target LC. Chemogenetics is a technique that allows modulation of specific cell types using the expression of Designer Receptors Exclusively Activated by Designer Drugs (DREADDs). DREADDs are engineered human muscarinic receptors inert for the endogenous ligand acetylcholine, and activated by designer drugs such as Clozapine-N-Oxide (CNO) and clozapine.

The focus of the experimental work in this thesis was set on achieving the two requirements necessary for chemogenetic modulation of the LC: 1) High cell-specific expression of the excitatory hM3Dq DREADD in LC; 2) Characterization of a selective DREADD agonist.

The aim of the first study was to assess the feasibility to use an AAV2/7 viral vector to introduce the hM3Dq excitatory DREADD selectively in LC-NA neurons using the specific PRSx8 promoter. Single unit recording under anesthesia was perfomed to determine the suitability of systemic administration of subclinical doses of clozapine as DREADD ligand. We demonstrated using immunfluorescence stainings, that the AAV2/7 viral vector is a suboptimal approach, since low levels of hM3Dq expression in LC-NA neurons and high aspecificity was observed probably due to its low tropism.

Secondly, we were not able to draw conclusions on the suitability of clozapine as DREADD agonist, showing no significant increase in firing frequency after 0.01 mg/kg clozapine

administration. However, we did observe an increase in LC activity after administration of the highest dose of clozapine (0.1 mg/kg) even in control animals, indicating a DREADD-independent effect and the need for further optimization.

Since achieving high levels of cell-specific hM3Dq expression in LC-NA neurons is the first requirement necessary to chemogenetically modulate LC, another type of viral vector was used. The aim of the second study was to optimise the transduction efficiency using the canine adenovirus type 2 (CAV2) vector carrying a plasmid containing the PRSx8-hM3Dq-mCherry construct. Animals were injected with different absolute numbers of CAV2-PRSx8-hM3Dq-mCherry physical particles using different volumes to obtain a condition with high and cell-specific transduction of LC neurons. Post-processing of the immunofluorescence images revealed that high titers of the CAV2-PRSx8-hM3Dq-mCherry viral vector induced signs of toxicity evidenced by a decreased LC size and presence of lesions. Reducing the number of viral particles to 0.1E9 induced high and safe cell-specific hM3Dq expression in LC with low aspecificity.

In this thesis an optimal viral vector approach was achieved for safe and specific transduction of LC with the excitatory hM3Dq DREADD to study the role of the LC-NA system in the healthy and epileptic brain. Future well-designed preclinical research is needed to further establish its effect on hippocampal excitability and potential clinical use.

Nederlandse Samenvatting

Het locus coeruleus-noradrenerg (LC-NA) systeem moduleert neuronale circuits over het gehele brein en beïnvloedt verschillende functies zoals slaap, cognitie, geheugen en neuroplasticiteit. Het wordt bestudeerd voor zijn rol in exciteerbaarheid van de hersenen en verschillende neurologische en psychiatrische aandoeningen zoals de ziekte van Parkinson, de ziekte van Alzheimer, depressie en epilepsie. Epilepsie is één van de meest voorkomende neurologische aandoening met een incidentie van 0.5-1% wereldwijd. Nervus vagus stimulatie (NVS) wordt toegepast bij patiënten met refractaire epilepsie die niet geholpen worden door de huidige anti-epileptische medicatie. Hoewel het werkingsmechanisme van NVS nog niet volledig gekend is, zijn er aanwijzingen dat het LC-NA systeem hierin een sleutelrol speelt, aangezien beschadiging van LC het aanvalsonderdrukkende en anti-depressieve effect van NVS verzwakt. Om de rol van het LC-NA systeem in hippocampale exciteerbaarheid en zijn mogelijke therapeutische toepassingen verder te ontrafelen, is selectieve modulatie van LC noodzakelijk. In het verleden induceerde elektrische en chemische LC stimulatie variabele effecten, mogelijks door aselectieve karakter van de methode en de complexiteit van het LC-NA systeem. Deze bevindingen benadrukken de nood voor een celspecifieke techniek om LC te moduleren.

Chemogenetica is een techniek dat celspecieke modulatie toelaat via expressie van Designer Receptors Exclusively Activated by Designer Drugs (DREADDs). DREADDs zijn gemodificeerde humane muscarinerge receptoren inert voor het endogene ligand acetylcholine, en worden geactiveerd door *designer drugs* zoals Clozapine-N-Oxide (CNO) en clozapine.

De focus van het experimentele werk in deze thesis lag op het behalen van twee noodzakelijke eigenschappen voor chemogenetische modulatie van LC: 1) hoge celspecifieke expressie van de excitatorische hM3Dq DREADD in LC; 2) karakterisatie van een selectieve DREADD agonist.

Het doel van de eerste studie was om de efficiëntie van de AAV2/7 virale vector te bepalen om de hM3Dq excitatorische DREADD selectief te expresseren in LC-NA neuronen door middel van een PRSx8 specifieke promoter. Unit recording onder anesthesie werd toegepast om na te gaan of subklinische dosissen van clozapine kunnen gebruikt worden als DREADD ligand.

Door middel van immunofluorescentie kleuringen werd aangetoond dat de AAV2/7 virale vector een suboptimale methode is om LC neuronen te transduceren, aangezien lage hM3Dq expressielevels in LC neuronen werden vastgesteld in combinatie met een hoge aspecificiteit. Waarschijnlijk door laag tropisme van de virale partikels voor LC neuronen. Verder konden er geen conclusies getrokken worden omtrent de geschiktheid van clozapine als DREADD agonist, aangezien er geen significante stijging in de vuurfrequentie werd waargenomen na toediening van 0.01 mg/kg. Niettemin, werd er na administratie van de hoogste dosis clozapine (0.1 mg/kg) een stijging in LC activiteit waargenomen zelfs in controledieren. Dit duidt op een DREADD-onafhankelijk effect en de noodzaak voor verdere optimalisatie.

Aangezien hoge celspecifieke hM3Dq expressie in LC-NA neuronen één van de belangrijkste voorwaarden is om LC chemogenetisch te moduleren, werd er een ander type virale vector gebruikt.
Het doel van de tweede studie was om de transductie efficiëntie te optimaliseren door gebruik te maken van een canine adenovirus type 2 (CAV2) virale vector dat het plasmide PRSx8-hM3Dq-mCherry construct draagt. Dieren werden geïnjecteerd met verschillende absolute hoeveelheden van virale partikels door middel van verschillende volumes te injecteren om een conditie met hoge en celspecifieke transductie van LC te bekomen. Post-processing van immunofluorescentie beelden toonde aan dat hoge titers van de viral vector tekenen van toxiciteit induceert zoals een gereduceerde grootte en de aanwezigheid van lesies. Reductie van het aantal virale partikels tot $0.1^{E}9$ induceerde hoge en veilige celspecifieke hM3Dq expressie in LC met een lage aspecificiteit.

Deze thesis werd een optimale virale vector approach bereikt die veilig en specifiek de LC kan transduceren met expressie van de excitatorische hM3Dq DREADD om de rol van het LC-NA systeem in het gezonde en epileptische brein verder te bestuderen. Toekomstig preklinisch onderzoek is nodig om het effect van LC op hippocampale exciteerbaarheid en zijn potentieel klinisch gebruik verder na te gaan.

Dankwoord

Ik heb geleerd dat een doctoraatstraject is zoals het lopen van een marathon. Overenthousiasme aan de start, harde realiteit dat voelbaar wordt in het midden van het traject. De vele ups en downs worden gedragen door de steun van alle supporters aan de zijlijn. Het is net daarom dat ik mijn laatste woorden wil toewijden aan het bedanken van iedereen die mij aangemoedigd heeft en mij direct of indirect heeft geholpen om dit werk tot een goed einde te brengen.

Allereerst zou ik graag mijn promotoren, **Prof. Dr. Kristl Vonck** en **Prof. Dr. Robrecht Raedt**, willen bedanken om mij de mogelijkheid te geven een doctoraatsonderzoek te starten in het toenmalige LCEN3, en mij te ondersteunen sinds mijn masterthesis. **Prof. Dr. Kristl Vonck**, zou ik graag bedanken voor haar kritische ingesteldheid en haar taalkundige talenten bij het vormgeven van de publicaties. **Robrecht**, het was uw wetenschappelijk enthousiasme dat mij deed nadenken over een doctoraat. U heeft mij niet alleen aangezet om kritisch en zelfstandig te werken, maar u heeft mij ook doorheen de jaren de kans gegeven mij te ontplooien in het managen van de praktische zaken die samengaan met het werken in een laboratorium en daarbuiten. Ik geef mijn toestemming om één van de ratten-EEG lokalen in de nieuwbouw naar mij te vernoemen!

Ik zou ook alle leden van de examencommissie, **Prof. Dr. Ir. Sarah Vergult, Prof. Dr. Apr. Christophe Stove, dr. Benedicte Descamps, dr. Chris Van den Haute en dr. Tim Van Langenhove** willen bedanken voor hun bijdrage aan deze thesis. Hun interessante vragen en wetenschappelijke discussie hebben deze thesis tot een hoger niveau gebracht, bedankt! Een speciale bedanking gaat uit naar **Chris**, die me doorheen de jaren met raad en daad bijstond omtrent de wondere wereld der virale vectoren. Ook **Benedicte** wil ik graag persoonlijk bedanken, voor de rust die zij brengt in INFINITY, en vooral om te luisteren wanneer nodig en haar expertise met enthousiasme te delen. Daarnaast zou ik ook graag **Prof. Dr. Marie-Anne Vanderhasselt** bedanken voor de rol van voorzitster op haar te nemen en zeer snel te antwoorden op mijn vele mailtjes.

Daarnaast zou ik graag **Prof. Dr. Paul Boon** bedanken om mij de kans te geven mijn onderzoek uit te voeren in het 4BRAIN labo en om mij te verzekeren dat alles goed zou komen wanneer ik rust nodig had. Graag bedank ik ook **Prof. Dr. Evelien Carrette, Dr. Jean Delbeke en Prof. Dr. Wytse Wadman** voor de pittige en leerzame feedback tijdens de peer-reviews.

Ook de huidige post-docs, **Lars en Mathieu**, verdienen een speciale vermelding, om mij al tijdens mijn masterproef een realistisch beeld te schetsen van wat een doctoraat nu écht inhoudt. Blijf de volgende generaties inspireren! Lars, hopelijk stromen de resultaten binnen en lees ik binnnkort een Nature paper over chemo- en optogenetica in LC. En wees voorzichtig met de probes he!

Graag zou ik ook de leden van het animalarium bedanken die mij ondertussen 6 jaar geleden uitnodigden in hun keukentje. **Chantal**, **Marit** en **Maxime**, jullie babbeltjes waren een welkome afwisseling op de lastige (operatie)dagen.

Verder zou ik ook graag mijn collega's bedanken, voor wie woorden mij te kort schieten om hun existentiële rol in dit werk te beschrijven. Mijn doctoraatstraject was er toch één met enkele ups en downs, zowel op wetenschappelijk als persoonlijk niveau. Zonder jullie zou het nooit gelukt zijn!

Graag start ik met de leden van ons **4BRAIN senior groepje, Marie en Charlotte G.** Onze wekelijkse wandelingen leverden mij een geslaagd stappendoel op in combinatie met de noodzakelijke zaag-en-ventileermomenten. We zijn er eindelijk geraakt (met meer dan een PhD in cleaning)! **Marie**, bedankt om mij te vergezellen op ons allereerste symposium, waar we meteen de belangrijkheid van goeie catering leerden kennen! Jij was de oneindige spraakwaterval in het labo, en bent nog steeds een sfeerbrenger op feestjes (bedankt voor de shotjes in den Delta, het heeft diepe emoties naar boven gebracht). **Charlotte G**, ons verhaal startte in het begin van ons LCEN avontuur (en nee, de hechte band is nog steeds niet stuk). Ik zal nooit onze rattenlokaalbabbeltjes en de isoflo-vibes in het OK vergeten. Bedankt voor de meest gepaste leuze te bedenken: "het kan rap gaan, maar het kan ook traag gaan". Vergeet ons plan B niet, die kinderboerderij lijkt nog altijd een goed idee! **Jana**, jij vulde ons vrouwengroepje perfect aan, wat dan al eens leidde tot veel te uitgebreide conversaties over restaurantjes, laatste modetrends en niet te vergeten de beste mémés van het moment. Dankzij jou was ik ook niet langer de enige vrouw in het labo dat de bierkaart gretig verkende, kannetjes karmeliet zijn voor altijd aan jou gelinkt! **Anirudh**, thank you for sharing your book collection and for being such an enthusiastic person on the dance floor! **Charlotte B**, jouw bakkunsten hebben mij meermaals uit een suiker- en vooral mentaal dipje gehaald. **Emma**, jij bracht rust in onze groep en ik ben nog steeds onder de indruk over jouw perfecte presentaties. Daarnaast wil ik ook de nieuwere generatie veel succes wensen. **Erine**, jij hebt de mamarol in het labo perfect overgenomen. Bedankt om mij van tijd tot tijd te overstelpen met de nieuwste Kate

Middleton outfits. Ik heb mijn royal wave skills aangesterkt, tijd for some high tea! **Silke,** je was een fantastisch bureau- en sportmaatje, en vergeet niet dat je nog altijd een carrière als ballerina kan starten! De nieuwere collega's **Simona, Jeroen en Helen** wens ik heel veel succes bij het doorlopen van hun eigen doctoraatsavontuur. **Jeroen,** bedankt om tijdens mijn afwezigheid de ratjes goed te verzorgen en ondanks mijn occasioneel pessimisme toch nog aan een doctoraat te starten.

Ook mijn trouwe studenten die mij doorheen de jaren bijgestaan hebben wil ik bedanken. Jullie begeleiden was één van de mooiste aspecten van mijn doctoraat en ik hoop dat ik jullie met mijn filosofische quotes heb kunnen inspireren. **Sielke**, jij was noch mijn student noch een collega, maar ik denk dat ik niet lieg wanneer ik zeg dat we meteen gelijkgezinden waren in het labo. Jouw spontaniteit en enorme hulp hebben mij doorheen de laatste maanden gesleurd. Binnenkort kunnen we onze babbeltjes verder zetten als buurvrouwen, samen met een frietje (vergeet de stoofvleessaus en chicken fingers niet)!

Daarnaast wil ik ook **Chris en Leen** bedanken om mij zeer plots te verwelkomen in uitdagende tijden, ik kijk al uit naar de "aperitiepmomentjes" onder de nieuwe pergola! **Liesbeth en Alison**, bedankt voor de verwelkoming in de schone zusjes groep, ik denk dat we een maandelijkse coquitoavond gaan moeten inplannen. **Jan**, dankzij jou heb ik vertrouwen in de emotionele capaciteiten van de mannelijke Van Lysebettens. **Tom**, jouw culinaire creaties en recente prikkelende wekelijkse columns waren een bron van inspiratie en doorzettingsvermogen de laatste weken in mijn doctoraat. **Daniël en Leo**, AKA Captain America en de Hulk van Gent, en sinds kort **Casje**, ik ben vereerd de rol van lante Tatoja op mij te mogen nemen!

Uiteindelijk wil ik ook **mama en papa** bedanken, voor letterlijk alles wat ik heb en ben vandaag. Ik ben dankbaar voor de kansen die jullie mij gegeven hebben, opportuniteiten die door de complexiteit van het leven niet aan jullie aangeboden werden. Dit alles heeft mij geleerd om steeds alles in vraag te stellen en soms te kritisch het leven te benaderen, maar ik veronderstel dat dit geen slechte eigenschappen zijn als wetenschapper! Verbonden door deze ervaringen, maakt dit alles van ons een ondoorbreekbaar blok, en geeft dit moment een waarde die enkel wij kunnen bevatten. Jullie zijn het perfecte voorbeeld van een echte symbiose, you are still an effective team! En mijn **Indymansje**, boelemansje, patoetermansje, patattemansje, schetemansje, versterkte mijn benen met veel geduld, vult mijn eigenwijze karakter perfect aan en verzacht mijn hart.

Als laatste wil ik **Wouter** bedanken, beter bekend als baby, woepeliepoepsie, of ook wel schatziee. Ik denk niet dat één van ons twee na onze eerste ontmoeting in het labo had gedacht dat wij uiteindelijk het beste resultaat zouden zijn van onze doctoraatsonderzoeken. Bedankt om mijn vragend koppie altijd van een uitgebreide uitleg te voorzien, om mijn "zorgen" te doen vergeten in den Delta, om herhaaldelijk te zeggen dat mijn kousen écht niet opvallen, om mijn oiskipoiski kapitinski momentjes te verdragen, mij te motiveren in het vinden van nieuwe dansmoves, om mij te begrijpen zonder woorden en vooral om mij de rust te geven waarvan ik dacht het nooit te vinden. Ik kijk uit naar alle avonturen die ons pad nog gaan kruisen, vol vertrouwen met jou aan mijn zijde, vergezeld van de nodige snulliegrapjes en wigglemomentjes. Ik zie je graag!

Curriculum Vitae

Personalia

Full name	Latoya Stevens
Address	Vlaanderenstraat 117/201, 9000 Ghent
Date of Birth	28/12/1993
Nationality	Belgian
Phone	+32 (0) 499 46 54 31
E-mail	Latoya.Stevens2@gmail.com

Experience

Sep 2021 – Present	**Pharmaceutical consultant,** Abylsen Belgium
Nov 2016 – Sep 2021	**PhD Candidate Health Sciences**, Ghent University
Jun 2016 – Dec2016	**Student Research internship Grant application** Ghent University
Sep 2014 –Jun 2016	**Student Research Internship Master thesis**, Ghent University

Educational Background

2016 – present	**PhD in health sciences**, Ghent University
2016 – 2020	**Doctoral Schools Training Program**, Ghent University
2014 – 2016	**MSc Biomedical Sciences**, Ghent University Summa Cum Laude Thesis: "The effect of hippocampal neurostimulation on epileptic seizures in a rat model for temporal lobe epilepsy"
2011 – 2014	**BSc Biomedical Sciences**, Ghent University Cum Laude
2005 – 2011	**Latin – Sciences**, Secondary school, IKSO Denderleeuw

Postgraduate courses

2020-2021	Networking for Researchers, online Workshop, Ghent University
2018-2019	Epilepsy Management Course, Ghent University Hospital
2017-2018	Guiding of writing assessments, Ghent University Statistical analysis in SPSS, Ghent University Summer school: Let's talk Science, KU Leuven
2016- 2017	Summer school: 6th Edition of the U4 Summer School "Ageing Brain", prize for best grant application

Publications (A1)

Stevens L, Larsen LE, Van Lysebettens W, Carrette E, Boon P et al. Transducing the locus coeruleus using canine adenovirus type 2 (CAV2) vector in rats for chemogenetic modulation research. Front Neurosci. 2021

Van Lysebettens W, Vonck K, Larsen LE, **Stevens L**, Bouckaert C, Germonpre C, et al. Identification of vagus nerve stimulation parameters affecting rat hippocampal electrophysiology without temperature effects. Brain Stimul. 2020;13(5):1198-206.

Germonpre C, Proesmans S, Bouckaert C, **Stevens L**, Sprengers M, Vonck K, et al. Acute symptomatic seizures following intracerebral hemorrhage in the rat collagenase model. Epilepsy Res. 2020;164:106364.

Stevens L, Vonck K, Larsen LE, Van Lysebettens W, Germonpre C, Baekelandt V, et al. A Feasibility Study to Investigate Chemogenetic Modulation of the Locus Coeruleus by Means of Single Unit Activity. Front Neurosci. 2020;14(March):162.

Conference Abstracts (C3)

Stevens L, Vonck K, Van Lysebettens W, Baekelandt V, Van Den Haute C, Carrette E, Boon P and Raedt R (2019). Genetic modification of Locus Coeruleus NE cells for chemogenetic activation remains challenging. Front. Neurosci. Conference Abstract: 13th National Congress of the Belgian Society for Neuroscience. doi: 10.3389/conf.fnins.2019.96.00009

Larsen LE, **Stevens L**, Acharya A, Bouckaert C, Craey E, Desloovere J, Goossens M, Germonpré C, Proesmans S, Boon P, Vonck K, Vanhove C, Van Mierlo P and Raedt R (2019). Evoked hippocampal seizures are associated with bursts of locus coeruleus neuronal activity in the anaesthetized rat: a mechanism of 'pathological memory formation' in epilepsy. Front. Neurosci. Conference Abstract: 13th National Congress of the Belgian Society for Neuroscience. doi: 10.3389/conf.fnins.2019.96.00016

Stevens L, Raedt R, Van Lysebettens W, Baekelandt V, Van Den Haute C, Boon P and Vonck K (2018). Induction of DREADD expression in the rat locus coeruleus and its effect on neuronal firing. Epilepsia.59.

Oral Presentations

Chemogenetic modulation of the locus coeruleus in rat. 3rd Neuroscience Day, Ghent, Belgium, December 2019.

Chemogenetic modulation of the locus coeruleus in rat. Neuromodulation Workshop, Ghent, Belgium, September 2019.

Presumed subclinical doses of clozapine not useful as selective ligand for chemogenetic activation of locus coeruleus neurons in rat. *Research Day and student symposium*, Ghent, Belgium, April 2019.

Genetic modification of locus coeruleus NE cells for chemogenetic activation remains challenging. *F-Tales Neuroplasticity and Neuromodulation at different scales*, Antwerp, Belgium, June 2019.

Chemo- and optogenetic modulation of the locus coeruleus in rat. *1st Neuroscience Day*, Ghent, Belgium. February 2019.

Toward selective modulation of locus coeruleus neurons using chemogenetics. *AMIE symposium: Optical and Chemical modulation of brain networks*, Ghent, Belgium, January 2018.

Poster Presentations

Stevens L, Raedt R, Van Lysebettens W, Baekelandt V, Van Den Haute C, Boon P and Vonck K. Genetic modification of locus coeruleus NE cells for chemogenetic activation remains challenging. *21th annual international symposium Epilepsy, Sleep and Neurocognition*, Heeze, The Netherlands; june 2019.

Stevens L, Raedt R, Van Lysebettens W, Baekelandt V, Van Den Haute C, Boon P and Vonck K. Genetic modification of locus coeruleus NE cells for chemogenetic activation remains challenging. *F-Tales Neuroplasticity and Neuromodulation at different scales*; Antwerp, Belgium, June 2019.

Stevens L, Raedt R, Van Lysebettens W, Baekelandt V, Van Den Haute C, Boon P and Vonck K. Genetic modification of locus coeruleus NE cells for chemogenetic activation remains challenging. Belgian Society of Neuroscience, Brussels, Belgium; May 2019.

Stevens L, Raedt R, Van Lysebettens W, Baekelandt V, Van Den Haute C, Boon P and Vonck K. Presumed subclinical doses of clozapine not useful as selective ligand for chemogenetic activation of locus coeruleus neurons in rat. *Research Day and student symposium,* Ghent, Belgium; April 2019.

Stevens L, Raedt R, Van Lysebettens W, Baekelandt V, Van Den Haute C, Boon P and Vonck K. Presumed subclinical doses of clozapine not useful as selective ligand for chemogenetic activation of locus coeruleus neurons in rat. *SWO midwinter meeting*, Amsterdam, The Netherlands, January 2019.

Stevens L, Raedt R, Van Lysebettens W, Baekelandt V, Van Den Haute C, Boon P and Vonck K. Induction of DREADD expression in the rat locus coeruleus and its effects on neuronal firing. *13th European Congress on Epileptology,* Vienna, Austria, August 2018.

Stevens L, Raedt R, Van Lysebettens W, Baekelandt V, Van Den Haute C, Boon P and Vonck K. Induction of DREADD expression in the rat locus coeruleus and its effects on neuronal firing. *Research Day and Student Symposium, Ghent, Belgium, April 2018.*

Stevens L, Raedt R, Van Lysebettens W, Baekelandt V, Van Den Haute C, Boon P and Vonck K. Induction of DREADD expression in the rat locus coeruleus and its effects on neuronal firing. *SWO midwinter Meeting, Amsterdam, The Netherlands, March 2018,*

Stevens L, Raedt R, Van Lysebettens W, Baekelandt V, Van Den Haute C, Boon P and Vonck K. Induction of DREADD expression in the rat locus coeruleus and its effects on neuronal firing. *20th annual International Symposium of Epilepsy, Sleep and Neurocognition, Kempenhaeghe, Heeze, The Netherlands, March 2018,*

Teaching and supervision of students

- Master thesis of Aki Van Zande: The applicability of optogenetics and chemogenetics to transduce the locus coeruleus in rat. (2019-2020)

- Master thesis of Jeroen Spanoghe: Chemogenetic and optogenetic modulation of noradrenergic neurons of the locus coeruleus in rat (2018-2019)

- Research project Master Biochemistry and Biotechnology of Nele Goossens: Chemogenetic control of epileptic seizures in temporal lobe epilepsy (2017-2018)

- Lesson on communication of neurons and the influence of hormones on brain and behavior, for master biology students, March 2017

Miscellaneous

- February 2021-April 2021: Volunteer Internal Contact tracer, AZ Maria Middelares, Ghent
- Member of organizing committee of the 3rd 4BRAIN Neuroscience Day, Ghent University, 2019
- Member of Animal Welfare Body – Faculty of Medicine and Health Sciences, Ghent University, 2018 – 2020
- First intervention team: first aid and evacuation, Ghent University, 2018-2020

Appendix A: The effect of chemogenetic activation of the locus coeruleus on hippocampal excitability – preliminary data

A.1 Material and Methods

A.1.1 Animals

Adult male Sprague-Dawley rats (Envigo, The Netherlands) were used in this preliminary study and treated according to European guidelines (directive 2010/63/EU). The local Ethical Committee on Animal Experiments of Ghent University (ECD 16/31) approved the study protocol. Animals were kept under environmentally controlled conditions: 12h light/dark cycles with artificially dimmed light, temperature and relative humidity at 20-23°C and 40-60% respectively with food (Rats and Mice Maintenance, Carfil, Belgium) and water ad libitum. All animals were grouped housed in Type IV cages (Tecniplast, Australia) on wood-based bedding (Carfil, Belgium). Cages were enriched with paper nesting material and cardboard tunnels (Carfil, Belgium).

A.1.2 Viral vector administration

Animals (n=17; 10-11 weeks old) were anesthetized with a mixture of medical oxygen and isoflurane (5% for induction, 2% for maintenance, Isoflo, Zoetis, UK); body temperature was controlled using a heating pad. Rats were placed in a stereotaxic frame (Stoelting, USA) and the skull was exposed. Bregma was lowered 2mm relative to lambda (15° head angle) to target the LC and avoid the transverse sinus. Using a Hamilton Neuros Syringe (Hamilton company, Nevada, USA) and Quintessential Stereotaxic Injection system (flowrate 150nl/min, Stoelting, USA), three injections of CAV2-PRSx8-hM3Dq-mCherry vector solutions ($5.9x10^9$ pp/µl undiluted, in PBS) were performed along the dorsoventral axis in the LC (3.9 AP, 1.15 ML relative to lambda, -5.8, -5.5, -5.3 DV from dura). Animals were injected bilaterally with the following injection conditions: 3x300 nl containing $1E^9$ pp of CAV2 (LowV_1E9, n=5), 3x300 nl containing 0.1E9 pp CAV2 (LowV_0.1E9, n=3) and 3x600 nl containing 0.1E9 pp of CAV2 (MediumV_0.1E9, n=5). Four control animals were injected with 3x600nl containing 1E9 pp of CAV2 control viral vector. After each injection the syringe was left in place for an additional 5 min and then slowly retracted to avoid backflow. Two-component silicone gel (Kwik-Sil; World Precision Instruments, FL, USA) was applied to the craniotomy to protect the brain surface. After surgery, animals were subcutaneously (s.c.) injected with the nonsteroidal anti-inflammatory drug meloxicam (1mg/kg metacam, Boehringer Ingelheim, Germany) and lidocaine (5% Xylocaine gel, Astrazeneca, UK) was applied to the incision site

to minimize discomfort. All animals recovered two weeks in their home cage to allow for optimal viral vector expression

A.1.3 Electrode implantation

Two weeks after viral vector administration, animals (n=17) were anesthetized with a mixture of medical oxygen and isoflurane (5% for induction, 2% for maintenance, Isoflo, Zoetis, UK); body temperature was controlled using a heating pad. Rats were placed in a stereotactic frame (Stoelting, USA) and the skull was exposed. Bipolar electrodes were used for stimulation of the perforant path and recording in the dentate gyrus. For recording, two twisted polyimide-coated stainless steel wires (California fine wire, USA) with a bare wire diameter of 70µm and 900µm intertip distance were used. For stimulation, two twisted, polyimide-coated, stainless-steel wires with a bare diameter of 110µm diameter (Science Products) and 900µm tip separation were used. Scalp electrodes made out of a copper wire soldered to a stainless steel microscrew (0.8mm diameter, Plastics One) were used as ground and reference electrodes and implanted in the *os frontale*. Two craniotomies were made at -3.8mm posterior and 1.9mm lateral relative to Bregma for recording in the dentate gyrus and at AP level from lambda and 3.9mm lateral for stimulation of the perforant path. First, the bipolar recording electrode was lowered in the brain parenchyma until the most dorsal electrode tip reached the dentate gyrus (approximate depth of 3mm relative to brain surface) and the ventral tip was situated in the CA1 using audiomonitoring. Secondly the bipolar stimulation electrode was slowly lowered and square wave biphasic pulses of 400µA, 200µs pulse width per phase were administered at 0.1Hz until a characteristic EP with clear fEPSP and max PS were detected in the dentate gyrus (approximate depth 2.5mm below brain surface).

A.1.4 Electrophysiology: set-up

Recorded signals were referenced to a scalp electrode placed in the os frontale. Recording and stimulation electrodes were connected to an amplifier. A constant-current stimulator (DS4 Bi Phasic Stimulator, Digitimer) was used for electrical stimulation. Evoked potentials were amplified 248 times and digitized at a sampling rate of 25 kHz using a data acquisition device (National Instruments). Acquisition of the data was performed in a Matlab-based application.

A.1.5 Electrophysiology: *in vivo* dentate gyrus evoked potential recording

After implantation of the electrodes and stabilisation for 15 min, DG EP were recorded under isoflurane anesthesia. During the entire recording, EPs were recorded as a result of biphasic charge balanced square wave pulses delivered to the perforant path with pulse width 200µs and interpulse interval of 10s. The protocol started with a baseline recording. The PP was stimulated starting at an intensity of 50µA increasing in steps of 50µA until 300µs was reached, continuing to 1000µA in steps of 100µA. Per EP recording session, this input-output (IO) curve was repeated five times. After a baseline recording session, subcutaneous injections of clozapine were made, starting with the lowest dose of 0.01 mg/kg. After 15 minutes, the same EP IO stimulation protocol was performed followed by a second injection of clozapine at a higher dose (0.1 mg/kg, s.c.). After the second injection, the stimulation protocol was repeated.

A.1.6 Histology

Double label immunostaining for DBH and the mCherry tag fused to the hM3Dq receptor was performed to quantify specificity of hM3Dq expression, and evaluate possible damage to the LC. Twelve histological sections were selected per animal starting approximately 10.5 mm posterior to Bregma, and keeping every third section (80 µm apart), towards anterior. Selected sections were rinsed twice for 5min in distilled water (dH_2O) followed by incubation in 0.5% and 1% H_2O_2 for 30 and 60min respectively to block endogenous peroxidase activity. After washing twice for 5 min in PBS, sections were incubated for 45min in blocking buffer (BB; 0.4% Fish Skin Gelatin (FSG) and 0.2% Triton X in PBS). For one hour at room temperature and subsequently overnight at 4°C, sections were incubated in BB with primary antibodies to visualize noradrenergic LC neurons (mouse anti-DBH, 1:1000, clone 4F10.2, Merck,) and mCherry tag (rabbit anti-red fluorescent protein, 1:1000, ROCK600-901-379, Rockland). The next day, sections were washed twice in BB for 10 min followed by one hour incubation in BB with the secondary antibodies Alexa Fluor goat anti-mouse 488 nm (1:1000, Ab 150113, Abcam) and Alexa goat anti-rabbit 594 nm (1:1000, Ab 150176, Abcam) diluted in BB for 1 hour. After washing twice in PBS for 5 min, a nuclear DAPI stain was performed. After two additional washing steps in PBS (2x5 min), sections were mounted on glass slides and cover slipped using Vectashield H1000 mounting medium (Vector Laboratories, USA) to prevent photobleaching.

Glass slides were scanned using a Pannoramic 250 slide scanner equipped with a Plan Apochromat 40X objective and a pco.edge 4.2 4MP camera to have overview images of all sections. Detailed images of the LC sections were acquired of the DREADD injected animals

using the Olympus IX81 confocal microscope using Olympus Fluoview FV1000 software or a Nikon A1R confocal laser scanning microscope (Nikon Benelux, Brussels, Belgium) equipped with a Plan Apo VC 20X, 0.75 NA objective lens (Nikon). Images were exported as .nd2 and tiff files for post-processing. For each rat, images of three tissue sections containing a clear LC nucleus were selected to qualitatively identify the presence and location of the hM3Dq expression. Expression levels were assessed as described in more detail in 6.2.3.

A.1.7 Data analysis

Successful recording was performed in all but one DREADD animal. EP data of animals showing high levels of bilateral hM3Dq expression (n=5) and control animals (n=4) were processed in Matlab 2019b (The Mathwork Inc, Natick, USA). Three main parameters were extracted: the fEPSP slope by fitting a line between the fEPSP start and the PS onset using the least square method; 2) PS amplitude measured as the vertical distance between the peak of PS and the line that connects the positive fEPSP peaks before and after the PS; and 3) the fEPSP amplitude by fitting a line between 0 and the peak of the fEPSP (Fig.A1). EP parameters were averaged over all animals within their respective group (DREADD versus control) and normalised to the baseline value at the maximum stimulation intensity.

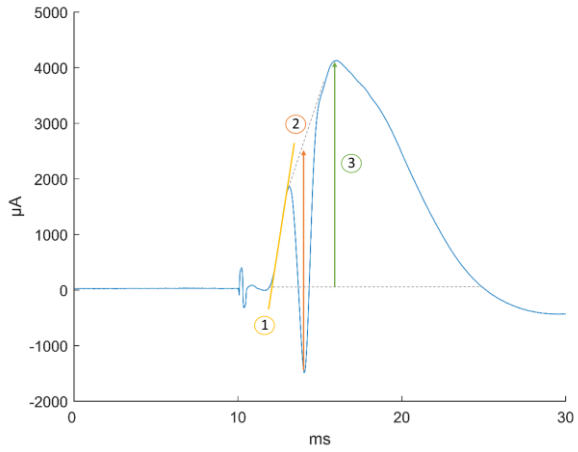

Figure A 1 Representative sample of DG evoked potential after stimulation of PP and parameters extracted: 1) fEPSP slope in yellow; 2) PS amplitude in orange and 3) fEPSP amplitude in green. X-axis time in ms, y-axis amplitude in µA.

A.2 Results

A.2.1 Viral vector expression

Bilateral expression was observed in 6/13 DREADD-injected animals. Five of these 6 animals were injected with 3x300nl and 1E9 particles, showing 79.6 ± 4.1% of LC neurons expressing the hM3Dq receptor. One animal with bilateral expression was injected with the MediumV_0.1E9 pp showing hM3Dq expression in 88.8 ±1.4% of LC neurons.

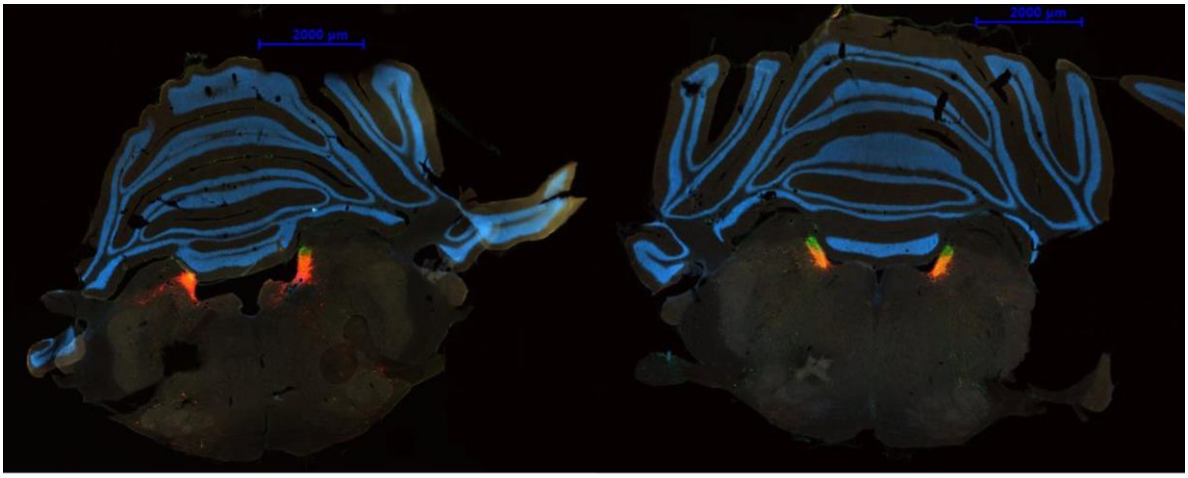

Figure A 2 Representative image of bilaterally injected animals expressing hM3Dq DREADD. Left panel. Overview of section (LowV_1E9). Right panel gives an overview of bilateral hM3Dq expression in MediumV_0.1E9. LC-NA neurons are visualized using primary anti-DBH antibody (green, AF 488nm) and expression of hM3Dq DREADD is visualized using anti-RFP (red, AF 594nm), cell nuclei are stained with DAPI (blue)Scale bar left 2000µm.

A.2.2 Effect of chemogenetic LC activation on dentate gyrus evoked potentials (DG EP)

Recording of DG EPs under anesthesia was performed before and after systemic administration of clozapine (0.01 and 0.1 mg/kg, s.c.) in DREADD animals (n=5) and control animals (n=4). The fEPSP slope (Fig A3 A), a measurement for the efficiency of presynaptic neurotransmission shows in the DREADD animals an average decrease, up to 10% at the highest stimulation intensities after clozapine 0.01 mg/kg administration. Whereas in control animals (dashed lines) no decrease in fEPSP slope is observable, not even after the highest dose of clozapine (red dashed line). The amplitude of the fEPSP, a measurement for postsynaptic depolarization, seems to decrease in a similar manner in the DREADD animals after both doses of clozapine, with the higest dose inducing decreases up to 20% at some given intensities. Again, no clear decrease was observed in control animals after both doses of clozapine, however, a small increase could be observed at the higher stimulation intensities, which could be normal physiological variance and/or due to the stimulation protocol (Fig.A3C). Figure A3B shows the average population spike amplitude for both conditions, which resembles the

summation of postsynaptic action potentials. Here, in contrast to the other EP parameters showing small changes, no difference could be observed between DREADD and control animals. A decrease in PS amplitude was observed in both conditions after administration of clozapine, lacking a clear DREADD-induced effect on postsynaptic firing. This sign of depression could be induced by the stimulation protocol itself, as reported both in vitro as in vivo when using a stimulation paradigm with interpulse interval of 10s(1, 2).

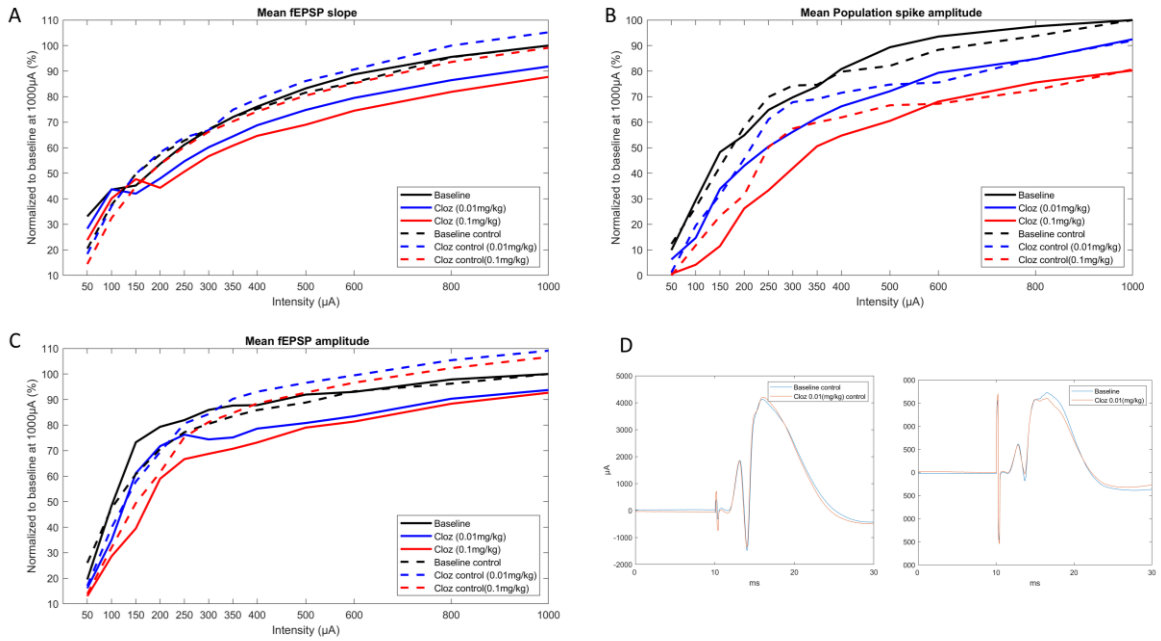

Figure A 3 Effect of clozapine on DG EPs in DREADD versus control animals. A) Mean EPSP slope; B) mean fEPSP amplitude; c) Mean PS amplitude. All data averaged per condition DREADD: full line and control dashed line, normalised to the baseline value at max stimulation intensity. Baseline (black), clozapine 0.01 mg/kg (blue) and clozapine 0.1 mg/kg (red); D) representative EP in control and DREADD animal and the effect of clozapine 0.01 mg/kg (orange)versus baseline (blue).

Bibliography

1. Harris EW, Lasher SS, Steward O. Analysis of the habituation-like changes in transmission in the temporodentate pathway of the rat. Brain Res. 1979;162(1):21-32.

2. Harris EW, Lasher SS, Steward O. Habituation-like decrements in transmission along the normal and lesion-induced temporodentate pathways in the rat. Brain Res. 1978;151(3):623-31.

Appendix B: AAV2/7 Viral vector conditions

Pilot trial experiments were performed to characterise the ability of AAV2/7-PRSx8-hM3Dq-mCherry of transducing LC noradrenergic neurons. In different preliminary trials, rats were injected in LC (-5.7 DV) with different volumes (10-50-125nl) of undiluted or diluted (in PBS) viral vector. Qualitative analysis of the cell-specific expression and hM3Dq expression in non-noradrenergic neurons was performed by experienced researchers underneath the epifluorescence microscope.

Initially, 125nl of viral vector induced cell-specific expression of hM3Dq, however a large presence of aspecificity was observed in the vicinity of LC. Therefore, the volume was decreased to 50 and 10nl, both resulting in lower but still significant presence of aspecific expression. Therefore, these volumes were diluted as depicted in Table B1.
In general, we observed a lack of hM3Dq expression after administration of diluted viral vector, indicating a possible caveat in the protocol.

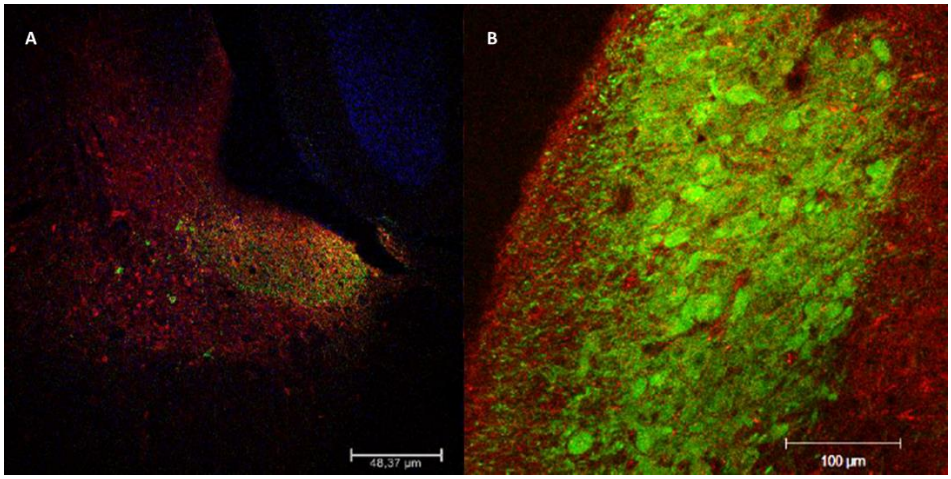

Figure B 1 Visualization of hM3Dq-mCherry expression in LC injected with different conditions of AAV2/7 viral vector. A. LC injected with 125nl of AAV2/7-PRSx8-hM3Dq-mCherry, showing clear aspecific hM3Dq expression (red) in the vicinity of LC. B. 50 nl injection of AAV2/7 viral vector, showing no transduced cell bodies. Scale bar in µm.

These conditions pointed out that 10nl of undiluted AAV2/7-PRSx8-hM3Dq-mCherry was the most optimized injection condition we assessed in the lab, where cell-specific expression was observed, although a signficant presence of hM3Dq was expressed in non-noradrenergic neurons (Chapter 5).

Table B.1 Overview of injection parameters used in preliminary experiments using AAV2/7-PRSx8-Hm3Dq-mCherry (5.99E+12 GC/ml).

Volume	Dilution	Cell-specific expression	Aspecific expression
125 nl	Undiluted	+/-	+++
50 nl	Undiluted	+/-	++
50 nl	1/500	-	-
50 nl	1/5000	-	-
10 nl	Undiluted	+/-	+
10 nl	1/10	-	-
10 nl	1/100	-	-
10 nl	1/1000	-	-

Since it was never our primary goal to perform titration experiments or compare different viral vectors to each other, some caveats in the methodology were present. This complicated the formation of hypothesis concerning the exact origin of differences observed in transduction efficiency with the AAV2/9 used in literature or the CAV2 (chapter 6). Therefore we suggest to perform standardised experiments when targeting a new cell-type, or when comparison of different serotypes or viral vectors is necessary.

Following parameters should be uniform along experiments, since all these factors might play a role in the observed transduction efficiency, as we observed during the course of experiments.

- Identical species, strain and sex
- Age of injection
- Handling of viral vector:
    - coating of syring with viral vector
    - sterile PBS for dilution and low binding pipet tips
    - avoidance of multiple freeze-thaw cycles
- Standardised injection parameters:
    - injection material (Hamilton syringe, glass capillaries)
    - stereotactic coordinates and number of injection sites
    - volume and number of particles (identical titer assay)
- Standardised analysis of outcome parameters: manual cell count (or unbiased stereology), or pixelvalues as a proxy.